

LOUGHBOROUGH  
UNIVERSITY OF TECHNOLOGY  
LIBRARY

AUTHOR

DODDS, J

COPY NO.

025140/01

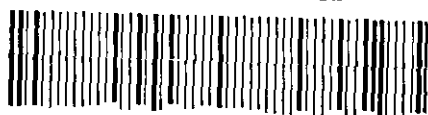
VOL NO.

CLASS MARK

ARCHIVES  
COPY

FOR REFERENCE ONLY

002 5140 01



To  
Katy, My Wife

THE PORE SIZE DISTRIBUTION AND DEWATERING  
CHARACTERISTICS OF PACKED BEDS AND FILTER  
CAKES

J.A. DODDS

Submitted for the degree of Doctor of Philosophy  
Loughborough University of Technology

Department of Chemical Engineering September 1968

Professor D.C. Freshwater Supervisor P.J. Lloyd

Department of Mechanical Engineering  
Loughborough University  
Leicestershire LE11 3TU

MEMORANDUM

Subject: [Illegible]  
Reference: [Illegible]

Date: [Illegible]  
By: [Illegible]

Loughborough University Of Technology Library	
Date	Oct. 68
Class	
Acc. No.	025140/01

## ACKNOWLEDGEMENTS

I wish to express my gratitude to my Supervisor Mr. P.J. Lloyd for his help and guidance throughout the course of this work. To Professor D.C. Freshwater in whose department the research was carried out. To members of staff Mr. R.H. Berresford, Mr. H.W. Kropholler and Mr. B. Scarlett for helpful discussion. To Mrs. Bayard Burford for typing the manuscript.

## SUMMARY

Dewatering may be defined as the displacement of fluid from a saturated porous medium. The mechanism of the process is not fully understood, but is known to be strongly dependent on the pore structure of the porous medium because of the action of capillary forces in the pores. This investigation attempts to describe the microscopic effects of moisture in porous media and to relate these to the macroscopic process of dewatering. This is divided into three parts: The first is concerned with the static effects of moisture retained in porous media, for which a model of pore space is developed; The second deals with the flow of fluids in partially saturated porous media and an attempt is made to relate the model of pore space to this; Finally a simple theory of dewatering is developed to demonstrate the effects of the various variables.

Chapter One Introduction and Dewatering Theories Page No. 1

- 1.1 Introduction
- 1.2 Empirical Correlations
- 1.3 Theory based on Flow in Porous Media
- 1.4 Capillary Theory of Dewatering
- 1.5 Discussion

Chapter Two Effects of Moisture in Porous Media Page No. 16

- 2.1 General
- 2.2 Capillary Pressure
- 2.3 Vapour Pressure Lowering
- 2.4 Range and Applicability of the Effects
- 2.5 Measurement of the Capillary Pressure Saturated Relationship
  - 2.5.1 Introduction
  - 2.5.2 Gravity Drainage Method
  - 2.5.3 Suction and Pressure Plate Methods
  - 2.5.4 The Mercury Porosimeter
- 2.6 Characteristics of Capillary Pressure Curves
- 2.7 Equal Size Spheres in Open and Close Packing
- 2.8 Moisture Distribution in Sphere Packs
- 2.9 Haines Theory of Capillary Pressure Curves
  - 2.9.1 Introduction
  - 2.9.2 Desaturation of Close Packing
  - 2.9.3 Imbibition in Close Packing
  - 2.9.4 Desaturation and Imbibition in Open packing
- 2.10 Experimental Verification of Haines Theory
- 2.11 Summary

Chapter Three Characteristics of Capillary Pressure Curves Page No. 37

- 3.1 Hysteresis
- 3.2 Residual Moisture
- 3.3 Surface Area
- 3.4 Correlations for Porosity Variation
- 3.5 Effect of Contact Angle
- 3.6 Pore Size Distribution and the Network Model
- 3.7 Capillary Pressure Curves for Sphere Size Mixtures
- 3.8 Discussion of Capillary Pressure Curves Related to Dewatering

- 4.1 Introduction
- 4.2 Particle Size Distribution and Packing
- 4.3 Wise Model of Random Packing of Unequal Spheres
- 4.4 Pore Space in the Wise Model
  - 4.4.1 Pore Size Distribution
  - 4.4.2 Continuity of Pore Space
- 4.5 Setting up and use of the Network Model
- 4.6 Preliminary Tests
- 4.7 Summary

- 5.1 Introduction
- 5.2 Description of Apparatus
  - 5.2.1 General
  - 5.2.2 Types of Cell
  - 5.2.3 Volume Measuring System
  - 5.2.4 Vacuum System
- 5.3 Calibration of the Apparatus
  - 5.3.1 Calibration of the Measuring Tube
  - 5.3.2 Correction to Pressure Readings
  - 5.3.3 Correction to Volume Readings
- 5.4 Experimental Procedure
- 5.5 Experiments Performed
- 5.6 Results and Discussion
  - 5.6.1 Experimental Results
    - 5.6.1.1 Reproducibility
    - 5.6.1.2 Porosity Variation
    - 5.6.1.3 Surface Area
    - 5.6.1.4 Full Correlation
    - 5.6.1.5 Summary
  - 5.6.2 Results from Theoretical Model
    - 5.6.2.1 Porosity Correlation
    - 5.6.2.2 Surface Area and Residual Moisture
    - 5.6.2.3 Full Correlation
    - 5.6.2.4 Summary
- 5.7 Conclusions



- 6.1 Introduction
- 6.2 Single Phase Flow in Porous Media
  - 6.2.1 Capillary Tube Theories
  - 6.2.2 Kozeny-Carman Theory
  - 6.2.3 Tortuosity
  - 6.2.4 Discussion
- 6.3 Two Phase Flow in Porous Media
  - 6.3.1 Experimental Study of Two Phase Flow in Porous Media
  - 6.3.2 Determination of Relative Permeability
  - 6.3.3 Characterisation of Two Phase Flow
- 6.4 Derivations of Relative Permeability
  - 6.4.1 Capillary Tube Theory
  - 6.4.2 Tortuosity from Electrical Resistivity
  - 6.4.3 Kozeny-Carman Applied to Relative Permeability
  - 6.4.4 Discussion
- 6.5 Theories including Pore Inter-connection
  - 6.5.1 Cutting and Joining Models
  - 6.5.2 Lattice Models
  - 6.5.3 Network Models
- 6.6 Summary

- 7.1 Introduction
- 7.2 Matrix Expression for the Resistance of a Network
- 7.3 Application of the Relationships to the Network Model of Porous Media
- 7.4 Use of the Matrix Method for Permeability and Relative Permeability
- 7.5 Results and Discussion
  - 7.5.1 Saturated Permeability
  - 7.5.2 Relative Permeability
- 7.6 Summary and Conclusions

Chapter Eight Dewatering as a Flow Process

Page No. 182

- 8.1 Introduction
- 8.2 Dewatering as a Flow Process with a Succession of Steady States
- 8.3 The Variables which affect Dewatering
- 8.4 Discussion
- 8.5 Conclusions

Chapter Nine Summary and Suggestions for Further Work

Page No. 199

- 9.1 Introduction
- 9.2 Capillary Pressure Curves
  - 9.2.1 Summary
  - 9.2.2 Experimental Works
  - 9.2.3 Extension of Theory
- 9.3 Permeability and Relative Permeability
  - 9.3.1 Summary
  - 9.3.2 Experimental Work
  - 9.3.3 Extension of Theory
- 9.4 Dewatering
  - 9.4.1 Introduction
  - 9.4.2 Experimental Work
  - 9.4.3 Extension of Theory

Appendices

Page No. 209

1. Geometrical Relationships of Tetrahedra Formed by Four Spheres
2. Computer Program for Wise Model Pore Space
3. Samples used in the Experiments
4. Example of obtaining Capillary Pressure Curves from Model
5. Experimental and Theoretical Results
6. Matrix Permeability Program
7. Relative permeability and dewatering curve program

NOMENCLATURE

A	Area	Pc	Capillary pressure
A	Mean solid angle	$\Delta P$	Pressure drop
a	Radius of capillary tube	$\rho$	Density
a,b	Constants for tortuosity term	q	Volume flow rate
a,b,c	Number of times a given sphere appears in a tetrahedron	Ros	Resistance
C	Curvature	R	Gas constant
d	Particle diameter	Re	Reynolds number
e	Porosity	Rw	Residual moisture (weight basis)
e *	Pseudo porosity	r	Sphere radius
e	Voltage	r	Radius of curvature
F	Formation factor	re	Equivalent radius
Fa	Dahlstrom approach factor	S	Surface area
Fe	Formation factor for partially saturated material	<del>Se</del>	<del>Effective</del> saturation
f	Lithology factor	So	Specific surface
f	Number frequency of a sphere in a mixture	Sr	Residual saturation
f	Friction factor	T	Surface tension
h	Vapour pressure	t	tortuosity
ho	Saturated vapour pressure	t	Temperature
h	Capillary height	t	Time
hm	Mean capillary height	u	Specific volume of water
i	Amperes current	V	Volume
j	Leverett function	v	Velocity
K	Permeability	v <sup>1</sup>	Apparent velocity
ko	Shape factor	x	Reciprocal sphere radius
L	Bed depth	y	Exponent to saturation in Brownell and Katz correlation
L	Length of capillary tube	Z	Impedance
Le	Effective bed depth	$\theta_d$	Dewatering time
li	Edge length of Floods unit pore	$\theta$	Contact angle
M	Molecular weight of water	$\theta$	Packing angle
M	Hydraulic radius	$\phi$	Angle of conical capillary
m	Exponents to porosity in Brownell and Katz	$\phi$	Integer between 1 and 9
n	Number of components in a mixture	$\eta$	Viscosity
n	Exponents to porosity in Brownell and Katz correlation	$\mu$	Microns
		Subscripts :	
		e	Effective
		s	Solid
		rL	Relative
		w	Water or wetting phase
		w	Weight basis
		nw	Non wetting phase

## CHAPTER ONE:

### INTRODUCTION AND DEWATERING THEORIES

#### 1.1 INTRODUCTION

In solid/liquid separation the cycle which starts with a slurry and ends with a moist cake is often referred to as dewatering. Thus in some processes certain filters or centrifuges are called dewatering filters or centrifuges. This is especially so in sanitary engineering practice where dewatering means the whole process of removing water from a sewage sludge. The term is used here however in a more restricted sense to refer to that part of the filtration cycle when filtrate is mechanically removed from an already formed filter cake. This definition also excludes vibration dewatering used in coal and sand preparation when drainage from a slurry is promoted by vibration on a screen. Filtration is therefore considered to be composed of two processes, the formation of a saturated cake by filtration proper, and the dewatering of that cake by applying pressure stress on the cake to remove some of the filtrate. Usually it is possible to remove moisture thoroughly by thermal drying but mechanical dewatering has the advantage of being much cheaper and does not involve loss of the liquid or possible damage to the solid. The process is however limited since there is always a residual moisture which cannot be removed by dewatering. The residual moistures reached in laboratory experiments and approximately predictable by theory are rarely reached in practice for reasons which are not properly understood.

The final moisture content of filter cakes can be of importance for several reasons. If the filter cakes is an intermediate in a process the moisture content may have to be reduced below a critical level for further processing. e.g. if the next operation is granulation. Furthermore, the filtrate itself or dissolved solids in it may be valuable or may contaminate the filter cake and have to be removed. It has been

observed (Himus 1958) that if water used in washing coal to reduce ash content is not itself removed it can constitute a larger percentage of impurity in the coal than did the ash originally. When the filter cake is a final product, moisture content can be important because it increases transportation costs per unit weight of solid as the water also has to be carried. Furthermore, moisture in stored materials can lead to degeneration or can cause handling difficulties in trucks or bunkers by causing caking or freezing up in winter.

If filtration is taken as being concerned with the separation of solids from liquids then both filtration and dewatering should be considered together in producing this separation, and the final moisture content should be chosen by optimisation of the whole filtering operation. The filtration part of this sequence has been studied intensively in recent years. The theory is well developed and has a large literature much being based on the work done in the general topic of fluid flow in packed beds. Grace (1959) has stated that the theory of filtration is in advance of the practical application of that theory. Dewatering and the allied topic of two-phase flow in packed beds have been studied to a lesser extent and are not yet fully understood. The authors of the recent Ministry of Technology review of solid liquid separation literature (Poole and Doyle 1965) stated that "No satisfactory theory exists to relate the degree of dewatering of a filter cake to its parameters".

Research into dewatering has been tackled in two ways. One an empirical approach in which the dewatering process is studied as a function of the variables which affect it. The other a theoretical approach which tries to describe the process mechanistically and mathematically.

In discussing these theories here, moisture contents are expressed as either a percentage of the void volume of the porous medium or as a percentage of the dry weight. The first method is

preferred and used when the porosity is available. The second is more convenient to calculate but does not allow easy comparison between different materials. It is however more useful than moisture contents expressed as a weight percentage on a wet basis as these give no grounds at all for comparisons even with the same material. Only the moisture existing between grains in a free state is accessible to dewatering and considered here. Water held by chemical or adsorption forces is taken as part of the solid phase and if it exists correction must be made to moisture contents determined by drying and weighing. For generality the fluids existing in a partially saturated porous medium should be termed either wetting or non-wetting phase, here however, water and air are used as representative of these.

## 1.2 EMPIRICAL CORRELATIONS

Dahlstrom and his co-workers (1952-61) have developed an empirical correlation for dewatering based on results obtained from a variety of sources. These include laboratory tests, pilot plant work and full scale plant tests, all on a variety of materials.

The factors taken as affecting moisture content are divided into two groups, filter feed variables and operating variables. The first includes, size distribution of solids, solids concentration, and the viscosity of liquid. The second includes, dewatering time, cake thickness, pressure drop across the cake and air rate through the cake. These variables are interrelated and no one variable can be separated, e.g. the cake thickness is dependent on the filtration time and this affects the time available for dewatering. The cake thickness also affects the air rate through the cake. The optimum conditions for cake dewatering are also not the same as for filtration and therefore the true optimum is always decided by economic criteria. This makes the correlation procedure very useful for practical problems. The

correlation was taken as

$$\left[ \frac{\Delta P}{L} \right] \left[ \frac{\theta_d}{\eta} \right] \left[ \frac{\text{air rate}}{\text{area}} \right] \text{ plotted against}$$

moisture content, Piros, Brusenback and Dahlstrom (1952). This results in two similar curves shown in Fig. (1). The higher curve

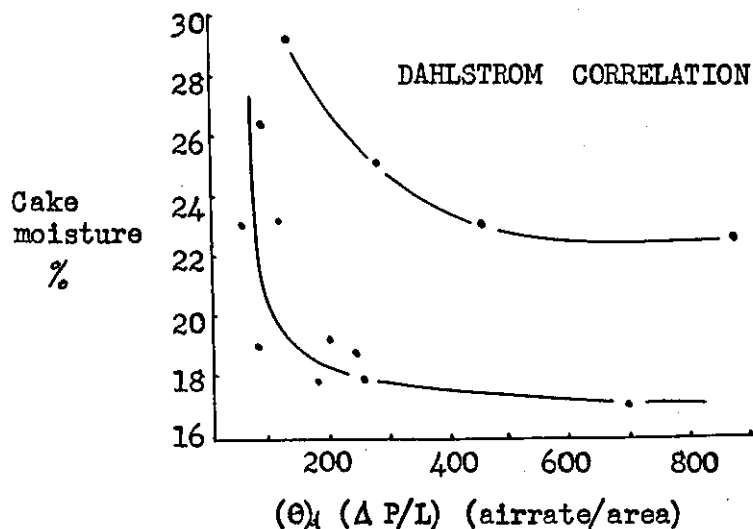


Fig. (1)

on the moisture content axis is for the case when a significant percentage of fines are present and the lower one when it is removed. The sharp corner in the curve indicates clearly that filters should be operated to the right of this point. Too far to the right would however mean expensive over design for little benefit in terms of reduced moisture content.

Silverblatt and Dahlstrom (1954) investigated the effects of surface tension and viscosity on the correlation. Laboratory scale experiments showed that viscosity had a large effect on the rate of approach to equilibrium and that surface tension did have a statistically significant, but nevertheless minor, effect on the equilibrium. The correlation was modified to include viscosity

$$\left[ \frac{\Delta P}{L} \right] \left[ \frac{\theta_d}{\eta} \right] \left[ \frac{\text{air rate}}{\text{area}} \right]$$

Nelson and Dahlstrom (1957) extended this using theoretical relationships for the permeability of filter cakes and developed the 'approach factor'

$$F_a = \left[ \frac{K}{\eta L} \right] \left[ \frac{\Delta P}{L} \right] \left[ \theta d \right]$$

This was found to be accurate but less convenient than the correlating factor for design purposes (Simons and Dahlstrom 1966).

Later papers, Emmett and Dahlstrom (1961), Henderson Cornell, Dunyon and Dahlstrom (1957) have used the correlating factor for a variety of materials and processes. The method has also been applied to the study of steam aided dewatering. Shoenberger and Burch (1964), Silverblatt and Dahlstrom (1964), Simons and Dahlstrom (1965), Simons and Dahlstrom (1966), Grice, Major-Marothy, Simons and Dahlstrom (1966). In this steam is applied to the face of the filter cake during dewatering and gives significant reductions in moisture contents. The improvement is taken to be caused by the reduction in viscosity at the steam/filtrate interface and the correlation is successful in dealing with it.

Lyons (1950) has reviewed dewatering practice in coal preparation and indicated a relationship between moisture content, particle size and ash content. He has also compared results obtained in dewatering coal by various types of centrifuge (May 1951) and correlated published results in industrial operations for dewatering coal by a log. log. plot of moisture content versus ash content (Oct. 1951). This correlation gives a series of straight parallel lines for different processes. He concluded that "apparently all the makes of filter currently available are equally effective from a moisture reduction standpoint". No theoretical development was included.



The empirical approach studies the dewatering characteristics of particular systems as a function of changes of the variables. The method therefore lacks generality in that the fundamental mechanism of the process is obscured. And whilst the Dahlstrom correlation, in particular, has been shown to be of value for the optimisation of many processes, it is not possible to attack the optimisation of the design of dewatering machines unless the actual mechanism of dewatering is properly understood. For this reason no matter how successful a correlating procedure is devised it is necessary to pursue theoretical enquiry which observes the phenomena occurring in dewatering and seeks to explain them. Two main lines of theory may be discerned. That based mainly on the flow of fluids in porous media and that based mainly on the capillary effects of moisture in porous media.

### 1.3 THEORY BASED ON FLOW IN POROUS MEDIA

The first significant work in this field is that of Brownell and Katz (1947). They developed a semi-empirical correlation for saturated flow in porous media which they extended for two phase flow and applied to dewatering.

The correlation is based on a Reynolds number, Friction factor plot analogous to that used for flow in pipes. The Reynolds number and Friction factor are extended to include parameters to describe the porous media, e.g. Particle size, sphericity and roughness and porosity of the packing.

$$Re = \frac{d v_p}{\eta e^m} \quad f = \frac{2 g d \Delta P e^n}{L v_p^2}$$

Data from a variety of sources was plotted on log log axes and a curve similar to that obtained for flow in pipes was obtained.

To extend this to two phase flow, one fluid is taken as wetting the solid and flowing in contact with it. The non-wetting fluid is

considered to be flowing in a porous medium modified by the presence of wetting fluid. Thus a Reynolds number and Friction factor can be defined for each phase in the same way as was done for saturated flow but with the parameters changed by the relative properties of each fluid.

Investigations showed that an important feature of two phase flow is the existence of a residual saturation of wetting fluid. This is considered to be the pore-space eliminated from flow by capillary forces. Saturations used in the correlation are therefore effective saturations that is actual saturation minus residual saturation. It is therefore necessary to know the residual saturation and for this it was shown that log log plots of residual saturation against a dimensionless group called capillary number gave a straight line

$$\text{Cap. No.} = \frac{K \Delta p}{L g T \cos \theta}$$

This is defined as the ratio of the forces driving the fluid out of the bed to the forces retaining the fluid in the bed.

The equation of the straight line obtained is,

$$S_r = \frac{1}{8.63} \left[ \frac{K \Delta P}{L g T \cos \theta} \right]^{-.264}$$

With this effective saturations can be determined and a Reynolds number and Friction factor can be defined for each phase

$$\text{Wetting phase} \quad \text{Re} = \frac{d v_p}{\eta e^m S_e^y} \quad f = \frac{2 \tau d \Delta P e^n S_e^{2y}}{L v^2 p}$$

$$\text{Non-wetting phase} \quad \text{Re} = \frac{d v_p}{\eta (e)^m} \quad f = \frac{2 \tau d \Delta P (e)^n}{L v^2 p}$$

where  $e$  is a wetted porosity defined as the ratio of the volume of the voids occupied by non-wetting fluid and residual saturation of wetting fluid divided by the volume of the bed.

The exponents of porosity and saturation which can be seen in the definitions are taken to be determined by particle size and shape. Roughness figures were taken for particles above 1/16" dia. to be caused by waves at the wetting fluid interface and below 1/16" to be the same as for saturated flow.

The method was used by Brownell and Katz (1947) and Brownell and Gudz (1949) to make calculations for the various parts of the cycle of a rotary vacuum filter. This included the deposition of the cake, washing and dewatering the cake, and also a calculation of the capacity required for the vacuum pump. Brownell and Crosier (1949) applied the method to a rotary filter dryer and calculated the flow of hot air through the filter cake. In these applications dewatering is taken to be equivalent to non-steady state two phase flow and the method used is a step-by-step application of the correlation. The method is therefore tedious to use. Furthermore, some of the terms required are difficult to evaluate accurately. The method has also been criticised for the way in which the various exponents have been used. (See Lapple in the discussion of part 1 of the series of papers). These can be taken as basically empirical correlation factors and have been applied without proper consideration of the actual characteristics of flow in porous media. For instance the exponent used for porosity can be shown to be only applicable around 40%. A more fundamental criticism is for the use of Reynolds number for flow in porous media. The use of such a correlation is only valid if the systems compared are dynamically similar. This cannot be assumed for porous media especially for the wide differences used in the correlation.

Furthermore, the onset of non-linearity in flow in porous media is not due to turbulence as in pipes but to the emergence of inertial effects in laminar flow caused by irregularities in the flow channels.

Another approach which essentially depends on concepts of saturated flow in porous media is that of Nenniger (1956) and Nenniger and Storow (1958) who have developed differential equations to predict the drainage rate of packed beds by gravity or by centrifugal force. They assumed that flow in the packed bed when the interface had penetrated the bed was the same as for saturated flow but with a constant retarding force due to the capillary pull in the pores of the bed. This was taken as numerically equal to the height of capillary rise in the bed. Thus the interface is taken as moving down the bed under this retarding force and leaving a residual moisture in the pores behind it. Residual saturation was taken from the Brownell and Katz correlation. Capillary rise was measured both conventionally and by a method based on the change in flow rate observed when the interface enters the draining bed. All the parameters required by the equations could therefore be obtained from a gravity drainage experiment.

The equation which was derived predicted a more rapid approach to equilibrium than was found in experiments and two possible explanations were put forward for this. Firstly that variation in capillary suction throughout the bed could occur. Secondly that as the interface falls through the bed film drainage of the liquid from the particles takes place. This latter explanation was adopted and a simple equation was derived and experiments carried out to test it on draining films in burettes and on strings of beads in contact. The equations were amalgamated and a series solution obtained. This gave results which agreed closely with experiments both for gravity drainage columns and centrifuge cakes.

#### 1.4 CAPILLARY THEORY OF DEWATERING

A more fundamental approach to the problem of dewatering is

based on a study of the effects associated with the retention of moisture in porous media by capillary or surface tension forces. This was promoted by investigations into dewatering by gravity drainage which is a quite widely used method of dewatering in coal preparation practice. This is similar to filter dewatering except that the displacing force is not air pressure but the hydrostatic head of the contained water. In this process capillary forces play an obvious and important role and the study of these has been extended to dewatering in general.

Gravity drainage as a method of dewatering coal was studied by Gillmore and Wright (1952). They packed columns with fine coal slurry and allowed them to drain for up to 24 hours. These columns were then sampled and the saturation at various heights determined. This showed a transition zone between residual moisture and complete saturation usually called the capillary height and analogous to rise in capillary tubes. This zone was shown to move down the column with time but became substantially stationary after about 24 hours. The equilibrium position of this capillary height was shown to be dependant on particle size distribution of the coal and surface tension of the water.

Burton and Thomas (1953) and Phillips and Thomas (1955) extended the technique by using an electrical moisture meter to determine the saturation at various points in the column without disturbing it. They fully recognised the importance of capillary effects and considered the problem in two parts. The quantity of water remaining as residual moisture, and the rate of approach to this state. "The equilibrium residual moisture represents a balance between surface tension and displacement forces such as gravity, hydrostatic head or air pressure". They showed that capillary rise is related

to some sort of mean pore size and this mean pore size also controls the permeability of the bed and hence the rate of approach to equilibrium residual moisture. They also recognised that residual moisture in the form of discrete amounts at the points of contact of the particles could not be caused to flow because they do not form a continuous phase. The effect of reduction of surface tension by surfactants and of viscosity by heating was investigated and shown to be in accord with their explanation but to be uneconomic for industrial use. The importance of particle size distribution in dewatering was emphasized and it was shown that coal slurries with a large proportion of -300 mesh were very difficult to dewater both because of the capillary height involved and the small pore size available for flow.

Batel (1954-61) has made an extensive study of the properties of granular materials containing moisture. This includes the effect of moisture on mechanical properties and granulation (1956), on sieving capacity (1955), as well as an investigation into dewatering as applied to gravitational drainage and centrifugal and filter dewatering (1954) (1961). He emphasises the importance of capillary effects in dewatering and has noted that dewatering can only occur when the displacing forces are greater than the capillary height, for which he presents an expression in terms of cake parameters. In considering the rate of approach of saturation to equilibrium residual moisture the process is taken as being composed of three parts. Part one in which the most rapid removal of

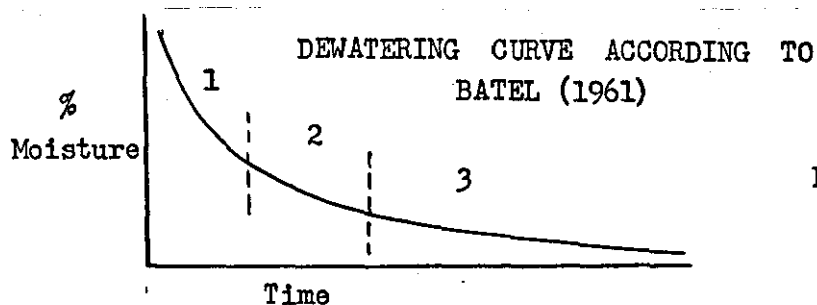


Fig. (2)

moisture occurs when the fluid is being driven out of the capillary spaces. Part two in which the rate of removal is slower since there are less capillary spaces to be emptied but with the rate augmented by some flow of the liquid from the film of moisture left on the pore walls. Part three in which the rate of removal of moisture is slowest of all and the equilibrium residual saturation is approached only by the flow of the remaining moisture from the pore walls. This description is essentially the same as that of Nenniger and Storrow, previously mentioned, but has only been developed qualitatively and shown to be capable of giving saturation time curves of the requisite shape.

Column drainage experiments have demonstrated the importance of capillary forces acting in the pores of materials during dewatering. They are however an unwieldy way of measuring these effects and a more simple and accurate method is available, called the capillary pressure technique, which has been used for a number of years in soils testing and other work. Harris and Smith (1957), Gray (1958), Harris (1959) and Morrow (1962) have introduced this into dewatering research.

The method essentially involves measuring the fluid removed from a sample of porous material allowed to come to equilibrium with a given displacing pressure. This is increased after each equilibrium until the sample is completely desaturated. The technique is analogous to gravity drainage experiments but requires less time to perform, less sample and is capable of a greater accuracy. The results can be analysed to give a pore size distribution of the sample used. Harris and Smith, Harris, and Morrow were concerned mainly with adapting the technique and its theoretical aspects to dewatering, which is covered more fully when the method is discussed in the next

section. Gray (1958) used the technique for the study of practical problems in fine coal dewatering such as the effect of particle size distribution, porosity and of chemical additives such as wetting agents and flocculants.

As mentioned, the pore size distribution of a filter cake can be measured using this technique and hence the mean pore size determined. The experimental results for mean pore size of filter cakes formed from various particle size distributions were correlated by Gray against the percentage of -120 mesh and -240 mesh in the distribution. A correlation of increasing porosity with increasing fines was also noted. Since the volume of water held in a bed at saturation is governed by the porosity of the bed and the difficulty of its removal is governed by the pore sizes in the bed, these results allow at least a qualitative assessment of dewatering problems from consideration of the particle size analysis of the filter feed. The possibility of splitting a particle size distribution of a slurry into two or more fractions and dewatering them separately before recombining was investigated but the improvement was shown to be small or non-existent. Flocculants were demonstrated to have a beneficial effect on dewatering, even though the porosity of the filter cake is increased and hence the volume of water retained at saturation also increased. This is because the mean pore size of the flocculated cake is greater and the moisture can be removed more easily. Wetting agents were shown to effect some improvement in the dewaterability of a slurry but the adsorption<sup>p</sup> of the agents on the solid surfaces meant that the amounts required were uneconomic (as was found by Phillips and Thomas). The addition of oil together with wetting agents was found to be a practical way of aiding dewatering because the coal surface is preferentially



wetted by oil and any oil residue after dewatering enhances the calorific value of the coal.

By considering a bundle of tubes as a model of the filter cake with a distribution of tube sizes derived from the experiments Gray was able to calculate the saturation versus time relationship for the dewatering process. These calculated results showed a much faster approach to equilibrium than did experiments. He concluded that the model used was too simple and that connectivity between capillary tubes should be incorporated.

### 1.5 DISCUSSION

The ultimate requirement of a theory of dewatering is the prediction of the saturation versus time relationship. The two types of theory outlined may be divided by the way in which they approach this by considering different aspects of the dewatering process. The capillary theory starts from a consideration of a microscopic description of the phenomena associated with moisture retention in packed beds. The flow theory concentrates directly on the way moisture flows out of a bed and relates this to the saturation versus time curve.

The second may be criticised because of the application of saturated flow relationships to what is essentially a two-phase flow problem. These two types of flow in porous media have important differences which should not be minimised. Saturated flow can be treated by using average pore properties and overall permeabilities, but when two fluids are occupying the same porous medium then these average and overall properties are not valid for either fluid. There is some reason therefore to think that Nenniger and Storrow should have applied the other of the two alternative explanations for the failure of the simple case.

Brownell and Katz attempted to overcome these criticisms by considering each of the two phases in the porous medium as separate fluids flowing in porous media defined by the presence of the other fluid. They also drew a clear distinction between the wetting and non-wetting phases. This approach however relies essentially on a correlation of saturated flow phenomena.

The capillary theory on the other hand avoids these difficulties by considering a microscopic description of the effects of moisture in packed beds. It has been able to show that the retention of moisture is controlled by the pore structure of the packed bed because of the way surface tension forces act in the pores. The flow of two phases in packed beds has also been shown to be strongly dependent on the pore structure of the bed by similar considerations. However Gray has demonstrated that the pore size distribution applied to a bundle of capillary tubes model is insufficient to describe this and a more realistic model of pore space in porous media is required.

Therefore it may be concluded that for an understanding of the dewatering process the nature of pore space in porous materials must be described as it is this which controls the process both in the way moisture is retained in a porous medium and the flow characteristics of its removal. The action of surface tension forces in porous media which produce the capillary pressure curve can give a description of the pore properties of porous media more simply and completely than most other measurements. Furthermore, it describes the pore space in terms which can be readily related to dewatering characteristics. The next sections are therefore devoted to a study of these capillary effects and the interpretation of them in terms of the characteristics of pore space operating in dewatering.

## CHAPTER TWO

### EFFECTS OF MOISTURE IN POROUS MEDIA

#### 2.1 GENERAL

Associated with the retention of liquid in porous media are phenomena caused by the action of surface tension forces in the pores of the material. The effects include, the depression of the freezing point, the vapour pressure lowering, and the capillary pressure exerted by the liquid retained in the pores. These effects may be related to the curvature of the menisci of the liquid in the pores caused by surface tension, which may in turn be related to the geometry of the pore space. Cronney, Coleman and Bridge (1952) have given a comprehensive review of the methods available for measuring these effects and the calculation of pore properties from them. However only the capillary pressure and the vapour pressure lowering will be discussed here as they are more generally encountered.

#### 2.2 CAPILLARY PRESSURE

A pressure difference exists across a curved liquid meniscus such that  $\Delta P \propto C$  where (C) is the curvature of the liquid/air interface. This is often called the pressure deficiency of the interface. The constant of proportionality is the surface tension of the liquid (T). The mean curvature may be expressed by the radii of two curves on which the surface cuts two mutually perpendicular planes containing its normal. If these are taken as  $r_1$  and  $r_2$ , conventionally considered positive if the centre of curvature lies on the same side of the interface as the non-wetting (i.e. air) phase the mean curvature is

$$C = \left[ \frac{1}{r_1} + \frac{1}{r_2} \right]$$

and the pressure drop across it given by the Laplace equation

$$\Delta P = \left[ \frac{1}{r_1} + \frac{1}{r_2} \right] T$$

If the liquid is contained in a circular capillary radius (a) and the interface has a contact angle ( $\theta$ ) against the wall of the capillary then the curvature is given in terms of the radius of the capillary tube  $r_1 = r_2 = a/\cos \theta$

$$\Delta P = hpg = 2T \cos \theta/a$$

This is the equation governing the well known phenomena of rise of liquid in a capillary tube.

In porous materials the curvature of the meniscus at a given saturation of capillary pressure from equilibrium considerations must be everywhere the same. The equation given shows that the curvature may be expressed in terms of the capillary pressure to which it gives rise. The actual shape however is extremely complex and is dependent on the geometry of the pore space as well as the degree of saturation. If circular capillaries are assumed the relationship between curvature of the menisci and pore size can be solved. Therefore for this simple case it is possible to relate the expression for capillary pressure to the radii of the capillaries. This was illustrated by the derivation of the equation for capillary rise of liquid in a tube. To displace the liquid in such a tube the pressure required is just greater than that given by the equation. Considering a bundle of tubes full of water. If the displacing pressure is increased from zero there will be no moisture movement until a pressure is reached which is just greater than that which the largest tube in the bundle can support. Tubes of this size will then be emptied. The pressure may then be increased to displace water from the next largest tube size and so on until all the water is removed. It is possible in this way to build up a tube size distribution since values of displacing pressure are inversely proportional to tube radii and the volume of water removed at a given

pressure is proportional to the volume of tubes of the corresponding size. Therefore a plot of pressure versus the summation of the volume of liquid displaced is equivalent to a cumulative tube size distribution. Fig. (3). This assumes that the porous medium is

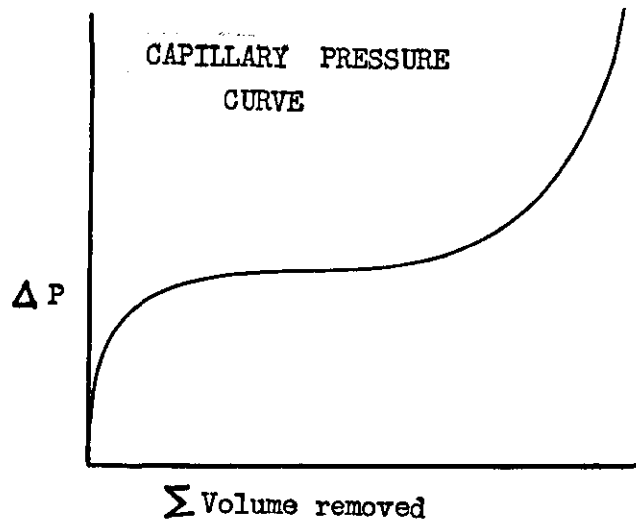


Fig. (3)

rigid and does not deform under the applied pressure stress.

### 2.3 VAPOUR PRESSURE LOWERING

It can be shown thermodynamically that at a curved liquid/gas interface the liquid exerts a lower vapour pressure than at a plane surface. The Kelvin equation gives the relationship

$$C = \frac{1}{T} \frac{Rt}{M_u} \ln \left[ \frac{h}{h_0} \right]$$

which can be related to capillary pressure

$$P_c = TC = \frac{Rt}{M_u} \ln \left[ \frac{h}{h_0} \right]$$

This phenomena may be treated in a similar manner to that adopted for capillary pressure by using a bundle of capillary tubes as a model. Consider a horizontal capillary, completely filled with water and not in contact with any outside source of liquid. Placed in an atmosphere of 100% relative humidity the liquid surfaces at the ends of the capillary will be plane. If the relative humidity is reduced a slight evaporation will create a concave

meniscus according to the equation given. If the surrounding relative humidity is reduced further a state will be reached when the radius of curvature of the meniscus will be equal to the radius of the capillary itself and any further reduction in the relative humidity will cause the meniscus to retreat into the tube and all the water will evaporate at this value. Therefore at a given relative humidity all the capillaries with a radius greater than a given value will be empty, and all those smaller than a given value will be full, if equilibrium is attained. Clearly by measuring the saturation of a given porous medium in equilibrium with atmospheres of a range of relative humidities it is possible to determine the curvature saturation relationship and for capillary tube bundles the pore size distribution.

#### 2.4 RANGE AND APPLICABILITY OF THE EFFECTS

The upper limit of applicability of these relationships is that when the curvature is plane, and the lower limit is when the curvature is of the order of molecular dimensions and interfaces have no real existence. Table I gives the capillary pressures,

TABLE I

pore radius $\mu$	Capillary Pressure cm Hg	Relative Humidity %
	0	100.000
110	1	99.999
22	5	99.995
11	10	99.990
78	14	99.986
5.4	20	99.980
1.1	100	99.901
.11	1,000	99.025
.011	10,000	90.668
.002	50,000	61.270

relative humidities and radii of various circular capillaries calculated for water with zero contact angle and surface tension 72.5 dynes/cm. The two effects, capillary pressure and vapour pressure lowering, can be seen to be of use in different pore size ranges. The relative humidity relation is not suitable for pore sizes greater than  $.01\mu$  and the capillary pressures become very large for pores smaller than  $.1\mu$ . In general here the pore sizes covered in the range of the practical applicability of capillary pressure effects will be considered. The capillary pressure effect is, moreover, better suited to studying dewatering, because the adjustment of equilibrium is by fluid flow in partially saturated porous material caused by a displacing pressure. It is possible therefore to say that capillary pressure saturation measurements are analogous to dewatering. Furthermore the results of capillary pressure experiments can be considered as a pore size distribution defined in terms of dewatering parameters.

The vapour pressure lowering effect on the other hand does not bear this analogy to dewatering as equilibrium is attained by mass transfer across the liquid/gas interface. This also means that the approach to equilibrium is slow and the technique is less convenient to use.

For these reasons therefore the capillary pressure saturation relationship will be used here in studying capillary phenomena applied to dewatering.

## 2.5 MEASUREMENT OF THE CAPILLARY PRESSURE

### SATURATION RELATIONSHIP

#### 2.5.1 Introduction

In the description of the capillary pressure saturation relationship in terms of a bundle of capillary tubes it was

mentioned that the method involves measuring volumes of water held in the porous material for various displacing pressures. Several methods exist for doing this and have been reviewed by Cronney, Coleman and Bridge (1952) and Coleman (1963), together with methods based on the other capillary phenomena.

#### 2.5.2 Gravity Drainage Method

Gravity drainage of a column of porous material is historically the first method used for investigating the capillary pressure saturation relationship. In a continuous water column the height of a point above a free water surface is the hydrostatic stress exerted at that height. Therefore if a saturated column is allowed to drain, or a dry column is allowed to imbibe, then water movement will continue until the menisci in the pores are able to support a column of water of a height corresponding to their size. The height at which a zone of a given saturation is found in the column gives the capillary pressure at that saturation.

This technique has been used since before the turn of the century by many workers, chiefly soil scientists, civil engineers and oil field researchers. For a review of this work see Prill, Johnson and Morris (1965). In the literature on dewatering the technique has been used by Leverett (1941), Dombrowski and Brownell (1954), Gillmore and Wright (1952), Burton and Thomas (1953), Phillips and Thomas (1954) and Harris and Smith (1957).

One of the main difficulties in using this technique for measurement of capillary pressure saturation relationships is in the measuring the saturations at various heights. Various methods have been used. Leverett cut his columns into sections and determined the saturation of each section directly. Gillmore and Wright took small samples of material at the various heights.



These methods however can only be used once on a given column and it is difficult to study the approach to equilibrium. Furthermore, these techniques may introduce errors as the column is disturbed to take samples and moisture may be redistributed. To overcome these criticisms Dombrowski and Brownell used an x-ray photographic technique, and Burton and Thomas and Phillips and Thomas used an electrical resistance method. Other workers (Prill, Johnson and Morris) have used manometers to measure directly the capillary pressures at various elevations.

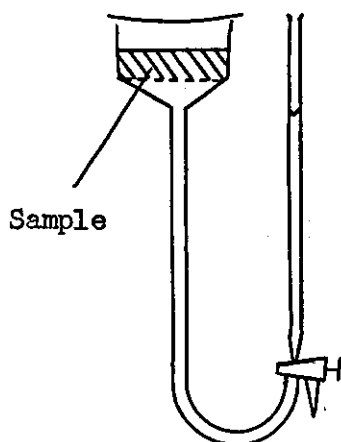
The time required for equilibrium to be reached in gravity drainage is excessive. King (1899) found that even after  $2\frac{1}{2}$  years, drainage was not complete. Other workers find that within acceptable experimental error a lesser time is required but this may still be in terms of days. More seriously the method is not capable of high accuracy because large quantities of sample, and for small pore sizes very long columns, are required. This can lead to difficulties in obtaining uniform packing along the length of the column.

### 2.5.3 Suction and Pressure Plate Methods

These are a more simple and convenient way of measuring capillary pressure saturation relationships. They consist of applying a displacing pressure directly to a sample of a porous material and measuring the volume of water removed or retained. The main feature of the technique is the use of a support plate for the sample which has smaller pores than the sample. Therefore in the range of pressures required to desaturate the porous material the support plate itself will remain saturated and able to conduct fluid. A range of suitable materials are available for this such as sintered glass, sintered metal and fine pored plastic

membranes. Other requirements are for a method of applying and measuring the displacing pressures and a method of measuring the volume of water removed. The technique was first used by Haines (1930)

Fig. (4) shows his apparatus.



HAINES'S  
APPARATUS

Fig. (4)

It consists of a buchner funnel with a fine pore support plate (Haines used a sealed in filter paper) on which the sample rests. The suction applied to the sample is the difference in level between the sample and the water in the burette. Adjustments to this can be made by moving the buchner funnel relative to the burette, or allowing some water to run out of the burette using the double stopcock. The water removed from the sample is measured by the change in level in the burette.

The apparatus has faults, notably that the water displaced from the sample changes the level in the burette and thus equilibrium is approached under varying pressure conditions. This is especially unfortunate due to the existance of a hysteresis in capillary moisture properties between the moisture advancing and the moisture receding conditions which is discussed later. Flexion in the rubber connections can also make the measurements of volume erroneous. Furthermore, the apparatus is limited by the length of burette to

capillary pressures below about 150 cms of water. This can be extended by using mercury as a manometric fluid when the upper limit becomes 1 atmosphere, since it is a suction method.

Richards and his co-workers (1943) have developed a pressure plate apparatus which is essentially the same but uses pressure instead of suction. The limits of this type of apparatus are those imposed by the size of pore in the support plate. Using regenerated uncoated cellulose membranes, pressures of up to 10,000 cms of water can be used. However with pores fine enough to support this pressure the approach to equilibrium is slow.

Many workers have used an apparatus of this general type for investigations where pore properties or capillary effects are important. In soil science it is a standard technique, it has also been used in Civil Engineering by Coleman (1963). Textile and Paper research, Christensen and Barkas (1955), and Preston and Nimkar (1952), Oil Field research Purcell (1949), Rose and Bruce (1949) and by Chemical Engineers Newitt and Conway-Jones (1958) and Pearce and Donald (1959).

In problems involved in dewatering the method has been used, as previously mentioned, by Harris and Smith (1957), Gray (1958), Harris (1959) and Morrow (1962). In the final form of their apparatus Morrow and Harris (1965) used a controlled vacuum source to provide displacing suctions and measured the volumes of displaced water in a horizontal measuring tube with a small bore to keep the meniscus vertical. This is very convenient for following the approach to equilibrium and is also very accurate.

The method can be used on very small samples, Morrow and Harris (1965) obtained reproducible results for samples of down to five particles thick. For these small samples the approach to

Capillary Pressure Apparatus  
Morrow (1962)

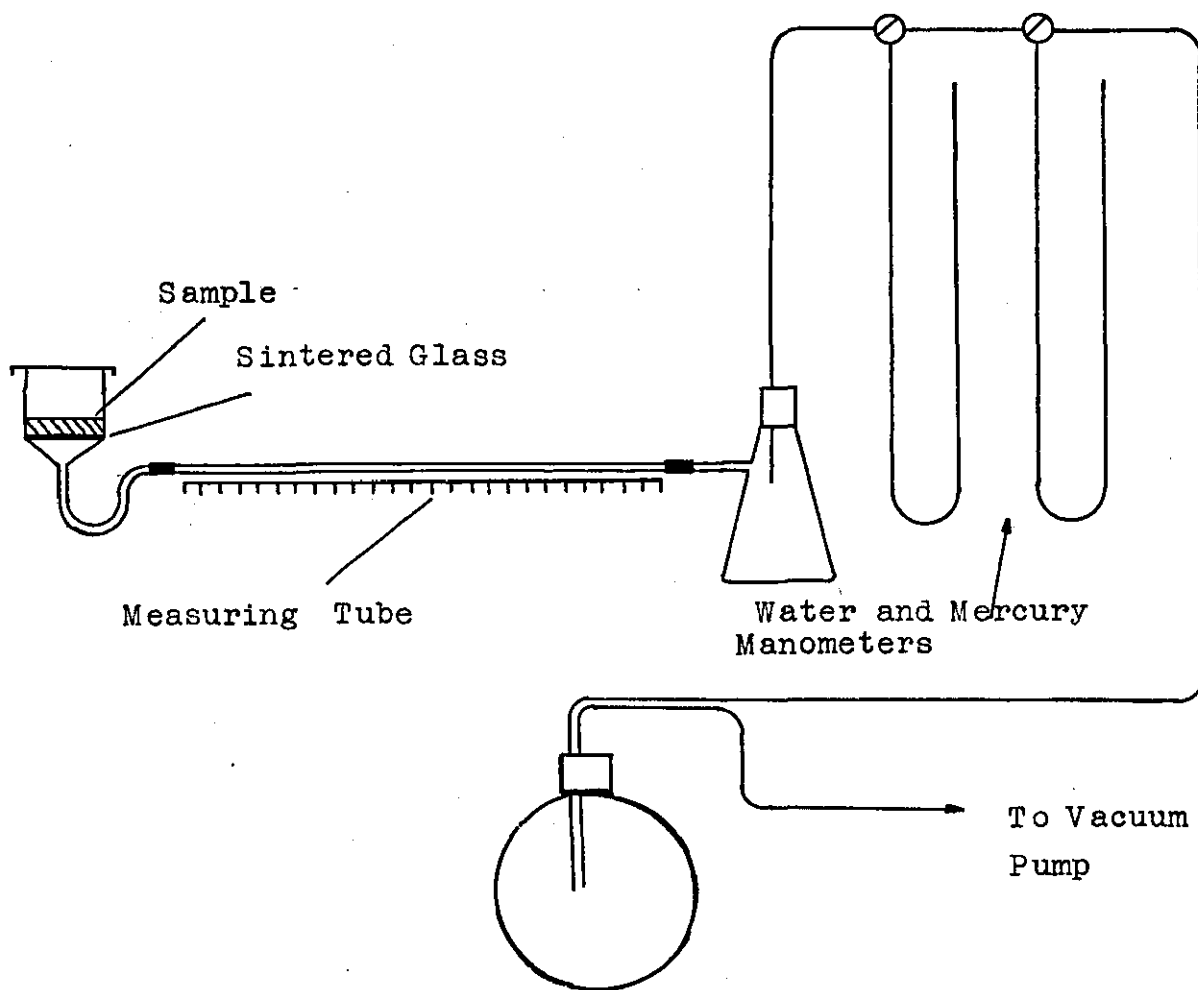


FIG. 5

equilibrium is quite rapid and a whole capillary pressure curve can be traced in a few hours. The essential simplicity and accuracy of the technique has led to a greater insight into the phenomena of capillary pressures and the properties of porous materials in general.

#### 2.5.4 The Mercury Porosimeter

This is a similar method to that of the pressure plate technique. Mercury which is a non-wetting fluid (analogous to the air phase in the preceding section) is forced into the porous material under pressure, the size of a pore determining its entry pressure.

The method has been used by Ritter and Drake (1945) to obtain pore size distributions of several different porous materials such as diatomaceous earth and sintered glass. In more recent years Kruyer (1958), Mayer and Stowe (1965) (1966) and Iczkowski (1967) have also investigated the technique. Several commercial instruments are available and have been reviewed in an article in 'Chemical Processing' volume 14 1968.

The method is not considered further here because the capillary desaturation technique is simpler and better suited for investigating dewatering. Furthermore for a given size of pore a greater pressure is required in this method than in capillary desaturation which increases the danger of disturbance of the sample, especially with unconsolidated media considered here. Uncertainty is also associated with the effect of contact angle which is mentioned later.

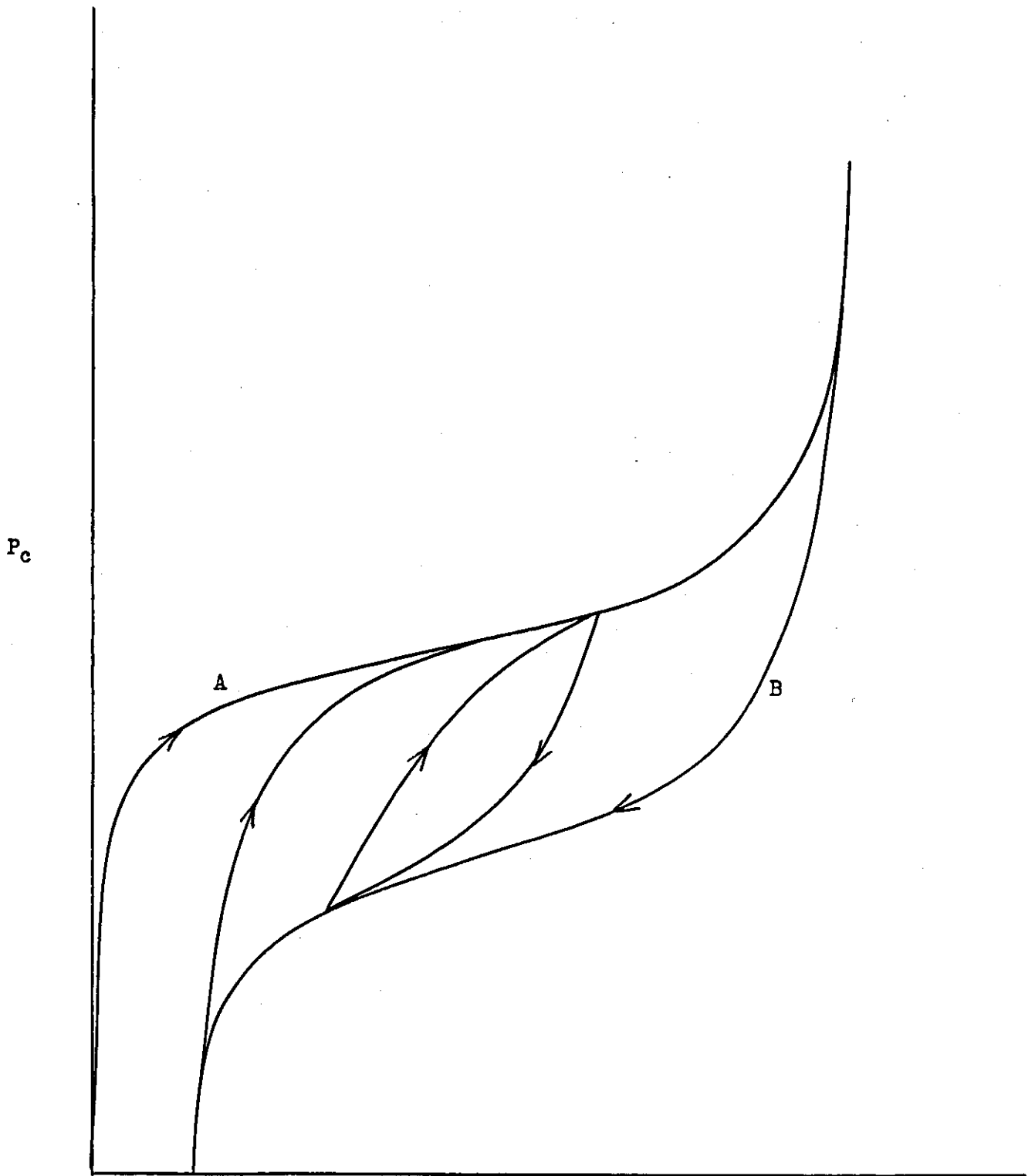
#### 2.6 CHARACTERISTICS OF CAPILLARY PRESSURE CURVES

The capillary pressure curve has been described in terms of a bundle of capillary tubes with a distribution of radii. In

general however the pores in porous media are not circular and it must be remembered that what is actually measured in the technique is the relation between the volume of liquid retained in (or removed from) a porous medium and the curvature of the menisci. This meniscus is of complex shape but of constant curvature at a given saturation when at equilibrium. It is possible to describe any part of it (and therefore the whole) by two radii of curvature  $r_1$  and  $r_2$ . When the curvature is  $\left[ \frac{1}{r_1} + \frac{1}{r_2} \right]$  then by considering  $r_1 = r_2$  this becomes  $\frac{2}{r_e}$  which can be defined as the radius of an equivalent spherical meniscus which will exert the same hydrostatic stress, or pressure deficiency, as the non-spherical meniscus. This gives a reasonable description of pore radius which for most purposes is not very different from the actual geometrical pore radius which may be indeterminate. Caution must be exercised however in using this to relate the volume of water displaced at a given pressure to the number of pores, since it is not a geometrical quantity and cannot be used as such. It is therefore more correct to say only that a given volume of water is held in pores of a given radius and not to use number of pores.

The bundle of tubes model can therefore give a good picture of capillary pressure curves from the point of view of pore size, and distribution and the nature of entry pressure. Capillary pressure curves of real porous media however exhibit further characteristics Fig. (6) which cannot be reproduced by the simple bundle of tubes concept. Most obvious of these discrepancies is the existence of a definite quantity of residual moisture which cannot be removed no matter how high a displacing pressure is applied.

Furthermore capillary pressure curves for real porous media exhibit a hysteresis: On desaturating a given porous material the



$\Sigma$  Volume removed

Fig. (6)

curve A in Fig. (6) is followed. Then if the returning or imbibition curve is traced by relaxing the displacing pressure in small amounts and measuring the amount of water imbibed for the new equilibrium, curve B is traced. This imbibition curve does not return to 100% saturation. . . On further desaturations of the sample the new desaturation curve rises to coincide with the first desaturation curve and then follows it. Further cycles of desaturation or imbibition can be made to follow this hysteresis loop. If the desaturation and imbibition are interrupted at intermediate saturations then minor hysteresis loops can be described as shown.

Thus a capillary pressure for real porous material is not a unique function of saturation and the previous saturation history of the sample must be known to define the capillary pressure for a given saturation or vice versa.

This behaviour cannot be reproduced by a simple capillary tube model. Explanations have been offered (Scheidegger (1956)) in ~~in~~ terms of the hysteresis in contact angle between moisture advancing and moisture receding but the magnitude of the effect is too great for this to successfully account for it.

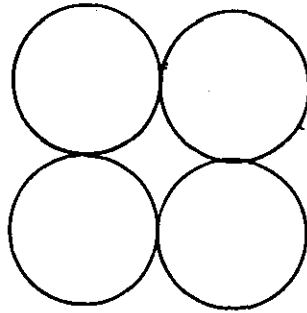
Furthermore it is necessary also to explain the trapping of air on imbibition. A better approximation to the pore space in unconsolidated media is provided by sphere packs and with some properties of such a model an explanation may be advanced.

## 2.7 EQUAL SIZE SPHERES IN OPEN AND CLOSE PACKING

Spheres may be packed in a variety of regular arrays but the most simple and useful of these are those arrays known as open and close packing. The geometrical properties of these were investigated by Slichter (1898).



He showed that in open packing Fig. (7) each sphere touches

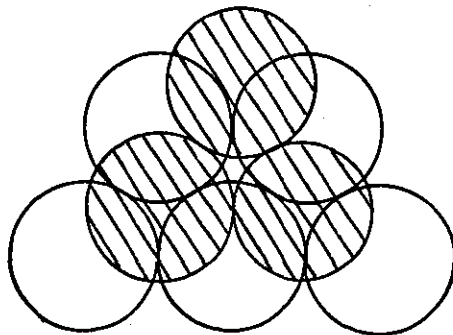


Open  
Packing

Fig. (7)

six others and the lines joining the centres of eight spheres forms a cube of side length  $2r$  which is the smallest representative element of the packing and called a unit cell. The porosity is 47.64%. The pore space may be taken to be composed of a central void which can hold a sphere of size  $.732r$  and is connected to other similar voids in the packing by six outlets, one in each face of the unit cell. The largest sphere which will fit through these is of size  $.414r$ .

In a close packed system Fig. (8) each sphere has twelve



Close  
Packing

Fig. (8)

points of contact and the unit cell is a rhombohedron or cuboid formed by passing planes through the centres of eight contiguous spheres. The length of side is  $2r$  and the face angles are  $60^\circ$

and  $120^\circ$ . This gives rise to adjoining cells of two kinds; a smaller having tetragonal form which can contain a sphere of size  $.225r$  and a larger having a cuboidal or rhomboidal form and which can contain a sphere of size  $.29r$ . The continuity of pore space can be imagined as joining the apices of the two kinds of cell. Each of the four apices of a tetrahedral cell being joined to an apex of four different rhomboidal cells, whilst eight apices of each rhomboidal cell are joined to eight tetrahedral cells. Thus there are twice as many tetrahedral cells as rhomboidal and communication is always between cells of different kinds. The waists between each cell are all the same size and can contain a sphere of size  $.155r$ . The porosity of close packing is 25.95% and is divided between large and small cells in the ratio 6 : 13.

## 2.8 MOISTURE DISTRIBUTION IN SPHERE PACKS

Versluys (1917) identified 3 states of moisture distribution in sphere packs. Capillary or saturation state in which the whole of the pore space is filled with water. The moisture content in this case is equivalent to the porosity of the packing. Pendular state in which water is held at the points of contact of the spheres as pendular rings. In this the air phase is continuous and can flow but the water phase is discontinuous and cannot. Therefore moisture can only be removed by evaporation. This state therefore corresponds to the residual moisture found in porous media at the end of a capillary pressure experiment. Using the geometrical properties of sphere packs it is possible to show, Keen (1924), that in close packing the maximum size of pendular rings which do not touch each other subtend a half angle of  $30^\circ$  at the centres of the spheres. In open packing this angle has a maximum of  $45^\circ$ .

Fig. (9)

## Pendular rings in Open and Close Packing

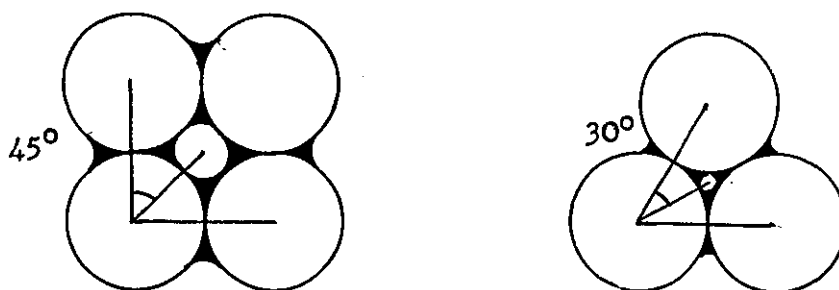


Fig. (9)

Using a simplification that pendular ring menisci are circular the volume of a pendular ring between two equal size spheres radius ( $r$ ) which subtends a half angle ( $\theta$ ) has been shown by Wilsdon (1924) to be:

$$V = \frac{8\pi r^2 \sin^4\theta}{\cos^2 2\theta} \left[ 1 - \tan 2\theta \left[ \frac{\pi}{2} - 2\theta \right] \right]$$

Therefore it is possible to calculate that the maximum amount of moisture held as pendular rings in open packing is 18.2% of the void space and 24.3% of the void space in close packing. Fisher (1926) has shown that the true shape of a pendular ring meniscus is a nodoid, however this makes little difference to the calculations of volume. The residual moisture found in practice in sphere packs is of the order of 5 - 10% of the void space, this discrepancy will be explained in the next section.

Intermediate between these two states is the Funicular state which can be imagined as when the pendular rings are large enough to meet at their points of nearest approach and to coalesce. They then form a network or mesh with air still occupying the wider spaces of the pores. Both the air and the water phases are continuous and can flow. This is the moisture state most concerned in capillary pressure curves.

## 2.9 HAINES THEORY OF CAPILLARY PRESSURE CURVES

### 2.9.1 Introduction

The effects as moisture distribution in sphere packs varies between capillary state and pendular state were the subject of a series of papers by Haines (1925-30). He was concerned with the cohesion found in packings due to capillary effects. In a controversy with Fisher (1926) (1928) he advanced a theory of capillary pressure in granular porous media which is still the most complete available.

The explanation is based on the two cases of regular sphere packs previously considered, namely open and close packing and the essentially cellular nature of the pore space. The various stages as water is removed from a packing can be followed for this example of the desaturation of a close packing.

### 2.9.2 Desaturation of Close Packing

At first when the packing is saturated a water interface will surround it which has negligible curvature. As water is removed the film is drawn into the surface pores, which have waist like constrictions and open into wider cells beyond (as previously described). As the menisci in the surface pores advance the curvature will increase and the pressure deficiency of the interface will rise until the narrowest part of the waist is reached. This has been shown to have a size of  $.155r$  and at this point under a pressure deficiency of

$$P = T/r \left[ \frac{1}{.155} + \frac{1}{.155} \right] = 12.9 T/r$$

at some pore minutely wider than the others, the meniscus passes the unstable point and abruptly expands into the cell beyond. The displaced water redistributes itself and the shape of the film

in the evacuated cell is made up of menisci at each corner (except the one of entry) ready to penetrate further into the packing by similar leaps. These menisci are joined round the cheeks of enclosing particles by films which are portions of not yet fully formed pendular rings. Further decrements of moisture are made at the same pressure deficiency since the waists are all the same size.

The process of evacuation extends cell by cell through the packing until only pendular rings are left as immobile residual moisture. The pendular rings in this case have a pressure deficiency of  $12.9T/r$ , the pressure existing at their formation and are therefore not at their maximum size of subtending a half angle of  $30^\circ$ . At this maximum size a pendular ring has two radii of curvature  $r_1 = .155r$  and  $r_2 = -.422r$ ,  $r_2$  is convex and therefore negative according to the convention. The pressure deficiency in this case is given by

$$P = T/r \left[ \frac{1}{.155} - \frac{1}{.422} \right] = 4.1 T/r$$

### 2.9.3 Imbibition in Close Packing

If a reversal of moisture movement is considered i.e. the case of imbibition. The capillary suction is decreased and the water film in each cell sags towards the centre until in one cell, minutely smaller than the rest the bubble detaches from the wall of a cell and collapses by evacuating air through the open pore. The point of instability in the rhomboidal cell (radius  $.29r$ ) is

$$P = T/r \left[ \frac{1}{.29} + \frac{1}{.29} \right] = 6.9T/r$$

Therefore the entry to the pore remains open up to this point because the pressure deficiency would have to fall to  $4.1 T/r$

before the pendular rings coalesce at the waist. The smaller tetragonal cell would fill at a higher pressure deficiency

$$P = T/r \left[ \frac{1}{.225} + \frac{1}{.225} \right] = 8.9 T/r$$

but these are always separated by the larger rhomboidal cells and hence the water movement will not be general until the larger cells are able to fill.

#### 2.9.4 Desaturation and Imbibition in Open Packing

The case for open packing is similar but simpler since there is only one size of cell as well as one waist size.

The entry value for decreasing moisture is controlled by the waist size and is

$$P = T/r \left[ \frac{1}{.414} + \frac{1}{.414} \right] = 4.8 T/r$$

all the moisture in the packing is removed at this value leaving pendular rings. For returning moisture the bubble in the cell will collapse at

$$P = T/r \left[ \frac{1}{.73} + \frac{1}{.73} \right] = 2.7 T/r$$

Since a pendular ring at its maximum size in open packing has two radii of curvature  $r_1 = .414r$  and  $r_2 = -.586r$  then this has a pressure deficiency of

$$P = T/r \left[ \frac{1}{.414} - \frac{1}{.586} \right] = .7 T/r$$

and therefore the waists will remain open to allow the collapse of the menisci in the cells.

#### 2.10 EXPERIMENTAL VERIFICATION OF HAINES THEORY

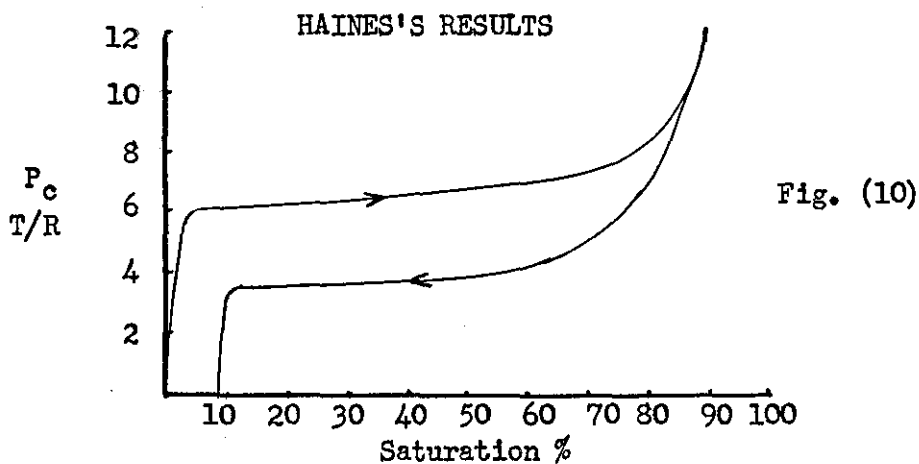
Haines was able to substantiate these theoretical results in two experiments carried out on real sphere packs. Firstly

he used 3/32" ball bearings arranged by hand in regular packings and observed the meniscus movements as paraffin oil saturating the pore space was removed. The results show good agreement with the theory and are listed in Table II.

TABLE II

	entry value	pendular rings coalesce	collapse of rhomboidal cell
Theory	12.9 T/r	4.1 T/r	6.9 T/r
Experimental	11.3 - 11.5 T/r	4.3 T/r	6.7 T/r

Further experiments were carried out using 190 $\mu$  glass spheres in random packing of between 36 and 37% porosity using the apparatus shown in Fig. (4) and described in section 2.5.3. The results of this experiment are shown in Fig. (10).



The irregular packing gives rise to a variable pore size, which is in general wider than the ideal case and thus gives lower values of pressure deficiency. The theoretical value for entry will therefore be expected at the end of the funicular stage just before the breakup into pendular rings. Conversely for returning moisture the closure will commence at the

theoretical value. From Fig. (10) it can be seen that for the desaturation curve general entry takes place at about 6.1 T/r at which pressure most of the moisture is removed indicating a uniform pore size. The final breakup into pendular rings occurs at about 11.0 T/r which compares well with the experimental and theoretical results shown in Table II. The closure of the cells in imbibition commences at around 6.5 T/r which also compares well with the theory and the previous experiment. General closure occurs at around 4.1 T/r. The trapping of air on imbibition, shown in Fig. (10) by the curve not returning to 100% saturation, was taken as being caused by the irregularities in the packing. Thus some cells, larger than the average may become isolated as the water front advances.

Further corroboration of Haines' theory has been provided by Hackett and Strettan (1928). They tested the assumption that the entry pressure required to overcome a meniscus in the pores of sphere packs could be taken as the largest possible inscribed circle in the pore. Ball bearings were arranged in groups in contact and the suction required to pull the water/air interface through the pore was measured. The result of 11.3 - 11.4 T/r is close to Haines' experimental result. This was considered also as good agreement with the theory bearing in mind the complexity of the phenomena and the simplicity of the assumption. The entry pressure for random packing of equal spheres of porosity of 36 - 40% was found to be 4.75 T/r which is lower than Haines' value for random packing of 36 - 37% porosity, which was 6.1 T/r.



## CHAPTER THREE

### CHARACTERISTICS OF CAPILLARY PRESSURE CURVES

#### 3.1 HYSTERESIS

The Haines theory demonstrates that hysteresis in the capillary pressure-saturation relationship is due to genuine alternative configurations of the menisci in the pore space. A general theory of hysteresis called the domain theory has been developed by Everett and his co-workers (1952-5) which considers the case of any system in which a physical property depends on an independent variable in a non-reversible manner. It is assumed that such a system comprises of a large number of small regions or domains which are each capable of taking up more than one meta-stable state for a single value of the external variable controlling the system. It is further assumed that transitions between these states occur at definite values of the external variable, these values differing according to whether this variable is increasing or decreasing. Enderby (1955, 1956) has extended this by allowing that changes from State I to State II may either aid or hinder the transition of neighbouring domains from I to II. Thus for a given domain the occurrence of a transition depends not only upon the behaviour of the external variable, but also upon the states of its neighbours.

The domain theory has been applied to capillary hysteresis by Poulovassilis (1962). The total volume of water taking part in a hysteresis loop can be divided into volume elements specified by the capillary pressures at which they empty or fill by experimentally determining the volumes involved as capillary pressure is relaxed or imposed. Assuming these elements retain their identity during changes in suction it is possible to predict the

state of the system after any sequence of capillary pressure changes. Excellent agreement was found between predicted and experimental curves. Philip (1964) has extended this on a less rigorous basis by assuming that the distribution in geometrical relationships between desaturation and imbibition curves is independent of pore size. This has the advantage of allowing a full description of hysteresis behaviour from only one curve, either desaturation or imbibition.

In dewatering only the desaturation curve is involved and the hysteresis behaviour is of interest only because it is related to the pore structure of the porous medium. Fig. (11) shows three different pore shapes and also their behaviour in emptying or filling.

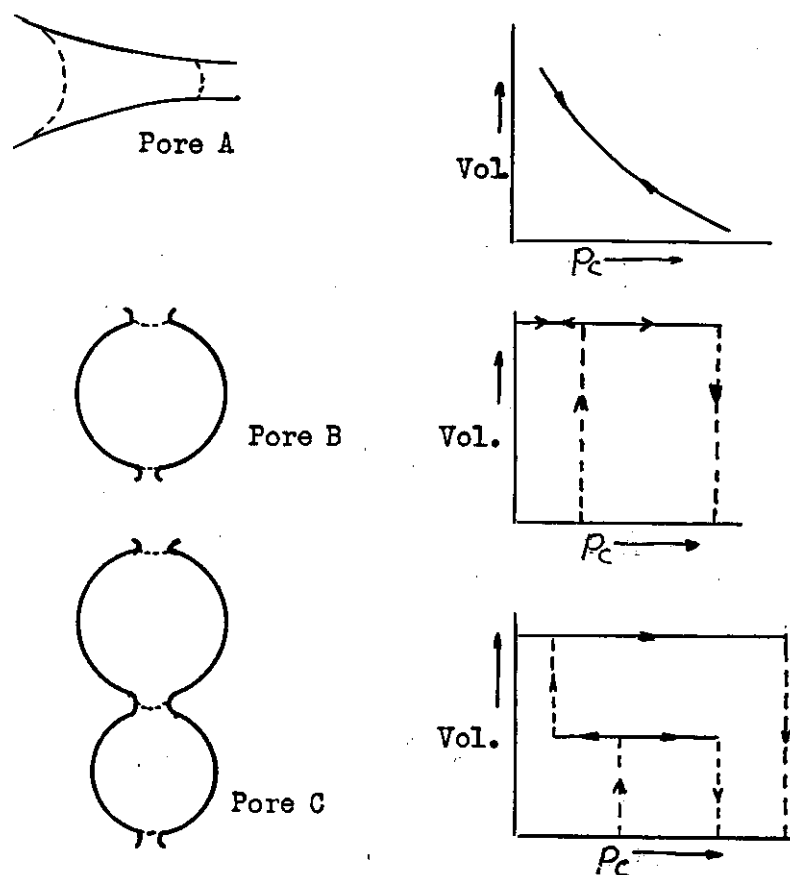


Fig. (11)

Pore (a) does not exhibit hysteresis and the relationship between displacement pressure and volume is reversible. Pore (b) represents an independent pore domain which empties at one pressure and fills at another. This is a contrast to pore (c) which empties at one pressure and fills in two stages of different pressures. This sort of non-independence was not detected by Poulovassilis and the whole pore space behaved as an assembly of pores of type (b). The domain theory may be considered as equivalent to that of Haines, but on a more general basis.

### 3.2 RESIDUAL MOISTURE

The residual moisture held in a porous medium at the end of a capillary pressure experiment has been shown to consist of pendular rings at the points of contact of the particles. The maximum amount of water held in this form in close packing has been shown to be 24.3% of the void volume and in open packing to be 18.2% of the void volume. These values were reconciled with the 5 to 10% moisture usually found at the end of a capillary pressure experiment by the Haines theory which shows that pendular rings have a size dependant on the pressure deficiency existing at their formation. The ideal case for close packing in which pendular rings are formed at  $12.9 T/r$  predicts a moisture content comparable with residual moistures obtained in practice.

As a consequence of this it is to be expected that different pendular rings in different parts of a desaturated packing will exist at different pressure deficiencies and have different volumes since they were formed at different capillary pressures. This has been confirmed by Harris and Morrow (1964) who made direct measurements of pressures in pendular rings with a micro-manometer.

Clearly in cases such as this when liquid in the bed is held at various pressure deficiencies true equilibrium conditions do not obtain. Since pendular rings are not in hydraulic contact with one another equilibrium can only be attained in such systems by evaporation and condensation. This will occur because of vapour pressure lowering at a curved surface. Pendular rings with a high curvature will grow by condensation and those with a small curvature will evaporate until they are all at the same curvature and pressure deficiency. This process is slow and the effects in terms of volume of water involved is small and may be ignored for all practical purposes.

Most theoretical calculations of the volumes of pendular rings rely on an approximation of a circular meniscus Wilsdon (1924), Keen (1924), Von Englehardt (1955) Rose (1958) and Mayer and Stowe (1966). Fisher (1926) however demonstrated that the true shape is that of a nodoid and that the gain in accuracy by using this to calculate the volumes of pendular rings was small but could be significant for large curvatures. Kruyer (1958) and Iczkowski (1966) took the shape to be that of a hyperboloid of revolution which gives a better approximation than that of a circle. Melrose (1966) (1967) has given mathematical functions for an accurate solution which are stated to be in a more convenient form than those given by Fisher in his accurate solution. All of these concern the pendular ring formed between two equal and touching spheres. Rose (1958) considered the general case of two non-touching unequal spheres. He showed that the separation and the non equality of sphere sizes do not have a very large effect on the volumes of residual moisture.

Residual moisture has been shown experimentally not to vary very much with either surface tension or contact angle (Morrow 1962). Nenniger and Storrow (1958) however, did find that the volume of a pendular ring formed in a bed as a water interface passed through the bed could vary slightly with the velocity of the interface. This effect is, however, insignificant and for most practical purposes a sufficiently accurate estimate of the volume of a pendular ring in a packing can be made by knowing the pressure deficiency when it was formed and assuming the meniscus to be circular.

### 3.3 SURFACE AREA

An interesting and useful feature of capillary pressure curves, mentioned by Haines, is that they can be used to give the surface area of the sample used. The work done in removing moisture from the sample is  $\int p \, dV$  which is the area between the capillary pressure curve and the volume displaced axis. This is equivalent to the work done in creating the new surface of the liquid, which at residual saturations tends to the surface area of the bed. The area of the hysteresis loop can be taken as energy wasted irreversibly. Haines showed that his results from Fig. (10) were in reasonable agreement with calculated surface areas of the glass beads used.

This relation was also derived independently by Leverett (1941) who studied column drainage. He considered the curvature saturation relation to be too complex for analytical treatment and used measured curves as functions which characterised the pore space in the packed bed. He derived on thermodynamic grounds the relationship

$$A_2 - A_1 = \int_{S_1}^{S_2} P \, dS$$

which in the limits of 100% and 0% saturation gives the surface area of the bed. Leverett also showed that there are uncertainties associated with using this. These are that the relative proportions of solid/liquid and liquid/gas interfaces are indeterminate and that residual moisture leads to predicted surface areas less than the true values. Furthermore the existence of hysteresis must also be considered.

Payne (1953) (1954) and Rinquvist (1955) investigated the method as an alternative to measurements of surface area by permeability. They obtained good results for a range of materials and particle size distributions with an error of not more than 10%.

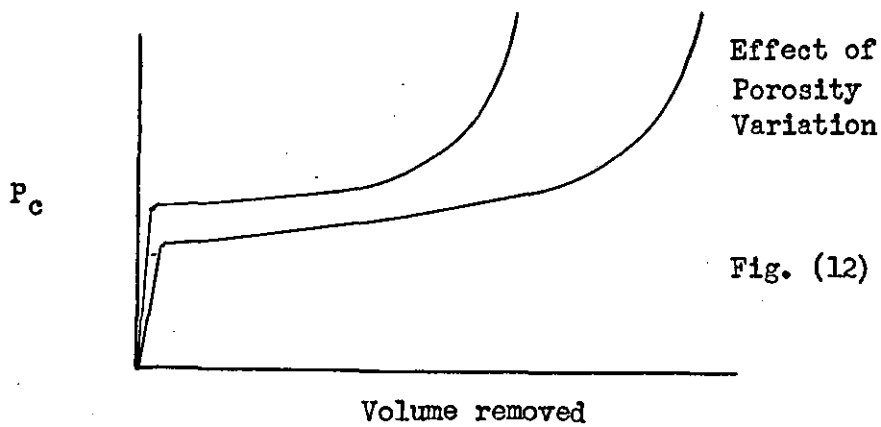
The main advantage is that a shape or tortuosity factor is not required as in permeability measurements and the method is independent of particle shape or size distribution. There is also an additional advantage in that it is possible to measure the area contribution of different size components of a packed bed by stopping the summation of the area at appropriate limits.

#### 3.4 CORRELATIONS FOR POROSITY VARIATION

An important feature of packed beds is that porosity is a variable which depends on the way a given bed is formed. For instance, particles packed into a container by pouring can have their porosity reduced by tapping or vibration. Scott (1960) had identified these two states as loose random packing and dense random packing. Macrae, Finlayson and Gray (1957) and Macrae and Gray (1961) have shown that in packing formed by pouring, an increasing impact velocity decreases porosity up to a limit. Packing formed by pouring particles in a liquid is generally looser

than that formed by the same particles in air although Rutgers (1962) has found that the porosity of the dense random packed state is reproducible in both air and water. Different materials of the same shape pack to different porosities dependent on their resilience (Macrae and Gray (1961)) and their surface roughness (Leva (1947)).

Theoretically porosity should be independent of particle size as it is the ratio of void volume and bed volume of a packing. It has however been demonstrated by Andreasen (1940) and Frazer (1935) that fine particles pack to a higher porosity than coarse ones. This is generally attributed (Gregg and Hill (1953)) to the larger surface areas of fine particles and the effect of surface forces or adsorbed layers. It is possible also that this could be due to the lower permeability of packings of small particles which inhibit air or liquid displacement necessary for compaction. McGeary (1961) attempted some packing experiments in a partial vacuum but the results were inconclusive due to air leaks causing transport of the particles. From the point of view of the capillary pressure curve porosity variation will affect both the volume of the pore space and the size of the pores. Considering a given pack of particles which may be packed in different porosities. At the end of a capillary pressure experiment the packing with the higher porosity will have released more water than the packing with the smaller porosity because it contains more. The values of capillary pressure will also be different because the packing with the lower porosity will contain smaller pores and hence give rise to higher capillary pressures. These effects may be seen in Fig. (12). The saturation axis may be normalised by expressing the volume of



water removed as a percentage of the volume of water which can be removed. On this basis all saturations in capillary pressure experiments are between 0 and 100% and residual moisture is ignored. The capillary pressure axis correlation is more complex since what is required is a correlation for the variation of pore size with porosity.

Smith, Foote and Busang (1931) attempted an analytical treatment of this based on an idealised packing. All packings were considered to be made up of close packing with spheres separated by a distance (d) which can be adjusted to give the required porosity. A relationship can be derived between sphere radius, separation and porosity

$$(2r + d)^3 = \frac{4 \sqrt{2} \pi r^3}{3 (1-e)}$$

It had earlier been shown that the capillary rise in an irregular pore could be related to the maximum value of perimeter/area.

The pore space governing desaturation may be defined by three different minimum pore sizes in the assumed unit cell. These are shown in Fig. (13) together with their relative frequency





This is called the Leverett  $j$  function is usually expressed  $(j)_s$  and gives two curves one for drainage and a lower one for imbibition for a variety of tested materials. The group can be derived from either of two assumptions. 1. That capillary height is inversely proportional to an equivalent circular diameter of the voids which is calculated from porosity and permeability. 2. That the interfacial surface area between two fluids at a given saturation is a definite fraction of the total surface of the <sup>particles</sup> sand. The correlation has been used by oil field research workers and was modified by Rose and Bruce (1949) to include contact angle

$$(j)_s = \frac{P_c}{T \cos\theta} \sqrt{\frac{K}{e}}$$

Carman (1941) showed that the Laplace equation could be expressed in terms of a hydraulic radius

$$\Delta P = \frac{T}{M}$$

where  $M = \frac{\text{volume of a column of water in a capillary}}{\text{area of wetted surface of a capillary}}$

this value of  $M$  is the diameter of a circular capillary with the same ratio of perimeter to area as a given non-circular capillary.

This was compared with values of  $\left[ \frac{1}{r_1} + \frac{1}{r_2} \right]$  for a variety of

regular shapes such as, parallel plates, ellipses, rectangles etc.

and found to show good agreement with both calculated values and

experimental results based on capillary heights in tubes of various

shapes. The hydraulic radius of a packed bed may be calculated.

The area of the wetted surface is  $L A S$  and the volume occupied

by liquid is  $L A e$ , therefore

$$M = \frac{L A e}{L A S} = \frac{e}{S}$$

but since  $S = (1-e) S_0$

therefore  $P = \frac{S_0 (1-e) T}{e}$

The same relationship for hydraulic radius has been derived by Debbaas and Rumpf (1966) from consideration of a random cross-section of any irregular packing.

The experimental results of Hackett and Strettan (1928), and of Smith, Foote and Busang (1931) show agreement with this. Furthermore, the Leverett (j) function can be derived from this by substituting the Kozeny-Carman equation for permeability.

Harris (1959) amplified this by noting that the same bed packed in different porosities would nevertheless have the same total surface area. Therefore in Fig. (12) the areas under the two curves should be the same.

Calculations of mean hydraulic radius from both the area underneath a capillary pressure curve and the average pore size are possible

$$M = \frac{e}{(1-e)} \frac{1}{S_o} \quad M = \frac{2 T}{h_m p g}$$

Harris found good agreement between these methods which corroborates the correlation relationship.

An alternative correlation has been proposed by Thomeer (1960) for consolidated samples in mercury porosimeters. He noted that capillary pressure curves plotted on log. log. co-ordinates approximate to hyperbolae. Assuming that this is always the case he has derived a relationship to define the location and shapes of capillary pressure curves in terms of a 'pore geometrical factor'. This is basically an empirical correlation and no data has been given to allow its extension to unconsolidated media nor to the effect of porosity variation.

It may be concluded that it is possible to produce a unique curve for a given pack of particles no matter what their

porosity variation. Both Gray and Phillips and Thomas experienced difficulty with reproducibility of packing and hence capillary pressure curves in their experiments. This could have been overcome by using the correlation method. Furthermore by including specific surface all capillary pressure curves for the same pore size distribution should be correlatable to the same curve and differences in pore size distribution will be shown by the shapes of the curves only.

### 3.5 EFFECT OF CONTACT ANGLE

The existence of contact angle has not so far been considered and it has been assumed that the solid phase has always been fullywetted by the liquid, that is the contact angle is zero. For greater generality the contact angle should be included in the capillary pressure relationship. For the case of a capillary tube this was demonstrated in section 2.2 and it is usually extended to other cases as a multiplying factor to the surface tension by analogy.

Bartell and Osterhoff (1927) used the relationship

$$P = 2 T \cos\theta / r$$

to determine contact angle in porous systems by measuring the pressure required to resist imbibition of liquid. Rose and Bruce (1949) incorporated the contact angle in the Leverett (j) function in a similar way

$$(j)_s = \frac{P}{T \cos\theta} \sqrt{\frac{K}{e}}$$

Bethel and Calhoun (1953) found that this was not sufficient to account<sup>t</sup> for the effect of contact angle in porous media. The horizontal part of the capillary pressure curve fitted the

correlation but at the extremes of saturation it did not.

The fallacy of using contact angle in porous media by analogy with the rise in a capillary tube may be seen by considering the capillary rise in a conical capillary of angle ( $\phi$ ) to the vertical, and radius ( $r$ ) at the liquid/air interface. If the meniscus can be assumed as having approximately spherical symmetry then

$$P = \frac{2 T \cos(\theta - \phi)}{r}$$

Thus the contact angle interacts with the geometry of the porous medium in a more complex way than the simple capillary tube can account for. A further complication is that contact angle exhibits a hysteresis between moisture advancing and moisture receding conditions.

Harris, Jowett and Morrow (1964) attempted to overcome these difficulties by discussing the effect of contact angle in porous media in terms of the correlation of capillary pressure curves. Using

$$C = \frac{\Delta P M}{T}$$

they took that capillary pressure relationships are always of the form

$$S = f(c)$$

and results of different capillary pressure experiments are correlatable if for zero contact angle the function above gives the same curve. For a correlatable bed having a contact angle greater than zero an experimental relationship may be obtained

$$S = f^{\theta}(c_{\theta})$$

where ( $f^{\theta}$ ) is analogous to ( $f$ ). To account for the effect of contact

angle a correlating factor is introduced in terms of an apparent contact angle ( $\theta$ ) such that

$$S = f(C_e / \cos\theta)$$

Therefore a plot of ( $C_e / \cos\theta$ ) against (S) gives the same curve (f) as was obtained when the contact angle was zero.

The apparent contact angle measured using this method for various treated coals, was compared with equilibrium contact angles measured by the sessile drop method on polished coal surfaces. It was shown that apparent contact angle for the imbibition case was equivalent to the equilibrium contact angle but for desaturation the equilibrium contact angle was three times greater than the apparent contact angle.

In practice unless the existence of a contact angle is definitely established it is usual to assume that the solid is fully wetted by the liquid. Mercury exhibits a contact angle on most solids of around  $140^\circ$  and this introduces fresh complexity in to the mercury porosimeter method for measuring pore size distribution.

The effect on variation of contact angle on residual moisture in both beds of glass spheres and fine coal was found by Morrow (1962) to be negligible.

### 3.6 PORE SIZE DISTRIBUTION AND THE NETWORK MODEL

The effect of pore size distributions in porous media on capillary pressure curves has been discussed in terms of a bundle of capillary tubes model of porous media by the method used by Ritter and Drake (1945) and Gray (1958). Real porous media however do not consist of single pores going from one face of the material

through to the other, but rather of a complex three dimensional network of small interconnected pores. These interconnections which are ignored in the bundle of tubes model, to make mathematical operations on the model simpler, are important when considering the effects of a pore size distribution on the desaturation mechanism. A more realistic model for pore structure has been proposed by Fatt (1956) and can be used to demonstrate this.

Fatt considered that the network of pores which exists in real porous media could be represented by a relatively small regular two dimensional array of capillary tubes.

This is equivalent to assuming that the actual irregular configuration of connectivity in the medium is less important than the fact that it exists, and that its three dimensional aspect can be represented in two. As a justification of this he noted that a very thin slice of sandstone sandwiched between two planes has the same properties as a cube of the material. It is also assumed that the whole porous medium can be represented by a relatively small number of tubes (Fatt used 200 to 400). Morrow (1962) (quoted in Morrow and Harris (1965)) found that capillary pressure curves were reproducible for very small samples of the order of five particles thick which lends support to this.

To obtain a capillary pressure curve from the network model a pore size distribution is divided into a number of pores or tubes which are then randomly located in a regular array as in Fig. (14). The volume of a tube of a given radius is required for this and since it can not be measured Fatt used an assumption, later tested, that the length of a cylindrical pore is inversely proportional to

## NETWORK SHAPES

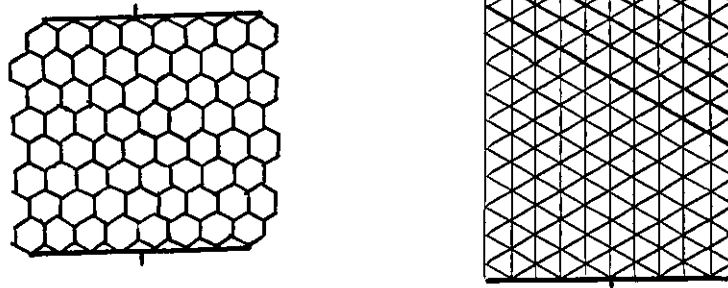


Fig. (14)

its radius. A stepwise desaturation procedure can now be followed by assuming the model to be filled with wetting phase and surrounded by non-wetting phase (i.e. water and air) and applying and imaginary displacing pressure in increments corresponding to the radii of the tubes in the network

$$\Delta P = 2 T/r$$

A tube may be emptied if the displacing pressure is sufficient to overcome the capillary pressure in it, and if there is a non-wetting phase path to it. For the first pressure increment the tube must therefore be connected to the edge of the network. Any tubes in the interior of the network will remain full if they can only be approached through smaller radius tubes. The network is examined for all displaceable tubes and their volume contribution summed. The values of pressure and displaced volume correspond to one point on the capillary pressure curve. Further points are obtained by increasing the displacing pressure until the model is completely desaturated and a full capillary pressure curve traced. It can be seen that as a contrast to the bundle of capillary tubes this model shows that a capillary pressure curve is not a true cumulative pore size distribution as it underestimates the



contribution of large pores and overestimates the contribution of medium size pores.

Residual moisture is not considered in the desaturation process described above, and may be taken to consist of immobile fluid acting like a part of the solid matrix. Alternatively the trapping of moisture can be simulated if, in addition to the other 'desaturation rules', the requirement of a continuous wetting phase path to allow removal of moisture from a pore to be displaced is stipulated. When this rule is adopted quite large amounts of wetting phase become trapped and it is more convenient to assume that this can be removed by film flow on the pore walls or through a connection in the third dimension.

Fatt tested the model by applying the desaturation procedure to several different pore size distributions and different network arrays with 4, 6, 7, and 10 tubes connected to each tube. In all cases the curves gained from the model were similar to usual capillary pressure curves. The results showed that as the number of connections per tube increase or the pore size distribution is narrowed, the capillary pressure curves more approached those given by the bundle of tubes model. The bundle of tubes model can therefore be considered as a well connected network best suited to mono-size pores. However the capillary pressure curve was more influenced by the pore size distribution than by the network type. The relationship between pore radius and length mentioned earlier as being needed to divide a continuous pore size distribution into a discrete number of tubular elements was found not to be very critical. Several relationships including a random combination of pore radius and length were tested and found to have little effect on the

derived capillary pressure curves. The assumption that the length of pore was inversely proportional to radius was preferred because of the flow properties of the network which are discussed in a later section.

A network model has also been used by Harris (1965) applied to a pore size distribution. He noted that any plane or straight line drawn through a random packing exposes a section which should be representative of the packing. This can be represented in two dimensions by the rows and columns of a latin square. Capillary pressure curves of the appropriate shape were obtained using a similar set of desaturation rules. Harris also included the effect of residual moisture in the form of pendular rings by designating the volume of a pendular ring formed by the penetration into a pore by the pressure difference existing at the time of entry. He also examined the effects of a variation in pressure stress through the model such as occurs in gravity drainage. Finally he mentioned the possibility of building up series of these latin square models to represent three dimensions in the packing, but did not <sup>a</sup>persue this.

A network model has also been used by Dodd and Kiel (1959) for capillary pressure curves, to investigate the effects of variable wettability in porous media.

It may therefore be concluded that the network model provides an intimate description of the desaturation mechanism which leads to a capillary pressure curve. This demonstrates that a capillary pressure curve is not a true cumulative pore size distribution as the contribution of large pores is under-estimated and that of medium pores over-estimated.

A quantitative assessment of these effects has been made by Meyer (1953). He used probability concepts based on an assumption that the different size pores in a porous material are distributed randomly, and did not include the factor of connectivity. An expression was derived by which correction could be made to a capillary pressure curve to give a true pore size distribution. The method of using this involves a trial and error procedure and is tedious to use but does give corrections of the right order. However it has not gained acceptance and the assumption of the bundle of capillary tubes is still used without correction in calculating pore size distributions from capillary pressure curves.

### 3.7 CAPILLARY PRESSURE CURVES FOR SPHERE

#### SIZE MIXTURES

The only quantitative prediction of capillary pressure curves mentioned so far are those applicable to regular packings of mono-size spheres. The main value in capillary pressure curves is however that they allow pore size distributions and their effects to be handled. The Fatt network model gives a qualitative description of the effects of pore size distribution but it requires a pore size distribution to do this. Some assumption is therefore required about the nature of pore space in non-regular packings such as those with a range of particle sizes. Naar and Wygal (1962) have developed a method which has successfully predicted capillary pressure curves for mixtures of up to 13 components.

In this the properties of mono-size random packs are considered as known. Binary mixtures of these are taken as consisting of two zones: one zone where the grains form the most dense mixture possible the properties of which can be calculated,

the other containing only small component or large component depending on which is in excess. The porosity of these binary mixtures can be computed when the respective volumes of the two zones are known. The permeability and capillary pressure curves are taken to be defined by a weighted average of the two zones for which the averaging functions can be determined experimentally and should be independent of the composition of the mixture and of the size ratio of the particles. Two exceptions to this are made which cannot be dealt with. If the small particles are small enough to flow through the pores in the packing of the large particles the mixture segregates into two distinct layers and the packing is anisotropic. When the small grains cannot flow through the packing of the large ones but can be retained in the pores then the number of grains per pore is not likely to be constant. This requires a probabilistic approach which was not attempted. The method is therefore restricted to particle size distributions with a spread of about 4.5:1.

Mixtures of more than two components can be considered as being made up of a number of binary mixtures. For example a ternary mixture will consist of three different binary mixtures  $1/2$   $2/3$   $3/1$ . If the theory is consistent the averaging functions found experimentally for binary mixtures can also be used in predictions for multi-component packs.

The theory does not make any assumptions about particle shape but since this will affect pore size distributions spherical particles were used to test the theory. The effect of particle shape could be investigated in isolation afterwards. Uniform pores resulting in flat capillary pressure curves will be exhibited

by mono-size packs of spheres and also binary mixtures at maximum density. The other binary mixtures will have capillary pressure curves which will be weighted averages of the flat curves given by the different zones and will also contain uniform pores. Multi-component mixtures will also display a narrow range of pore sizes due to the limitations on the ratio of the size of large particles to small ones.

Extensive tests were made on binary mixtures with a range of size ratios and on multi-component packs of 3, 5 and 13 different sizes. The results confirm the theory and also compare well with porosity results for ternary mixtures given by Gratton and Frazer (1935).

The method is limited to size ratios less than 4.5 to 1 and also relies on a rather rigid conception of how different sizes of particles interact with one another in random packing. It is also difficult to use the technique in a microscopic description of the moisture effects in porous media which would allow extension to illustrate the mechanism of dewatering.

### 3.8 DISCUSSION OF CAPILLARY PRESSURE CURVES

#### RELATED TO DEWATERING

From this survey of the capillary pressure effects in porous media it can be seen that the capillary pressure curve provides an intimate description of the nature pore space in porous media in a way which other properties such as permeability or porosity cannot. The curve can be interpreted to give surface area, pore size distribution or mean pore size, and the results can be used to calculate porosity. The nature of residual moisture is illustrated and the existence of hysteresis also allows further characteristics of the structure to be analysed.

From the point of view of dewatering the capillary pressure curve provides information on how moisture is held in packed beds and shows that this is controlled by the pore structure of the bed especially the distribution of pore sizes. Furthermore, since the various quantities which can be measured from the capillary pressure curve are equivalent to those used in permeability relationships it should be possible to use them to predict the way moisture flows out of a desaturating packed bed without involving specifically saturated flow phenomena.

However, the analytical treatment of the capillary pressure curve, such as is provided by the Haines theory, only deals quantitatively with ideal packings of mono-sized spheres. Deviation from ideal behaviour such as is shown by the shapes of the curves and the trapping of air during imbibition were recognised by Haines to be due to the inevitable irregularities present in real porous media but were not treated quantitatively. These effects and the effects of a particle size distribution must be included in the theory because of their importance in dewatering.

Two approaches have been discussed which try to account for these. The qualitative description provided by Fatt's network model (section 3.6) and the quantitative prediction of capillary pressure curves from a sphere size distribution by Naar and Wygal (section 3.7).

The Naar and Wygal approach, although it is supported by experimental evidence, relies on a rather rigid conception of how particles of different sizes and relative proportions interact in a packing. Furthermore, it is restricted to a small range of particle size distribution which only involves relatively uniform

size pores. It is also difficult to see how the approach can be extended to give further insight into either capillary pressure curves or the mechanics of dewatering.

A more satisfactory extension of present theory would be if the network model could be made predictive. This would allow a more rigorous test of the model than the subjective ones possible in its present form and would provide a detailed description of the action of the two fluid phases in a porous medium during dewatering.

---

## CHAPTER FOUR

### PROPOSAL OF THEORY

#### 4.1 INTRODUCTION

The need for a theory to represent the pore space in packs of particles with a distribution in sizes has been emphasized. The Fatt network of capillary tubes model has been shown to be successful in representing qualitatively the effect of pore size distribution and the inter-connections of pore space on capillary pressure curves. But in this the tube radius distribution must be derived from a pore size distribution and the lengths of the individual tubes cannot be properly specified. (For example a long narrow tube may have the same volume as a short fat one). Furthermore as the model was derived mainly for consolidated media the effect of porosity variation was not considered. In order to make this model predictive and applicable to unconsolidated media the pore space in a particle pack must be described.

#### 4.2 PARTICLE SIZE DISTRIBUTION AND PACKING

The effects of particle size distributions on packing has been the subject of inquiry for many years because of its importance in many fields of technology. It has been established that packings of mono-size particles have in general higher porosities than those composed of a distribution of sizes. Thus two different sets of uniform particles having separately the same porosity will when mixed together produce a packing of a lower porosity.

As a first step to the problem it is possible to compute the sizes of spheres required to just fill the interstices in regular packings. Horsfield (1934) and White and Walton (1937) have made calculations of this sort and shown that close packing



can have its porosity of 25.95% reduced to 14.9% by the addition of sets of smaller spheres of five selected sizes. If finer and finer sizes are added the porosity will tend to zero. This however takes no account of the complexity of the interactions of different sizes and relative proportions in random packing.

Experimental investigation of the problem has resulted in empirical methods for predicting the minimum porosity of mixtures. Furnas (1929) (1931) added fine particles to coarse ones and represented his results as a series of curves. These can be used to predict minimum porosity for different numbers of components from their relative proportions and size ratios. Andreasen (1940) has made a similar study. Other empirical investigations have been carried out on irregular particles by Fuller and Thompson (1907), Westman and Hugill (1930), Adwick and Warmer (1966) and on spheres by Graton and Fraser (1935), Smith and Lea (1960), Parrish (1961), Epstein and Young (1962), Bo, Freshwater and Scarlett (1965), Ayer and Soppett (1965), McGeary (1961) (1967) and Ridgeway and Tarbuck (1968).

Several theoretical treatments have also been advanced. Lewis and Goldman (1966) have given two theorems by which the characteristics of particle size distributions may be used to predict weight ratios of different sized components to achieve maximum packed density. Weickowski and Streck (1966) have given equations to predict porosities of mixtures in terms of the properties and relative proportions of components in a mixture. Ben Aim and Le Goff (1968) investigated the effect of the container wall on the radial variation of porosity and have extended the treatment to binary mixtures. These theories are usually based

on an assumption of a perfect ordered mixture of the various sizes. Rose and Robinson (1965) have shown that this state is unobtainable with practical mixers and the best that can be hoped for is a perfect random mix. This leads to higher porosities than the theories would predict.

None of these treatments are capable of the extension required here, as they mainly concern the bulk property of porosity and leave aside pore size distribution. More fundamentally however the nature of random packing has not yet been adequately described even for mono-sizes. Much interest has been directed to the problem because of its relevance to the theory of the structure of liquids, Bernal (1964). Random packing of spheres by computer simulations have been attempted. Walkley and Hillier (1967), Mason (1967) and Smalley (1962). In general these are not satisfactory because of the unrealistic methods adopted to produce the packing, involving expanding spheres, or progressive removal of overlapping spheres etc. These types of operation are made necessary by the fact that particles occupy a finite amount of space and cannot overlap one another. In addition to these geometrical effects, which are even more complex for mixtures of sizes, must be added statistical effects due to the randomness of the packing. A study of this for unequal spheres has been made by Higuti (1961).

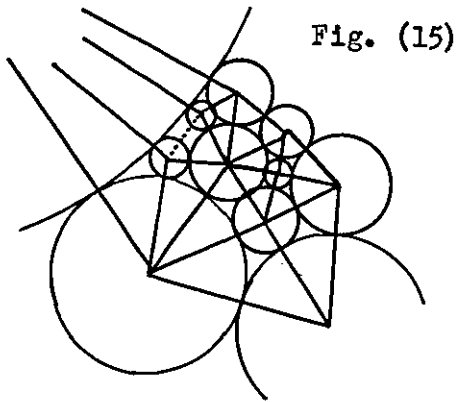
The complexity and importance of the interactions of these two effects have led Blum and Wilhelm (1965) to state that the solution of the packing problem requires a new discipline called, by them, statistical geometry. Debbas and Rumpf (1966) have used an amalgamation of geometry and statistics applied to a random packing. This was done by application of an expression derived

by Wicksell (1925) by which the particle size distribution in a packed bed can be related to the particle cross-sections exposed by a random section of the packing. It is difficult to see how this can be made predictive as it depends on the situation already existing in a given packed bed. A more direct application of statistics and geometry to the problem has been made by Wise (1952). He described how the properties of a packing of unequal spheres at its minimum porosity could be related to the sizes and relative numbers of spheres in a packing. This approach is covered in the next section and is extended to predict a tube size distribution for a network model.

#### 4.3 WISE MODEL OF RANDOM PACKING OF UNEQUAL SPHERES

Representations of pore space already existing, such as those of regular packings are used because the geometry is manageable and adequate for the applications considered. Here however the distribution of particle sizes in a random packing must be considered. Wise (1952) and Hogendijk (1963) have provided a mathematical description of one limiting case of this type of packing which can be used to extend the network model.

An assumption is made that in the densest packing possible of a set of unequal spheres each sphere touches its neighbours. Thus the space in the packing can be divided up by imaginary lines joining the centres of touching spheres forming tetrahedral units containing both solid and void. Fig. (15) shows this in two dimensions. In practice this assumption is false and there will always exist gaps such as that marked in the figure. The filling of these gaps will be promoted the wider the sphere size distribution



but they may never be completely eliminated. Here however they are assumed not to exist. The packed bed is therefore divided into tetrahedral units which completely fill the space occupied by the packing. The properties of the packed bed can then be given in terms of these units.

Assuming  $(n)$  different radii of spheres in the packing the number of different tetrahedra that are possible is given by

$$n(n+1)(n+2)(n+3)/4!$$

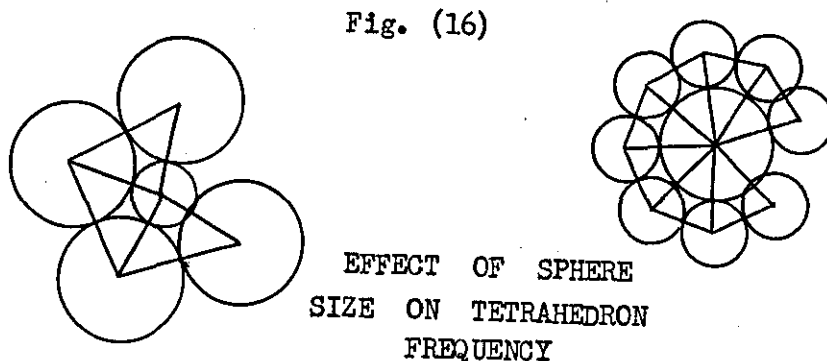
Hogendijk (1963). Therefore in a 3 component pack there exist 15 different tetrahedra which can be constructed from these 3 different sphere sizes, they are listed in Table III

TABLE III

(1) 1111	(4) 1122	(7) 1222	(10) 1333	(13) 2233
(2) 1112	(5) 1123	(8) 1223	(11) 2222	(14) 2333
(3) 1113	(6) 1133	(9) 1233	(12) 2223	(15) 3333

The relative frequency of occurrence of these tetrahedra in a random assembly of spheres will depend both on the relative numbers of the different spheres and also their relative sizes. This can be illustrated by considering a three component pack with spheres of

radii 1, 2, and 3 units and relative proportions by number 50, 30, 20 say. Since there are more spheres of radius (1), then tetrahedra containing (1) will be favoured. From the point of view of size however a smaller sphere can fit less other spheres around it than a large one, and so can take part in less tetrahedra. Therefore tetrahedra with (3) in will be favoured Fig. (16) shows



this in two dimensions. For a three dimensional measure of this Wise used the solid angle subtended at the centre of a sphere by another touching sphere expressed as a fraction. Therefore the probability of a sphere taking part in a tetrahedron will be related to

$$f / A$$

where (f) is the number frequency of the sphere in the packing and (A) is the average solid angle subtended at that sphere by the others in the packing. Assuming that the tetrahedron system in a packing is obtained by a random combination of groups of four spheres then the relative frequencies of the various tetrahedra are given by the respective terms of the expansion of the expression

$$\left[ \frac{f_1}{A_1} + \frac{f_2}{A_2} + \frac{f_3}{A_3} \right]^4$$

For example the tetrahedron 1233 will have a relative frequency

$$\frac{4!}{2!} \frac{f_1}{A_1} \frac{f_2}{A_2} \left[ \frac{f_3}{A_3} \right]^2 = 12 \frac{f_1}{A_1} \frac{f_2}{A_2} \left[ \frac{f_3}{A_3} \right]^2$$

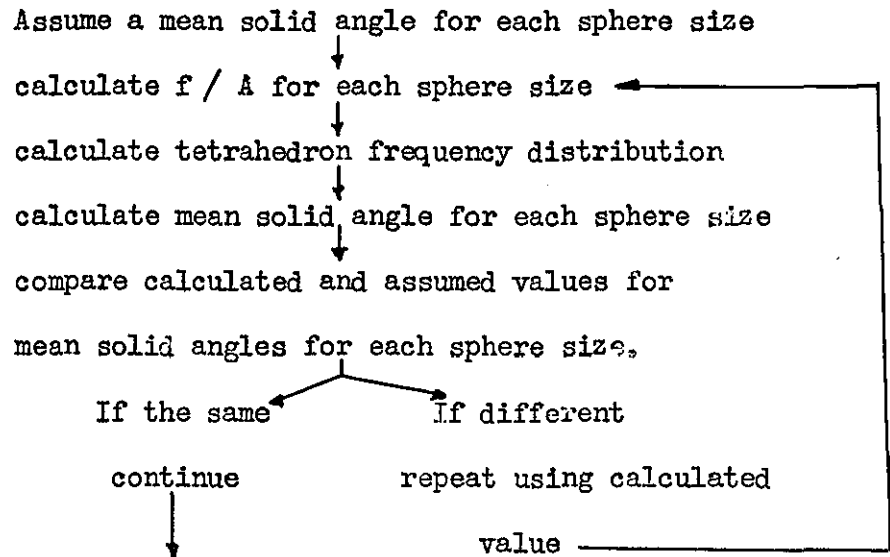
This can be generalised to

$$\frac{4!}{a! b! c!} \left[ \frac{f_1}{A_1} \right]^a \left[ \frac{f_2}{A_2} \right]^b \left[ \frac{f_3}{A_3} \right]^c$$

where (a) (b) and (c) are the number of times 1, 2 or 3 appear in the given tetrahedron. For the example above this becomes

$$\frac{4!}{1! 1! 2!} \left[ \frac{f_1}{A_1} \right]^1 \left[ \frac{f_2}{A_2} \right]^1 \left[ \frac{f_3}{A_3} \right]^2$$

However the mean solid angle (A) for each of the different spheres in the packing cannot be determined analytically unless the frequency distribution of the tetrahedra in the packing is known. This in turn cannot be determined without knowing the mean solid angle for each sphere size. Therefore a solution must be gained by successive approximations. The logical scheme below may be used



It is therefore possible to obtain the frequency distribution of the tetrahedra constituting the packing. From this Wise has shown that porosity and number of contact points can be calculated. This has been verified theoretically by Wise (1952) for a log. normal distribution of sphere sizes and by Hogendijk (1963) for a discrete radius distribution. No experimental verification has yet been reported.

#### 4.4 PORE SPACE IN THE WISE MODEL

##### 4.4.1 Pore Size Distribution

The unit of pore space enclosed by a tetrahedron of four spheres can be taken to consist of a large central void from which protude four narrow waists. Using the Haines simplification, this can be taken as a central spherical void and four capillary tubes, see Fig. (17).

PORE SPACE IN A TETRAHEDRAL  
UNIT

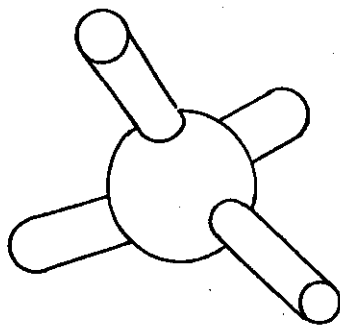


Fig. (17)

Knowing the radii of the spheres making up a given tetrahedron it is possible to calculate the radii and lengths of the individual tubes and the radius of the central spherical void. Wise (1960) has given an expression for the radius of the interstitial sphere in a tetrahedron formed by four spheres.

Letting the reciprocal of the radius ( $r_i$ ) of a given sphere be represented by ( $x_i$ )

$$x_i = 1 / r_i \quad \text{for } i = 1 \text{ to } 4$$

then

$$x_{\text{interstitial}} = 1/2 (x_1 + x_2 + x_3 + x_4) + 1/2\sqrt{3p}$$

where

$$p = (x_1 + x_2 + x_3 + x_4)^2 - 2(x_1^2 + x_2^2 + x_3^2 + x_4^2)$$

The relationships for calculating the lengths of the tubes and their radii are given in appendix 1.

In a 3 component pack it has been stated that there exist 15 different tetrahedra possible. Therefore 15 different sizes of interstitial sphere are possible. A tube extending from an interstitial void has a radius dependent only on the 3 spheres bounding it, and therefore in an (n) component pack there are

$$n (n + 1) (n + 2) / 3!$$

different tube radii possible. In a three component pack that is 10, as listed in Table IV.

TABLE IV

(A) 111	(C) 113	(E) 123	(G) 222	(I) 233
(B) 112	(D) 122	(F) 133	(H) 223	(J) 333

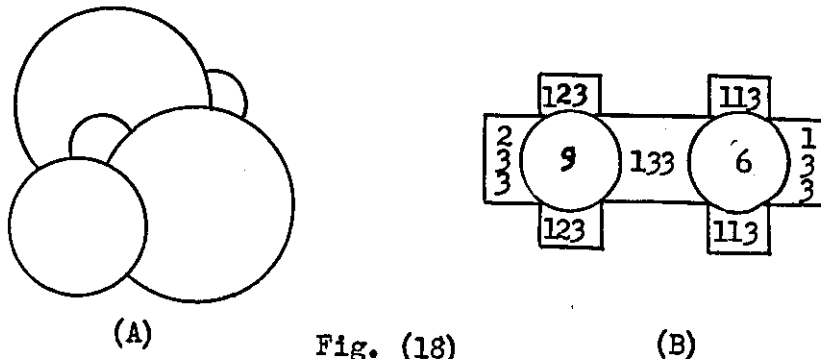
The lengths of these 10 different tubes will however depend on the fourth sphere in the tetrahedron and therefore each of the tubes can have (n) different lengths and hence volumes. In this case that is 3 different lengths. Thus a pore size distribution for the packing is calculable from the sphere radii making up the various tetrahedra and the relative frequency of occurrence of these tetrahedra. A computer program has been written to perform these calculations and is given in appendix 2.



#### 4.4.2 Continuity of Pore Space

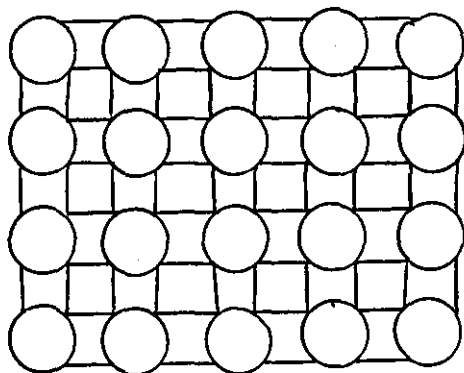
To use this information the continuity of the pore space must be specified. Fig. (18a) shows an assembly of the spheres

PORE SPACE APPROXIMATION



1, 1, 2, 3, 3. This is equivalent to two tetrahedra 1233 and 1133 connecting together at a 133 face. The pore space can be taken as being represented by Fig. (18b). Further tetrahedra can be formed on the system by adding on spheres in the same manner. Pore connectivity is therefore always between interstitial cells by two meeting tubes both having the same radius but not necessarily the same length. In theory therefore the structure of the pore space can be described. In practice however this is much too complicated to be used since the tubes will extend from the central voids at different angles. Furthermore the assumption of gapless packing will quickly breakdown as it becomes apparent that there must be discontinuities.

An approximation to pore space connectivity may be made by assuming the Fatt type regular network. The tetrahedral system dictates a 4 tube per junction network of the form shown in Fig. (19). Each circle in this represents one interstitial void and each connecting link between voids represents two tubes of the same radius.



4 CONNECTION  
NETWORK FORM

Fig. (19)

To assign the pore sizes in this network the tube size distribution is considered separately from the void size distribution. This is because it is not possible to keep the tetrahedral pore unit intact and still have the two tubes meeting between each pair of voids always of the same radius. The tubes are therefore located randomly in the network and for simplicity each pair of tubes in one connection is taken to be of the same type i.e. length.

The void spaces can be assigned in several ways. For instance by selecting the void for a given junction on the basis of the predominant tube size at that junction; or dependent on the largest tube size at the junction. These schemes show little difference from assigning the void sizes in the network randomly and since this is simpler this procedure was used.

#### 4.5 SETTING UP AND USE OF THE NETWORK MODEL

The largest practicable number of different components in a particle size distribution before the model becomes too unwieldy for pen and paper operations is 3.

For example using 4 components provides 35 different tetrahedra and 20 different tube radii, as compared with 15 and 10 for 3 components. The network configuration is fixed by the

tetrahedral unit of pore space at 4 connections per junction, but the size and shape of the array must be decided upon. These will affect capillary pressure curves obtained from the model in two ways. Firstly the size of the network must be large enough to statistically represent the whole whilst still being small enough for convenient use. Secondly the shape of the network will affect the initial part of the capillary pressure curve, in that the proportion of the displacable pores trapped in the interior of the model at each increase in displacing pressure, will be related to the ratio of the number of pores on the perimeter of the model, to those in the interior, as well as to the pore size distribution. There is no absolute method of deciding on these matters and a qualitative choice only is possible based on results from the model.

From the relative numbers and the radii of the three components in a packing the computer program given in appendix 3 calculates the porosity of the most dense packing, the relative numbers of the 15 different tetrahedra and also the cell radii and the tube radii and lengths associated with each of them. The cells are numbered 1 to 15 and the tube radii A to J (see Tables III and IV). The length of each tube is defined by the tetrahedron in which it occurs, therefore a complete specification of a tube size is given by a combination of a letter and a number e.g. A1, A3 or G12, etc.

The number of times a given tube size occurs in a given tetrahedron is also known. For instance tetrahedron (8) 1223, has faces 122, 123, 123, 223. That is face D once, E twice and H once. Therefore a complete specification for tetrahedron (8)

is, one D8 tube, two E8 tubes and one H8 tube. Since the relative number of tetrahedron 8 in the packing can be calculated then so also may the relative numbers of the different tubes.

Knowing the relative numbers of the various size cells and tubes the network model can be constructed. Each cell location in the network is numbered consecutively and the various size cells to be fitted in these are listed and given a random number between 1 and the number of cells in the network. These random numbers are matched with the numbered cell locations in the network, and so the cell sizes are randomly assigned. The same procedure is adopted for the tubes.

This network model is now little different from that used by Fatt and the desaturation rules used by him may be followed to obtain a capillary pressure curve. Two differences exist: one edge of the network is designated as an outflow face as opposed to the single pore used by Fatt; and there exists a void space at each junction. The desaturation procedure needs modification for this latter difference.

The rule adopted is that as soon as wetting phase enters a pore then the voids connected to that pore will also be emptied. It can happen that in a wide distribution of pore sizes the largest tube radius is bigger than the smallest cell size and because of the way of fitting the sizes in the network these may be connected to one another. Therefore logically in this case the cell could not be emptied. However, in practice the cell size connected to any tube must be always larger than the tube and the rule is therefore not unreasonable. No other modification of Fatts rules were made and therefore capillary pressure curves

may be obtained in the same way as previously described.

The necessity for this representation of the pore space in the network form is greater here than in the model used by Fatt. In the Fatt model it is possible to compare the results for capillary pressure curve with a capillary tube model since the only extra effect is that of isolation of large pores by small ones. This is not possible in this model as there is no way of assigning the volume of a given cell to a given pore size in desaturation without the network form being available.

#### 4.6 PRELIMINARY TESTS

The justification of the model can only be made by comparison between experimental and predicted capillary curves but as a preliminary the model was tested to give some idea of the size and shape of the array needed.

Three different sizes of model were tested with 90, 190 and 285 cells or junctions. That is with roughly twice these numbers of tube sizes each tube representing two pores connected together. The resulting capillary pressure curves are shown in Fig. (20). Little difference is exhibited between the 285 and the 190 cell models and not much more between these and the 90 cell model. Therefore the 190 cell model was adopted. This is about the same size as that used by Fatt.

The figure also shows the results for two different shapes of 190 cell models, one of 10 x 19 cells the other of 7 x 27 cells. The long 7 x 27 cell model gives results tending towards those of the small 90 cell model and the 10 x 19 cell one is almost the same as the larger 285 cell model. A 10 x 19 shape was adopted.

These simple tests cannot be considered as exhaustive but

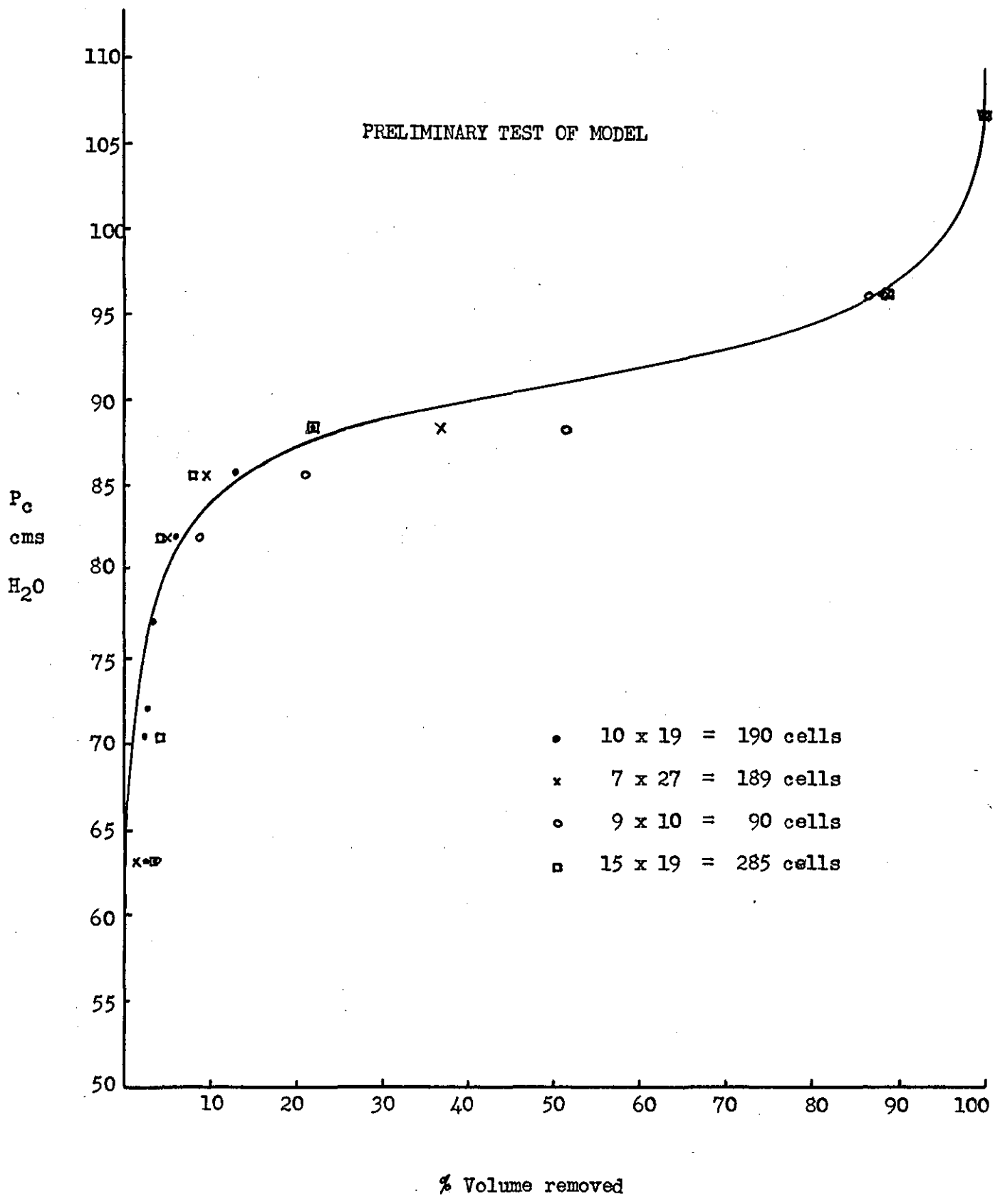


Fig. (20)

the results for each model are not very different and therefore bear out Fatts conclusion that with a network model the pore size distribution is the major factor in determining the shape of capillary pressure curves. To this extent this model is successful in that quite widely different model types do not mask the effect of pore size distribution.

To apply the model to continuous sphere size distributions a method must be devised of reducing this to a discrete number of components (3 in this case). To do this 3 points on a particle size axis of a distribution were selected which are roughly the mid points of 3 equal sections of the spread of the distribution. The number frequency associated with these selected sizes was then taken. To test the effect of this rather crude procedure, four such sets of 3 components were selected from an assumed sphere size distribution of approximately normal shape. Fig. (21). Capillary pressure curves were obtained from these sets by using the model, and are shown also in Fig. (21). Little difference can be seen between these results for the different sets. This may be taken to indicate that as the relative positions of the selected components are moved the change in particle size is matched by the change in relative number and the resulting pore size distribution is corrected.

In applying the model to experimental results this method of obtaining the 3 components was only applied to much less wide distributions than that used here. The spread of the distribution used in this test is  $240\mu$  for a mean size of  $280\mu$ . The widest distribution split by this method in the experimental section had a range of  $15\mu$  about a mean of  $55\mu$ . Wider distributions were made by mixing sets of 3 selected components.

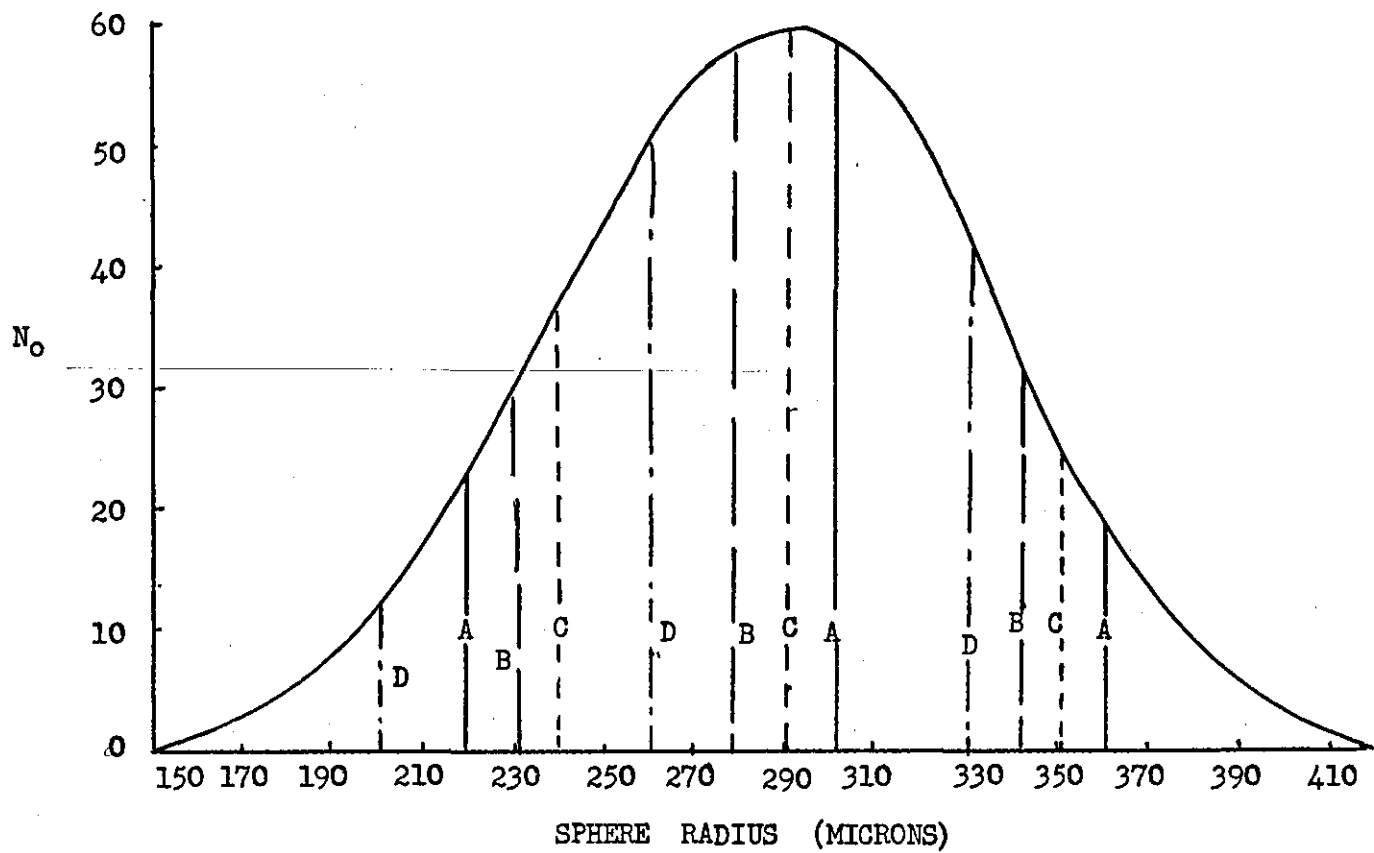


Fig. (21) (A)

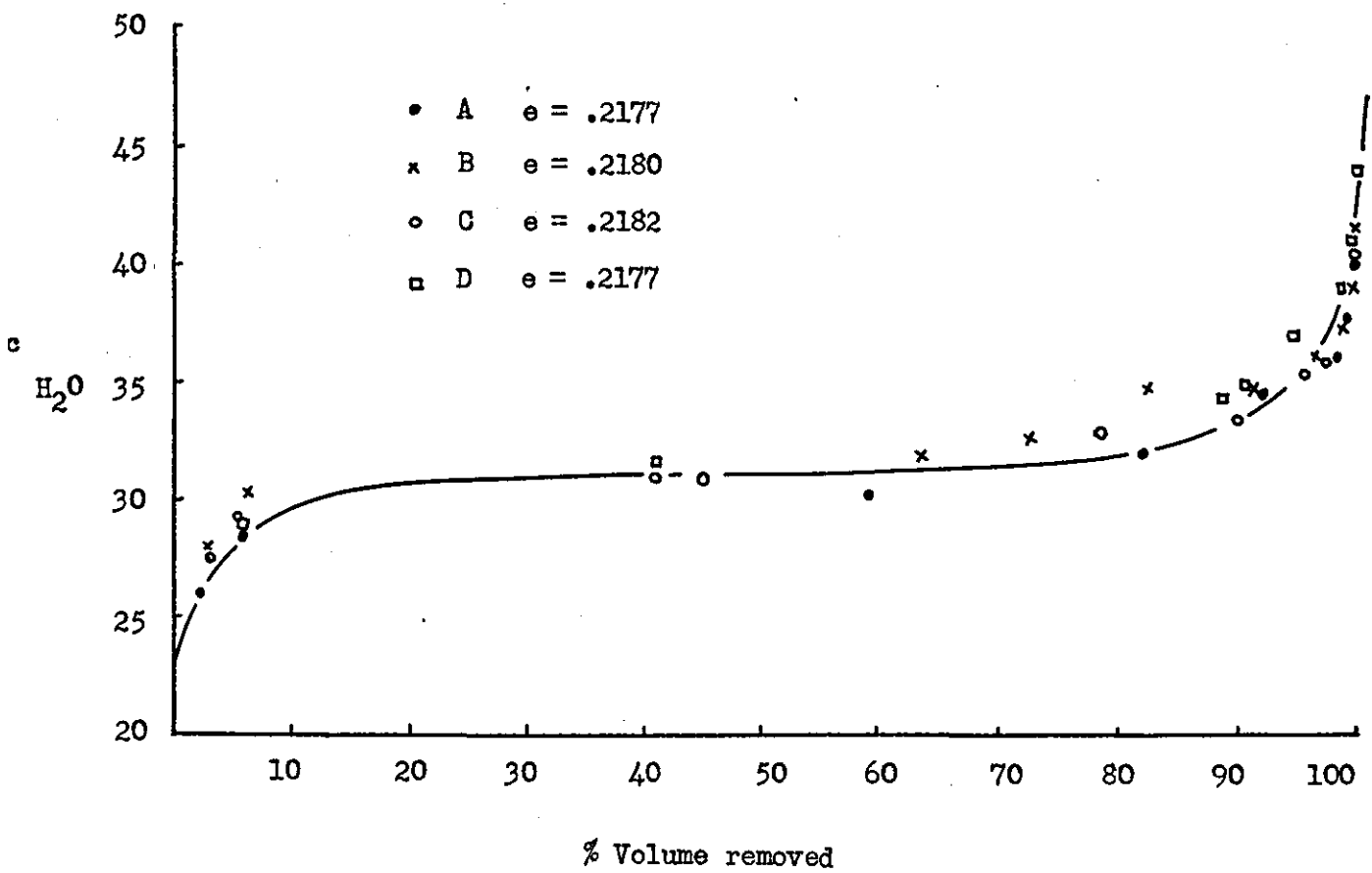


Fig. (21) (B)



#### 4.7 SUMMARY

The Wise model of random packing of unequal spheres has been extended to describe the pore space existing in such a packing. This description of pore space has been used to construct a Fatt type network model using 4 connections per junction.

Preliminary tests indicate that for a 3 component packing of spheres a 380 tube 190 cell model with a shape of 10 x 19 cells is adequate to give capillary pressure curves. A simple method of splitting a continuous sphere size distribution into a set of 3 components has been tested and found to give consistent results when applied to the model.

## CHAPTER FIVE

### EXPERIMENTAL TEST OF THEORY

#### 5.1 INTRODUCTION

Capillary pressure curves have been obtained from the theoretical model and compared with experimental results for similar size distributions of glass beads. The comparison is made by means of the previously mentioned correlation method.

The size distributions used in these experiments were various mono-size and three component packs of glass beads. Each sample has been tested in both of two reproducible porosities.

Capillary pressure curves have also been determined for a range of grades of filter aid material and compared using the same correlations.

#### 5.2 DESCRIPTION OF APPARATUS

##### 5.2.1 General

The apparatus used in the experiments is shown in Fig. (22). It follows the design used by Morrow (1962) which is shown in Fig. (5). There are three main components, the sample cell, the volume measuring system, and the vacuum system.

##### 5.2.2 Types of Cell

Three different cells were used in the experiments. Each has a different size and fine pore support plate. The largest cell and the one used in most of the experiments is shown in the general layout Fig. (22) and in Fig. (23). It has a diameter of 10.8 cms. and a fine pore support plate of a sintered bronze disc with a pore size of approximately  $3\mu$  set in a perspex holder. This could be used to support a cellulose acetate membrane which are available in pore sizes down to fractions of a micron.

GENERAL LAYOUT FOR APPARATUS

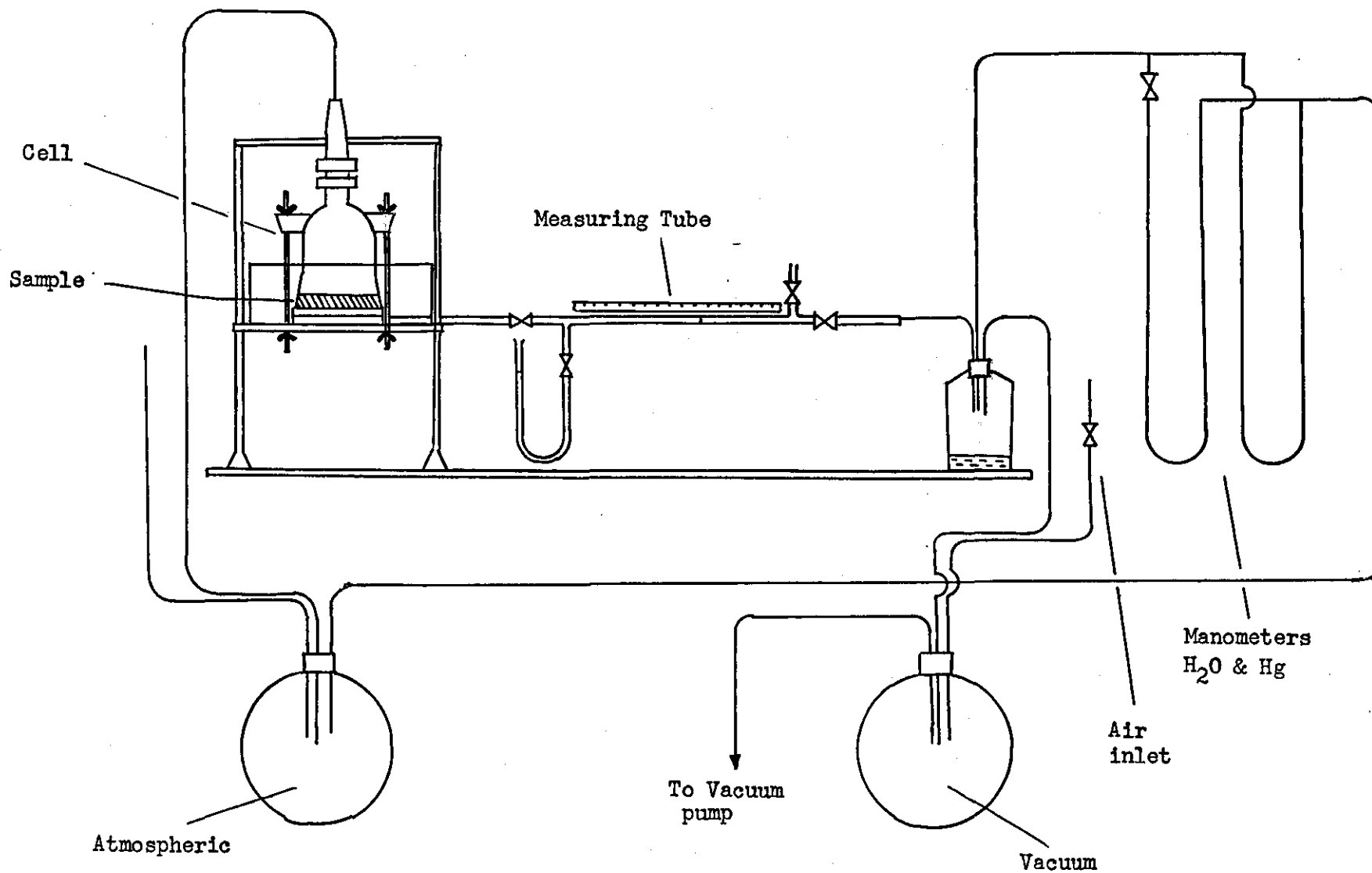
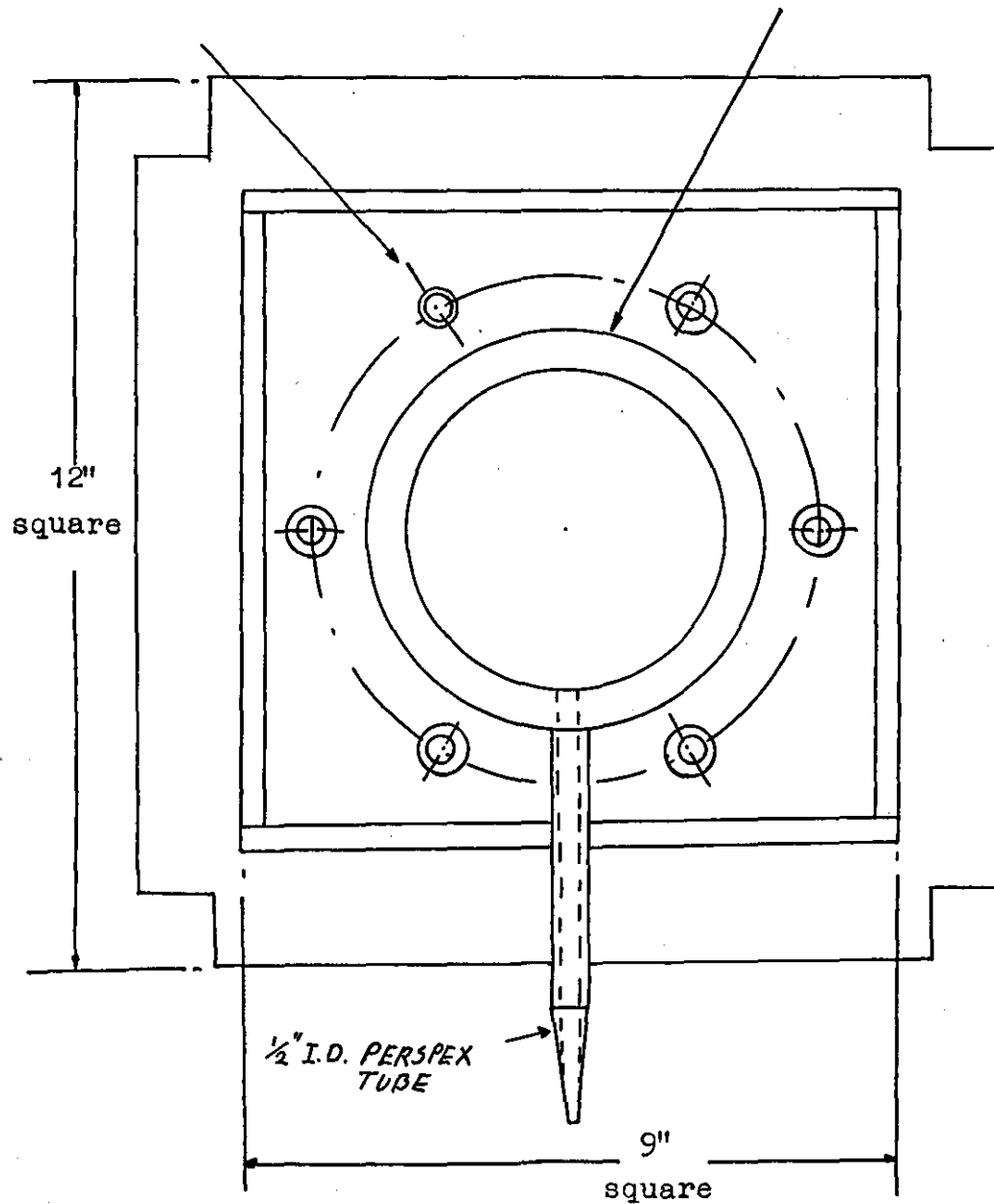


Fig. (22)

6 Holes on 7" P.C.D.  
with rubber grommets

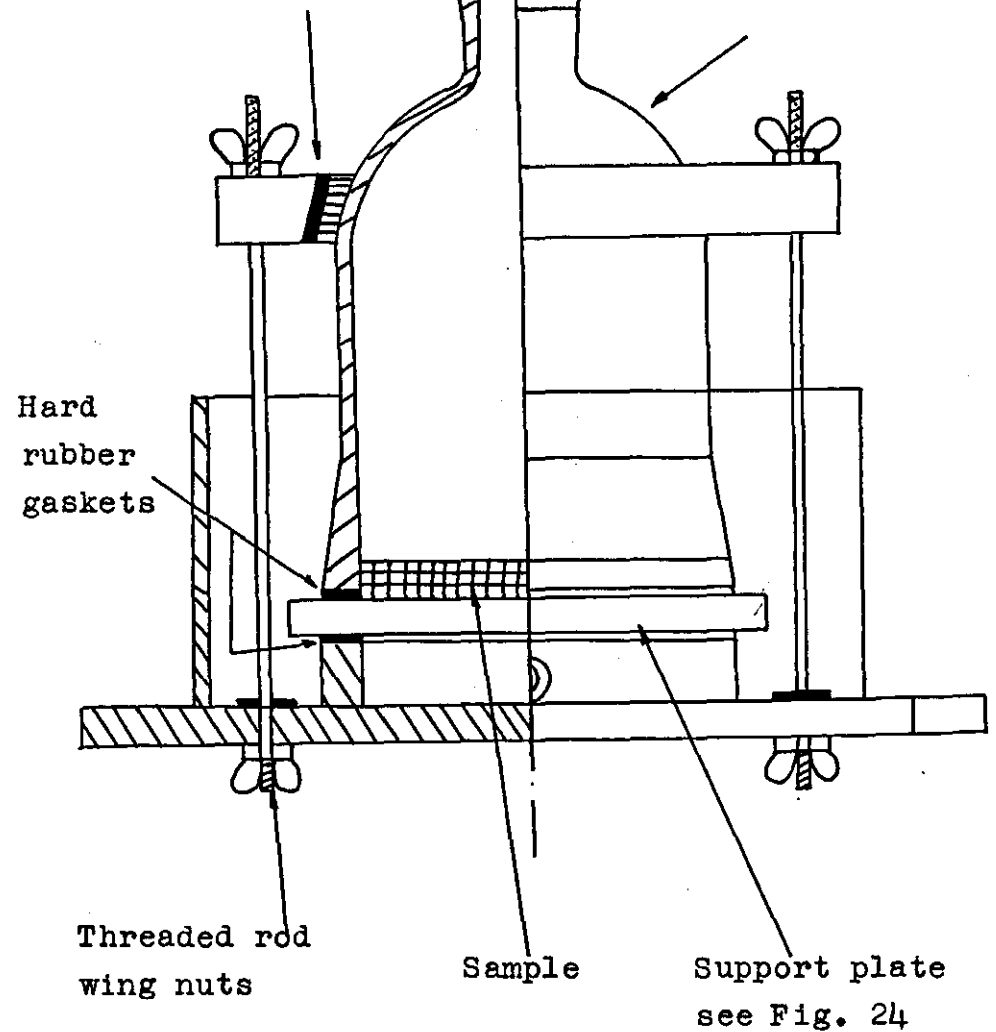
### CAPILLARY PRESSURE CELL

4½" I.D.  
5¼" O.D.



4" QVF flange with  
wooden former

4" to 1½" QVF  
column head piece



Materials :  
¼" and ½" Perspex.  
QVF column head.

FIG. 23

Two support plates were constructed: One in which the porous disc was the same diameter as the glass container and relies on Araldite for sealing into the perspex (Disc A); The other, in which the gasket on the joint face of the glass cover also seals the sintered disc together with the Araldite, in the perspex holder. (Disc B). This latter design was found to be more satisfactory from the point of area available for flow. Both are shown in Fig. (24).

The sample in the cell is enclosed and connected to a buffer container of about 45 litres as shown in Fig. (22) as recommended by Morrow (1962). This serves to control the atmosphere above the sample and inhibit evaporation.

The cell is fitted with a bath which can be filled with water to allow assembly of the cell components under water. This feature was included because of the difficulty in excluding air bubbles underneath the sintered disc or between it and the plastic membrane when used.

The water can be removed before experiments are started in case it should leak in to the cell and cause errors in the volume measurements, or alternatively it can be left to serve as a constant temperature jacket if required.

Using a plastic membrane this cell should be capable of supporting more than one atmosphere without air penetration of the support plate. However the fragility of the plastic membranes and the large area used meant that in practice this was difficult to achieve. The large area also lead to difficulties with variability of calibration (see section 5.3.3) which also made the use of plastic membranes in the cell unreliable.

# SUPPORT PLATE FOR LARGE CELL

## Section AA

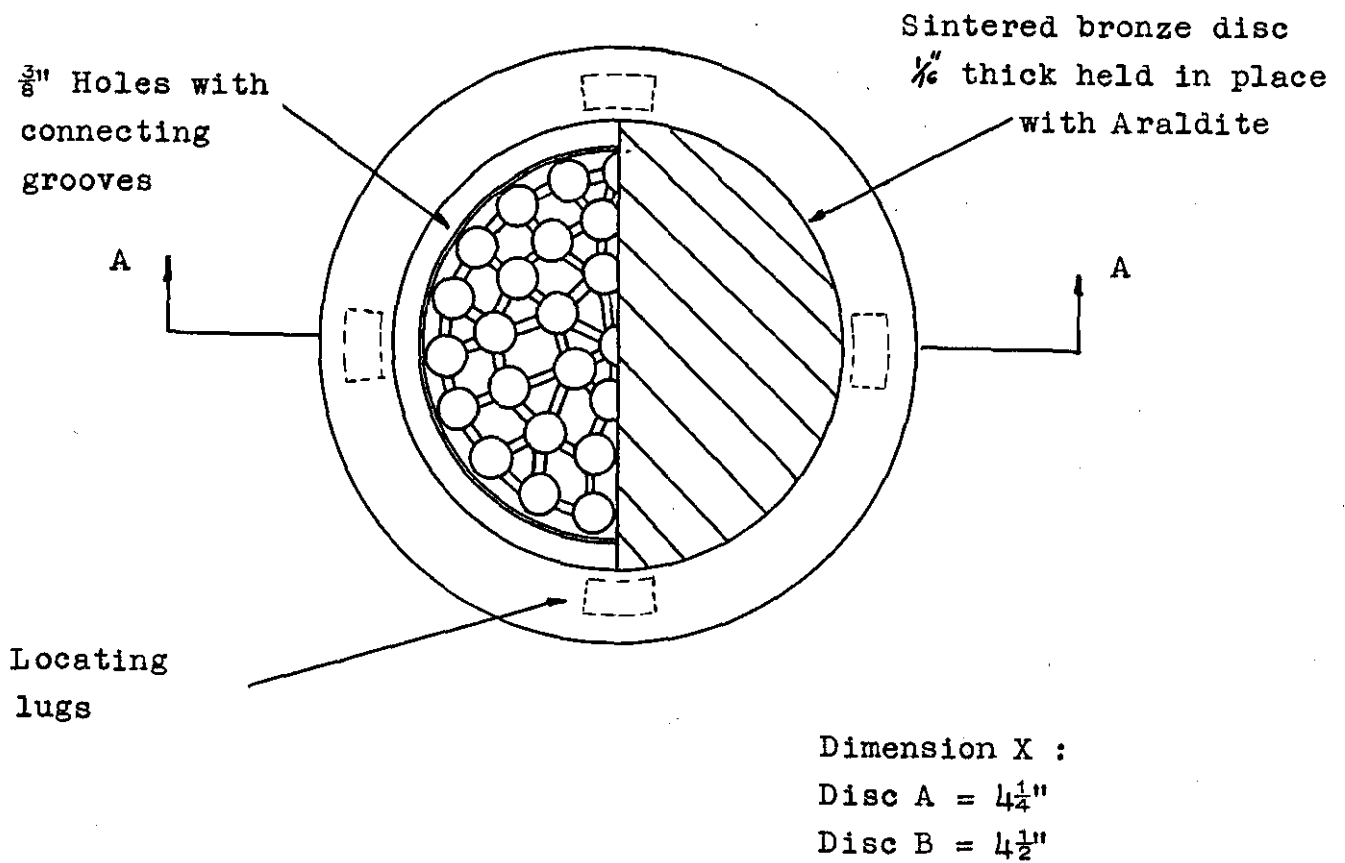
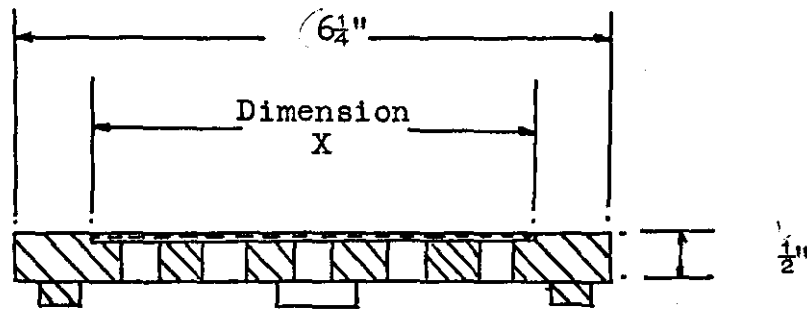


FIG. 24

For experiments therefore which required displacing pressures greater than about 250 cm. of water, the limit of the sintered metal disc, an alternative cell was used. This was constructed from the filter holder of a "milli-pore" filter which has a diameter of 3.6 cms. and is shown in Fig. (25). The plastic membrane is supported on a ground flat sintered glass support plate and the components are held together by a spring clamp. A lid was fitted to inhibit evaporation.

A third type of cell was also used and is shown in Fig. (25)1. It was constructed from a sintered glass buchner funnel and has a diameter of 6.5 cms. This is the largest diameter of sintered glass disc available with a plane surface, larger ones being domed to help support pressure. A lid was fitted to inhibit evaporation.

### 5.2.3 Volume Measuring System

The different cells were used on a wide range of sample sizes and therefore the measuring system must be capable of flexibility. The system used is shown in Fig. (26). Displaced volumes are measured differentially in the horizontal tube and collected cumulatively in the burette. This allows high accuracy and a large capacity. The horizontal measuring tube system is also convenient for following the approach to equilibrium at each pressure increment.

The tube has an accurate bore of about .3 cms. and is about 50 cms. long. It can therefore contain nearly 3.5 cc's, which is sufficient in most cases for the volume removed in one pressure increment. This volume can be transferred to the burette without relaxing the pressure on the sample, or disturbing the pressure system, by using the appropriate stopcocks. Measurements are made

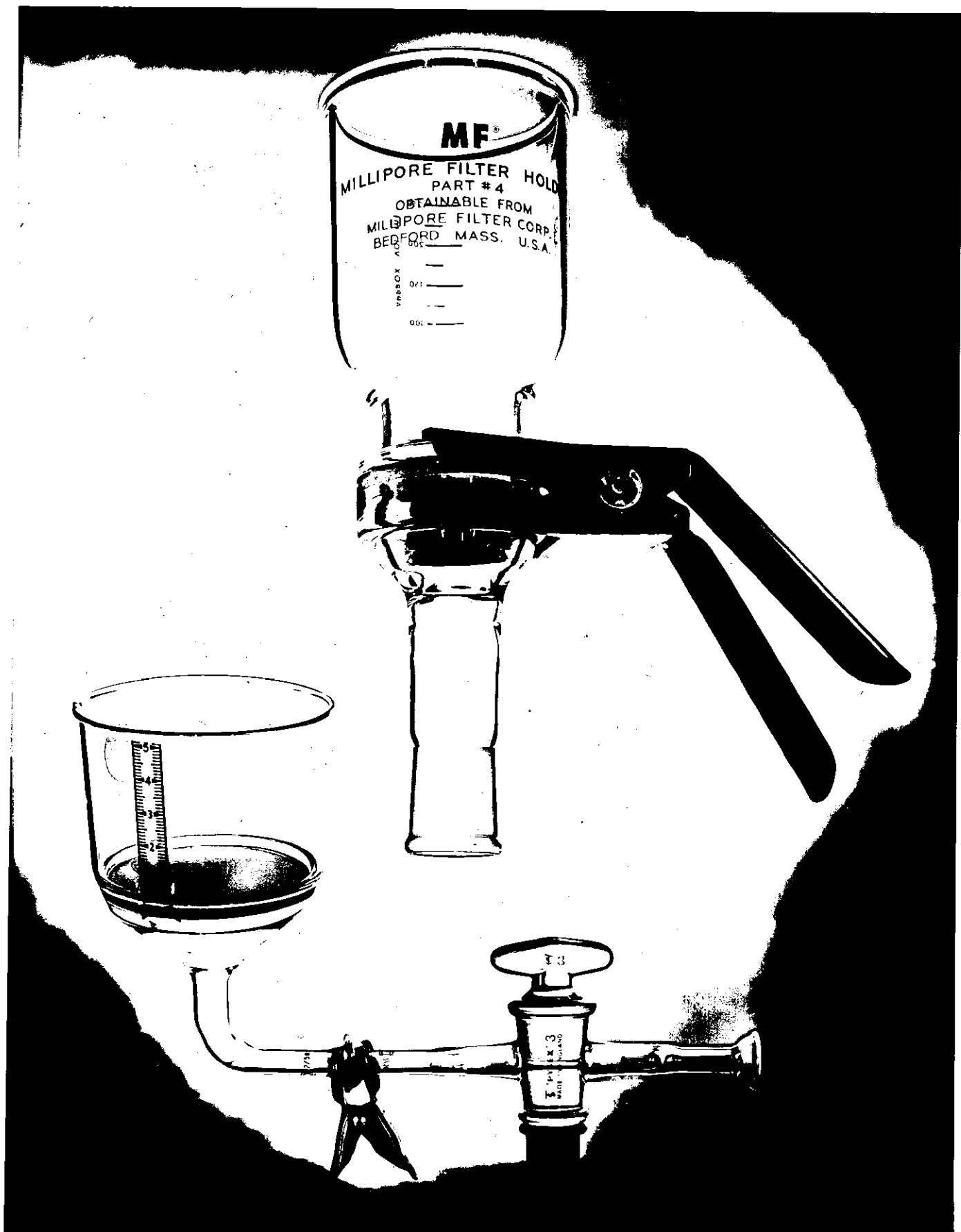


Fig. (25)



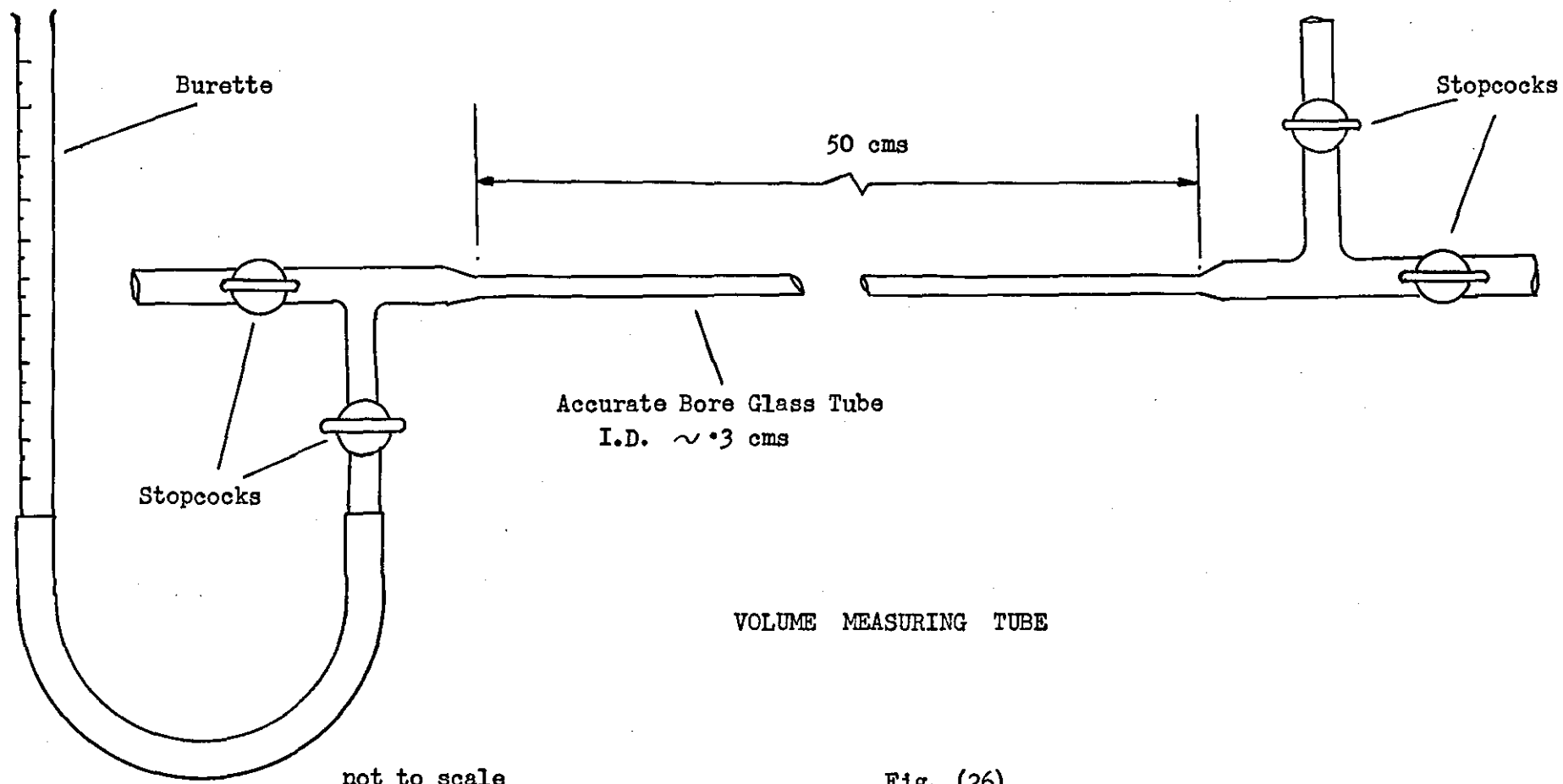


Fig. (26)

on a centimetre scale which may be read to within one millimetre. The tube was calibrated (section 5.3.1) against this scale for conversion in to cc's. One millimeter on the scale represents about  $\frac{1}{3}\%$  of the total volume of water removed from a 100 gm. sample of glass beads.

To minimise discharge errors as the meniscus is moved back and forth, the tube was treated with 'Repelcote' which is a 2 per cent v/v solution of dimethyldichlorosilane in carbon tetrachloride for giving a water repellent surface to glass.

#### 5.2.4 Vacuum System

Displacing pressures are applied by vacuum using the system shown in Fig. (22). A vacuum pump evacuates a large container (approximately 45 litres) in which vacuum is controlled by a two valve air bleed system (one coarse, one fine). The pressure across the sample is measured by a 250 cm. water or a 76 cm. mercury manometer. Accuracy of control of better than  $\frac{1}{2}$  cm. of water was obtained.

Using the large cell, previously described, it is possible to use positive pressure for displacement, this was not attempted.

### 5.3 CALIBRATION OF THE APPARATUS

#### 5.3.1 Calibration of the Measuring Tube

The measuring tube was calibrated for volume after treatment with the silane solution. The tube was filled with distilled water which was run out in small amounts which were collected and weighed. Two calibrations were performed, each with 17 readings, which showed that 14.304 cms. length on the scale was equivalent to 1 cc. with a standard deviation of .27 cm. on the individual readings. No variation in diameter along the length of the tube was detected.

The calibration was carried out at room temperature of 18°C which was the temperature usually obtaining during all the experiments.

### 5.3.2 Correction to Pressure Readings

To obtain the pressure stress on a sample correction must be made to the manometer readings for the height of the sample above the measuring tube, and for the slight capillary pull of the meniscus in the measuring tube. These two corrections may be measured in one operation. The burette connected to the measuring tube is clamped near to the cell. Water in it is allowed to flow into the measuring tube until an equilibrium is reached between the level in the burette and the meniscus in the measuring tube. The water level in the burette is now at the same height as the measuring tube with the height equivalent of the capillary effect in the measuring tube included. The difference in levels between the top of the support plate in the cell and the water level in the burette can be measured to within a millimetre. This value is a constant for each type of cell and must be added to all pressure readings from the manometers to give the pressure stress on the sample.

In addition correction must also be made for the height of the water level inside the sample during an experiment. This varies with the saturation, being equal to the sample height at 100% saturation, and zero at 0% saturation. For a full correction therefore the capillary pressure curve would have to be known beforehand. But with samples used here, which are less than 1 cm. thick a correction of sufficient accuracy may be made by adding half the height of the bed. This correction therefore applies strictly only at about 50% saturation, but this is the most

vulnerable part of the curve from the point of view of error in the pressure readings. Some experiments were performed on beds of up to 5 cm. thick to test this assumption.

### 5.3.3 Correction to Volume Readings

The measurements of displaced volume of water must be corrected for the flexion of the support plate. For this a calibration curve was obtained for each plate by performing an experiment in the usual way but without a sample. A curve may then be drawn of volume of water displaced against pressure from which interpolated results can be used to correct experimental data, making the assumption that the presence of a sample will not affect the calibration. This is reasonable for the rigid support plates, sintered metal and glass, but when a plastic membrane is used care must be taken to seat this on its support plate by employing a high initial pressure. This difficulty was never successfully overcome on the large cell when using a plastic membrane, and this led to the construction of the other cells used when high displacing pressures were required.

Calibrations were performed several times on each support plate and were found to be reproducible. The maximum correction applied is about 3% of the void volume of a sample of 100 gm. of glass beads. The 'milli-pore' cell did not require a calibration.

One short-coming of disc A was detected during calibration. The dead zone at the edge of the disc where the Araldite sealed it in the perspex holder tended to retain water which extended the initial drainage period for the experiments to about 30 minutes. The modification introduced in Disc B overcame this as it allows full use of the whole area of the cell.

#### 5.4 EXPERIMENTAL PROCEDURE

Before an experiment is commenced the apparatus must be assembled. This involves ensuring that the support plate is fully saturated and that no air bubbles are retained beneath it. The latter point was taken care of, as mentioned, by assembly of the various components underwater. To saturate the support plate it was kept in a high vacuum for several hours, then air free distilled water was flooded in on to it. The support plate was not taken out of the water during assembly. This procedure need not be performed often, as it is possible to remove samples from the cell without dismantling it.

To obtain capillary pressure curves after the apparatus is assembled the following procedure was used.

The sample was weighed and prepared as a slurry with distilled water using an ultrasonic probe. This ensured that no air becomes trapped in the beads and the whole sample is thoroughly wetted. The sample was then introduced into the assembled cell which contained a few centimetres of water, by being washed down a funnel and tube projecting under the surface of the water in the cell. This prevents inclusion of air in the packing. The shallow depth of water in the cell inhibits segregation as particles sediment on to the support plate. Care was taken that none of the sample was lost in these operations as its weight is important in calculating the results.

The surface of the sample was then levelled out under water using a wire probe. This was found to give a reproducible packing with a porosity of around 39% for mono-size beads. A more dense reproducible packing was obtained by vibrating the bed formed in this way with an electric vibrator, which gave porosities of around 35%.

All glass bead samples were tested with both of these types of packing. When beds of glass beads with a greater depth than a centimetre were used, the reproducibility of the packing is more difficult to ensure. Therefore in experiments of this sort only the dense packing was used and this was formed by vibrating the bed as the glass bead slurry was run into the cell.

Having prepared the packed bed the excess water above it was allowed to drain through into the measuring tube. This is equivalent to applying a constant pressure of the height difference between the sample and the measuring tube, to remove the water. This difference in levels is small compared with the capillary height of the samples used but provides a starting point when the packing may be taken to be just 100% saturated. Usually about 15 minutes was allowed after the meniscus in the measuring tube had stopped moving to ensure the accuracy of this point.

The capillary pressure curve is then obtained by measuring the incremental volumes of water removed by increments in displacing pressure. The equilibrium at each pressure level can be found by following the meniscus in the measuring tube and waiting until movement had ceased. The time required for this depends on the size of the pressure increment, the amount of water to be removed, the saturation of the bed at that point and the pore size of the bed. This can be as much as an hour, but by careful planning of the pressure increments used, a full curve can be traced in about 6 hours.

At the end of the experiment, when no more water can be removed by increasing the pressure, several samples of the bed were taken without relaxing the pressure, using a scoop. A moisture content determination was made on each sample by drying and weighing. Care

was taken in this operation to ensure that no beads were lost, all may be then returned to the cell afterwards and a repeat of the experiment may be made.

The data taken of, weight of sample, total volume of water removed after corrections have been made, and the moisture content at the end of the experiment together with the specific gravity of the beads, can be used to calculate the porosity of the bed. The surface tension of the water used was checked by the Du Nouy ring method.

The procedure followed in the experiments using filter aid material was slightly different. Precautions against segregation by sedimentation as the cake was being formed in the cell were necessary, because of the wide particle size distribution of the material. This was done by using a thick slurry which was poured directly on to the support plate. The weight of slurry used was found by difference, and the dry weight of solid found by a material balance by following the amount of water removed in each of the subsequent operations. When the cake was formed its surface was pricked with a pin to puncture any surface layer of fines which could not be avoided and which would inhibit drainage. This technique was used by both Gray (1958) and Harris (1959) in their experiments on fine coal samples. The rest of the procedure was the same as previously described.

#### 5.5 EXPERIMENTS PERFORMED

Capillary pressure curves have been measured for a series of samples which may be divided into three types. Mono-size packs of glass beads, three component mixtures of glass beads and samples of filter aid material. All the experiments on glass beads were

performed with both of the two types of packing previously described, i.e. poured or vibrated. Bed depths were of the order of half a centimetre except where special experiments were conducted to test the correction to the pressure readings for bed depth. In these cases depths of up to 5 cm. were used.

Four different mono-size packs of beads were used with a range of sizes. Two of these, 36/52 and 150/120, were produced by a sieve cut from the appropriate grade of glass bead. The other two, 52/60 and 72/85, were prepared by elutriation of a sieve cut to produce a narrower distribution. Size distributions were obtained by microscope counting and are given in Appendix III. The samples are labelled by the sieve cut producing them.

Four three-component mixtures of glass beads were also used. These were prepared from mono-size packs which had had their mean diameter determined from a microscope count. The details of these mixtures are also given in Appendix III. The sizes of beads used in these packs were not very different, the main variation between the packs being in the spread of the distribution of sizes. The mixtures are labelled 1 to 4 in ascending order of the spread of their distributions.

Five different samples of filter aid material were used, all from the Johns Manville Celite range. They were, Celite 560, 545, 535, 503 and Hyflow Super Cel. Particle size distributions taken from the manufacturers literature are given in Appendix III as a guide to the differences. The surface areas of these samples were measured both by a Fisher Sub-sieve Sizer, which is a permeability method, and also by a Strohliem gas Adsorption Area Meter.



## 5.6 RESULTS AND DISCUSSION

### 5.6.1 Experimental Results

#### 5.6.1.1 Reproducibility

Each capillary pressure curve obtained for the glass bead samples is the result of at least two experiments in both porosity conditions used. With the exception of those for mixture 4 which were only done once for each porosity, and the 36/52 and 150/120 packs which were tested more times, as the results of the deep bed experiments are also included.

The reproducibility as shown by the figures may be seen to be satisfactory, with the exception of the initial part of the curves near saturation for the thick bed samples. It was realised in using the pressure correction for depth of bed that this would only apply strictly to the horizontal part of the curve, this discrepancy is therefore not unexpected. The correction may be seen to be successful in the horizontal part of the curves.

In the experiments using filter aid only the curve for Celite 560 was repeated to test reproducibility. This shows consistency. All experimental results are tabulated in Appendix V.

#### 5.6.1.2 Porosity Variation

The effect of porosity variation on capillary pressure curves can be seen most clearly in Fig. (27) which is a plot of capillary pressure against volume of water removed for a given weight of the 52/60 bed in poured and vibrated packing. This is taken as representative of the other glass bead samples. It can be seen that the curves tend to retain their shape but higher porosities give larger pore sizes and lower capillary pressures than lower porosities, and the volume of the pore space is also greater. The normalisation of capillary pressure curves has been described (section 3.4) Fig. (28) and (29) and (30) show the first stage in

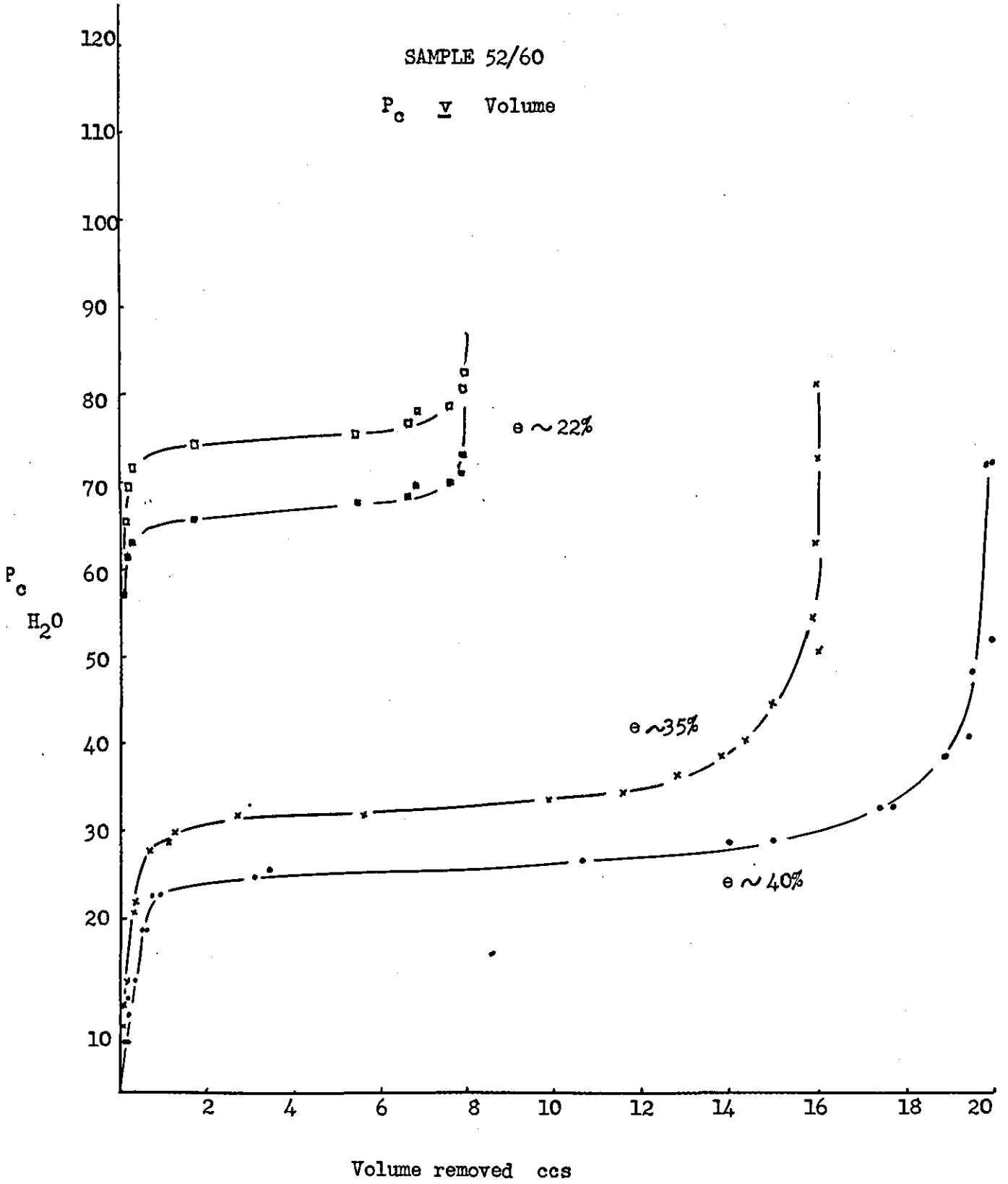


Fig. (27)

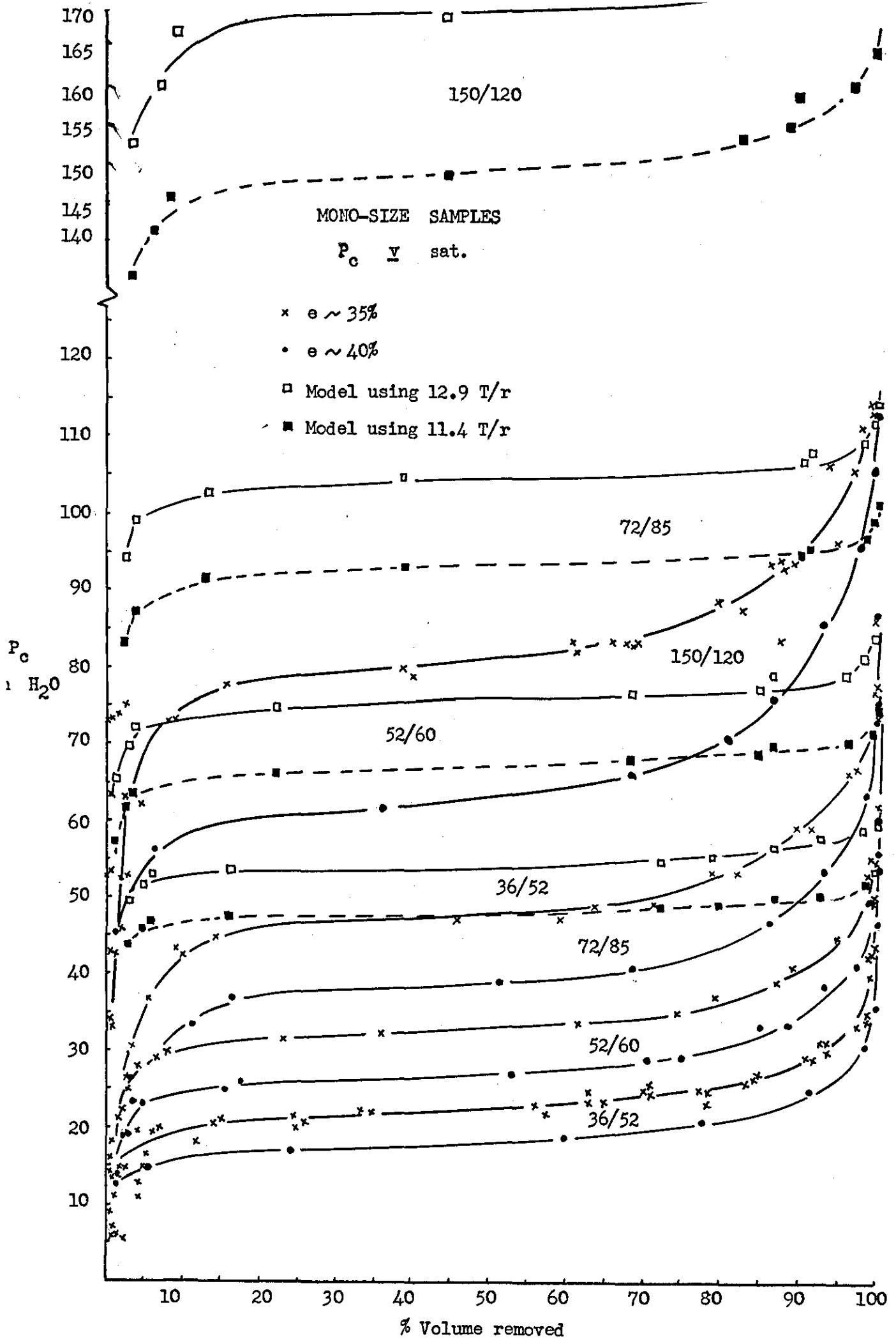


Fig. (28)

MIXTURE 1 and MIXTURE 2

$P_c \underline{v}$  sat.

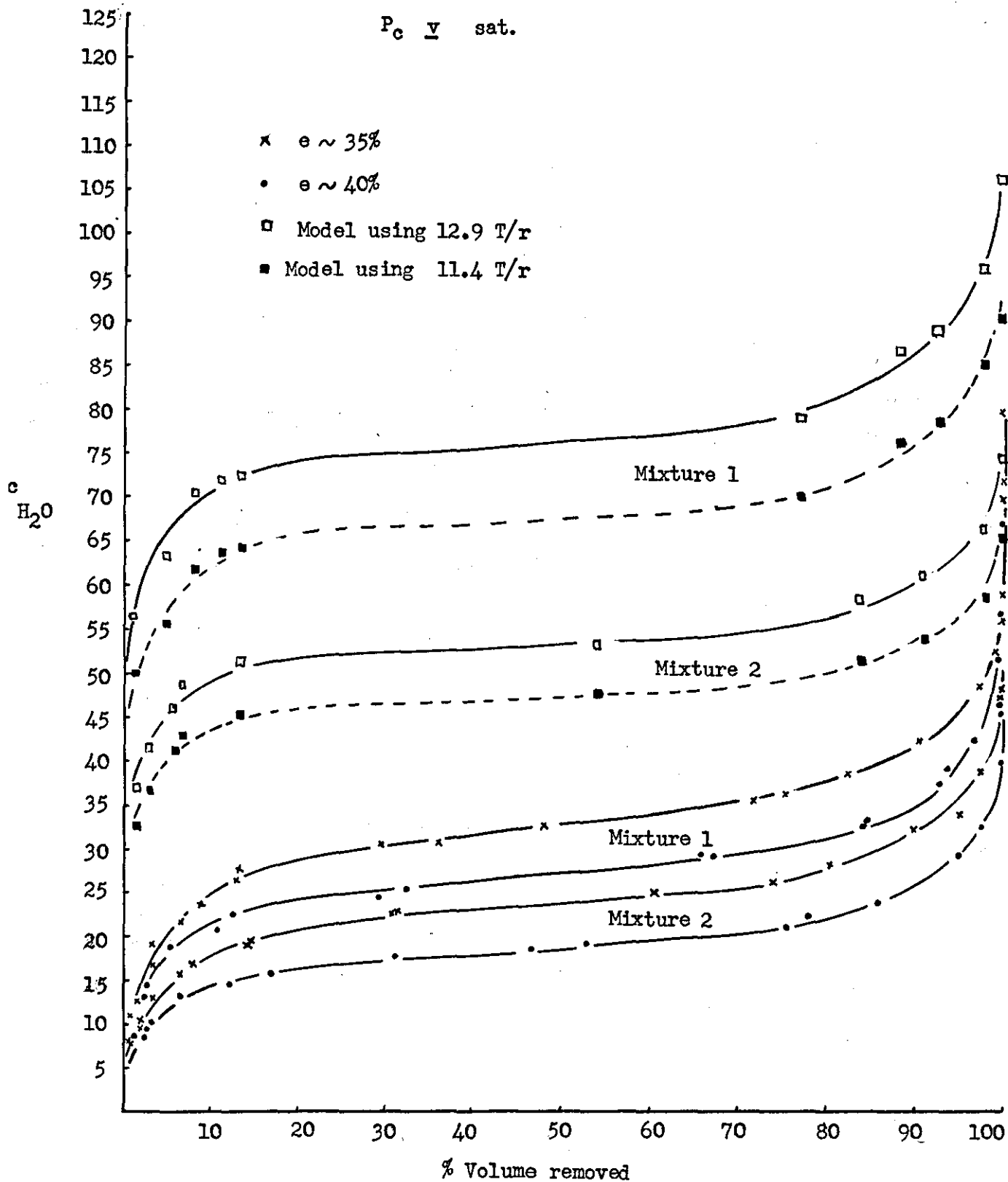


Fig. (29)

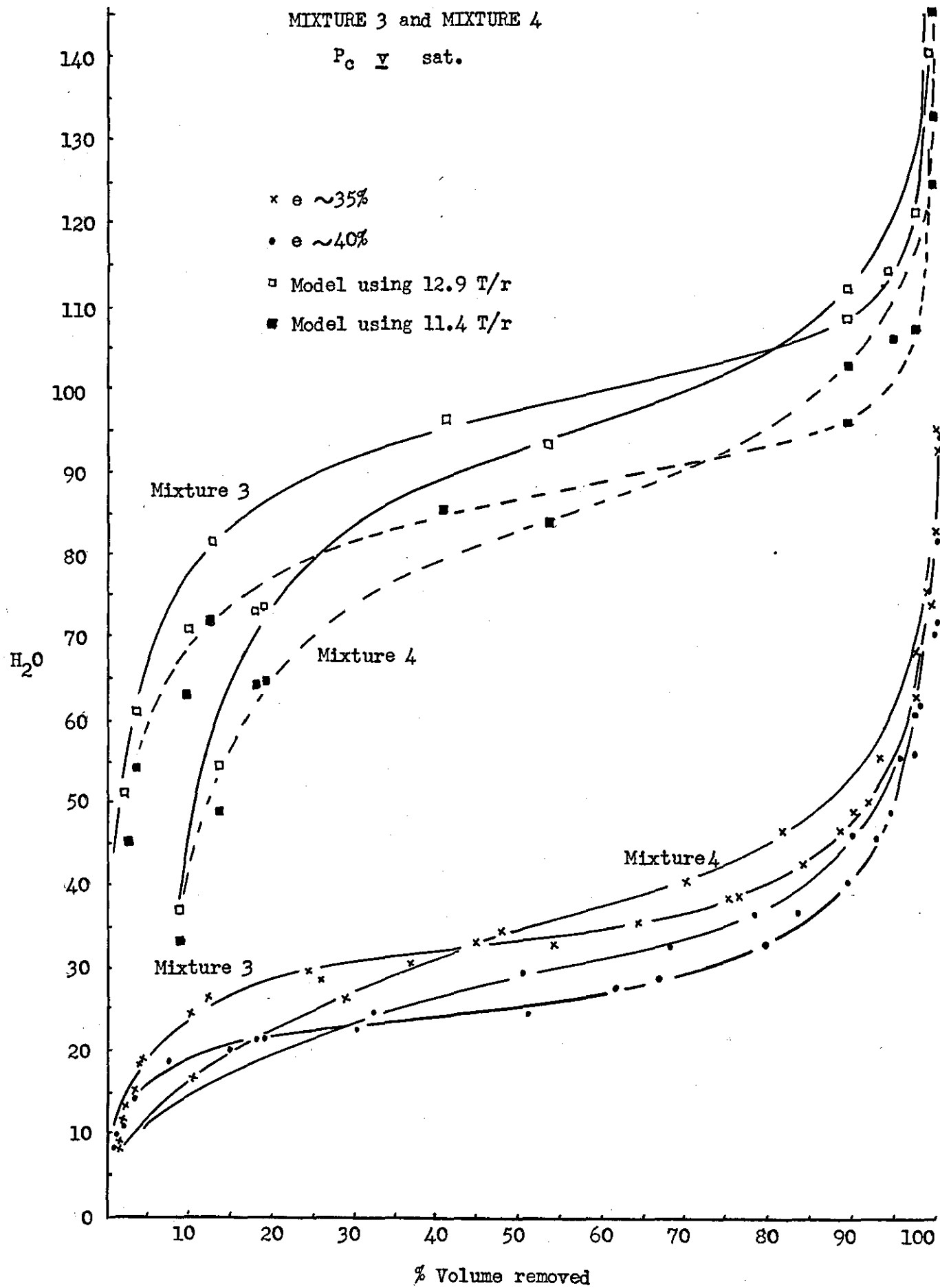


Fig. (30)

this where the results of displaced volumes are plotted as percentages of the total volume displaced in a run versus capillary pressure for the various samples. The similarity in the shapes of the curves for different porosities is now more easily seen. The next stage in the normalisation procedure can be followed in Figures (32), (33), (34). Here all the results for the various classes of samples used have been plotted. The figures show that the correlation

$$\frac{P}{T} \frac{e}{(1-e)} \text{ versus saturation}$$

is successful in reducing capillary pressure curves for a given sample to the same curve for any porosity. This function has not been applied to the filter aid samples since each is a distinct material and each have been tested at only one porosity. If plotted the correlation would only show the curves in their respective positions as on a plot of capillary pressure versus saturation.

#### 5.6.1.3 Surface Area

It was previously mentioned in section 3.3 that it is possible to calculate surface areas from capillary pressure curves using the relationship

$$A = \frac{1}{T} \int P \, dv$$

If curves are plotted in terms of saturation and capillary pressure, expressed in terms of centimetres of fluid, it is necessary to modify the equation. For example

$$P = h \rho g$$

$$\therefore A = \frac{\rho g}{T} \int h \, dv$$

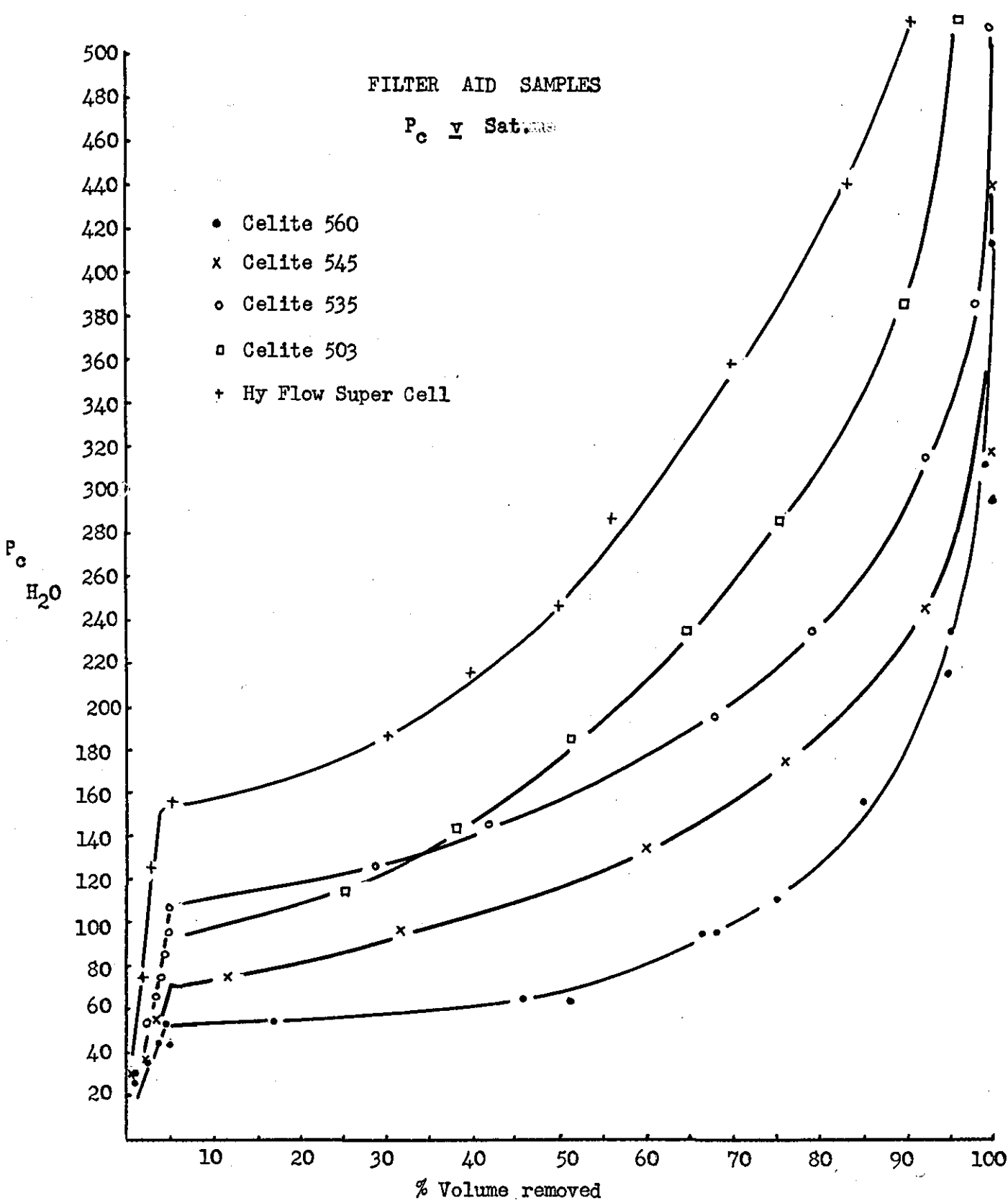


Fig. (31)

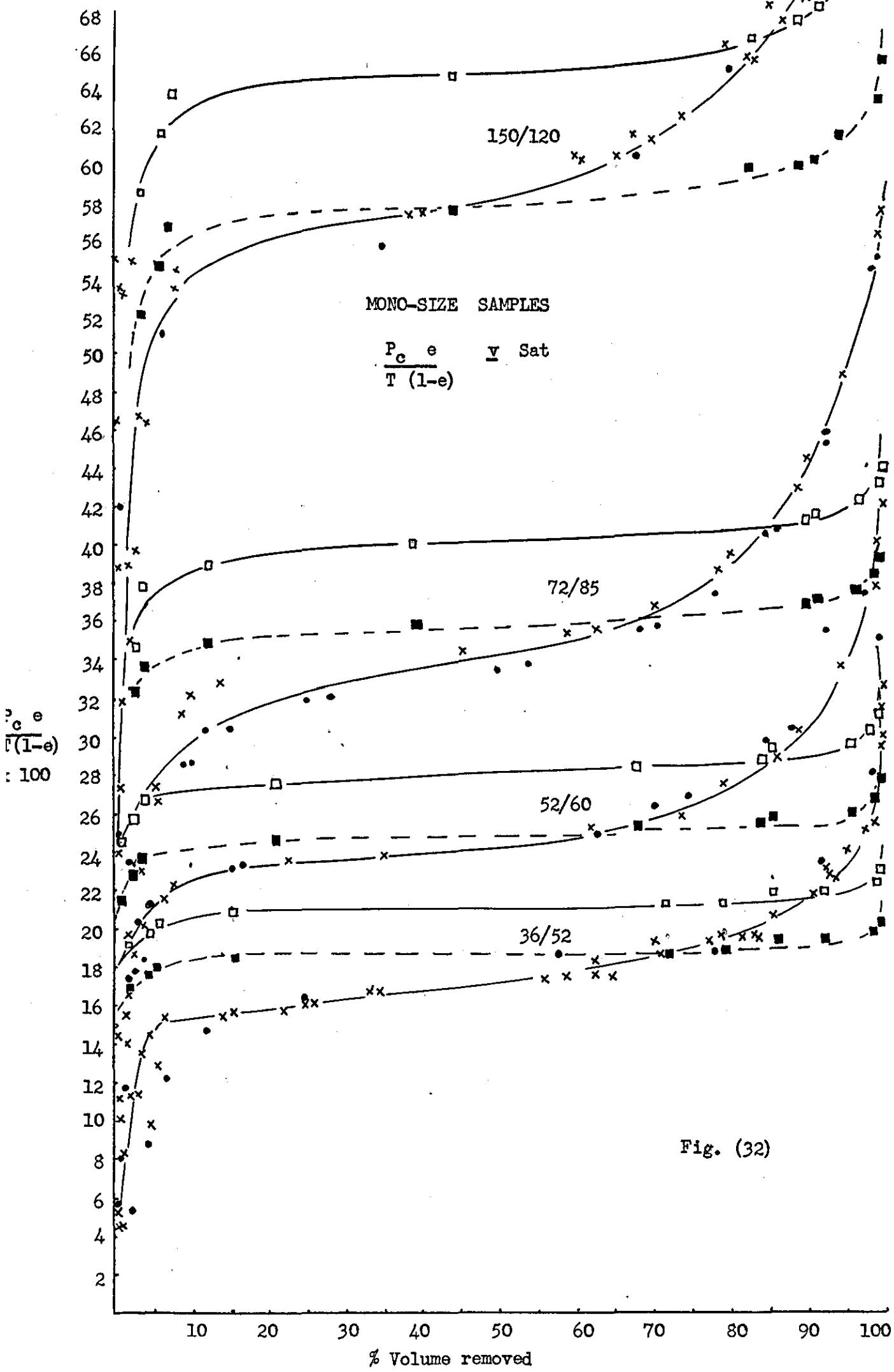


Fig. (32)



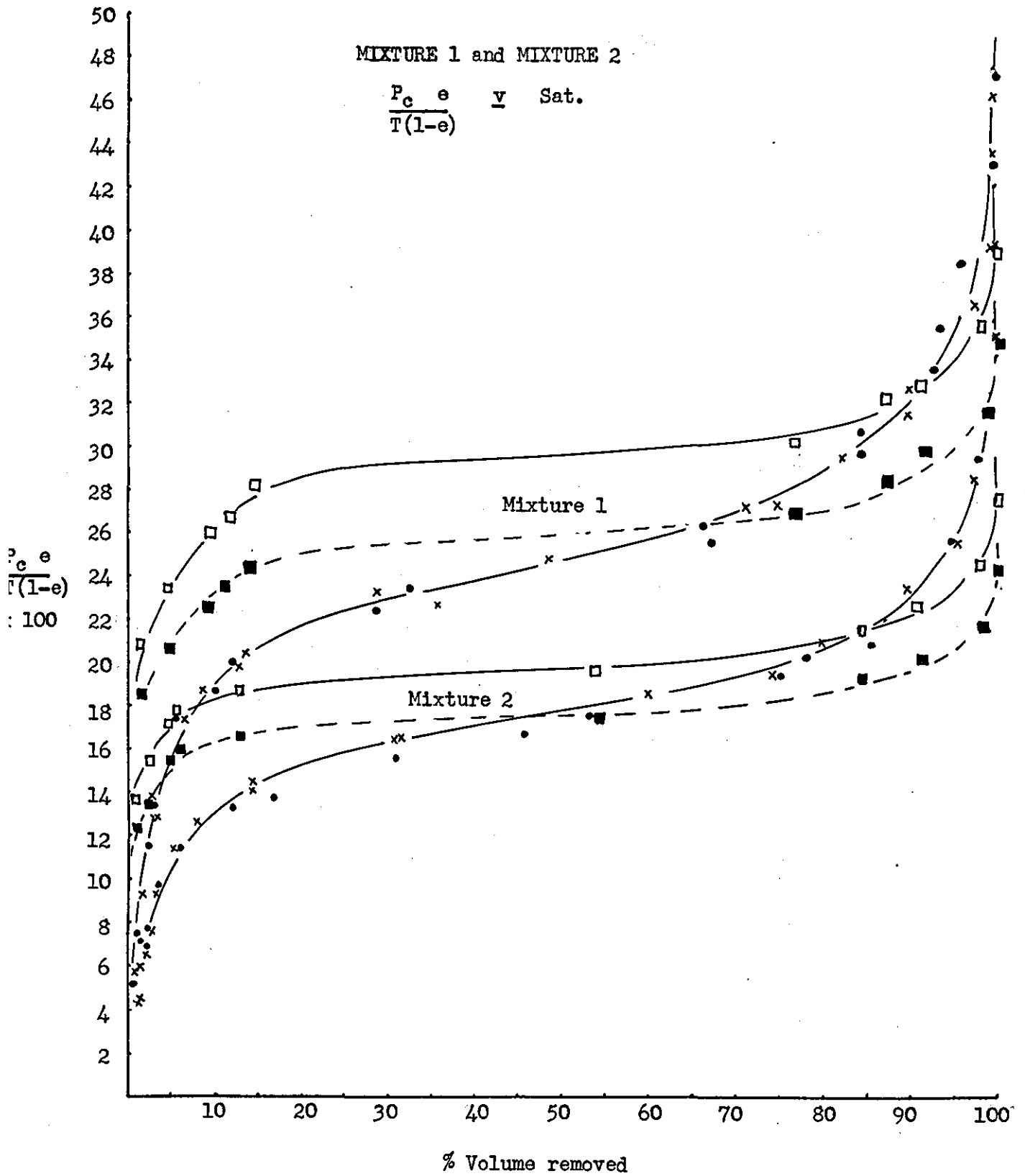


Fig. (33)

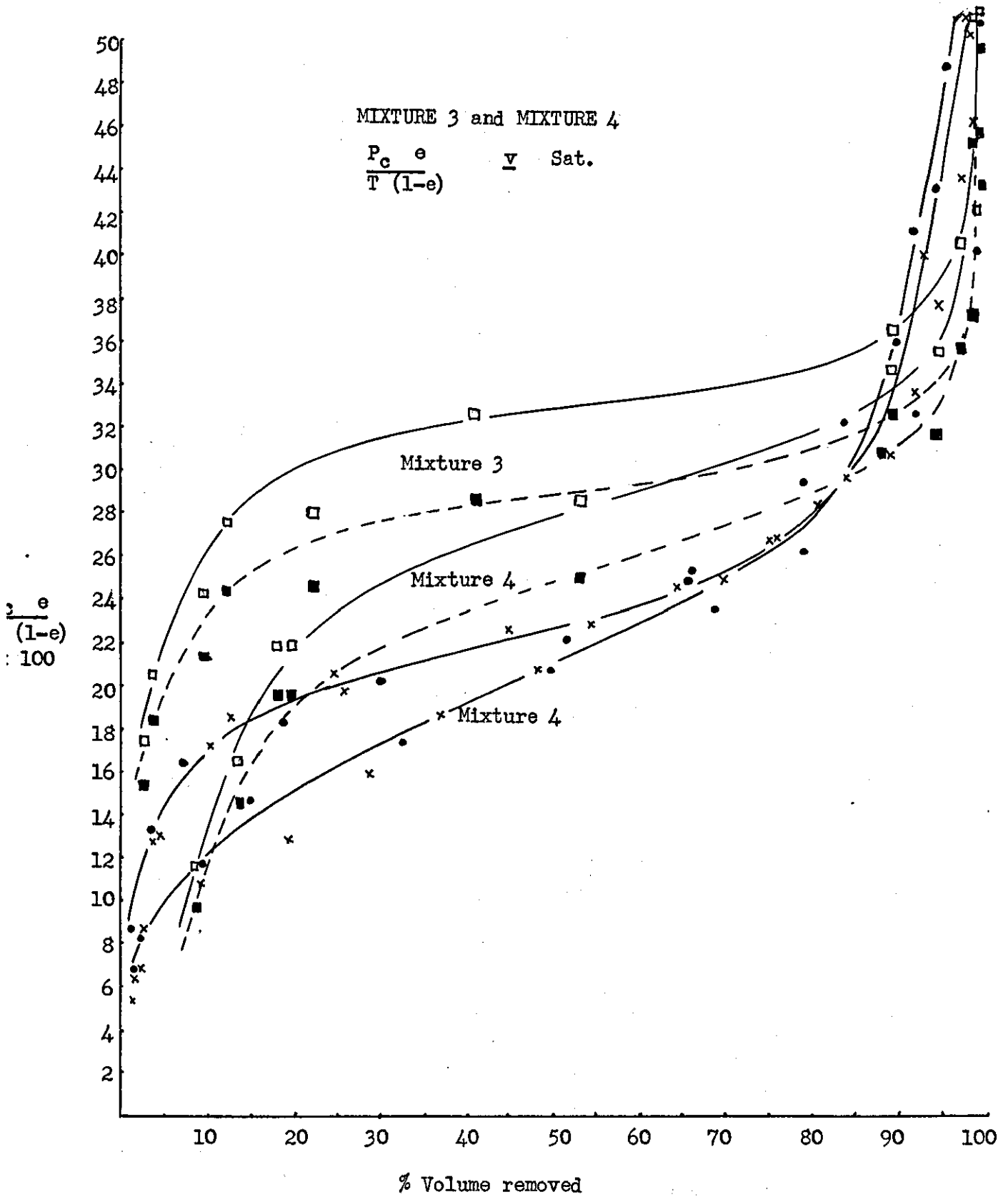


Fig. (34)

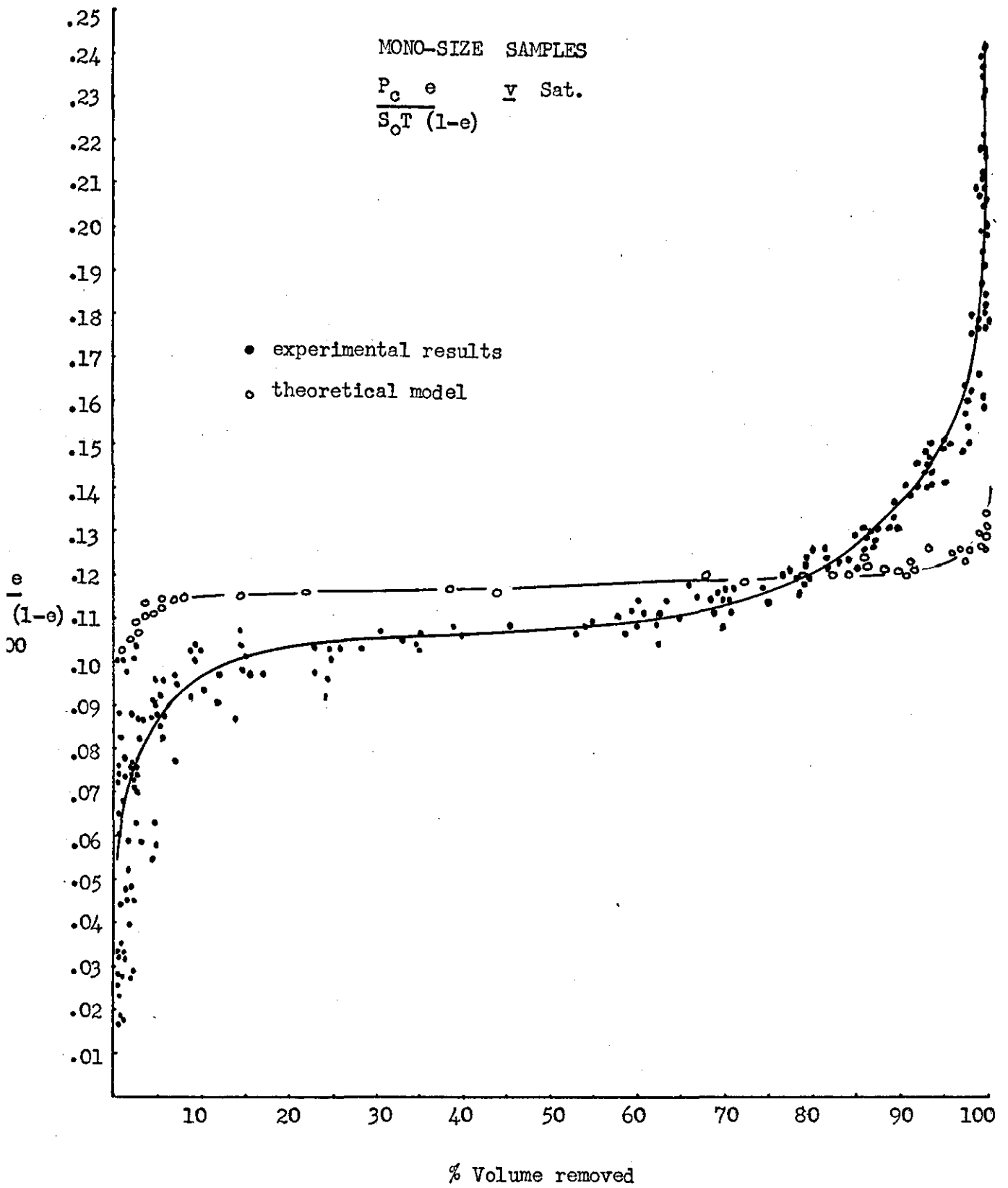


Fig. (35)

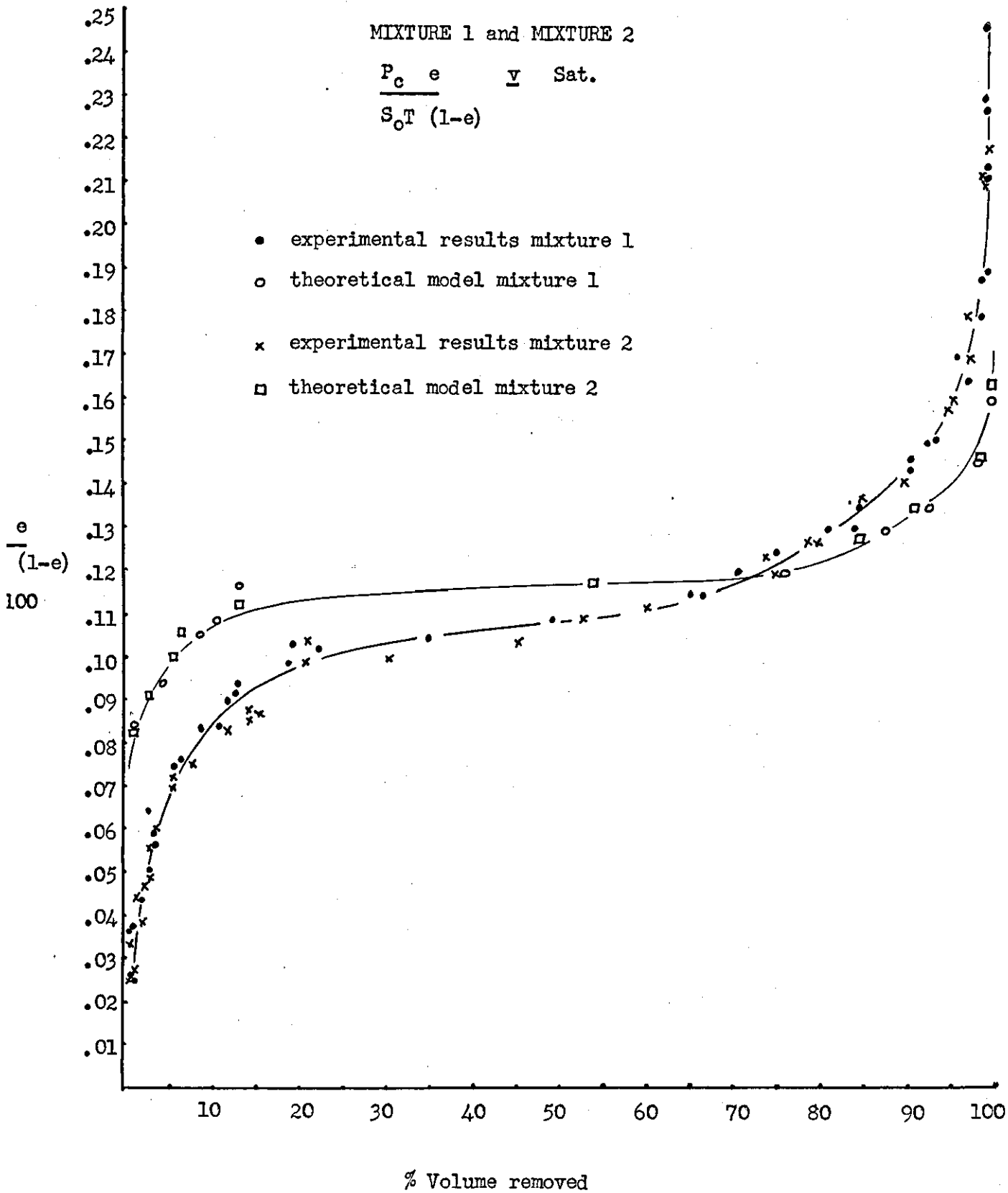


Fig. (36)

The relationship between saturation (as defined here) and volume of fluid is easier to derive if a 'pseudo' porosity ( $e^*$ ) is defined. This is taken as the porosity of a bed calculated by assuming the volume of fluid removed in capillary pressure experiment is the void volume of the pack. That is the residual moisture is considered as part of the solid phase which is the same assumption as that used in calculating saturations. Therefore

$$e^* = e - \frac{p_g}{p_w} \frac{R_w}{100} (1 - e)$$

in which ( $R_w$ ) is the residual moisture expressed as a weight percentage. Therefore for a given sample the volume of fluid associated with a value of saturation may be given as

$$V = \frac{S}{100(1 - e)} \frac{e^*}{p_g} \frac{Wt}{p_g}$$

therefore 
$$A = \frac{e^*}{(1 - e)} \frac{p_w g}{T} \frac{Wt}{p_g} \frac{1}{100} \int_0^{100} h \, dS$$

or 
$$S_0 = \frac{e^*}{(1 - e)} \frac{p_w g}{T} \frac{1}{100} \int_0^{100} h \, dS$$

Surface areas have been calculated from the curves using a straight line interpolation between the points and the above expression. These results are given in Table V and VI together with surface areas which for the glass beads have been calculated from microscope counts, and for the filter aid samples were measured experimentally by both a permeability method, using a Fisher Sub-Sieve Sizer, and a gas adsorption method, using a Strohliem Gas Adsorption Area Meter.

TABLE V

Specific Surfaces of Glass Bead Packs ( $\text{cm}^2 / \text{cm}^3$ )

Sample	Calculated	Results from Theory using		Experimental Results				
		11.4 T/r	12.9 T/r					
36/52	162.3	157.1	177.9	160.3	158.4	159.4	162.2	175.6
				177.8	161.2	159.2	152.4	
52/60	236.1	210.4	238.1	230.0	222.4	240.8	233.7	
72/85	319.6	304.1	351.2	315.2	313.3	310.0	311.2	
150/120	514.3	491.2	556.1	520.8	538.6	547.1	529.9	
				533.0	539.2	538.7		
Mixture 1	233.8	218.3	246.8	218.4	228.7	227.3	231.0	
Mixture 2	160.9	149.7	169.2	167.3	160.4	160.6	159.9	
Mixture 3	226.4	239.2	271.0	216.9	213.3	227.2	231.0	
Mixture 4	202.2	199.1	225.1	196.9	196.4			

TABLE VI

Specific Surfaces of Filter Aid Samples ( $\text{cm}^2 / \text{cm}^3$ )

	Gas Adsorption	Permeability	Experimental
Celite 560	13,400	9,100	7,164 7,414
Celite 545	14,700	11,900	9,733
Celite 535	20,800	13,300	12,389
Celite 503	24,800	18,200	14,529
Hy flow Super Cel	43,500	22,600	18,823

The specific surface<sup>s</sup> calculated from the capillary pressure curves compare quite well with the calculated specific surfaces. They are, in general, lower than the results from microscope count data, which is to be expected since what is measured is the area of the air/water film which will not exactly be that of the solid bed, due to the existence<sup>e</sup> of residual moisture.

The results for the filter aid samples given in Table VI show less good agreement. Comparing the two standard laboratory methods, the gas adsorption<sup>p</sup> method, as expected, gives much higher specific surfaces than those given by the permeability method, as it includes minute cracks and pores on the particles which are not accessible to the permeability method. The permeability results are closer to those from the capillary pressure curve but cannot be taken as absolute values for comparison since in their calculation, using the Kozeny-Carman equation, a factor is introduced which cannot be independently checked. The value usually assumed could be in error, bearing in mind the irregular nature of the particles, the high porosity of the bed (approximately 88%) and the wide size distribution. Nevertheless there is correspondence between these results and those calculated from the capillary pressure curve. The error is again on the expected side and in this case, since residual moistures of around 20% of the void volume, this is more exaggerated.

It is therefore possible to conclude that surface areas calculated from the capillary pressure curve compare with those calculated from microscope counting for glass beads, and from permeability for filter aid material which is a very extreme case. The errors may be in part attributable to the surfaces in the bed covered by residual moisture at the end of a capillary pressure

curve. The fact that the surface area measured by this method is comparable with surface areas involved in permeability relationships is important for further extension.

#### 5.6.1.4 Full Correlation

The first steps in the correlation of capillary pressure curves has been covered and illustrated in Figures (32), (33), (34). It is now possible to introduce the full correlation given by Carman (1941) and in section 3.4 where

$$\frac{1}{T} \frac{P}{S_0} \frac{e}{(1-e)} \quad \text{versus Saturation}$$

is plotted and normalises all capillary pressure curves. It is obvious that dividing similar shaped curves by the area underneath them will always give a single curve on replotting. In this case however it has been demonstrated, both theoretically in section 3.3, and experimentally, that the area under the capillary pressure curve has a physical meaning. Its use in this way is therefore reasonable.

The correlation applied to mono-size packs is given in Fig. (35) and for the 3 component mixtures and filter aid samples in Figures (36), (37)&(38). In each case the correlation normalises all the curves between the axes. These three sets of curves are all plotted together on Fig. (40).

It was realised that the correlation does not affect the shapes of capillary pressure curves, it merely moves them up and down the pressure axis to make them co-incident. The mono-size packs all have a similar particle size distribution, and therefore pore size distribution, and hence they all correlate to one curve. This curve is flat showing a predominantly uniform pore size in the packs. The particle size distributions in the 3 component packs



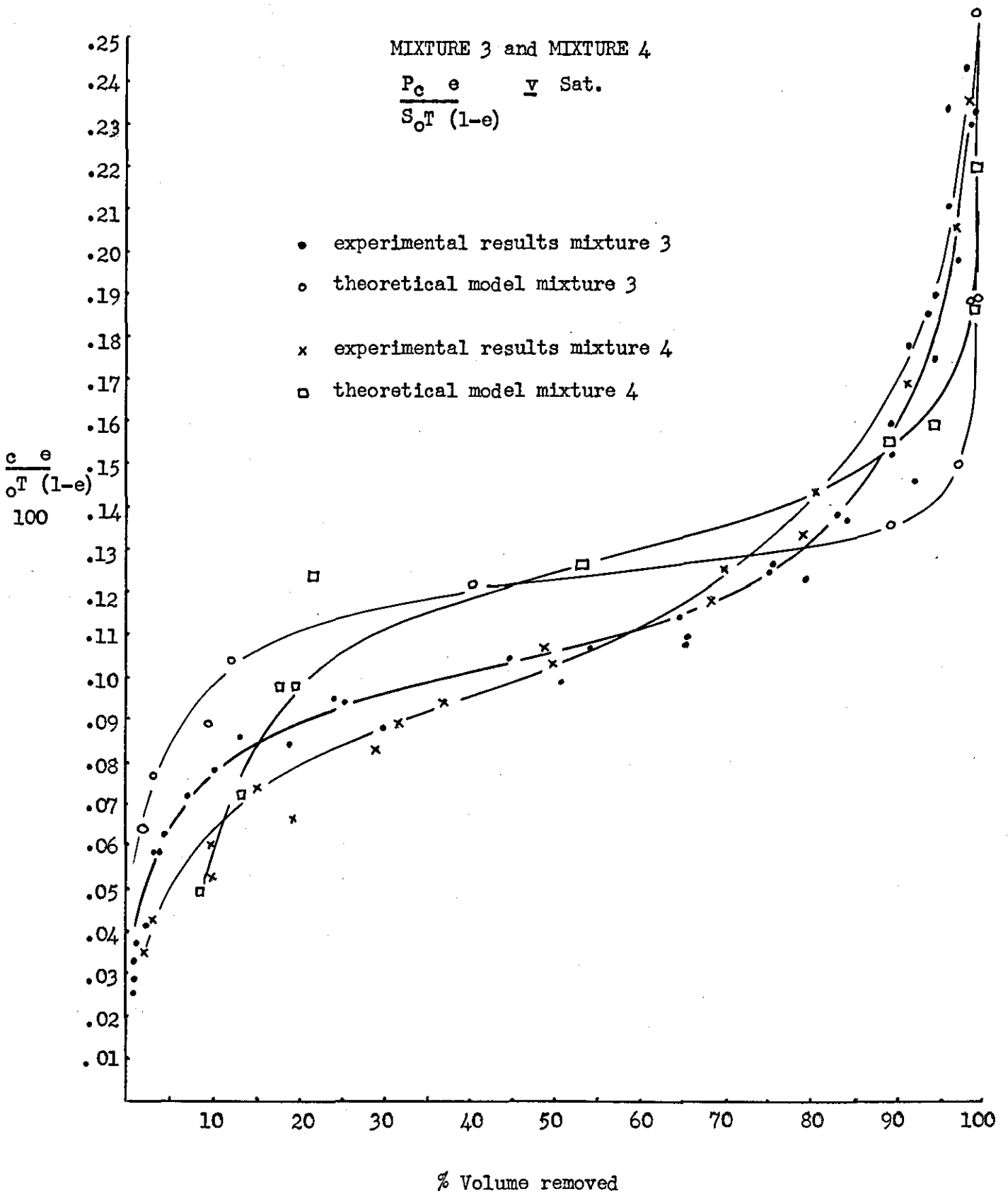


Fig. (37)

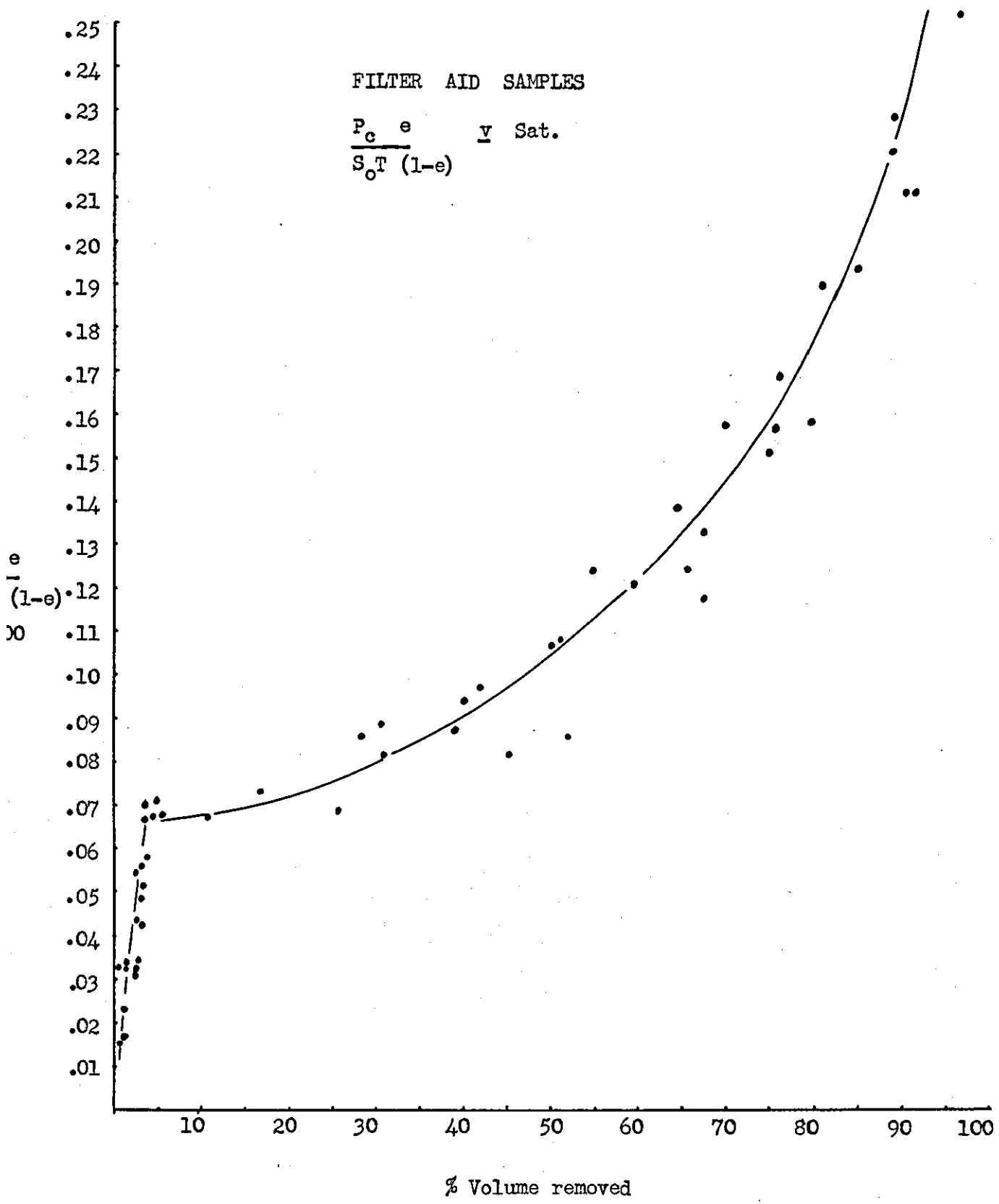


Fig. (38)

RESULTS FROM THEORETICAL MODEL

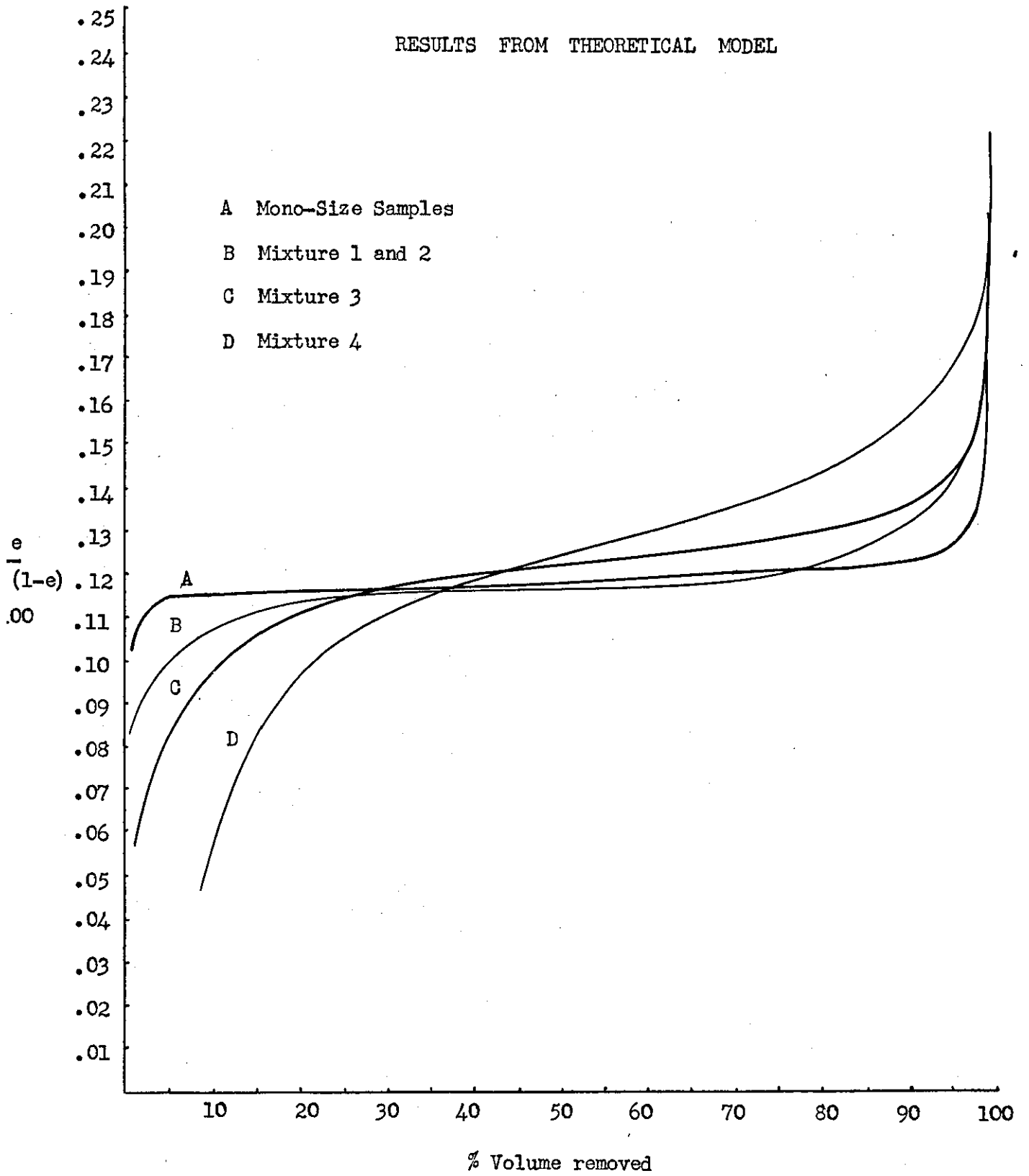


Fig. (39)

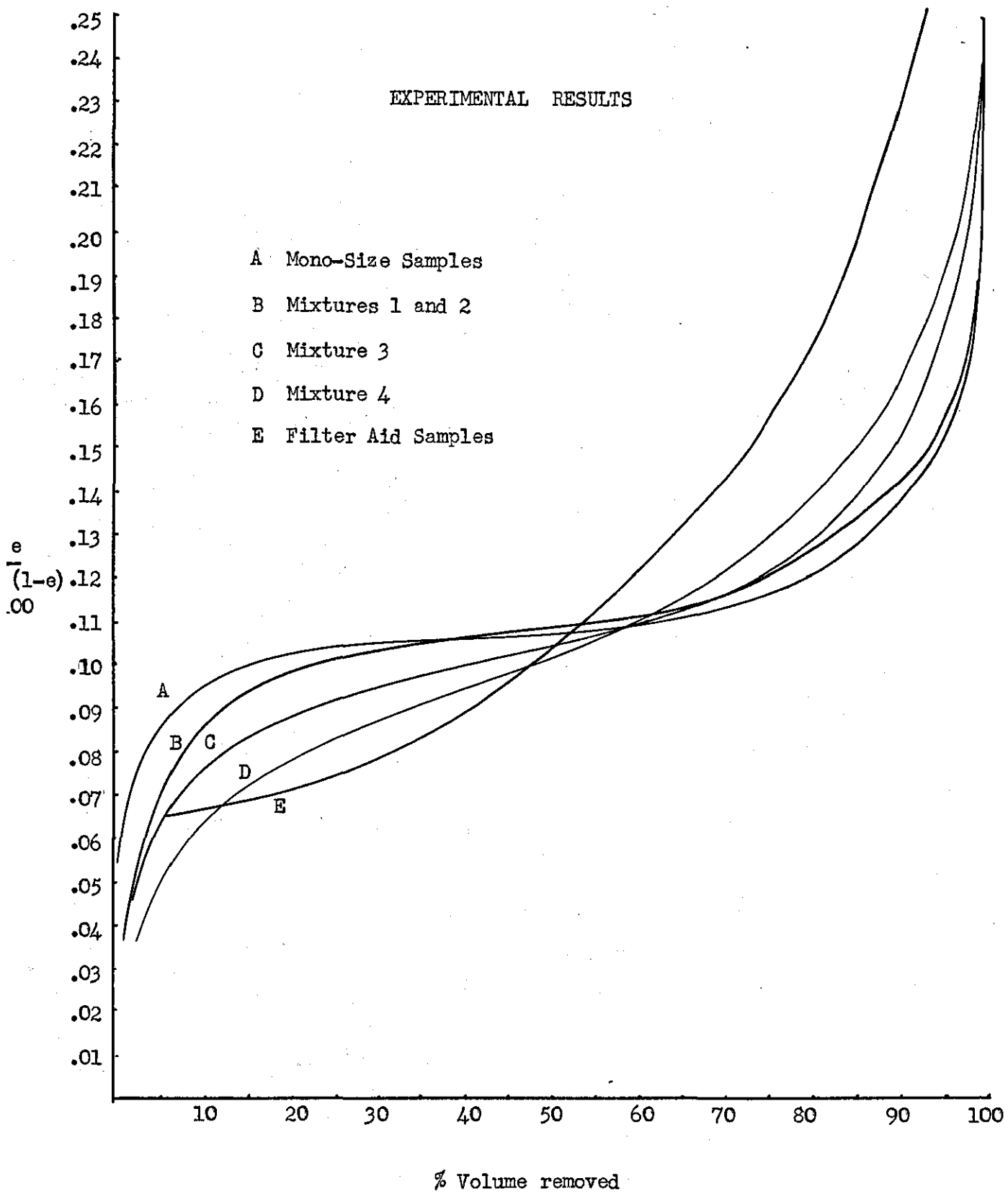


Fig. (40)

were not the same and the correlation in this case shows a family of curves for the different samples. It may be noticed that the wider the spread of sizes in the pack, the wider the pore size distribution indicated by a greater inclination of the middle parts of the curves to the horizontal. The results for the filter aid samples follow this. These samples have a very wide particle size distribution and give a very wide pore size distribution, the irregular shape of the particles also promotes this dispersion. The fact that one curve can be drawn through all the points plotted for the various grades of filter aid indicates the similarity of the pore size distribution of the various grades.

These effects may be seen more closely in Fig. (40) where all the correlation results are plotted on the same graph. This correlation which uses the same function as the Kozeny-Carman equation for permeability indicates both the success and the failure of the equation. The correlation shows that the function does give a reasonable mean pore size in that all the curves for the different samples come to the same point at around 50% saturation. However the correlation cannot account for the spread of pore size distribution as is shown by the shapes of the curves. This point is <sup>u</sup> pursued at greater length later.

#### 5.6.1.5 Summary

The capillary pressure curves measured experimentally have been shown to be reproducible.

The correction applied to displacement pressures to account for the depth of the bed has been shown to be successful for the horizontal part but not the initial part of each curve.

Specific surfaces calculated from the capillary pressure curves compare well with surface areas obtained by other means and are equivalent to the surface areas involved in permeability equations.

The correlations introduced in the literature survey have been shown to be successful in reducing all capillary pressure curves for a given particle size distribution to one curve. The correlation also emphasises the differences due to pore size distributions.

#### 5.6.2 Results from Theoretical Model

##### 5.6.2.1 Porosity Correlation

Having justified the use of the correlation method on experimental results it is now permissible to use the methods in comparing the experimental results with the results from the theoretical model. This is made necessary because the model refers to a dense random packing of around 20% porosity which can never be obtained experimentally. It has been pointed out in section 3.4 and section 4.2 that the porosity of a pack of particles depends both on the mode of formation of the packing and the properties of the particles themselves. The porosity of a given pack can be taken to be determined by a balance of the forces causing lessening of porosity, i.e. vibration compaction, and the ability of the particles to rearrange themselves. In practical cases the lack of freedom of movement of the particles to rearrange themselves is the main limit to porosity reduction below about 30%. The Wise model may be taken therefore to predict the pore space in a pack of particles not subject to this restraint and able always to rearrange themselves to the limit of porosity determined by the particle size

distribution. It follows from this also that a particle size distribution which will give the most dense packing is that which gives the best chance of the particles to flow and arrange themselves and is not a static geometrical problem. The Wise model cannot do this but the porosity results do tend to follow the experimental results (Mixture 3 and 4).

The capillary pressure curve results from the theoretical model have been plotted on the appropriate figures 27 - 40, and are tabulated in Appendix V. In Fig. (27) for the 52/60 bed, which is taken as representative of the other results, capillary pressure versus displaced volume has been plotted. The model does not provide absolute values of volumes removed and this data has been calculated, for comparison purposes, from saturation data using a value of 100 gms. for the weight of the bed, which is approximately that used in the experiments. The trend of the curves for porosity variation is demonstrated. This is continued in Fig. (28) to (30) where the saturation axis is normalised. The first stage of the correlation plotted in Figs. (32 - 34) shows however that the model predicts too high a capillary pressure (or too small a pore size) for the porosity of the bed. That is the assumption that the pressure required to blow a bubble through a group of three spheres can be calculated from the size of sphere which will just pass through the assembly gives an over estimate, and the pore size governing this is slightly larger. Alternatively the value of capillary pressure calculated may be correct and the porosity calculated by the model be too small.

This first conclusion is supported by the experimental results of both Haines (1930) and Hackett and Strettan (1928) who

found a value of 11.4 T/r experimental for this pressure as opposed to 12.9 T/r calculated on the assumption used. A correction of 11.4 / 12.9 has been applied to the capillary pressures on the theoretical curves and is shown on the figures in dashed lines. The correspondence between theory and experiment is improved.

#### 5.6.2.2 Surface Area and Residual Moisture

To calculate specific surfaces from these theoretical curves an estimate is required of the residual moisture existing in a pack of spheres at around 22% porosity. The experimental results for porosity and residual moisture are too close together to allow any predictions on this basis, it may however be done theoretically.

The change in residual moisture with porosity is governed by two opposing effects. As a packing becomes more dense the number of contact points per particle increases and also the values of capillary pressures in desaturation rises. The first effect will tend to give an increase in residual moisture as porosity becomes lower, since there will be more pendular rings formed. The second effect will tend to reduce residual moisture as porosity becomes smaller, since a pendular ring in a packing takes up a size dependent on the capillary pressure existing at its formation being smaller for higher pressures. To make calculations for these effects three relationships are required. Firstly the volume of a pendular ring as a function of its formation pressure, secondly the variation of capillary pressure with porosity, and thirdly the variation of co-ordination number with porosity. The first has been given in tabular form by Fisher (1926) for capillary pressures expressed in terms of T/r. The second may be given by the correlation

$$P \frac{e}{(1 - e)} = \text{constant}$$



by using one value of the capillary pressure at one porosity to calculate the others. An estimate of the third has recently been given by Pietsch and Rumpf (1967) as

$$C e = 77$$

This follows the results of Smith, Foote and Busang (1929) who found an almost straight line relationship between co-ordination number (C) and porosity.

Using both 11.4 T/r and 12.9 T/r as the capillary pressure at 22% porosity in a mono-size bed, calculations have been made using the relationships. The results are given in Table VII.

TABLE VII

e	P	Vol./r	Residual Moisture		P	Vol.	Residual Moisture	
	T/r	$\times 10^2$	Wt.%	Vol.%	T/r	$\times 10^2$	Wt.%	Vol.%
22	12.9	.70	.80	8.5	11.4	.80	1.2	12.8
35	6.7	1.85	1.34	7.4	6.0	2.23	2.1	11.8
40	6.1	2.10	1.32	5.9	4.8	2.65	2.2	9.9

There is little to choose between the two sets of results for residual moistures as the predictions for 35% and 40% all lie in the range of experimentally determined residual moistures, though the results for 11.4 T/r are a little closer. The agreement is good considering the coarsness of the assumptions. Also the predicted value of capillary pressure in a random packed mono-size bed of 6.0 T/r calculated from the value of 11.4 T/r at 22% is very close to experimental results given by Haines, and Hackett and Strettan for random packing of 35% porosity.

Specific surfaces have been calculated from the theoretical capillary pressure curves using both of these values. The results

are given in Table V. The results using 11.4 T/r show a better correspondence. This is not as obvious as it might appear from the positions of the curves on Fig. (32-34) Since the corrections applied by the residual moistures are quite large (of the order of 10% of the void volume at 22% porosity). The same value of residual moisture has been applied to both mono-size packs and the 3-component packs. This agreement supports the use of 11.4 T/r for the pressure required to blow a bubble through a pore formed by three spheres as opposed to the value of 12.9 T/r. Full justification can however only be made by a full theoretical treatment of the problem.

#### 5.6.2.3 Full Correlation

Using the values of specific surface calculated from the capillary pressure curves the correlation may be completed and is plotted in Figs. (35, 36, 37, 38, 39 and 40) . There is no difference on this basis between the curve using the 11.4 T/r value of entry pressure and that using 12.9 T/r this is because the areas under the respective curves are used in the correlation. In the case of the 11.4 T/r value however the specific surface values do correspond with measured results and the correlation is justifiable.

The capillary pressure curves predicted from the model do exhibit the correct shape and tend to follow the curves determined experimentally. In general however they exhibit a narrower range of pore sizes than do the experimental results. This variation of pore size distribution with porosity may be a real effect, not detectable in the small range of porosities available experimentally. Or more likely it may be due to ignoring the effects of gaps in sphere packing in the Wise model. These would tend to promote

more randomness in the packing and consequently a wider pore size distribution. It may also be that if a proper evaluation of the pressure required to blow an air bubble through an array of three spheres were available this would increase the distribution of pore sizes. If the assumption used breaks down for three equal spheres it is also likely to be more in error for an array of say two large spheres and a small one.

Despite this however the theoretical results do show that a dispersion in particle size in a 'mono' size sphere pack as small as  $30\mu$  in  $130\mu$  is significant enough to be exhibited in the curves. This particle size distribution is much narrower than that given in a sieve cut which is often used as a way of preparing mono size packs. Furthermore the results for the 3 component mixtures have a tendency for the correct shape and as plotted in Fig. (39) and do show the correct relative positions even though they are very close together.

It must also be remembered that the sphere size distributions used in the model are much abbreviated from that actually existing in the packing. Since the model has been shown to be sensitive to quite small dispersions in particle size a closer correspondence may be obtained if more components were used in the calculations than three. Also the approximation of the pore space in the packing given by using tubes and spherical cells is very coarse. Calculation shows that this accounts for only about 50% of the real pore space in the tetrahedral packing. If these improvements were to be incorporated then the setting up of the network and the desaturation procedure would have to be carried out automatically on a computer. This would not be impossible.

One point on the curve for mixture 4 has been left out in drawing the curves. This may be justified by an inspection of the results tabulated in the appendix. It can be seen that this point includes a very large proportion of isolated pores which are available for emptying if a path to them was established. As this is a wider distribution than the others it may be taken that the size of array used is too small in this case.

#### 5.6.2.4. Summary

The theoretical model predicts the properties of a dense random packing of around 20% porosity and these can only be compared with experimental results on the basis of the correlation.

Using the correlation methods the capillary pressure curves derived from the model can be seen to exhibit the correct shape, and position relative to experimental results for the same sphere size distributions.

Improved correlation with experimental curves is achieved if an experimental value for entry pressure into the assumed pore shape is used instead of the theoretical value derived from a simplification.

This improvement is reflected in values of specific surface calculated from the curves obtained from the model.

Estimates are made of the variation in residual moisture with porosity variation in sphere packs these show reasonable comparison with experimental results.

#### 5.7 CONCLUSIONS

The correlations for capillary pressure curves mentioned in section 3.4 are successful for experimental results.

Specific surfaces calculated from experimental capillary pressure curves show agreement with those obtained by other methods for the same samples.

The theoretical model predicts a low porosity relating to the densest possible packing.

Capillary pressure curves obtained from the theoretical model of pore space in sphere packs are of the correct shape but give a narrower pore size distribution than experimental results for the same particle size distribution.

The entry pressure into the pore formed by three equal and touching spheres is nearer  $11.4 T/r$  than  $12.9 T/r$ .

Using this value for entry pressure into a pore the results from the theoretical model correlate with experimental results. This indicates that the model gives correct values of porosity, specific surface, residual moisture and pore size. The agreement is less good for pore size distribution.

The model shows that the particle size distribution in so called mono-size packs is important in promoting pore size distribution.

## CHAPTER SIX

### FLOW OF FLUIDS IN POROUS MEDIA

#### 6.1 INTRODUCTION

The capillary pressure curve only involves the equilibrium effects of moisture in porous media, but dewatering is a flow process and the rate of flow from the desaturating porous medium is the main factor involved in any optimisation of the operation. Therefore, having studied the equilibrium effects of two fluid phases in a porous medium, this section is concerned with the flow of two immiscible fluids in porous media. This is a particular part of the general topic of flow of fluids in porous media. There are many points of contact between the equilibrium and dynamic effects of two fluids in porous media and these will be emphasised.

#### 6.2 Single Phase Flow in Porous Media

##### 6.2.1 Capillary Tube Theories

The permeability of a porous medium is introduced by the Darcy equation as a characteristic of the porous medium. It is determined by the structure of the bed but this is so complex in practice that if further description is required, simplification must be introduced. This is in the hope that theoretical considerations can show how to attach physical significance to the various parameters which can affect permeability.

A common analogy for flow in porous media is with straight capillary tubes. The Navier-Stokes equation, fundamental for fluid flow, can be solved for this case and the result is known as the Hagen-Poiseuille equation

$$v^1 = \frac{r^2}{8\eta} \frac{\Delta P}{L}$$

$v^1$  in this case is the flow velocity in a single capillary tube. If the analogy is made between a porous medium and a bundle of capillary tubes, the apparent velocity ( $v$ ) over the whole pack of tubes is given by

$$v = v^1/e$$

This is called the Dupuit-Forcheimer assumption and is only valid for an assembly of capillaries if the pore velocity is an actual statistical average. Combining ( $n$ ) capillary tubes as a bundle gives

$$v = \frac{n r^2}{8 \eta} \frac{\Delta P}{L} \quad \text{or} \quad q = \frac{n \pi r^4}{8 \eta} \frac{\Delta P}{L}$$

where ( $q$ ) is a volume flow rate. By analogy with Darcy's law the ~~total~~ permeability  $K'$  is then

$$K' = n \pi r^4 / 8$$

Assuming unit cross-sectional area for the tube bundle

$$e = n \pi r^2 / 8$$

$$\therefore K = e r^2 / 8 = e r^2 / t$$

The factor  $8$  is usually replaced by a factor ( $t$ ) which is termed the tortuosity factor and is introduced to correct for the differences between the model and an actual porous medium. To introduce

isotropy into the model it is possible to arrange 1/3 of the capillary tubes in each direction and insert a factor 3 in the equation. This does not alter the essentials of the model as this can be incorporated in the tortuosity factor. However it invalidates the implicit use of the Dupuit-Forcheimer assumption in that a factor 3 must also be introduced in this.

### 6.2.2 Kozeny-Carman Theory

The average radius of the capillary tubes is required for

the above equation and it is a difficult quantity to realise in practice, especially as in general the pores in porous media are not circular. In empirical correlations for flow in non-circular channels it is found that a hydraulic radius ( $M$ ) defined as the ratio of cross-sectional area to the perimeter of the cross-section can be used in its place. Therefore

$$K = \frac{e M^2}{k_o t}$$

where ( $k_o$ ) is a factor which is determined by the shape of the cross-section. For a circular capillary  $k_o = 2$ , for flow between two parallel plates  $k_o = 3$ , and for most other shapes ( $k_o$ ) varies between 2.0 and 2.5, Carman (1948). In a porous medium, as was shown in the previous section

$$M = \frac{\text{pore volume}}{\text{pore surface area}} = \frac{e}{(1 - e)} S_o$$

$$\therefore K = \frac{e^3}{k_o t (1 - e)^2} S_o^2$$

This equation is the same as the Kozeny-Carman equation which was derived by Kozeny on a different theoretical basis. Kozeny took that the porous medium was not a system of pores which require a definition of average radius but as one large channel of complex shape. This channel retards flow by friction at its surface. The tortuosity factor was introduced by Carman. Scheideggär<sup>e</sup> (1953) has stated that although the Kozeny-Carman equation makes use of fewer assumptions than the capillarc model, only involves concepts of internal surfaces and leaves aside pore size distribution, it is fundamentally the same. An inspection shows that it is based on a two dimensional analysis of the cross-section and is therefore



equivalent to a parallel set of capillaries. Debbas and Rumpf (1966) have derived (M) on the basis of the inter-section of a plane in a random packing which emphasises this point. Nevertheless the equation is accepted as one of the most useful descriptions of permeability in terms of pore structure that is available.

### 6.2.3 Tortuosity

The factor ( $t$ ) in the Kozeny-Carman equation is usually taken as  $(L_e / L)^2$  which is the square of the ratio of the actual flow path length in the porous medium to the thickness of the porous medium. The value of  $k_o (L_e / L)^2$  has been shown by Carman (1937) to be about 5.0 for a wide variety of unconsolidated media. Bartell and Osterhoff (1928) have shown that  $(L_e / L)$  is equal to  $\pi/2$  for close packing of equal spheres which gives a value of  $k (L_e / L)^2$  approximately equal to 5. Coulson (1949) has made extensive tests on a variety of regular shaped particles in different packings and has found the factor to vary with both shape and porosity mainly between 4 and 5, but it can be as low as 3.5 or as high as 6. Sullivan and Hertel (1942) measured tortuosity values for arrays of parallel fibres and found it to be given by  $1 / (\sin^2 \theta)$ , where  $(\theta)$  is the average angle of orientation of the fibres. Wyllie and Gregory (1955) have shown that pore size distribution and porosity can affect tortuosity and Bo (1968) has shown theoretically how  $(L_e / L)$  varies with porosity for random packing. Values of tortuosity much different to these mentioned have been reported by Wyllie and Rose (1950) for consolidated media and Grace (1953) who found values ranging from 5 to several thousand for flocculated filter cakes. Drennan (1964)

introduced the concept of inert porosity in consolidated media to correct these to more normal values. This may be applied to flocculated systems by excluding the pore space in flocs from flow calculations, but it is usually taken that these systems are beyond the true range of applicability of the Kozeny-Carman equation.

#### 6.2.4 Discussion

The Kozeny-Carman <sup>equation</sup> is widely accepted as giving good results for many different materials and is often used to measure the specific surface of powders. If tortuosity values are properly evaluated this can be quite accurate, Wyllie and Gregory (1955). There are however important conditions which must be observed for the validity of the equation which have been listed by Carman (1948)

- 1/. No pores must be sealed off, this would affect the value of absolute porosity but not the porosity available to flow.
- 2/. The particles must be in random distribution and reasonably uniform.
- 3/. The porosity must not be too large.
- 4/. Diffusion and surface effects must not be involved in the flow.

In addition to this Scheidegger (1954) states that the equation implies a well connected space lattice to allow the pressure profile in the medium to be even and perpendicular to the flow.

Childs and Collis-George (1950) have severely criticised the equation on a more fundamental basis. They show that surface area can be altered almost independently of permeability since large pores contribute most to permeability but small pores contribute most to specific surface. For example in fissured clays the fissures can contribute negligibly to porosity and specific surface but dominate permeability. Furthermore the equation cannot be

applied to anisotropic permeability since neither ( $e$ ) nor ( $S_o$ ) are directed quantities. Wyllie and Spangler (1952) have pointed out that tortuosity can be varied to account for anisotropy and they cite the example of Sullivan and Hertel's work on flow past fibres. This however seems to place too great an emphasis on tortuosity as a factor in the flow. And since tortuosity was not introduced in Kozeny's treatment it must be seen as essentially a correction to a bundle of tubes model.

The Kozeny-Carman equation was developed by Childs and Collis-George for a bundle of tubes with a distribution in sizes, to make the error more apparent. In such a tube bundle each group of capillaries of a given size has associated with it a portion of the solid to give each group the same porosity ( $e$ ) as the total. The cross-section of the group ( $a_r$ ) with capillaries radius ( $r$ ) contributes to the total permeability

$$K = \frac{\sum a_r K_r}{\sum a_r}$$

where ( $K_r$ ) is given for each group by the summation of Poiseuille's equation for  $n$  capillaries

$$q = n \frac{\pi r^4}{8 \eta} \frac{\Delta P}{L}$$

$$K_r = \frac{n \pi r^4}{8 \eta} = \frac{n \pi r^2}{8 \eta} \left[ \frac{2 \pi r^2}{2 \pi r} \right]^2$$

which may be written

$$K_r = \frac{1}{2 \eta} \left[ \frac{V}{A} \right]^2 \frac{e^3}{(1-e)^2}$$

where ( $V / A$ ) is the reciprocal specific surface of the particles.

Therefore

$$K = \frac{1}{2 \eta} \frac{e^3}{(1-e)^2} \frac{\sum a_r (V / A)_r^2}{\sum a_r}$$

The final term may be written as  $(\bar{V} / \bar{A})^2$  which represents the mean value of  $(V / A)^2$  for all the groups. This is not the same as the overall value of  $(V / A)^2$  for all the channels together since the first is dominated by the larger and the latter by the smaller channels. The only sense that the equation has applicability is if two structures are considered such that for every group ( $m_r$ ) in the other structure then

$$\frac{(\bar{V} / \bar{A})^2_r}{(\bar{V} / \bar{A})^2_{m_r}} = \frac{(V / A)^2_r}{(V / A)^2_{m_r}} = \frac{1}{M^2}$$

Childs and Collis-George conclude that it is impossible to obtain a sufficiently wide range of porosities or pore size distributions to test equations properly, and furthermore the success of the Kozeny-Carman equation may only reflect the essential similarity of most porous media.

Brooks and Purcell (1952) have studied the Kozeny-Carman equation from the point of view of surface area measurement and they conclude that it is only valid for uniform pore size. This study relies on concepts of pore size distribution and will be mentioned later. The correlation used in the previous chapter also illustrates these points as it is essentially the Kozeny-Carman function. It can be seen from Fig. (40) that it correlates for value of 50% saturation for all shapes of distribution, but it does not involve the shape of the distribution. Therefore in the wide distribution curves, such as those in the figure for Celite, there are fewer large size pores than in the more uniformly flat distributions and it is the large pores which contribute most to permeability. It is of course possible to correct any value of permeability or surface area obtained from the Kozeny-Carman

equation to a correct one by using an appropriate tortuosity factor. This is however not sufficient if concepts of pore structure are investigated.

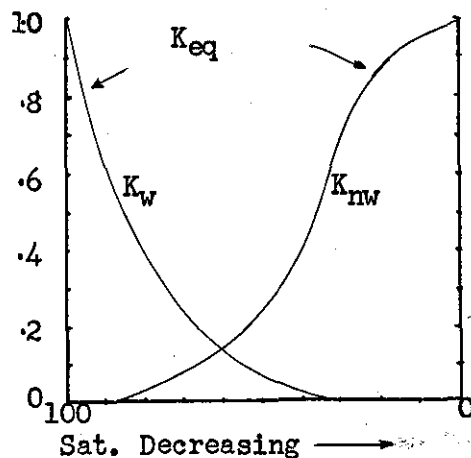
### 6.3 TWO PHASE FLOW IN POROUS MEDIA

#### 6.3.1 Experimental Study of Two Phase Flow

##### in Porous Media

In considering the flow of two fluid phases in porous media it is necessary to start from Darcy's Law where permeability is the constant of proportionality between rate of flow of fluid and pressure drop. When two phases are flowing in a porous medium, differentiated as wetting phase (water), and non-wetting phase (gas), it is possible to define a permeability for each phase. These permeabilities will vary for a given porous medium with the relative degrees of saturation.

An experimental study of this was made by Wycoff and Botset (1936). They flowed water and carbon dioxide mixtures through a horizontal tube 10 feet long and 2 inches diameter containing granular packings. The total pressure drop and the individual rates of flow of each phase were measured conventionally and the saturation of the packing measured by an electrical resistance method for which the water was made slightly conducting. Their results are best discussed by reference to Fig. (41). The



Relative Permeability  
Wycoff & Botset  
(1936)

Fig. (41)

permeabilities for each phase are expressed as a fraction of the saturated permeability and range therefore from 0 to 1 and are termed relative permeabilities. Saturations are expressed as percentages of the void spaces and range from 0 to 100%.

Considering the wetting phase (water) it can be seen that the permeability drops sharply as the saturation is reduced from 100%. At 80% saturation the relative permeability is .5 and at 50% it is .1. The curve reaches zero permeability at a finite saturation (10 - 15%) which corresponds to the residual saturation which exists as phase continuity is broken. The non-wetting (or gas phase) shows a similar shape. It can be seen that phase continuity ceases at about 90% saturation and also that from 0 - 20% saturation the permeability is substantially 1.0. That is the residual wetting phase has little effect on the non-wetting phase permeability. The two curves cross at between 50 - 60% saturation and about .15 relative permeability. By adding the two curves together the total permeability at a given saturation can be arrived at. It can be seen that this is only 1 at 0% and 100% saturation and that there is a pronounced minimum. The experiments were repeated for various sands with saturated permeabilities ranging from 17.2 to 262 Darcy's ( $1 \text{ Darcy} = 9.87 \times 10^{-9} \text{ cm}^2$ ) all of which gave the same curves. An interesting point is that marked ( $K_{eq}$ ) on the curves. At very low gas/liquid ratios i.e. below this point, the steady state of flow is not attained. Gas accumulates in the pores until the saturation reaches this point and flow begins. This is a definite characteristic which varies with the porous medium and was called equilibrium permeability or saturation. It has been mentioned by Eisenklam (1956) as being one of the causes

of anomalous permeabilities in saturated flow.

Some experiments were also performed on oil/water mixtures which gave similar curves but with a wider scatter of the points. Wycoff and Botset concluded that the curves applied generally to the flow of gas/liquid mixtures in unconsolidated sands and were probably valid also for immiscible liquids. These findings have been supported by Leverett (1939) for oil/water mixtures in unconsolidated sands and by Botset (1940) for gas/liquid mixtures in consolidated sands. Leverett in his work concluded that relative permeability is substantially independent of viscosity and is related to pore size distribution, as the non-wetting phase tends to flow in the larger pores and the wetting phase in the smaller ones, at any given saturation.

### 6.3.2 Determination of Relative Permeability

Multi-phase phenomena are of great importance in oil production and the measurement of relative permeability of rock cores is a routine laboratory technique. The methods available for this have been reviewed by Osoba, Richardson, Kerver, Hafford and Blair (1951) and Richardson, Kerver, Hafford and Osoba (1952). Using rock core samples which are much less long than the 10 feet used by Wycoff and Botset, difficulties are experienced with the boundary effect. This boundary effect was described by Leverett (1941) and is caused when fluids flow past a discontinuity in capillary properties. In the interior of a uniformly saturated porous mass the capillary pressure acts in all directions and hence cancels itself out, at the in-flow and out-flow faces however, the fluids are flowing in a region of no capillary pressure and this leads to a distortion of the saturation profile. The effect is

not critical in long samples but must be overcome for small samples such as rock cores.

The various methods used in relative permeability may be divided into three groups.

1/. Experiments in which measurements are made under steady-state flow conditions with both fluids flowing simultaneously. The boundary effect can be overcome by having independent systems for each phase to hold a pressure difference between them or by making measurements only on the central part of the sample.

2/. Experiments made under steady-state conditions with only one fluid flowing. One fluid is held stationary by capillary forces exerted through fine pore membranes and flow measurements made on the other fluid.

3/. Experiments in which measurements are made under transient saturation conditions. The boundary<sup>a</sup> effect is not eliminated but is included in the theory by which the calculations are made.

Richardson et. al. (1952) found good agreement between the different methods of measuring relative permeability except for the method using transient saturation conditions. All the methods however suffer from complexity and require upwards of a day to complete a permeability saturation plot. Moreover the methods are not well adapted for unconsolidated media and for high permeabilities generally.

Childs and Collis-George (1950) in their work used a method rather similar to that of Wycoff and Botset. They noted that when water flows down a sufficiently long packed column to a water table the moisture content is uniform over an appreciable length of the column. The zones of variable moisture being limited to each end



of the column. In the zone of uniform moisture the pressure is solely gravitational and therefore known, and the moisture content adjusts itself to provide the necessary permeability to conduct the imposed flow. The permeability may therefore be calculated from the rate of flow and the moisture content of the column. This latter determination must be made indirectly and an electrical method was used.

The method suffers from the same shortcomings as the column drainage method for determination of capillary pressure curves. That is saturations must be determined indirectly, large amounts of sample are required and the experiments take a long time. A method based on the pressure plate technique for capillary pressure determination has been reported by Gardner (1956). In this relative permeability is determined from flow data at each pressure increment using two assumptions. The slope of the capillary pressure curve is constant for small increments of pressure and the flow resistance of the fine pore support plate is negligible. This latter assumption can lead to error and Richards (1965) has given a method for allowing for a non-negligible support plate resistance.

All of these determinations are however tedious to perform and open to error, furthermore relative permeability curves do not vary very much even between different materials. A more attractive approach is therefore to investigate the mechanism involved in two phase flow and to produce relative permeability curves from more easily obtained characteristics of porous media.

### 6.3.3 Characterisation of Two-Phase Flow

Initially it was assumed by analogy with Darcy's Law for

single phase flow that relative permeability could be defined for each phase in two phase flow. Using experimental techniques this has been established within the limits which also apply to Darcy's law for homogeneous flow in porous media. That is within the laminar region and also including gas slippage effects for gas phase relative permeability. However the existance<sup>e</sup> of capillary hysteresis leads to different results depending on the direction of saturation changes. In general permeability at a given saturation is greater when wetting phase is decreasing than when it is increasing. Naar and Henderson (1962) report that this is true for unconsolidated media but the reverse applies to consolidated media, no explanation was offered.

Visual studies have been made on two phase immiscible flow. Chatenever and Calhoun (1952) studied a mono layer of glass or perspex beads contained between two flat glass or perspex faces. When a mixture was flowed through the system each fluid was observed to flow in its own network of interconnecting channels which varied from one grain diameter to many in width. These meandered tortu<sup>o</sup>sly through the bed but maintained fixed geometries and positions with steady-state flow. With a change in saturation the geometry of the channels was altered, an increase in water saturation was accompanied by a general growth in the size of the water channels and a decrease in the size of oil channels. There was a tendency for the channels to hold their position in the flow bed and in the case of temporary disturbances the channels adjusted elastically, returning to their former configuration when the disturbance was past.

At static equilibrium the distribution of two fluids in

a porous medium has been shown to depend essentially on capillary forces and the structure of the porous medium in which they act. Rapoport and Leas (1951) described the change as the static equilibrium is turned into a dynamic one. "For each static interface the dynamic (i.e. flowing) pressure gradient will act as a local disturbance and this will be super-imposed on the static capillary pressure. This breaks down the equilibrium since the pressure drop over each interface will vary. Each interface will therefore have a tendency to modify its position to assume a new equilibrium which will include capillary and dynamic forces. However in general the dynamic pressure gradient will be orders of magnitude less than the capillary pressure gradient and the dynamic equilibrium will not be much different to the static equilibrium". That is the flow of non wetting phase will tend to be in the large pores and the wetting phase in the small pores. Templeton (1954) studied displacement in uniform glass capillaries down to  $4\mu$  in diameter and found that capillary pressure was independent of interfacial velocity. This gives some corroboration of this view.

On the closer examination it has been shown that the presence of one fluid contained in a porous medium can be taken as a factor which controls the geometry of the paths available to the other immiscible fluid which is also saturating the porous material. Each fluid acts on the other in the same way that the porous medium acts on them both. In this sense the application of Darcys law to each phase is not unreasonable.

## 6.4 DERIVATIONS OF RELATIVE PERMEABILITY

### 6.4.1 Capillary Tube Theory

With this explanation for relative permeability it is possible to make structural assumptions about porous media and arrive at mathematical expressions for unsaturated flow as was done for saturated flow. There is an extra incentive for this in relative permeability work since the curves do not vary much for different materials and because the determination of relative permeability is tedious, difficult and therefore open to error.

The simplest possible description is that provided by a bundle of tubes model of uniform capillaries. This would give two straight lines on a permeability-saturation plot for non-wetting and wetting phase which would intersect at 50% saturation and relative permeability of .5. The sum of these two lines would be constant and equal to saturated permeability. The obvious failure of this model has led to pore size distribution being included in the model.

Purcell (1949) assumed a bundle of tubes model and used the capillary pressure curve as a description of the pore size distribution. Starting with Poiseuille's equation

$$q = \frac{\pi r^4}{8\eta} \frac{\Delta P}{L} = \frac{V r^2}{8\eta} \frac{\Delta P}{L^2}$$

when  $V =$  volume of a tube  $\pi r^2 L$

Using the capillary pressure to define the radius of a pore

$$r = 2 T \cos\theta / P_c$$

$$v = \left[ \frac{T \cos\theta}{P_c} \right]^2 \frac{V \Delta P}{2\eta L^2}$$

Considering a bundle of  $n$  capillary tubes with a distribution of radii

$$q = \frac{(T \cos\theta)^2}{2nL^2} \Delta P \sum_{i=1}^n \frac{V_i}{(P_c)_i^2}$$

from which

$$K = \frac{(T \cos\theta)^2}{2AL} \sum_{i=1}^n \frac{V_i}{(P_c)_i^2}$$

The volume of each capillary ( $V_i$ ) may be expressed as a percentage ( $S_i$ ) of the total void volume ( $V_{tot}$ )

$$\therefore S_i = 100 V_i / V_{tot}$$

and since  $A \times L$  is the volume of the porous medium

$$e = (V_{tot} / AL) \times 100$$

$$\therefore K = \frac{(T \cos\theta)^2 e}{2 \times 100^2} \sum_{i=1}^n \frac{S_i}{(P_c)_i^2}$$

The quantity  $\sum S_i / (P_c)_i^2$  can be shown to be equal to

$$\int ds / (P_c)^2 \text{ and is the area underneath a plot of } 1 / P_c^2$$

versus saturation. Finally a factor ( $F$ ), so called lithology factor is introduced to account for differences between the model and a real porous medium. It may be seen that ( $f$ ) is equivalent to reciprocal tortuosity

$$K = F \frac{(T \cos\theta)^2 e}{2 \times 100^2} \int_0^{100} \frac{ds}{(P_c)^2}$$

Gates and Leitz (1950) extended this expression to relative permeability

$$K_w = \frac{K_{sw}}{K_{tot}} = f \frac{\int_0^{sw} ds / P_c^2}{\int_0^{100} ds / P_c^2}$$

This assumes that the term  $(T \cos\theta)^2 e$  can be cancelled out. The lithological factor is now used to correct observed relative permeability curves to those that were calculated. This was shown to require variation with saturations but was taken as an average value by using that obtained at 65% saturation. No relation was formed between tortuosity and either porosity or permeability. Gates and Leitz expressed saturations as percentages of total void space though it is more normal to express them as percentages of total void volume less residual moisture. In the discussion on this paper it was stated that if this was done the correlation is closer.

In the previous section the Leverett (j) function was shown to correlate different capillary pressure curves to one curve when

$$(j)_{sw} = (P_c / T \cos\theta) \sqrt{K/e}$$

is plotted against saturation. Rose and Bruce (1949) used this relationship in a similar expression for relative permeability as that just given. This allows relative permeability curves to be predicted from one point on the capillary pressure curve.

Fatt and Dykstra (1951) made an improvement in the method by taking the tortuosity to be a function of saturation. During desaturation the wetting phase retreats into smaller pores and it is assumed that liquid in these pores has a more tortuous flow

path. This is allowed for by making (t) vary with (r).

$t = a/r^b$  where a and b are constants. Using a similar derivation to Purcells,

$$K = \frac{(T \cos\theta)^2 (1+b) e}{3 a^2} \int_0^{100} \frac{ds}{P_c^2 (1+b)}$$

in relative permeability the constant (a) is cancelled out

$$\text{and } K_w = \frac{\int_0^s \frac{ds}{P_c^2 (1+b)}}{\int_0^{100} \frac{ds}{P_c^2 (1+b)}}$$

which if b is taken as  $\frac{1}{2}$  becomes

$$K_w = \frac{\int_0^s \frac{ds}{P_c^3}}{\int_0^{100} \frac{ds}{P_c^3}}$$

*Equation*

Gates and Leitz<sub>Λ</sub> can be seen as a special case with b = 0.

The expression can be evaluated from a plot of  $(1/P_c^3)$  versus saturation. Comparison with experimental results show that (b) must also vary with the type of porous medium for best fit.

#### 6.4.2 Tortuosity from Electrical Resistivity

The analogy between fluid flow<sub>Λ</sub><sup>and</sup> the conduction of electricity has allowed tortuosity values to be derived from resistivity data. Winsauer, Shearin, Masson and Williams (1952). Formation factor (F) is defined as the ratio of the resistivity of a porous material saturated with conducting fluid to the resistivity of the fluid itself

$$F = \frac{R_o}{R_w} = \frac{\text{Resistivity of Saturated Sample}}{\text{Resistivity of Fluid}}$$

Wyllie and Spangler (1952) show that

$$F = \frac{R_o}{R_w} = \frac{L_e / L}{e} = \frac{t^{1/2}}{e}$$

therefore  $t = F^2 e^2$

If the Kozeny-Carman equation is used with a pore size distribution given by the capillary pressure curve

$$K = \frac{e^3}{k_o t S^2} = \frac{e}{k_o F^2} \frac{T^2}{P_c^2}$$

this is only strictly valid for a set of uniform pores but it may be claimed that at any saturation ( $S_w$ ) and corresponding capillary pressure ( $P_c$ ) a fictitious porous medium is considered which has a porosity of ( $e \Delta S_w$ ) and has uniform pores of mean hydraulic radius ( $e \Delta S_w$ ) /  $S_{oi}$  where ( $S_{oi}$ ) is the specific surface of that group of pores.

$$K_i = \frac{(e \Delta S_w) T^2}{k_{ot} P_c^2} \quad \text{and} \quad Q = \frac{K_i P}{\eta L}$$

since the quantity of fluid passed by all such groups

$$Q = \frac{K P}{\eta L} = \sum \Delta Q \quad \text{where } K \text{ is the overall}$$

permeability of the porous medium

$$\therefore K = \frac{e T^2}{k_o F^2} \sum \frac{\Delta S_w}{P_c^2}$$

by the method of Purcell in the previous section

$$K = \frac{e T^2}{k_o t} \int_0^{100} \frac{dS_w}{P_c^2} = \frac{T^2}{(F^2 e) k_o} \int_0^{100} \frac{dS_w}{P_c^2}$$



this is clearly the same and can be used in an expression for relative permeability. However with the electrical definition of resistivity this can be developed further. Thornton (1949) has shown that for partially saturated porous media

$$F_e = 1 / I S_w$$

where (I) is the resistivity index  $F_e / F$  for the saturation  $S_w$ .

If the permeability at any saturation is given by

$$K_e = \frac{T^2}{(F_e^2 e S_w^2)} k_o \int_0^{S_w} \frac{dS_w}{P_c^2}$$

and relative permeability by  $K_e / K = K_{rL}$

$$K_{rL} = \frac{T^2}{(F_e^2 e S_w^2)} k_o \frac{(F_e^2 e) k_o \int_0^{S_w} \frac{dS_w}{P_c^2}}{\int_0^{100} \frac{dS_w}{P_c^2}}$$

$$K_{rL} = \left[ \frac{F}{F_e} \right]^2 \frac{1}{S_w^2} \frac{\int_0^{S_w} \frac{dS_w}{P_c^2}}{\int_0^{100} \frac{dS_w}{P_c^2}}$$

$$K_{rL} = \frac{1}{I^2 S_w^2} \frac{\int_0^{S_w} \frac{dS_w}{P_c^2}}{\int_0^{100} \frac{dS_w}{P_c^2}}$$

this assumes that the shape factor ( $k_o$ ) is invariant with saturation. It has also been demonstrated Hassan and Nielsen (1953) and Archie (1942) that (I) can be expressed as a function of saturation

$$I = S_w^{-n}$$

This is called Archie's law. Wyllie and Spangler (1952) showed that the relationship holds for the full range of saturations even to the final breakup of wetting phase into pendular rings.

6.4.3 Kozeny-Carman Applied to Relative Permeability

An alternative approach has been taken by Rapoport and Leas (1951) in using the Kozeny-Carman equation

$$K = \frac{e^3}{k_0 t S^2}$$

This can be extended to two phase flow by replacing porosity by effective porosity for the phase considered and using the area bounding that phase

$$K_L = \frac{(S_2 e)^3}{k_0 t (A_L)^2}$$

and for relative permeability

$$K_{rL} = \frac{S^3}{(A_L/A)^2}$$

It was shown in a previous section that surface areas can be calculated from capillary pressure curves by taking the integral of, or measuring the area underneath, the curve. The existence of residual moisture can be taken into account by considering it as part of the solid matrix and using effective saturation and effective total area

$$K_{re} = \frac{S_e^3}{(A_L/A_e)^2}$$

For any moisture content less than 100% saturation several interfacial areas can exist. Solid/liquid, solid/gas and gas/liquid and it is not possible to arrive at definite expressions for each.

It is however possible to take the limiting cases which are

$$K_{rL} \text{ (min)} = s^3 \left[ \frac{A_e}{A_{L \text{ max}}} \right]^2$$

and

$$K_{rL} \text{ (max)} = s^3 \left[ \frac{A_e}{A_{L \text{ min}}} \right]^2$$

for the case of ( $K_{rL} \text{ min}$ ) this is physically that the fluid distribution is such that the liquid interface is a maximum which means that the gas interface is a minimum, the opposite is the case for ( $K_{rL} \text{ max}$ ). Experimental results were shown to lie between maximum and minimum relative permeability curves. For a synthetic alundum core the agreement was good and for a natural core was less good, though still reasonable. This was ascribed to the greater homogeneity of the synthetic core.

#### 6.4.4 Discussion

The limitations which apply to the bundle of tubes model are the same for multi-phase flow as for saturated flow. This is made clear by the need for the tortuosity parameter. It has been mentioned that a bundle of uniform capillaries leads to a straight line relationship between relative permeability and saturation and the two lines intersect at 50% saturation and 0.5 relative permeability and add together to a constant value equal to saturated permeability. The adoption of a pore size distribution leads to an improvement in this in that at 50% wetting phase saturation the wetting phase will be contained in the smaller pores and thus have a permeability less than 0.5. However the non-wetting phase will be contained in the larger pores and will therefore have a permeability or more than 0.5. The sum of the

two curves will still be constant and equal to saturated permeability. Therefore pore size distribution alone is not sufficient to describe relative permeability curves.

Tortuosity is seen therefore to be more than a correction for path length of flow and must be related to the structure of the porous medium. In particular it must be related to the way the networks of wetting and non-wetting phase interact with one another. Therefore though the connection between resistivity and tortuosity may be valid it cannot overcome the way the parameter is used in the equations.

The same limitations also apply to the use of the Kozeny-Carman equation in multi-phase flow as were mentioned in the section on saturated flow. Wyllie and Spangler (1952) in their derivation, as given previously, take note of the criticisms of Childs and Collis-George (1950) but since the end result is the same as other derivations they cannot be taken as having overcome the criticism. The criticisms moreover have more validity in multi-phase flow. It was shown that the equations cannot be used for porosity and pore size distributions too far away from the usual. In relative permeability the effective porosities range from (0) to (e) and the effective pore size distribution is truncated at each given saturation. Childs and Collis-George discussed the use of average pore properties and how this must be properly defined and be representative. This is impossible in multi-phase flow as large pores in general conduct one fluid and the small pores the other. The relative sizes and proportions of these change with saturation and cannot be represented by average properties. From this even the similarity criterion advanced for

saturated flow requires more rigorous application.

A further demonstration by Brooks and Purcell (1952) will serve to emphasise these points. It has been shown that the Kozeny-Carman equation can be derived from a bundle of tubes model by using functions of surface area. It has also been shown that the surface area of a porous medium can be taken as

$$A = \frac{e}{(1-e)} \frac{1}{T} \int_0^{100} P_c dS \quad \times \frac{1}{100}$$

which is independent of pore size distribution. Furthermore the equation

$$K = \frac{e T^2}{k_{ot} 2 \times 100^2} \int_0^{100} \frac{dS}{P_c^2}$$

has been derived for a bundle of capillary tubes with a distribution of sizes. By combining these two equations to eliminate the surface tension term

$$K = \frac{e^3}{k_{ot} (1-e)^2 A^2} \int_0^{100} \frac{dS}{P_c^2} \left[ \int_0^{100} P_c dS \right]^2 \times \frac{1}{2 \times 10^4}$$

this only reduces to the Kozeny-Carman equation if

$$\left[ \int_0^{100} P_c dS \right]^2 \times \int_0^{100} dS / P_c^2 = 10^4$$

which will only occur if  $(P_c)$  is constant for all values of saturation. That is if all the pores are the same size.

It may be concluded that for multi-phase flow, relationships must allow use of pore size distribution and that pore interconnection is important and cannot be fully described by tortuosity parameters.

## 6.5 THEORIES INCLUDING PORE INTER-CONNECTION

### 6.5.1 Cutting and Joining Models

The need for inclusion of pore inter-connections in expressions for relative permeability has been realised and attempts have been made to do this to give better representation of unsaturated flow. The cutting and joining model was first suggested and used by Childs and Collis-George (1950) and since then has been developed by a number of workers Marshall (1958) Wyllie and Gardner (1958) and Millington and Quirk (1961). Reviews of this work have been made by Marshall (1962), Wall (1965) and Laliberte, Brooks and Corey (1968).

Consider a bundle of capillary tubes with a distribution of tube radii. A slice through the pack normal to the length will expose two planes, (A) and (B) showing the same pore size distribution. Many such slices may be made and rearranged in random juxtaposition to reform the porous medium. Childs and Collis-George in their treatment arrived at an equation for permeability in terms of the pore size distribution, porosity, and an unknown factor. Experimental justification of the equations was made for unsaturated flow but the range of materials used was not sufficient to say much about the character of the factor, which was gained by graph fitting. The treatment here is that given by Marshall (1958) which is fundamentally the same but which arrives at an equation with no indeterminate factors.

The assumption is made that permeability is controlled by the cross-sectional area of the necks formed between pores at the joins in the planes. The cross-sectional area of the neck when the fit of one pore to the next is perfect is taken as that of

the smaller pore. Since the fit is often imperfect, allowance is made in this case for a reduction in the size of the neck when the two pores in random alignment do not fit perfectly on to one another. A mean cross-sectional area of all the necks is obtained and is taken to represent that of a tube through which flow occurs. It is assumed that the material is isotropic that is the fractional pore area exposed in a slice is the same as the void volume. The pore size distribution is divided up in to n equal pore classes each of area  $1/n$ . The mean neck area for each of n portions of surface (B) with pores ( $r_1$ ) in contact with the first portion of (A) will be

$$e\pi r_1^2, e\pi r_2^2 \dots e\pi r_n^2,$$

taking the smallest pore in a sequence as determining the resistance thus  $r_1 > r_2 > r_n$ . Also on average the area of contact is taken to be (e) times its area. Similarly the portion (A) containing pores ( $r_2$ ) contacting with (B) will be

$$e\pi r_2^2, e\pi r_2^2, e\pi r_3^2 \dots e\pi r_n^2$$

This series is continued in this way until the nth portion of surface containing pore radii ( $r_n$ ) has been considered. This last portion will provide a neck area of  $e\pi r_n^2$  for each of the n portions of surface (B) with which it makes contact. Therefore the average area of neck cross-section for all  $n^2$  portions of surface is

$$e\pi/n^2 \left[ (r_1^2 + r_2^2 + r_3^2 \dots r_n^2) + (2r_2^2 + r_3^2 + \dots r_n^2) + \dots + n r_n^2 \right]$$

or

$$e\pi/n^2 \begin{bmatrix} r_1^2 & r_2^2 & r_3^2 & \dots & \dots & r_n^2 \\ r_2^2 & r_2^2 & r_3^2 & \dots & \dots & r_n^2 \\ r_3^2 & r_3^2 & r_3^2 & \dots & \dots & r_n^2 \\ \dots & \dots & \dots & \dots & \dots & \dots \\ r_n^2 & r_n^2 & r_n^2 & \dots & \dots & r_n^2 \end{bmatrix}$$

this area of neck is taken to represent the cross-sectional area of tube radius (r) controlling flow, where  $r^2$  is divided into the above. From this and Poiseuille's equation

$$K = \frac{e^2}{8n} \left[ r_1^2 + 3r_2^2 + 5r_3^2 + \dots + (2n-1)r_n^2 \right]$$

The averaging procedure is only valid because equal areas for each pore class were used. In the particular case for uniform pore sizes this equation reduces to

$$K = \frac{e^2 r^2}{8}$$

which is analogous to the Kozeny equation

$$K = \frac{e^3}{S^2 k_o t}$$

if  $k_o t$  is taken a  $2/e$ . That is  $k_o t = 5.0$ . Therefore the porosity must be 0.4 which is reasonable.

Millington and Quirk (1961) used the same treatment but differed in the pore area resulting from interaction. The probability of continuity of pore space in the model is dependent on  $(e)$ . Therefore the pore area resulting from an interaction will lie between  $(e)$  and  $(e) \times (e)$ . The area resulting from an interaction can be taken to be  $e^{2x}$  that is  $e^x$  interacting with  $e^x$  to give an effective area for flow. Furthermore  $e^x$  may be regarded as a



maximum area and  $e^{2x}$  a minimum area. Therefore the maximum area occupied by solid is  $(1 - e)^x$  and the minimum pore area given by  $1 - (1 - e)^x$ . These minimum pore interaction areas should be identical

$$\therefore e^{2x} + (1 - e)^x - 1 = 0$$

for values of  $e$  between 0.1 and 0.6  $x$  is between 0.6 and 0.7 and may be taken a  $2/3$  the equation for permeability is therefore given as

$$K = \left(\frac{e^{2/3}}{8 n^2}\right)^2 \sum_{i=1}^n (2i - 1) r_i^2 = \frac{e^{4/3}}{8 n^2} \sum_{i=1}^n (2i - 1) r_i^2$$

Wyllie and Gardner (1958) allowed for a reduction in area and of individual pore size and their equation contained a factor  $e^3$

$$K = \frac{e^3}{8 n} \frac{B}{a} \sum_{i=1}^n r_i^2$$

The factors  $B$  and  $a$  are introduced in the derivation and go out when the equation is used for relative permeability.

Generally the equations if used for unsaturated permeability have the summation stopped at the appropriate pore size and also the porosity junction modified by the saturation. Thus Millington and Quirk give the following for non-wetting and wetting phase permeabilities

$$K_{nw} = \frac{(e S_{nw})^{4/3}}{8 n^2} \sum_{i=1}^{S-1} (2i - 1) r_i^2$$

$$K_w = \frac{(e S_w)^{4/3}}{8 n^2} \sum_{i=1}^n 2(i - 1) r_i^2$$

these must be divided by  $K_{sat}$  to give relative permeabilities.

The cutting and joining model when the pore interaction factor is taken as  $e^2$  gives an essentially two dimensional model of pore space continuity. It neglects the routes in the third dimension which are available in real porous media. The  $(e^{4/3})$  factor in the Millington & Quirk equation is an attempt to recognise this and provide opportunities for these extra connections. The equation has been shown to give a better fit for relative permeability values, Marshall (1962), Wall (1965), and this must emphasise this point.

Marshall (1962) extended the model into 3 dimensions by considering stacks of cells each containing uniform pore sizes which together gave a distribution

$$K = \frac{C}{n} \sum_1^n \left[ \frac{2r_1^2 r_i^2}{r_1^2 + r_i^2} + \frac{2r_2^2 r_i^2}{r_2^2 + r_i^2} + \dots + \frac{2r_n^2 r_i^2}{r_n^2 + r_i^2} \right]$$

if the smaller pores in two connecting cells are taken as dominating the permeability then this reduces to

$$K = \frac{C}{n^2} \sum_1^n (2i - 1) r_i^2$$

where C is a constant determined by the material.

### 6.5.2 Lattice Models

Lattice models, in which the structure of pore space is taken to be composed of small units which can be added together to form a porous medium, have been proposed by Flood (1958) and Le Goff (1967).

Le Goff (1967) approached the problem from consideration of a framework which allows repeating space filling elements to be used to characterise the flow regimes in two phase flow in packed columns. The simplest element which does not require orientation for space filling is the cube. Relatively few parameters are required to characterise the flow properties of this model and they can be determined by experiment. Knowing these parameters allows prediction of behaviour under a range of conditions.

A similar model has been described by Flood (1958) to allow statistical representation of pore space. It has been extended by Wall (1965) to provide an expression for permeability in terms of the pore size distribution and the pore structure defined by the porosity and the formation factor.

The cubical elements comprising the porous medium have a range of edge sizes ( $l_i$ ). Each cube contains a model pore, as shown in Fig. (42), where the square capillary neck has a side

Flood (1958)

Unit Pore

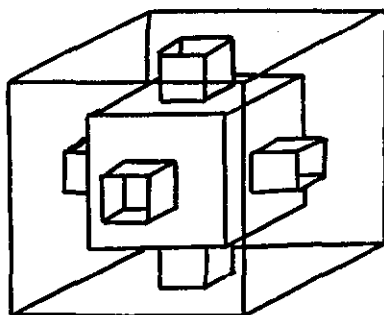


Fig. (42)

of  $l_i/a$  and the central cubical void a side of  $b l_i/a$ . This allows the porosity and the formation factor to be calculated

$$e = \frac{b^3 + 3a - 3b}{a^3} \quad F = a(a - b) + \frac{a}{b} - \frac{2a(a - b)}{b^2(b^2 - 2a - 2b)}$$

Plots of porosity versus formation factor can be made for various values of (a) and (b). Therefore if (F) or (e) is known for a real system it is possible to evaluate an expression for permeability in terms of the pore space parameters. Wall derives the equation

$$K = \frac{1}{8a(a - b)} \frac{\sum r_i^2}{n}$$

where ( $r_i$ ) is the equivalent radius of the capillary neck. This is essentially similar to the other expressions, but really considers pore space as a sequence of identical pores. The extension to relative permeability may not therefore be successful.

### 6.5.3 Network Models

A more direct introduction of pore space connectivity was made by Fatt (1956) with the network of tubes model of porous media. This is the same as previously described in the capillary pressure section but utilized for permeability studies and more especially two phase permeability. Fatt was not able to calculate the permeability of the model directly for a reasonable size of network because the number of variables was too great for convenient working with the size of computer then available. He therefore constructed an electrical analogue using the correspondence between Ohms Law and Poiseuilles Law

$$V = R I \quad \Delta P = \frac{8 \eta L}{\pi r^4} q$$

$$\text{Resistance} = \frac{8 \eta L}{\pi r^4} = \frac{C L}{r^4}$$

If only relative values are required it is sufficient to use resistance proportional to  $L / r^4$ . Knowing the radius and length of each tube in the network it is therefore possible to calculate an equivalent electrical resistance. A network of appropriately sized resistances was then set up and the total resistance (or permeability) of the network measured directly. By removing resistances to simulate desaturation (as previously described) it is possible to measure the permeability of the network at different saturations. The removed resistances were fitted into an equivalent network which represents the non-wetting phase flow path and the resistance of this was also measured. Thus a complete relative permeability saturation plot was obtained for both wetting and non-wetting phases. The relation between resistivity and saturation was also investigated. This however requires another set of resistances since the electrical resistance of a fluid filled tube is proportional to  $L / r^2$  as compared with  $L / r^4$  for the flow resistance.

Fatt applied the technique to different network configurations and a range of pore size distributions including mono-size pores, just as in his capillary pressure work. He was able to show that the shape of the relative permeability curves could be reproduced by this network model and that the sum of non-wetting and wetting phase relative permeabilities was always less than unity. This even applied to a network of mono-size tubes which were desaturated in random sequence. The non-wetting phase relative permeability was found to be more sensitive to changes in network shape than the wetting phase, but the characteristics of two phase flow in general were shown to be mainly a consequence of the inter-connections in

the network. The measurements of resistivity for different saturations followed Archie's Law,

$$\text{Relative Resistivity} = S_w^{-n}$$

for all saturations. The exponent (n) was shown to be related to the number of inter-connections per pore in the network but not the pore size distribution. From measurements of relative resistivity on unconsolidated media Fatt concluded that networks in these have between 4 and 13 connections at each junction.

In a similar but independent work Probine (1958) used a 6 connection <sup>per</sup> junction network arranged in three dimensions. This was chosen to represent the pore space occurring in a cubical packing of equal spheres. Even with a relatively small network of 64 resistances this gave a better fit with the measured relative permeabilities of Childs and Collis-George than did their expression for permeability.

Rose (1957) extended Fatt's network concept to larger sizes by using a digital computer. He considered a three dimensional tetragonal network which has a high degree of connectivity and pore path possibility. This could be altered to other less well connected networks by fitting in zero pores randomly. Rose showed that the number of connections per pore is not sufficient by itself to specify network configurations in three dimensions as it cannot account for the number of pore paths available between adjacent junctions. Therefore Fatt's conclusion from his essentially two dimensional model that the shape of relative permeability curves is mainly determined by number of inter-connections per pore must be seen as too simple.

Two methods were outlined for operating on the large network

with a computer; one was a direct method of following consecutive processes in pores, the other a network relaxation method as described by Dykstra and Parsons (1951). Rose was not primarily concerned with using the model as a microscopic description of fluid flow in porous media but rather of using it to represent the macroscopic processes involved in oil reservoirs. The techniques are applicable in principle to microscopic descriptions since he merely used a less fine network in which the correspondence is not on the basis of individual pores.

So far no expression for permeability in term of the parameters of porous media has been derived from network models.

#### 6.5 SUMMARY

The flow of fluids in porous media has been discussed in terms of expressions for permeability given by parameters of pore space. It has been shown that models based on the bundle of tubes concept including the Kozeny-Carman equation rely on tortuosity factors to account for the true nature of pore space in an unrealistic way. These relationships are not very satisfactory for single phase flow in porous media but breakdown seriously in characterising two phase flow. This is because of the way two immiscible fluid phases distribute themselves in a porous medium which does not allow average properties to be used. It has been emphasised therefore that in expressions for relative permeability pore size distribution and pore space connectivity must be incorporated. The network model of Fatt is important in this respect as it successfully reproduces relative permeability characteristics for even a system of mono-size pores. The theoretical model which is similar to Fatts model may therefore be applied to this problem.

## CHAPTER SEVEN

### NETWORK MODEL APPLIED TO FLUID FLOW

#### 7.1 INTRODUCTION

Existing relationships for the permeability of porous media have been mentioned and their short-comings discussed. In general they are not satisfactory because they do not take full account of the true nature of pore space. This is especially so for two phase immiscible flow where pore size distribution and pore connectivity have been shown to be critical factors. In Chapter IV a theoretical model of the pore space in a pack of unequal spheres in dense random packing was developed, in which the connectivity of the pores was approximated by a regular two dimensional array. Capillary pressure curves were obtained from this model which compare quite well with experimental results. The model is based on that used by Fatt (1956) who obtained permeabilities of the model by constructing electrical resistance analogues and directly measuring the total resistance of the arrays. The use of electrical relationships is based on the analogy between Ohms law for electrical resistance and Poiseuilles law for flow in capillary tubes

$$I = V / R \quad q = \frac{\pi r^4}{8 \eta L} \Delta P$$

$$\frac{1}{R} \equiv \frac{\pi r^4}{8 \eta L} \quad \therefore R \propto L / r^4$$

Thus the flow resistance of a network of different sizes of capillary tubes can be represented by the electrical resistance of a network of appropriately sized resistors. The direct measurement of the resistance of specially constructed arrays of resistors is of limited use, but Kirchoffs laws can be applied to the network and the total resistance calculated. In the next sections a matrix



expression of Kirchoff's laws is developed which is related to the permeability of the network of capillary tubes model developed in Chapter IV. The derivation is taken from electrical network theory but the inter-changeability of these and capillary tube relationships has been demonstrated.

## 7.2 MATRIX EXPRESSION FOR THE RESISTANCE OF A NETWORK

The following treatment is based on that given in textbooks on electrical network theory such as those by Stigant (1964) and Tropper (1962) which are based on the work of Kron (1939).

The performance of any given network may be derived from the performance of the individual elements in the network. In Fig. (43) the real network (a) may be reduced to the so-called

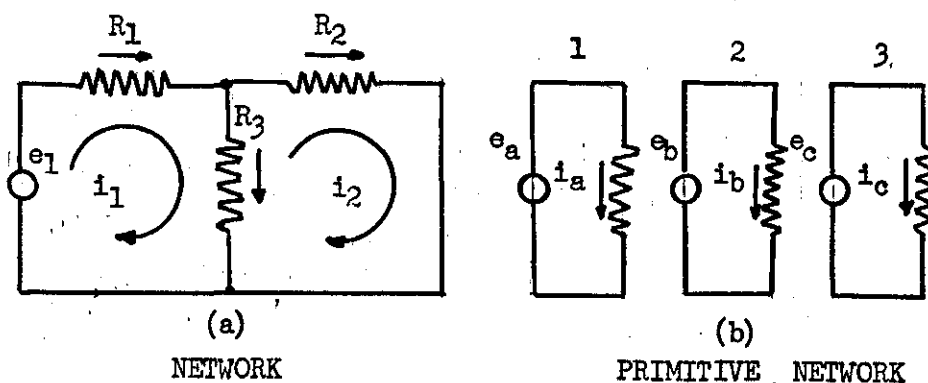


Fig. (43)

"primitive" network form (b) and the relation between the two systems can be represented by a transformation or connection matrix. In Fig. (43) (b) Ohms law may be expressed

$$\begin{bmatrix} e_a \\ e_b \\ e_c \end{bmatrix} = \begin{bmatrix} R_1 & 0 & 0 \\ 0 & R_2 & 0 \\ 0 & 0 & R_3 \end{bmatrix} \begin{bmatrix} i_a \\ i_b \\ i_c \end{bmatrix}$$

$$[e'] = [R] [i']$$

But from the real network in Fig. (43) (a)

$$\begin{aligned} i_a &= i_1 \\ i_b &= i_2 \\ i_c &= i_1 - i_2 \end{aligned}$$

which may be expressed

$$\begin{bmatrix} i_a \\ i_b \\ i_c \end{bmatrix} = \begin{bmatrix} 1 & 0 \\ 0 & 1 \\ 1 & -1 \end{bmatrix} \begin{bmatrix} i_1 \\ i_2 \end{bmatrix}$$

$$[i'] = [C] [i]$$

where  $[C]$  is the transformation or connection matrix and provides the relationship between the currents in the actual network and the primitive network.

Similarly the relationship between the voltages in (a) and (b) may be given in terms of a matrix which is the transpose of  $[C]$

$$\begin{aligned} e_1 &= e_a + e_c \\ e_2 &= e_b - e_c \\ [e] &= [C]_t [e'] \end{aligned}$$

The connection matrix is a rectangular matrix with (i) rows and (j) columns where (i) is the number of elements and (j) is the number of loops in the actual network. To define the connection matrix for a network the elements and the loops in the network are numbered and the directions of current flow arbitrarily assigned. Here loop currents are taken as being clockwise and currents in elements taken as either left to right for horizontal

elements or top to bottom for vertical elements. The elements of the matrix may be designated according to these rules:

- $C_{ij} = 0$  If element (i) is not part of loop (j)  
 $C_{ij} = +1$  If the assumed direction of current flow in element (i) coincides with the assumed loop current flow in (j)  
 $C_{ij} = -1$  If the assumed direction of current flow in element (i) is opposite to the assumed loop current flow in (j)

Therefore going back to the expression of Ohms law for the primitive network

$$\begin{aligned}
 [e'] &= [R] [i'] \\
 \therefore [e] &= [C]_t [R] [i'] = [C]_t [R] [C] [i]
 \end{aligned}$$

∴ Ohms law for the actual network may be expressed

$$[e] = [Z] [i]$$

$$\text{where } [Z] = [C]_t [R] [C]$$

In electrical terminology this is called the 'mesh impedance matrix' and is an operator which acts as the resistance of the whole network.

In the network shown in Fig. (43) (a)

$$[Z] = \begin{bmatrix} 1 & 0 & 1 \\ 0 & 1 & -1 \end{bmatrix} \begin{bmatrix} R_1 & 0 & 0 \\ 0 & R_2 & 0 \\ 0 & 0 & R_3 \end{bmatrix} \begin{bmatrix} 1 & 0 \\ 0 & 1 \\ 1 & -1 \end{bmatrix}$$

$$[Z] = \begin{bmatrix} (R_1 + R_3) & -R_3 \\ -R_3 & (R_2 + R_3) \end{bmatrix}$$

This  $[Z]$  is a symmetrical square matrix with its order given by the number of loops in the network, in this case  $2 \times 2$ . This may also be defined directly by a set of rules:

$$Z_{ii} = \text{The sum of resistances in loop (i)}$$

$$Z_{ij} = Z_{ji} = - (\text{The sum of resistances common to loops (i) and (j) })$$

Thus a matrix expression for the performance of a network may be given by

$$[e] = [Z][i]$$

where  $[e]$  and  $[i]$  are column vectors representing the current and the voltage sources in each loop. The matrix  $[Z]$  may be defined either from the connection matrix and a diagonal matrix of the resistance elements

$$[Z] = [C]_t [R] [C]$$

or directly from the configuration of the network and values of the resistances.

It must be remembered that a matrix may only be used as an operator on other matrices and is not a definite quantity, therefore the total permeability or resistance of a network may only be obtained in terms of potentials and the currents in the network. That is, where in general the potential drop across an array of resistances is known, the mesh impedance matrix can be used to calculate the loop current matrix from

$$[Z]^{-1} [e] = [i]$$

Therefore knowing the potential drop across the network and the current it causes, the total effective resistance of the network may be calculated. In general therefore the problem is one of finding the inverse of the mesh impedance matrix.

7.3 APPLICATION OF THE RELATIONSHIPS TO THE NETWORK MODEL OF POROUS MEDIA

The matrix relationships may be used in calculating the performance of the network of capillary tube model. The form of the network used in Chapter IV for capillary pressure curves is slightly changed for convenient operation by using a square array and removing the voids at each junction. This latter change is equivalent to assuming that the permeability of the network is governed by the narrow tubes between junctions. An example of the network form used is shown in Fig. (44) in which there are 13 loops and 21 elements

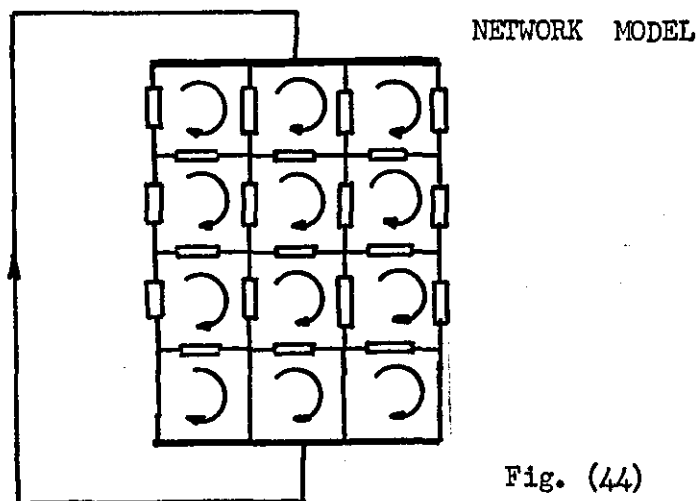


Fig. (44)

In this by analogy between Ohms law and Poiseuilles law

$$\text{Resistance} \propto L / r^4$$

and

$$\text{voltage} \propto \Delta P$$

$$[Z]^{-1} \begin{bmatrix} \Delta P \\ 0 \\ 0 \\ \vdots \\ 0 \end{bmatrix} = \begin{bmatrix} i_1 \\ i_2 \\ i_3 \\ \vdots \\ i_{13} \end{bmatrix}$$

Since there is only one potential source in this problem then the whole of the inverse of  $[Z]$  is not required. Assuming the inverse of  $[Z]$  to be  $[X]$

$$[Z]^{-1} \begin{bmatrix} \Delta P \\ 0 \\ 0 \\ \vdots \\ 0 \end{bmatrix} = \begin{bmatrix} X_{11} & X_{12} & \dots & X_{113} \\ X_{21} & X_{22} & \dots & X_{213} \\ X_{31} & X_{32} & \dots & X_{313} \\ \vdots & \vdots & \vdots & \vdots \\ X_{131} & X_{132} & \dots & X_{1313} \end{bmatrix} \begin{bmatrix} \Delta P \\ 0 \\ 0 \\ \vdots \\ 0 \end{bmatrix} = \begin{bmatrix} \Delta P X_{11} \\ \Delta P X_{12} \\ \Delta P X_{13} \\ \vdots \\ \Delta P X_{113} \end{bmatrix} = \begin{bmatrix} i_1 \\ i_2 \\ i_3 \\ \vdots \\ i_{13} \end{bmatrix}$$

Therefore it can be seen that only the first column of the inverse of  $[Z]$  is required. By definition of the inverse of a matrix

$$[Z] [Z]^{-1} = [I]$$

Where  $[I]$  is the unit matrix which is a diagonal matrix in which each non-zero element is unity. Therefore the first column of the inverse of  $[Z]$  may be obtained by the solution of a set of simultaneous equations in which the right hand side co-efficients are given by the first column of  $[I]$

$$\begin{bmatrix} Z_{11} & Z_{12} & \dots & \dots & Z_{113} \\ Z_{21} & Z_{22} & \dots & \dots & Z_{213} \\ Z_{31} & Z_{32} & \dots & \dots & Z_{313} \\ \vdots & \vdots & \vdots & \vdots & \vdots \\ Z_{131} & Z_{132} & \dots & \dots & Z_{1313} \end{bmatrix} \begin{bmatrix} X_{11} \\ X_{21} \\ X_{31} \\ \vdots \\ X_{131} \end{bmatrix} = \begin{bmatrix} 1 \\ 0 \\ 0 \\ \vdots \\ 0 \end{bmatrix}$$

The overall permeability of the network shown in Fig. (44) may then be obtained from

$$K = i_1 / \Delta P$$

but since  $i_1 = \Delta P X_{11}$

therefore  $K = X_{11}$

Thus the overall permeability of the network is given by one element of the inverse of the mesh impedance matrix.

This applies generally no matter which way the loops in the network are numbered as the required solution will always be given by the equation with a right hand side co-efficient of 1. This is obtained from the appropriate column of the unit matrix. The solution may therefore be seen to be an application of Kirchoffs voltage law that, the algebraic sum of the products of current and resistance in each part of a closed circuit is equal to the applied voltage in the circuit.

However the statement of the relationships in the form given by the mesh impedance matrix allows the contributions due to the individual elements and the contribution of the network to be differentiated

$$[Z] = [C]_t [R] [C]$$

The matrix  $[R]$  can be taken to be related to a pore size distribution since the terms it contains are made up of the resistances of individual pores. This may be defined almost independently of the actual configuration of the porous medium by a capillary pressure curve. Furthermore capillary pressure curves for similar particle size distributions have been shown to be correlatable to one unique curve for any porosity or absolute particle size by using the relation

$$\frac{e}{(1-e)} S_o$$

This could therefore be incorporated in  $[Z]$  as a scalar multiplier to the  $[R]$  matrix. Thus the individual resistive elements in a porous medium may be defined by a function similar to that used by the Kozeny-Carman equation. Here however an additional factor of the structure of the pore space is also included. The success

of the Kozeny-Carman equation may be therefore understood by the success of the correlation used in Chapter V for capillary pressure curves, and also that the  $[C]$  matrix for an actual porous medium either does not vary very much or, is not critical, in most cases and can be represented by a single coefficient such as the tortuosity.

#### 7.4 USE OF THE MATRIX METHOD FOR PERMEABILITY AND RELATIVE PERMEABILITY

The matrix expression for the performance of a network has been shown to be equivalent to a statement of Kirchoffs voltage law and to require the solution of  $n$  simultaneous equations where  $n$  is the number of loops in the network. It may be possible to give the solution of the equations for the one element required in terms of a series expression involving the coefficients of the equations. This would then be equivalent to other relationships for permeability. In practice however it is more convenient to retain the matrix form and to treat the problem on this basis as a set of simultaneous equations. The main limitation on the use of the method is in the size of computer storage required for the matrices. For example a network of 100 loops requires solution of 100 simultaneous equations which means storage of 10,000 coefficients. Therefore the direct method of defining the mesh impedance matrix is preferred as the expression in terms of  $[C]$  and  $[R]$  requires storage of these also.

The largest network able to be solved with the computer available has 91 loops and contains 171 resistances, using the method given as a computer program in appendix 6. A list of the radii and the volumes of the capillary tubes calculated from the Wise model



of pore space is used. The flow resistance of each of these is calculated from Poiseuille's law (i.e.  $l / r^4$ ) and the resistance values are then arranged in random order in the network by using the library sub-routine ZORMAL ( $\phi$ ). From this the mesh impedance matrix is specified by the sub-routine Z (I, J) by assuming the network form in Fig. (44). This sub-routine defines the matrix from the number of loops in the network and the appropriate number of resistance values to fill the network, and thus the matrix need not be stored. The 91 simultaneous equations defined by this and the first column of the unit matrix are then solved using the library sub-routine F2SOLVE. This is a sub-routine for the solution of simultaneous equations with partial row pivoting and row normalisation. The permeability of the network is then picked out of the solution.

To apply the method to relative permeability, simplification has been introduced. As the network desaturates, that is the larger tubes empty and no longer contribute to the network permeability, the connectivity of the network changes. Therefore at each stage in the desaturation a new [C] and [R] should be evaluated. Here however the desaturation is taken to be simulated by the substitution of very high resistances for tubes which have been emptied. The network form and the [C] matrix are therefore considered to be unchanged by desaturation. Also for convenience the network desaturation procedure used in defining the capillary pressure curves from the network is not used and therefore isolation of large tubes by smaller ones is not considered. This greatly simplifies the operations on the matrix and may be used as a first approximation.

These methods of using the relationships are capable of

improvement since the mesh impedance matrix is symmetrical (as shown in 7.2) and is also quite sparse, for the network form used here. It should therefore be possible to reduce the storage required for the matrix by using these properties. A solution of the equations in terms of the compressed coefficient matrix will then have to be devised. This must be an accurate solution using pivoting as a simple elimination procedure was tried and found to be unsatisfactory.

## 7.5 RESULTS AND DISCUSSION

### 7.5.1 Saturated Permeability

The matrix expression of the permeability of a network has been applied to networks of capillary tubes calculated from the Wise model of sphere packing given in chapter IV. From this the radii lengths and relative numbers of the various capillary tubes making up a network are known and their individual resistances can be calculated. It is possible to apply the method to radii or pores determined from an experimental capillary pressure curve by making some assumption about the relationship of pore volume to radius but this was not attempted and the method is only applied to the derived network models. That is relating to the four mono-size packs of beads and the four 3-component mixtures previously mentioned.

The various resistances are fitted into the model network in random order using the library sub-routine ZORMAL ( $\phi$ ). Where ( $\phi$ ) is an integer between 1 and 9 which is used to vary the starting point for the calculation of the random number series. The effect of changing the randomising order on the calculated permeabilities is shown in Table VII.

TABLE VII

Bed	Permeabilities for different random arrangements						Average value	Average value $\times S_0 \times 10^{-2}$
36/52	9.44	9.45	9.44	9.44	9.58	9.49	9.47	15.34
52/60	3.41	3.42	3.41	3.41	3.46	3.46	3.42	8.07
72/85	1.33	1.33	1.31	1.32			1.32	4.22
150/120	.31	.31	.31	.31			.31	1.59
Mixture 1	2.83	3.15	2.86	2.91			2.93	6.85
Mixture 2	7.69	8.60	8.81	8.18			8.32	13.39
Mixture 3	1.56	1.56	1.56	1.52	1.54	1.56	1.55	3.50
Mixture 4	1.36	1.25	1.21	1.26	1.36		1.27	2.58

It can be seen that in general the variability of the results is greater for the three-component mixtures than for the mono-size packs. This is because there is a greater capability of variation in these networks as the pore size distribution and therefore the resistance distribution is wider. This variability should be reduced if the network size was greater.

To compare these results with other results for permeability it must be remembered that the relationship between the size and shape of the network, to the element of the porous material it represents must be included. The network form and shape has been kept constant for each bed and therefore each network represents a similar element of pore space. However for the given constant number of tubes in the network the system represents a larger element of the pore space for the 36/52 bed with an average sphere diameter  $370\mu$  than that of the 150/120 bed with an average sphere diameter of  $117\mu$ . The average values of the network permeabilities given in Table VII must

therefore be divided by the average sphere diameters of the pack they represent. That is multiplied by the specific surface as is presented in the last column of Table VII. These values are not absolute values of permeability for the various sphere packs but may be only taken to be proportional to the absolute permeability as a constant multiplying factor for the network shape used must also be included.

Permeabilities for each of the samples used has been calculated using both the Kozeny-Carman equation,

$$K = \frac{e^3}{5.0 (1 - e)^2 S_o^2}$$

and also from the experimental and theoretical capillary pressure curves using the expression of Millington and Quirk given in 6.5.1

$$K = \frac{e^{4/3}}{8r^2} (r_1^2 + 3r_2^2 + 5r_3^2 + \dots + (2n - 1) r_n^2)$$

KMQ = Permeability by Millington & Quirk

KKC = Permeability by Kozeny-Carman

TABLE VIII

PERMEABILITIES OF MONO SIZE PACKS  $\text{cm}^2 \times 10^{-8}$

36/52

e	.2197	.3575	.3547	.3528	.3524	.3508
KMQ	15.58	113.16	113.45	109.53	108.15	91.25
KKC	13.22	84.04	81.37	79.60	79.23	77.77
KMQ/KKC	1.17	1.34	1.39	1.37	1.36	1.17

e		.3532	.3725	.3583	.3926	
KMQ		91.16	138.31	117.29	196.92	
KKC		79.97	99.67	84.82	124.54	
KMQ/KKC		1.13	1.38	1.38	1.58	

52/60

e	.2135	.3528	.3519	.3952	.4003
KMQ	7.68	52.50	54.23	84.23	92.49
KKC	5.64	37.60	37.21	60.53	63.97
KMQ/KKC	1.36	1.39	1.45	1.39	1.44

72/85

e	.2199	.3517	.3445	.3844	.3839
KMQ	4.19	26.54	24.40	42.45	41.41
KKC	3.42	20.26	18.63	29.34	29.18
KMQ/KKC	1.22	1.30	1.30	1.44	1.41

150/120

e	.2195	.3471	.3504	.3466	.3469
KMQ	1.58	8.82	8.83	8.56	8.78
KKC	1.31	7.42	7.71	7.37	7.40
KMQ/KKC	1.20	1.20	1.14	1.16	1.18

e		.3420	.3495	.3967	
KMQ		8.18	8.63	16.38	
KKC		6.99	7.63	12.97	
KMQ/KKC		1.17	1.13	1.26	

TABLE IX

PERMEABILITIES OF 3-COMPONENT MIXTURES ( $\text{cm}^2 \times 10^{-8}$ )

Mixture 1

e	.2122	.3503	.3537	.3924	.3952
KMQ	6.69	53.74	52.29	87.30	86.55
KKC	5.63	37.26	38.76	59.88	61.74
KMQ/KKC	1.18	1.44	1.34	1.45	1.40

Mixture 2

e	.2112	.3434	.3434	.3871	.3881
KMQ	13.75	88.73	92.11	168.33	164.84
KKC	11.69	72.53	72.53	119.24	120.56
KMQ/KKC	1.17	1.22	1.26	1.41	1.36

Mixture 3

e	.1975	.3316	.3325	.3902	.3867
KMQ	3.87	44.32	46.91	91.18	85.17
KKC	4.67	31.85	32.20	62.36	60.01
KMQ/KKC	.82	1.39	1.45	1.46	1.41

Mixture 4

e	.1792	.3033	.3404		
KMQ	3.64	63.96	40.39		
KKC	4.18	44.37	28.13		
KMQ/KKC	.87	1.44	1.43		

TABLE X

PERMEABILITY OF FILTER AID SAMPLES  $\text{cm}^2 \times 10^{-8}$

Sample	$e$	$S_o$ $\text{cm}^3/\text{cm}^2$	KM <sub>Q</sub>	KKC	KM <sub>Q</sub> /KKC
560	.8650	7,164	27.16	13.84	1.96
560	.8747	7,414	29.68	15.51	1.91
545	.8633	9,733	11.64	7.08	1.64
535	.8566	12,389	6.47	3.98	1.62
503	.8611	14,529	6.35	3.14	2.02
Hy Flow Super Cel	.8547	18,823	2.52	1.67	1.50

These show that the permeabilities calculated by the Millington and Quirk expression are higher than those calculated by the Kozeny-Carman equation by a constant factor of about 1.3 except for the filter aid results for which it is around 1.8. Also the tables show that the permeabilities calculated from the results of the theoretical model are consistent with those calculated from experimental results. These calculated permeabilities for the model are compared with permeabilities for the network model obtained by the matrix method in Table XI.

TABLE XI

	Matrix method	KM <sub>Q</sub>	$\frac{K \text{ matrix}}{KM_Q}$	KKC	$\frac{K \text{ matrix}}{KKC}$
36/52	15.34	15.58	.98	13.22	1.16
52/60	8.07	7.68	1.05	5.64	1.43
72/85	4.22	4.19	1.00	3.42	1.23
150/120	1.59	1.58	1.00	1.31	1.21
Mixture 1	6.85	6.69	1.02	5.63	1.21
Mixture 2	13.39	13.75	.97	11.69	1.14
Mixture 3	3.50	3.87	.90	4.67	.74
Mixture 4	2.58	3.64	.70	4.18	.61

The results shown for the three different methods of calculating the permeability of the model sphere packs are each different by a constant value, they may therefore be taken to be consistent with one another. Comparison with the experimental results for the Kozeny-Carman equation and the Millington and Quirk expression have been shown to be consistent with the calculated values for the model results and may therefore be also taken to support this.

Permeabilities calculated for the network model by the matrix method are therefore consistent with other methods of calculating the permeability of the model and also with calculated permeabilities from experimental results.

#### 7.5.2 Relative Permeability

The permeability equation of Millington and Quirk may be used to calculate relative permeabilities from capillary pressure curves by a modification of the porosity term to include saturation and by stopping the summation of the radius terms at the appropriate point. Thus

$$K_w = \frac{(e S_w)^{4/3}}{8 n^2} \sum_s^n (2i - 1) r_i^2$$



$$K_{rw} = \frac{(e(1 - S_w))^{4/3}}{8n^2} \sum_{i=1}^{S-1} (2i-1)r_i^2$$

and the relative permeabilities are given by these expressions divided by the saturated permeabilities. These expressions have been applied to the measured capillary pressure curves using 100 increments in the summation and a straight line interpolation between the experimental points. The results are plotted as relative permeability curves for the mono-size packs in Fig. (45), for the three-component packs in Fig. (46) and the filter aid samples in Fig. (48). The same results calculated from capillary pressure curves obtained from the theoretical model are shown with the mono-size pack results on Fig. (45) and for the three-component separately on Fig. (47).

These curves exhibit all the characteristics noted by Wycoff and Botset and mentioned in Chapter VI. The permeabilities of both the wetting and non-wetting phases approach zero for quite appreciable saturations. Residual moisture is excluded from the expression of saturation, therefore a margin of an extra 5% - 10% must be added to the low saturation side of these plots in which the wetting phase permeability is zero and the non-wetting phase relative permeability is 1.0. In each case the wetting and non-wetting phase curves cross below about .25 relative permeability and only add up to 1.0 at 0% and 100% saturation.

The results from the experimental capillary pressure curves for the mono-size samples all lie on the same curve with the results from the theoretical capillary pressure curves slightly to one side. Comparison with the results for the three-component packs and for the filter aid material show that wider pore size distributions

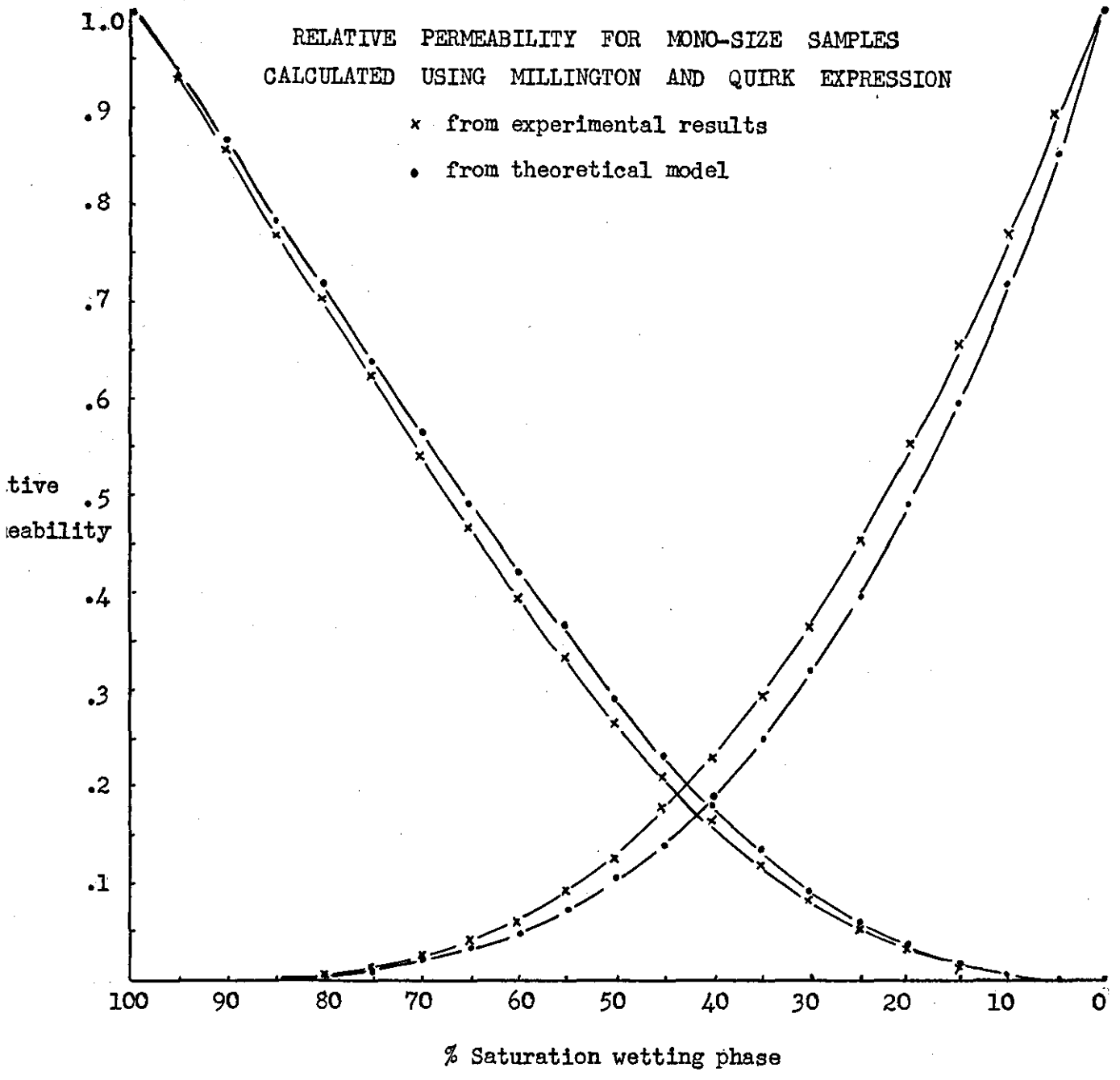


Fig. (45)

RELATIVE PERMEABILITY FOR 3-COMPONENT MIXTURES CALCULATED  
USING MILLINGTON AND QUIRK EXPRESSION

- × Mixture 1
- Mixture 2
- △ Mixture 3
- Mixture 4

Relative  
Permeability

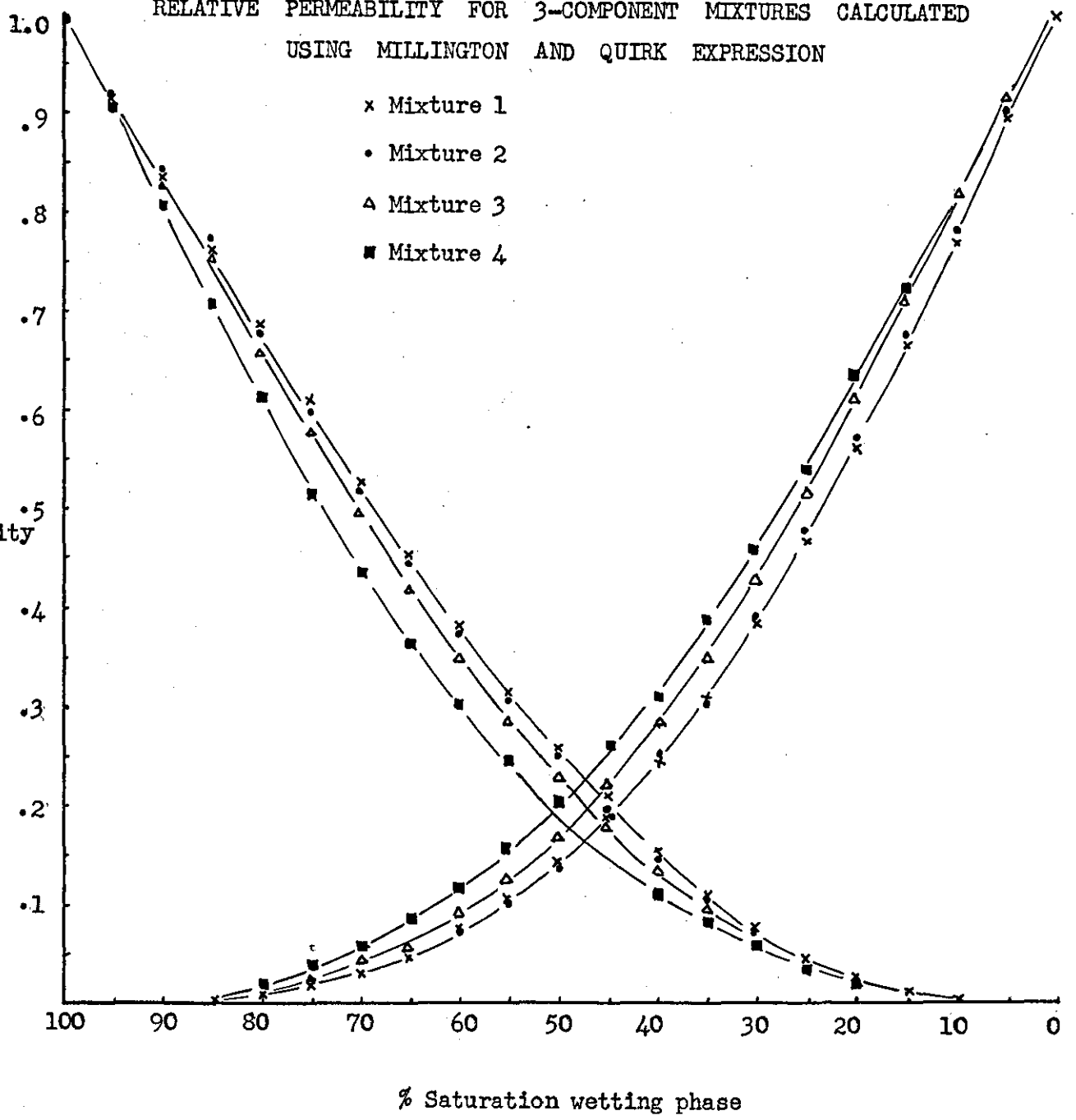


Fig. (46)

RELATIVE PERMEABILITY OF THEORETICAL MODEL FOR 3-COMPONENT MIXTURES USING MILLINGTON AND QUIRK EXPRESSION

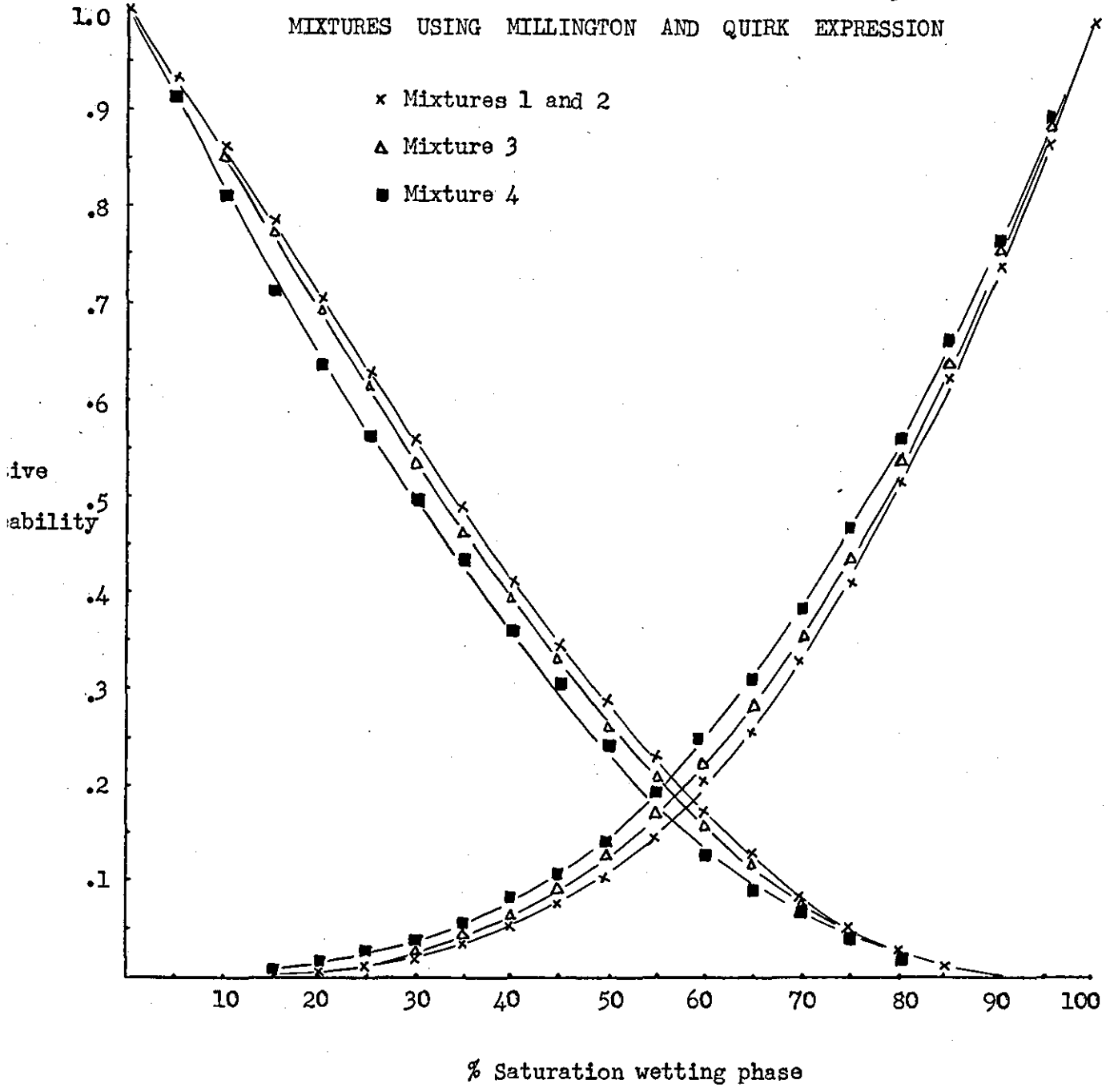


Fig. (47)

RELATIVE PERMEABILITY OF FILTER AID SAMPLES  
USING MILLINGTON AND QUIRK EXPRESSION

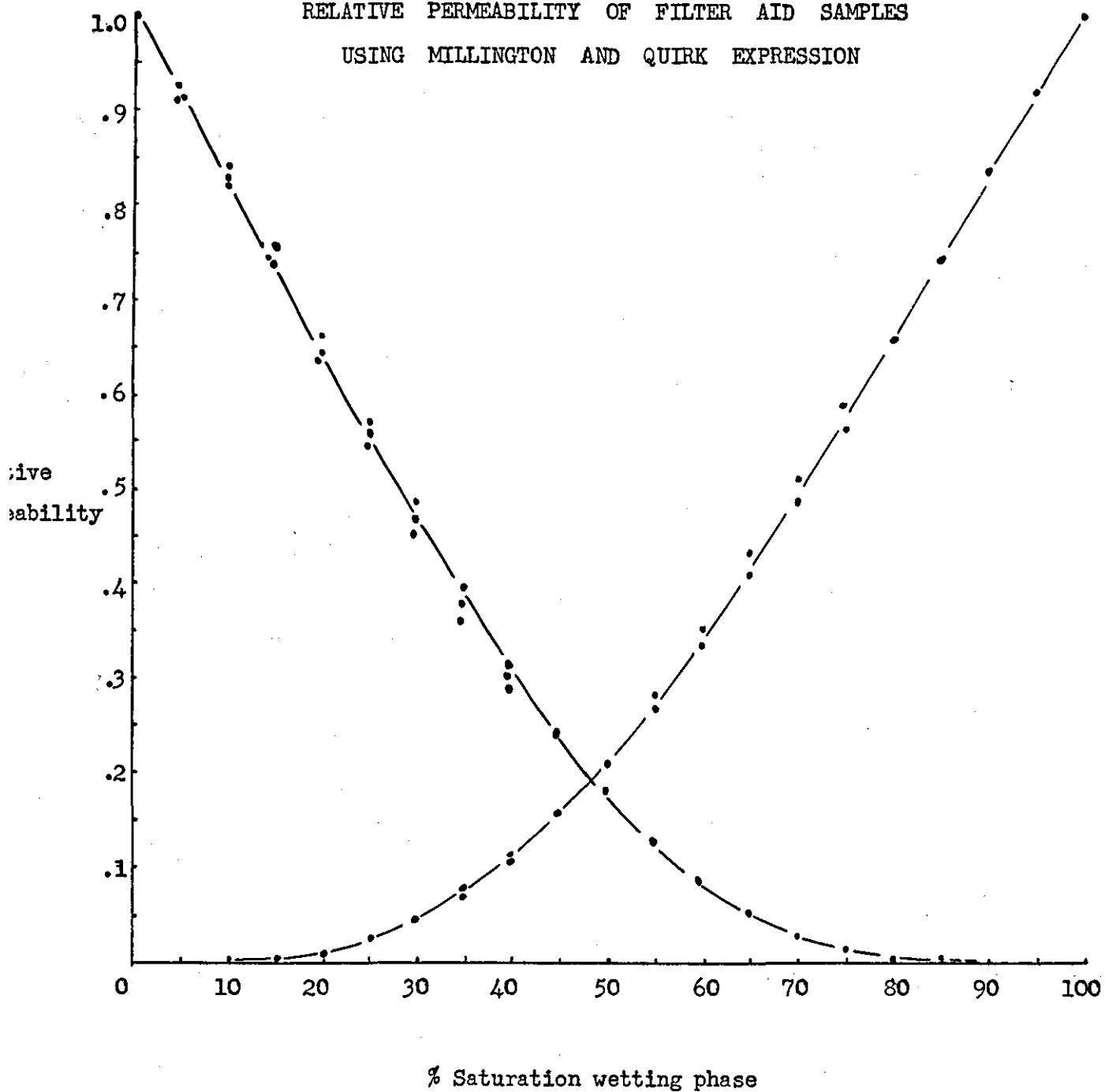


Fig. (48)

RELATIVE PERMEABILITY BY MATRIX METHOD

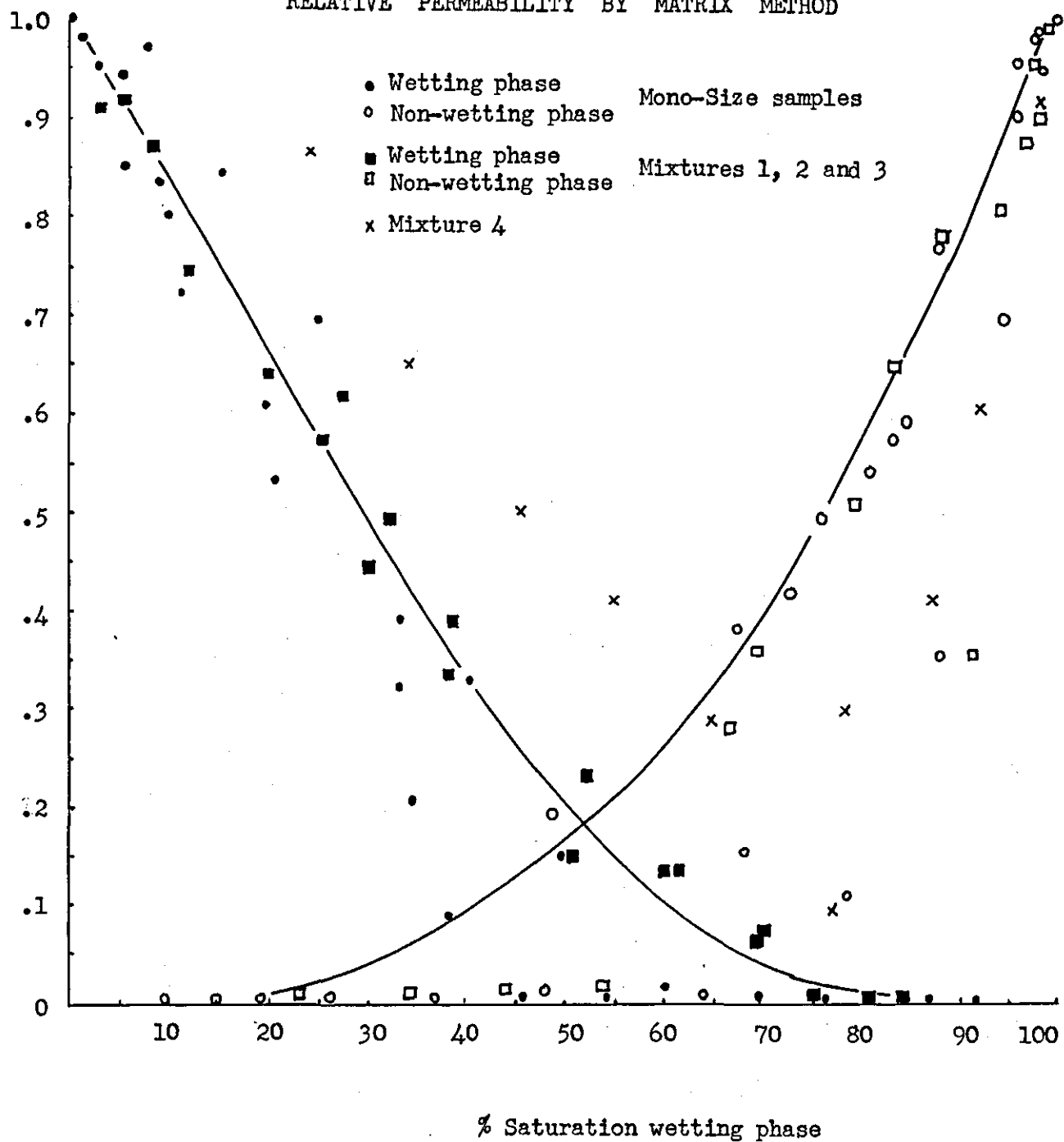


Fig. (49)

move the cross-over point of the pairs of curves towards the higher wetting phase saturations. Therefore since in general the theoretical model predicts a narrower pore size distribution than was found in practice, the relative permeability curves are to the right of the results calculated from the experimental curves to which they relate.

Relative permeability curves have also been calculated for the theoretical model using the matrix method. The results are shown for all the eight particle size distributions on Fig. (49). In these calculations only one value of the randomising function has been used which goes some way to explaining the wide scatter of the points. The variability may also be ascribed to the small size of the network used and to the limitations of the pore size distribution derived from the Wise model and mentioned in Chapter V. The main deviation is that due to mixture 4 which has the widest particle size distribution and which gives the greatest variation for different values of the randomising function and also the poorest fit for saturated permeability results. There is also doubt attached to the values of saturation at each point since the desaturation procedure used in determining capillary pressure curves is not used and also the void spaces which contribute a great deal to the total pore volume are not included. However a curve can be drawn through the points which follows the main features of the relative permeability <sup>u</sup> curves given by the Millington and Quirk expression. It is however not possible to pick out the features due to pore size distribution.

Considering the assumptions made in the derivation of the pore size distributions used in these calculations from the Wise model, the simplification introduced in setting up the network and

the small size of the network used the agreement is not unreasonable and at least justifies a further investigation of the procedure. However the main point may be taken as the corroboration of the conclusion made by Fatt that the characteristic shape of relative permeability curves is a result of both the pore size distribution and the structure of the pore space of porous media. Of these the most important feature in relative permeability curves may be taken to be the structure since the effect of pore size distribution can be shown to be quite small and only to make minor alterations in the configuration of the curves.

#### 7.6 SUMMARY AND CONCLUSIONS

A matrix expression for permeability has been developed from electrical network theory which includes terms for both the pore size distribution and the structure of a porous medium.

Permeabilities for the packs of beads used in the experiments in Chapter V have been calculated using the matrix method, the Kozeny-Carman equation and the expression derived by Millington and Quirk. The results for each method bear a constant relation to the others which is taken as indicating self consistency.

Relative permeability curves have been calculated from experimental and theoretical capillary pressure curves using the expression of Millington and Quirk. These curves show all the characteristics outlined in Chapter VI. The effect of pore size distribution on the curves has been noted and the results calculated from the theoretical capillary pressure curves show the effect of the narrowness of their pore size distribution.

Relative permeability curves calculated by the matrix method show a scatter about curves which are similar to the previous calculated curves. Reasons for this scatter have been advanced.



## CHAPTER EIGHT

### DEWATERING AS A FLOW PROCESS

#### 8.1 INTRODUCTION

The capillary theory of dewatering has been applied by previous workers to filter cakes by discussing the effects shown by capillary pressure curves. However dewatering is primarily a flow process and for any optimisation of the operation the relationship between saturation and time during dewatering is essential. Nenniger and Storow and Batel have described saturation versus time curves for dewatering by including the flow of water as a film on the pore walls. But the existence<sup>e</sup> of this phenomena in porous media has not been supported by any of the work covered in the literature survey. Gray calculated saturation versus time curves for fine coal filter cakes using a bundle of tubes model of porous media but showed that this gave poor correspondance<sup>e</sup> with experimental results. The failure of this model may be understood from the criticism of it in Chapter VI.

The discussion on two phase flow phenomena in Chapter VI has shown that a permeability may be defined for each phase, in a given partially saturated porous medium, in terms of the saturated permeability which is dependant<sup>e</sup> only on the saturation of the material to the phase considered. Using these considerations a description of the dewatering process may be advanced as a succession of steady-state flows governed by relative permeability. An analysis is presented on these lines which, though it is not complete, does enable the effects of the various variables to be illustrated.

8.2 DEWATERING AS A FLOW PROCESS WITH  
A SUCCESSION OF STEADY-STATES

The dewatering of a filter cake by a displacing pressure may be considered as taking place in two stages. In the first stage water alone flows from the material and at a uniform rate of flow. This gives way to a second stage when the zone of change in saturation reaches the outflow face of the filter cake and both water and air flow simultaneously. This stage is characterised by a steady decline in the rate of flow of the water phase.

The process may be represented by a cell model of the form shown in Fig. (50). The filter cake is divided horizontally into

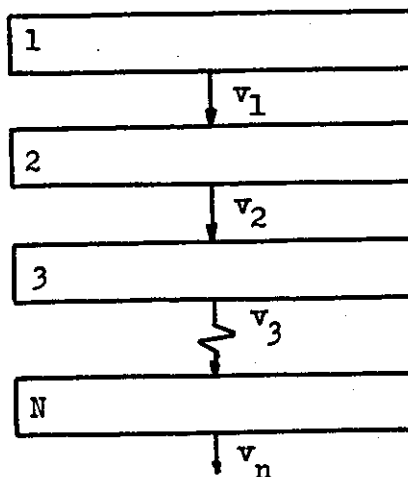


Fig. (50)

(N) sections as shown, with no. (1) section connected to the inflow face and no. (N) to the outflow face. Flow in the filter cake is through these sections connected in series, where the Darcy equation applies to each section. A pressure drop is applied across the porous medium to displace the saturating water. Small increments of time are considered and a volume ( $V_1$ ) can be calculated which flows from each section in to the next in the series. The saturation change in each section is therefore given by  $(V_{1-1} - V_1)$ . For the

first time increment each section is 100% saturated and therefore has the same permeability.  $(V_1)$  is therefore the same for each section and all remain fully saturated except for the first. The whole filter cake is reduced in saturation by the amount  $(V_N)$  which the section (N) releases to the outside. In the next time increment the permeability of (1) is now less than previously since its saturation is less, therefore  $(V_1)$  is smaller. Thus section (2) becomes less than 100% saturated since  $(V_2 > V_1)$ . All the other volumes flowing from section to section are the same and the total saturation of the whole porous medium is again reduced by the same amount. This procedure may be followed for further increments of time and the progress of the saturation changes in the various sections and the whole bed may be traced. The saturation change for the whole assembly of sections may be seen to be always given by section (N) and as long as this element remains 100% saturated the rate of flow out of the filter cake will be uniform. From the point when the zone of saturation change reaches this section the rate of flow out of the filter cake declines according to the relative permeability saturation plot and the saturation changes in (N).

Calculations on this model using relative permeabilities calculated from capillary pressure curves by the method of Millington and Quirk mentioned in the last chapter, were performed. The model as described does not make any assumptions about the nature of relative permeabilities used but this expression has been shown to give at least the correct sort of result and may be used here for demonstration purposes. In the calculations incremental times for each steady-state flow are chosen to give a saturation change at

each increment of about 1%.

As a preliminary test the effect of the choice of number of divisions of the porous medium was checked. Calculations were made with  $N = 1, 5, 10, 20$  and  $30$ . These results are plotted on Fig. (51) and show that 20 divisions is sufficient to achieve consistency<sup>e</sup> in the calculated curves. The case represented by  $N = 1$  is equivalent to the dewatering curve of an infinitely thin filter cake.

Several simplifications are introduced in this treatment. The main one is that the effect of the air entering the desaturated spaces in the filter cake is ignored. This is equivalent to assuming that the viscosity of air compared to that of the water is small enough to be neglected. The effect of the air flow through the cake on the pressure drop across the cake is also ignored. In practice this will depend on the relative permeability characteristic of the filter medium and the capacity of the vacuum pump. The displacing pressure gradient across each section of the bed is assumed constant and the effect of the medium resistance is not included.

Even with these assumptions the model is able to show dewatering curves of the correct shape, as described by Nenniger and Storrow, Batel, and Gray, without using assumptions about film flow etc. It is also able to show the relative effects of the various variables in the process and the true nature of residual moisture.

### 8.3 THE VARIABLES WHICH AFFECT DEWATERING

The procedure for calculating the dewatering curve used in the computer program is basically an application of the Darcy equation

EFFECT OF NUMBER OF DIVISIONS ON DEWATERING MODEL

Sample 52/60 P 300 cm H<sub>2</sub>O Viscosity .01 Poise

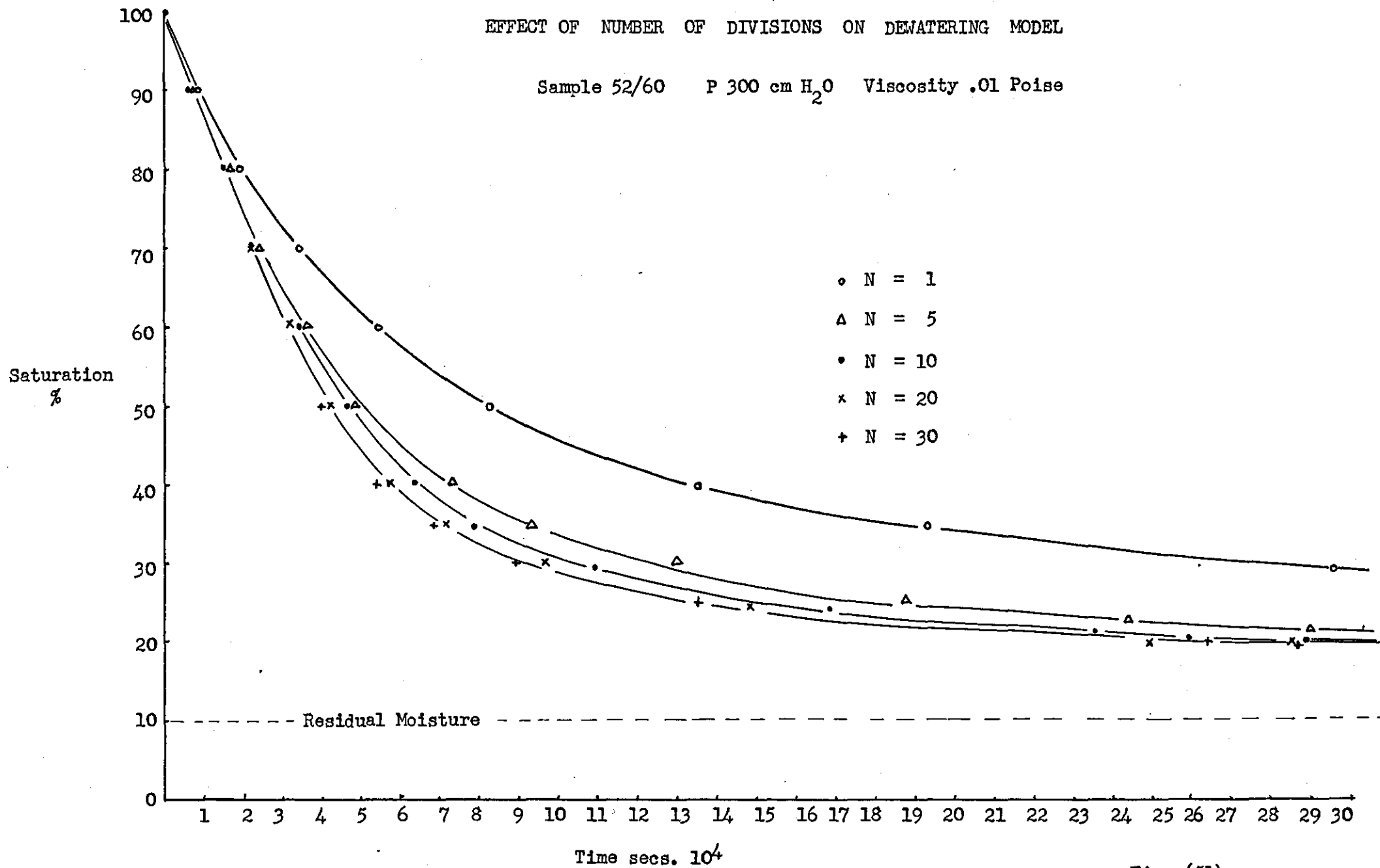


Fig. (51)

$$\frac{\Delta v}{\Delta t} = \frac{K A \Delta P}{L \eta}$$

Since  $\Delta S = \Delta V / A L e$

$$\Delta S = \frac{(K) (\Delta P) \Delta t}{L^2 \eta e}$$

In this both (K) and ( $\Delta P$ ) vary with saturation. The variation of permeability with saturation is given by the relative permeability curve and it is this which dictates the shape of the saturation versus time curve. The effective pressure causing flow varies with saturation due to the contribution of capillary pressure

$$\Delta P = (P_d - P_c)$$

where ( $P_d$ ) is the applied displacing pressure and ( $P_c$ ) is the capillary pressure at the saturation at a given time. From this it is clear that unless  $P_d > P_c$  no saturation will take place.

The effects of changes in these variables given in the equation is shown in Figs. (52) to (58). Figs. (52) (53) and (54) show the effect of changes in the direct variables of viscosity bed depth and displacing pressure. Fig. (55) shows the effect of surface tension which acts on the displacing pressure. Figs. (56) (57) and (58) show the effects of variations in permeability due to porosity changes, changes in particle size and in particle size distribution. In all these plots an assumed value for residual moisture left due to pendular rings is taken to be 10% and has been added to the curves.

#### 8.4 DISCUSSION

In general the variables which affect the dewatering curves do so in the same way as they affect saturated permeability. It would therefore be possible to normalise dewatering curves by plotting a function such as

EFFECT OF VISCOSITY ON DEWATERING CURVE

52/60 P = 600 cm H<sub>2</sub>O e = .3528

- viscosity .010 poise
- x viscosity .015 poise
- Δ viscosity .020 poise

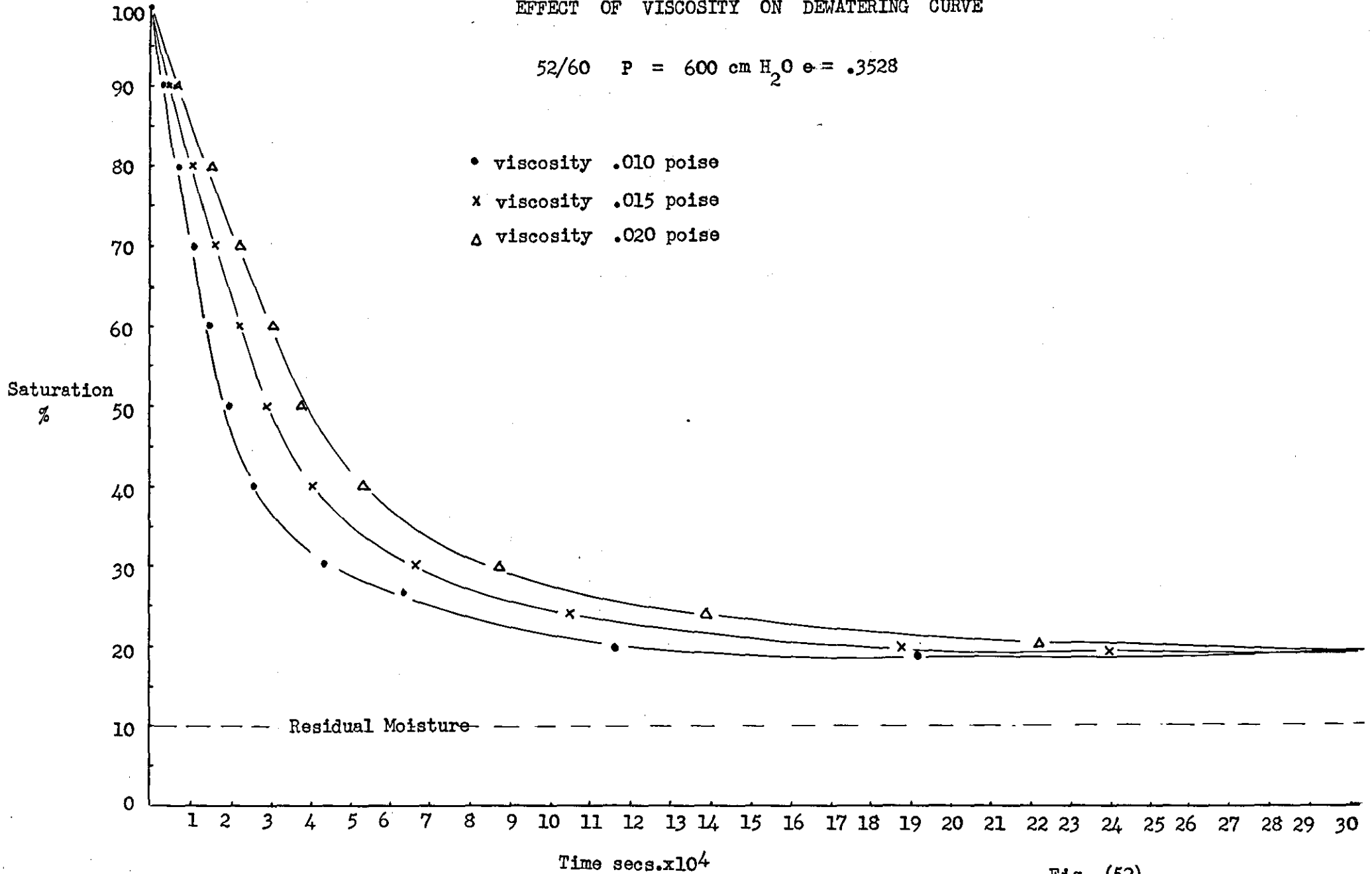


Fig. (52)

EFFECT OF BED DEPTH ON DEWATERING

52/60 Viscosity .02 poise P = 600 cm H<sub>2</sub>O e = .3528

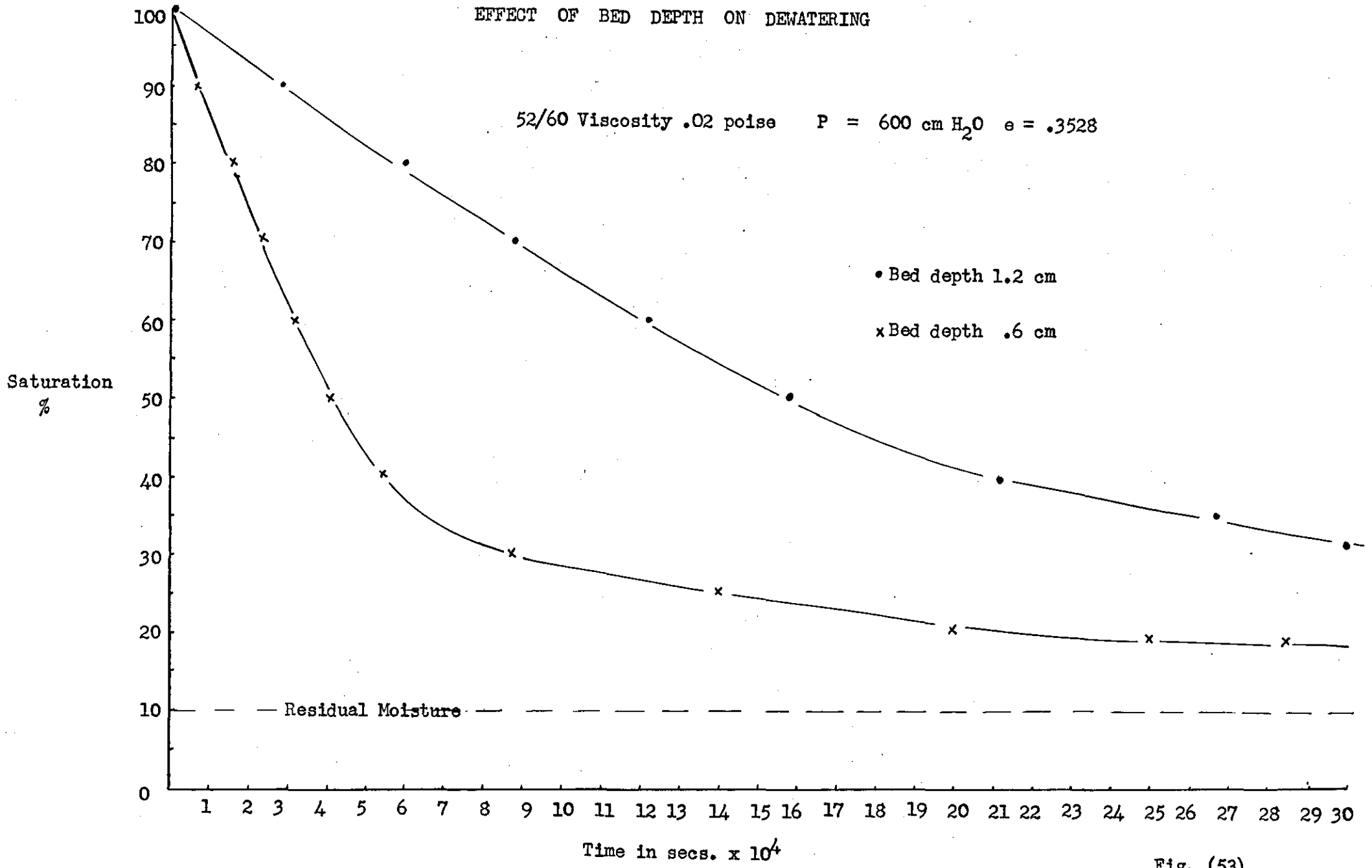


Fig. (53)



EFFECT OF DISPLACING PRESSURE ON DEWATERING

52/60 Viscosity .010poise  $e = .3528$

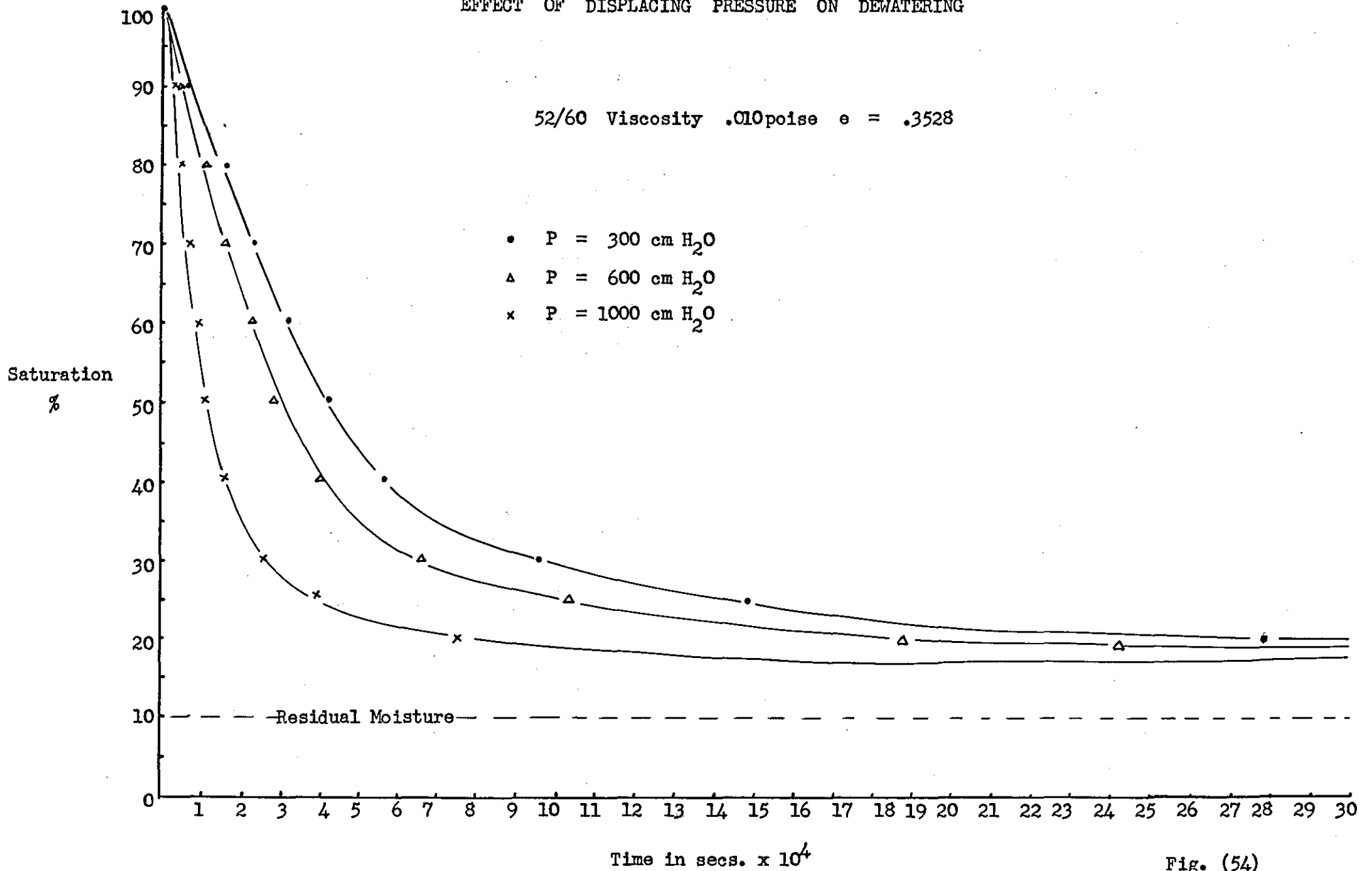


Fig. (54)

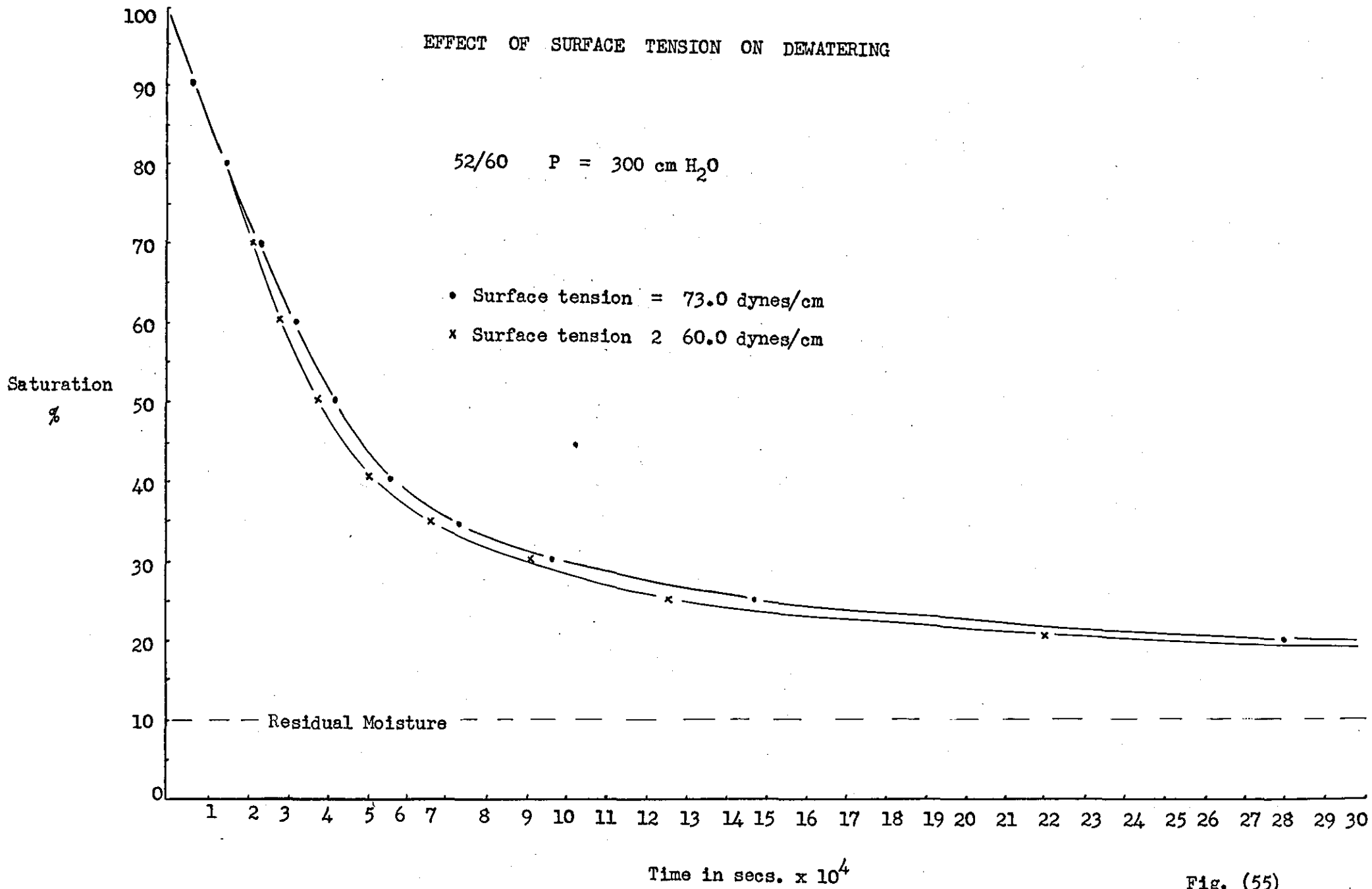


Fig. (55)

EFFECT OF POROSITY ON DEWATERING

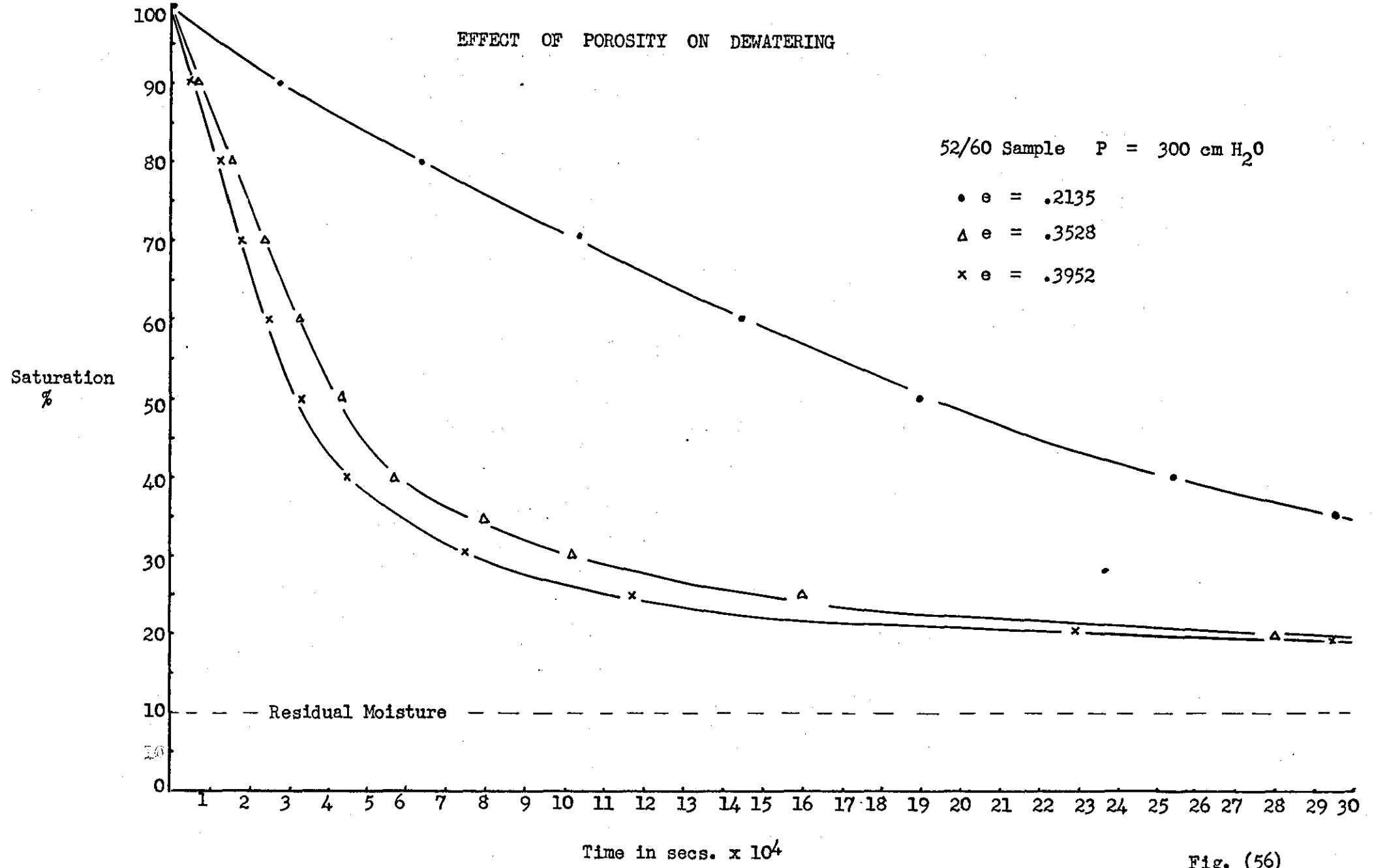


Fig. (56)

EFFECT OF PARTICLE SIZE ON DEWATERING

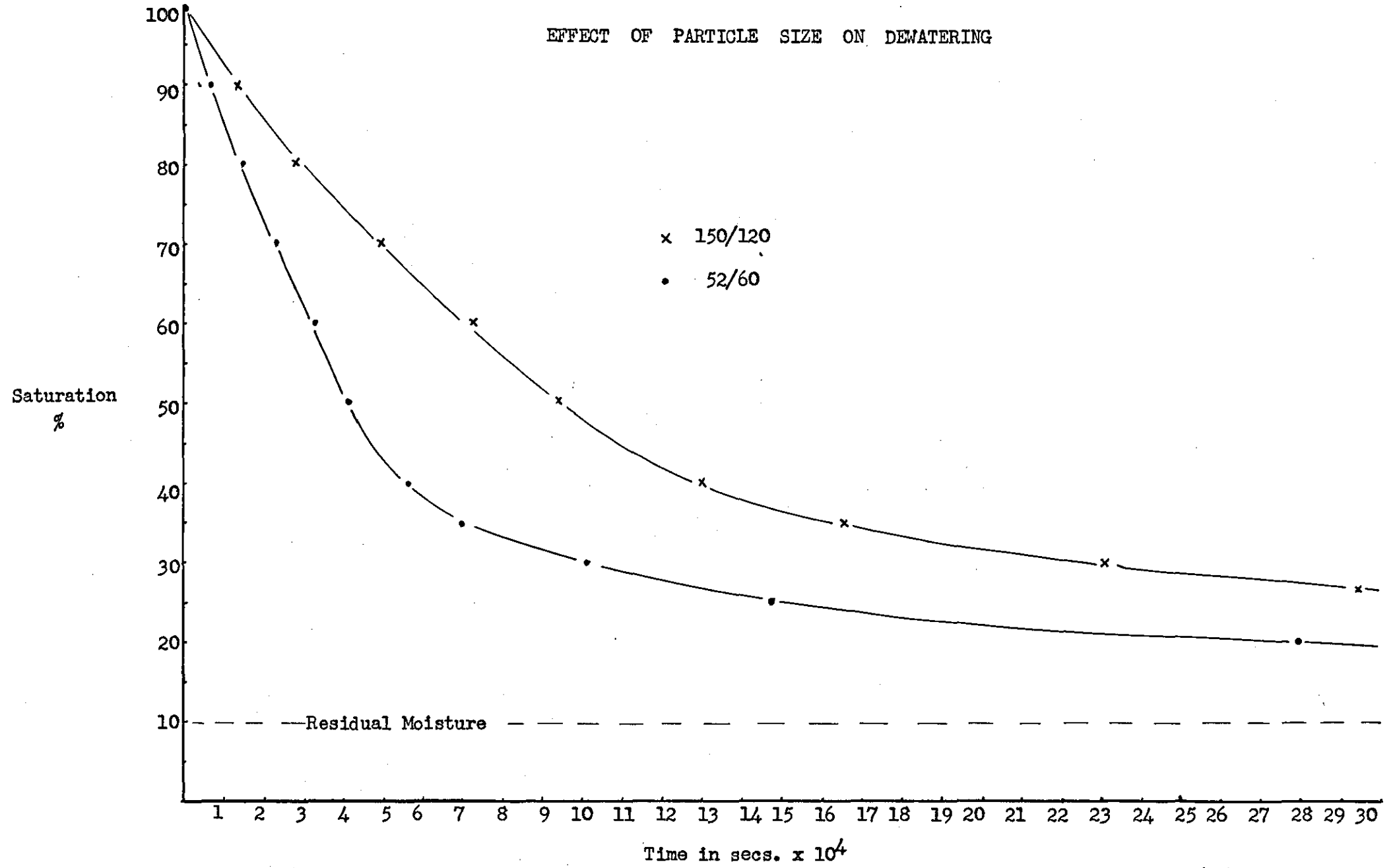


Fig. (57)

EFFECT OF PORE SIZE DISTRIBUTION ON DEWATERING

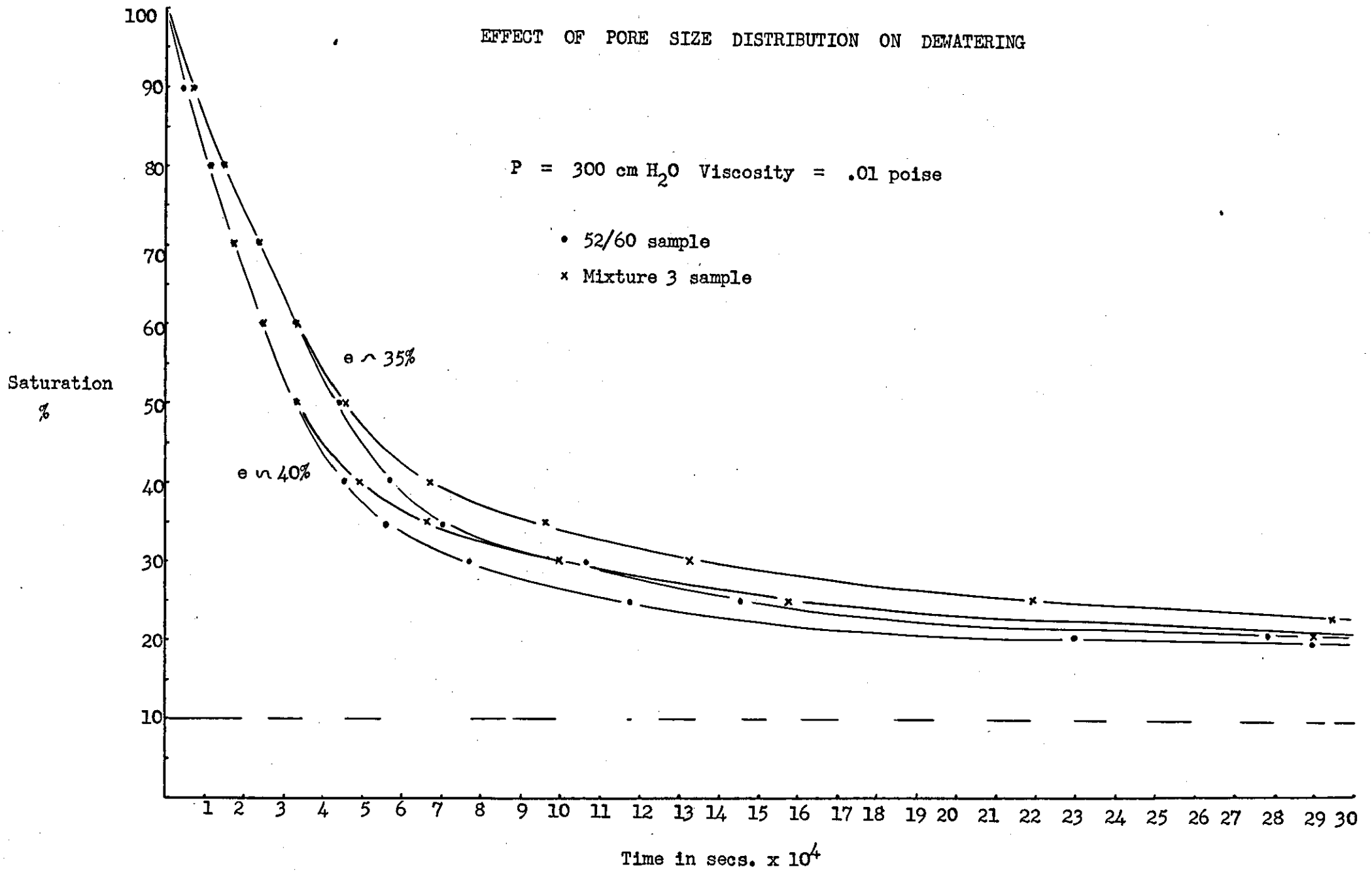


Fig. (58)

$$\frac{e L^2 n}{K_{sat}} \frac{\Delta t}{\Delta P} \quad \text{versus saturation}$$

This could be extended to include porosity and specific surface by including a Kozeny-Carman type function.

This does not include the effects of relative permeability or capillary pressure. However according to the Millington and Quirk expression, relative permeability curves do not vary very much as may be seen from Figs. (45), (46) and (48). The result of these small changes may be seen from Fig. (28) where dewatering curves are plotted for a mono-size pack and a 3-component pack with similar saturated permeabilities. The mono-size pack has a permeability characteristic which is higher for a given saturation than the pack with a distribution of pore sizes. Thus for a given set of conditions, after break through of air, the mono-size pack becomes desaturated slightly faster. The effect may however be seen to be small. From the way capillary pressure is included in the expression for giving the effective pressure causing flow, it may be taken to have a quite large effect on the curves. However variations in capillary pressure by changing surface tension will have a quite small effect and the variation due to saturation may be taken to be also small. Therefore in general the effective pressure causing flow will only vary with the applied pressure. The main variables which affect dewatering curves may all therefore be included in normalising functions of the type shown and a unique curve may be plotted which would give the dewatering characteristics of a wide range of materials. The success of the Dahlstrom correlation may be understood from these considerations.

Emphasis must however be placed on the nature of residual

moisture shown by the dewatering curves given in the figures. The change of saturation with time rapidly becomes small at saturations shown here of around 30% because the wetting phase permeability at these saturations is very small. If a sufficient amount of time were allowed the saturations would eventually reach those obtained in capillary pressure experiments, but for all practical purposes the saturations cease to change at values about 10% saturation above true residual moisture. The residual saturation reached in dewatering is therefore also an effect given by the shape of the relative permeability curve. From this the success of the Brownell and Katz 'capillary number' correlation for residual saturation may be taken to depend also on the similarity of relative permeability curves for most materials, and also on the fact that residual moisture as pendular rings is constant for a wide range of materials, and is not affected by the variables mentioned.

The importance in the model of the last section ( $N$ ) has been emphasised. In practice the last section consists of the filter medium and the characteristics of this may therefore have a large effect on the performance of a dewatering operation. In capillary pressure experiments a fine pore filter medium which always remains saturated and allows flow of wetting phase is used. In practical dewatering operations the permeability saturation characteristics of the filter medium may be such that it desaturates faster than the filter cake when the air/liquid interface reaches it, restricting and eventually stopping flow whilst the filter cake is still able to lose some more water. This effect would be difficult to predict in actual filter media as it would depend on the interaction of the filter cake and the medium, and also on the lateral

connectivity of the pores in the filter medium.

The relative permeability characteristics of the filter medium also exercise another important effect. Apart from the residual saturation reached in a given time the efficiency of a dewatering operation is dependent on the permeability of the filter cake to air as it is this which mainly determines the capacity required for the vacuum pump. The model used here is capable of calculating this, given relative permeability data for the non-wetting phase, and it would show that the air flow rate at a given saturation is always smaller for a mono-size pack than a bed with a wider distribution in pore size. However the decisive effect is that of the relative permeability characteristic of the filter medium. Suggestions have been made, Gray (1958) that fine pore media as used in capillary pressure experiments would allow the use of a much smaller capacity vacuum pumps and a consequent gain in economy. However, practical difficulties have not yet been overcome, mainly with regard <sup>to the</sup> fragility of high permeability fine pore media such as cellulose acetate membranes, and the low permeability of strong fine pore media such as sintered metal. Proper evaluation of these effects has been inhibited by the lack of a proper description of the mechanism of dewatering, but using the model given here at least preliminary calculations could be made.

For proper evaluation the filtering and dewatering operations should be both considered together and a true optimisation of the whole of a solid/liquid separation process could then be attempted. The similarity of the variables for these two stages should allow this to be done. The value of a theory of dewatering is mainly that improvements to the process such as the application of fine pore membranes or steam aided dewatering may be evaluated more



precisely. Furthermore, as mentioned by Dahlstrom (Nov. 1966), if the variables which affect dewatering are isolated then instrumentation can be carried out to control a process by operating on the variables. This removes the need to measure such things as cake thickness or moisture content which require more complicated devices than those for flows or pressure.

### 8.5 CONCLUSIONS

Dewatering must be considered as a flow process and the cell model presented here, despite simplifications, predicts the major characteristics of the saturation versus time curves. The shape of these curves is dictated by the permeability saturation relationship and the variables which affect saturated permeability. A significant feature is the small effect of surface tension on dewatering. Residual saturation reached in dewatering is also a direct result of the relative permeability characteristics. The filter medium is shown to have important effects on the efficiency of a dewatering operation. These findings generally support empirical correlations such as that of Dahlstrom for dewatering and that of Brownell and Katz for residual saturation.

## CHAPTER NINE

### SUMMARY AND SUGGESTIONS FOR FURTHER WORK

#### 9.1 INTRODUCTION

The dewatering process in packed beds and filter cakes was shown by previous workers to be dependent on the structure of the pore space in porous media, as a consequence of the capillary properties of liquid retained in porous media. However a satisfactory description of the mechanism of dewatering and an expression of the relationships involved in the saturation versus time curve was not available. This investigation has therefore attempted to follow the microscopic effects occurring in unsaturated porous media due to the retention and flow of water and also to relate these to the macroscopic process of dewatering.

The investigation may be taken as a discussion of the properties of porous media which are important in dewatering, this has been divided into three parts. The static properties of moisture in porous media are discussed with reference to the capillary pressure curve and the nature of the pore space which it reveals. The dynamic properties of unsaturated porous media are discussed with reference to relative permeability curves and the way in which the nature of pore space in porous media is simplified for use in expressions for permeability. The conclusions from these investigations have been used in a simple theory to explain the main features of dewatering curves and which allows a discussion of the role of the main variables of dewatering. These three divisions are followed in the next sections.

## 9.2 CAPILLARY PRESSURE CURVES

### 9.2.1 Summary

The properties of moisture retained in porous media have been investigated using the capillary pressure curve and the characteristics of these curves described by relation to the nature of pore space in unconsolidated media. The analytical treatment of capillary pressure curves has been extended to multi-component mixtures by using the Wise model of random packing of unequal spheres applied to the Fatt network model. Capillary desaturation curves obtained from this model have been compared with experimental results by using established correlations. The model gives a reasonable prediction of porosity, residual moisture, surface area and pore size, but predicts a narrower pore size distribution than was found in practice. The chief feature of the model is that the nature of pore space is considered in two separate parts, the distribution of pore sizes, and the connectivity of the pores.

### 9.2.2 Experimental Work

The comparison here of capillary pressure curves obtained from the model with experimental results provides, as far as is known, the only experimental test of the Wise model of sphere packing. One feature of the derived model which is not fully utilized is the specification of the void spaces in the interior of each tetrahedral pore element. The existence<sup>e</sup> of these is supported by the fact that their inclusion does not destroy the shape of desaturation curves, but to test properly for their validity the experimental study should be extended to imbibition curves which are chiefly determined by these voids.

The treatment given of capillary pressure curves is almost exclusively for sphere packs. The extension of the theory to

irregular particles is difficult to envisage but an experimental treatment could be useful. In general the greater the deviation of particle shape from that of a sphere, the wider will be the resulting pore size distribution for the same particle size distribution. This will be shown in the capillary pressure curves and may offer a useful definition of particle shape for use in other work, especially in permeability expressions.

### 9.2.3 Extensions of Theory

The capillary pressure curves obtained from the theoretical model predict too small a pore size, if the entry pressure into a pore in a sphere packing is calculated on the basis of the largest possible sphere which will fit in the pore. When an experimentally determined value for this is used the correspondance becomes much closer. This use of the experimental value requires to be supported by a theoretical treatment for its validity to be established. If such a theoretical treatment could be made for an assembly of 3 unequal touching spheres it may also improve the description of pore size distribution as the error which has been noted for an assembly of 3 equal spheres is likely to be much greater for 3 unequal spheres.

The model used to obtain capillary pressure curves is an assembly of two parts. The Wise model to provide a description of pore size distribution and the Fatt model to provide a description of pore connectivity. Both of these may be considered separately and improved independently.

The Wise model has not been used primarily as a model of packing but as a description of how the various sizes and relative numbers of particles in a multicomponent mixture interact with one another in 3 dimensions. From this point of view the assumption

that the particle arrangement is a perfectly ordered mixture should be improved to be more in accord with practical cases which can at best only be perfect random mixtures. Such a treatment may result in a better description of pore size distribution as it will in general make it wider.

Considering the Wise model as a description of the packing of particles, the main doubt is in the neglect of the gaps which exist between spheres. It may be that the method of testing the model used here cannot reveal this sort of effect. For example if a gap exists between two spheres in a packing the result will be that two tetrahedra will open into one another without an intervening small pore. By the independent<sup>e</sup> domain concept of capillary pressure curves, two independent<sup>e</sup> domains become one and take up the entry pressure of the lower of the two previous cases. This sort of effect may be revealed by a careful analysis of a full hysteresis loop but this is not certain. An extension to the model by including open tetrahedra is known to be in progress, Berresford (1967) and this may reveal more detail.

The hydraulic radius correlation of capillary pressure curves for porosity variation may only be checked experimentally in a very small region. In view of its importance here, a theoretical extension to both low and high porosities would be of great value. The Wise model modified by open tetrahedra may be capable of this sort of analysis as porosity variation in packings must be accompanied by either an increase in size or number of the gaps between particles. Alternatively extension of the Debbas and Rumpf theory, which is also known to be in progress, Scarlett (1968), may also be capable of covering changes in capillary rise due to porosity variation. Such

theoretical treatments may show that the narrow pore size distribution predicted by the model used is a real effect caused by the low porosity.

The Fatt network model used here is primarily a simple approximation to real three dimensional connectivity in porous media which only retains the actual fact that connections exist. This is sufficient for the major features of capillary pressure curves which are mainly dependant<sup>e</sup> on pore size distribution. However if the treatment of capillary desaturation were extended to include the trapping of moisture due to lack of phase continuity, more refinement should be included. The network form ought to be developed to include an approximation of 3 dimensional connectivity. The nature of 3 dimensional connectivity is indicated by the description of pore space given by the Wise model and this may provide a starting point for progress.

Extension to the network model should be made with computer models. These would allow far more extensive and accurate tests to be made on much larger arrays than can be managed by hand. A calculation of the transient phenomena between each equilibrium in a capillary pressure experiment may also be possible. From the point of view of dewatering filter cakes this sort of elaboration might not be justified but such models are of use in oil production where the same sort of problems are involved.

More immediately the assumption of simple network forms may allow an expression to be <sup>e</sup>drived<sub>A</sub> to correct pore size distributions calculated from capillary pressure curves. The expression given by Meyer may be valid but a more useable, if less accurate relationship would be more useful.

## 9.3 PERMEABILITY AND RELATIVE PERMEABILITY

### 9.3.1 Summary

Existing expressions for permeability have been discussed by relation to their assumptions about the nature of pore space. The flow of two immiscible fluids in porous media has been shown to be characterisable by relative permeability curves and the discussion of the expressions is extended to this case.

The uncertainty about permeability expressions centres on their treatment of pore size distribution and pore connectivity which are shown to be especially important for two phase flow. Using the model derived in the capillary pressure section and applying electrical network theory an expression for the permeability of the model has been derived. This involves separate matrix expressions for pore size distribution and network connectivity.

Permeability and relative permeabilities have been calculated using the expression and compared with values calculated using other relationships.

### 9.3.2 Experimental Work

Permeabilities and relative permeabilities calculated using the matrix expression compare reasonably well with results calculated in other ways. But this correspond<sup>e</sup>nce also requires experimental verification.

A method has been mentioned of using measurements on the rate of approach to equilibrium in capillary pressure experiments which appears attractive. In one experiment a large amount of data could be obtained about the nature of a porous medium such as porosity, pore size and distribution, surface area, permeability and relative permeability. The theory for the extension of this

sort to flow problems is however not complete.

More directly the nature of the model used could also be tested experimentally using miscible displacement, residence time, or perhaps frequency response methods. These techniques allow more information about the internal structure of a porous medium to be obtained, which could be compared with results from the network model.

### 9.3.3 Extension of Theory

The main limitation to the matrix expression for permeability is the large computer storage required for the coefficients. This has led to the application of the method to quite small networks which give rather variable results. Using the properties of the matrix solution it should be possible to extend the method by deriving a series expression for the permeability of a given network, or by devising a computer solution for the matrix which does not require storage of the zero elements. Once the problem of size of the network is solved a study of both the effects of pore size distribution and the structure of the porous medium could be attempted. It might also be possible to relate this to the extensive tests of the Kozeny-Carman equation which have been made and expressed by the variation of the tortuosity factor with such as porosity and particle size distribution.

The relative permeability curves were shown by Fatt to be a consequence of the connectivity of pore space. His tests however, and those here, were essentially static and the conclusion could be checked for a dynamic case by a computer simulation of unsaturated flow in a network. This could be extended by testing various network forms including three dimensional ones.



Here the pore size distribution and the connectivity of pores in a porous medium are considered to be independent of one another. The discussion about the continuity of pore space shown by the Wise model (section 4.4.2) indicates that this is only an approximation. If the network form in real porous media were to be investigated this should be borne in mind. Furthermore the variation in permeability with porosity has been taken to be determined by the changes in pore size given by the correlation function. Thus pore size distribution and pore connectivity have been assumed to remain constant. If theoretical treatment of porosity variation mentioned in 9.2.3 was successful then this view might have to be revised. For instance if the changes in porosity in packed bed were shown to take place by variation in the size or number of gaps between spheres the fourfold connectivity of the assumed network would no longer be sufficient. For instance two tetrahedra which open into one another due to a gap between spheres would then give a void with sixfold connectivity. This seems likely and the inclusion of porosity in the matrix expression as a scalar multiplier to the  $[R]$  matrix may have only restricted validity.

#### 9.4 DEWATERING

##### 9.4.1 Introduction

Using the conclusions gained from the study of the static and dynamic effects of water in unsaturated media a simple cell model for the mechanism of dewatering has been devised. Despite the simplification introduced the model shows the main features of dewatering curves and allows evaluation of the various variables which can affect dewatering. The results support existing correlations.

#### 9.4.2 Experimental Work

The dewatering curves derived using the cell model have not been tested experimentally. For this to be done satisfactorily relative permeability data must be available for the material involved, as the data used in the model is derived from an expression which had not itself been tested. The uncertainty attached to the effect of the filter medium in dewatering has been mentioned and experimental verification may be more satisfactorily made on a system using a fine pore filter medium. For this a medium should be used which has a higher permeability than the sample, otherwise the rate of flow out of the bed will be more affected by the medium than the saturation changes in the sample. Difficulty will also be associated with following the saturation changes as this is not an easy quantity to measure, especially as it will not be constant over the whole of the sample. A test program on the dynamics of dewatering has been reported using x-rays, Rozkydalek (1967).

If the process is as sensitive to the effects of the filter medium as has been indicated it may be more fruitful if further experimental work on dewatering is performed on actual equipment to test the effects of the variables given here. This could be done in conjunction with tests on the value of improvements such as using fine pore filter media, steam aided displacement or modifications to cake structure by vibrations. The true value of these can only be fully assessed in full-scale tests.

#### 9.4.3 Extension of Theory

The theory presented for dewatering is simplified because the viscosity of air in relation to water can be neglected. The use of liquids to displace liquids has been mentioned by Atkinson

(1949) as having some advantages in certain circumstances and it may be of value to extend the cell model to the general case and include the viscosity of the displacing fluid.

The difficulties inherent in experimental verification of the theory have been mentioned. A check could also be made by a computer simulation of the transient phenomena as a network desaturates. This has been mentioned as being of value for the other sections of theory and may provide a more convenient test here also.

This investigation has been solely concerned with displacement dewatering but this can only be performed if the displacing pressure exceeds the capillary pressure of the filter cake. This therefore only applies to relatively coarse materials ( $> 20 \mu$ ). For filter cakes with particles smaller than this a pressure applied to the cake can only displace filtrate by compressing the cake. This problem is in many ways analogous to displacement dewatering as it is also a flow process in which the permeability of the cake varies with the progress of the process, in this <sup>case</sup> due to the change in porosity. Furthermore preliminary experiments which were performed using the apparatus described earlier for the filter aid samples, indicate that a pressure/saturation equilibrium curve can be plotted which is analogous to both a capillary pressure curve and a stress/strain plot of mechanical properties.

An additional feature of this sort of dewatering is the occurrence of cake cracking which can be a problem in industrial filtrations. A greater understanding of the process would lead to a better understanding of cake cracking.

APPENDIX ONE

GEOMETRICAL RELATIONSHIPS OF TETRAHEDRA FORMED  
BY FOUR SPHERES

The pore space in a tetrahedron formed by four touching spheres has been approximated to a central spherical void from which protrude 4 cylinders. The dimensions of these may be calculated from the radii of the spheres forming the tetrahedron.

Wise (1960) has given an expression for the size of an interstitial sphere in such a tetrahedron which is quoted in (4.4.1).

The radius of the tubes protruding between 3 spheres is a two dimensional problem as shown in Fig. (59). The area of a triangle

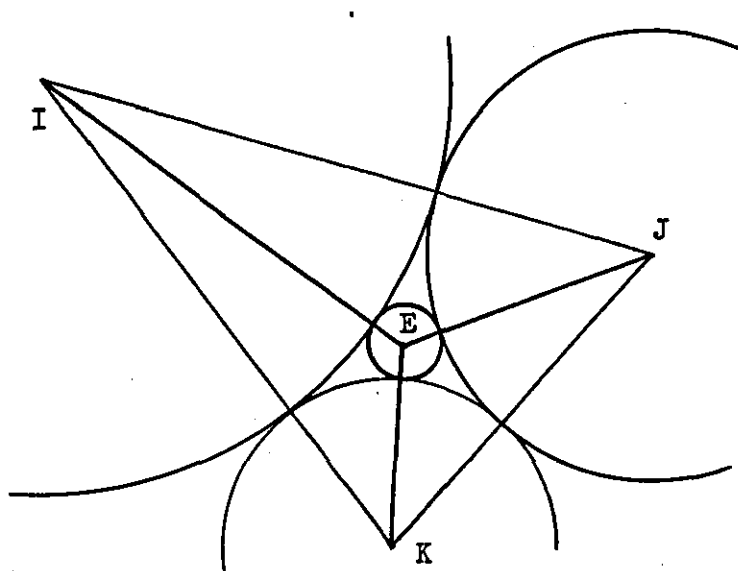


Fig. (59)

in terms of the lengths of its sides is

$$\Delta = \sqrt{S(S-a)(S-b)(S-c)}$$

where a, b, and c are the lengths of the sides and

$$S = (a + b + c)/2$$

For the triangle formed by 3 touching circles radii RI, RJ, RK

$$S = (RI + RJ + RK)$$

$$\begin{aligned} \therefore \text{ the area} &= \left[ S (S - (RI + RJ)) (S - (RI + RK)) (S - (RI + RK)) \right]^{\frac{1}{2}} \\ &= \left[ (RI + RJ + RK) RI RJ RK \right]^{\frac{1}{2}} \end{aligned}$$

In Fig. (59) Area IJK = Area IJE + Area IKE + Area JKE

$$\begin{aligned} \therefore \left[ (RI + RJ + RK) RI RJ RK \right]^{\frac{1}{2}} &= \left[ (RI + RJ + RE) RI RJ RE \right]^{\frac{1}{2}} \\ &+ \left[ (RI + RK + RE) RI RK RE \right]^{\frac{1}{2}} + \left[ (RJ + RK + RE) RJ RK RE \right]^{\frac{1}{2}} \\ \text{dividing throughout by} &\left[ (RI + RJ + RK) RI RJ RK RE \right]^{\frac{1}{2}} \end{aligned}$$

$$\left[ \frac{1}{RE} \right]^{\frac{1}{2}} = \left[ \frac{(RI + RJ + RE)}{(RI + RJ + RK) RK} \right]^{\frac{1}{2}} + \left[ \frac{(RI + RK + RE)}{(RI + RJ + RK) RJ} \right]^{\frac{1}{2}} + \left[ \frac{(RJ + RK + RE)}{(RI + RJ + RK) RI} \right]^{\frac{1}{2}}$$

No way was found of isolating (RE) but as the expression was to be incorporated in a computer program a trial and error solution was used. An assumed value of (RE) was used in the right hand side to calculate a value of (RE) which was used for the next substitution. This may be seen included in the program in Appendix 2.

The length of a tube from the face of a tetrahedron to the surface of an interstitial sphere is a 3 dimensional problem see Fig. (60).

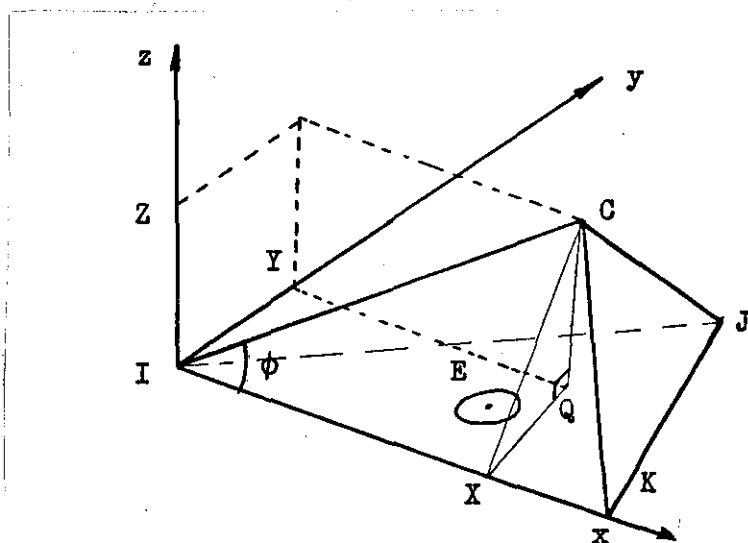


Fig. (60)

I, J and K are the centres of three of the four spheres making up a tetrahedron. C is the centre of the interstitial sphere formed

by these and the fourth sphere not shown.

The volume of a tetrahedron in terms of the radii of the spheres constituting it has been given by Wise (1952)

$$\text{Volume} = \left[ 2 (aa \, bb - aa^2 \, cc) / 9 \right]^{\frac{1}{2}}$$

$$\text{where } aa = RI \, RJ \, RK \, RC$$

$$bb = RI \, RJ + RJ \, RK + RI \, RC + RJ \, RK + RJ \, RC + RK \, RC$$

$$cc = 1 / RI^2 + 1 / RJ^2 + 1 / RK^2 + 1 / RC^2$$

also the volume of a tetrahedron = (base area x height) / 3

$$\therefore \text{z co-ordinate of sphere C} = (3 \times \text{volume of tetrahedron}) / \text{height}$$

This can be found from the above relationship for volume and the preceding one for area.

The x co-ordinate of sphere C is  $(RI + RC) \cos \phi$

$$\text{where } \cos \phi = \frac{(RI + RC)^2 + (RI + RK)^2 - (RK + RC)^2}{2 (RI + RC) (RI + RK)}$$

The y co-ordinate of sphere C may be found from the right angle triangle GXQ using Pythagoras theorem. The co-ordinates of the centre of the circle in the face of the tetrahedron marked E in Fig. (60) may similarly be found

$$\text{z co-ordinate} = 0 \text{ (by choice)}$$

$$\text{x co-ordinate} = (RI + RE) \cos \theta$$

$$\text{y co-ordinate} = (RI + RE) \left[ 1 - \cos^2 \theta \right]^{\frac{1}{2}}$$

$$\text{where } \cos \theta = \frac{(RI + RE)^2 + (RI + RK)^2 - (RE + RK)^2}{2 (RI + RE) (RI + RK)}$$

The length of the tube joining these two points (d) may be found from the expression

$$d = \left[ (x_2 - x_1)^2 + (y_2 - y_1)^2 + (z_2 - z_1)^2 \right]^{\frac{1}{2}}$$

The length of the tube in the model is therefore  $(d - RC)$ . These relationships are included in the computer program given in Appendix 2.

## APPENDIX TWO COMPUTER PROGRAM FOR PORE SPACE

## IN THE WISE MODEL

```

MASTER D000
DIMENSION R(3),X(3),YMEN(15),XMEN(15),FX(15),SOL(50),FREQ(50)
0 READ(1,40)N
IF(N.EQ.99)STOP
M=N*(N+2)*(N+1)/6.
NM=N*(N+3)/4.
DO 35 I=1,N
READ(1,41)A,B
R(I)=A
X(I)=B
YMEN(I)=1.
5 CONTINUE
50 DO 10 I=1,N
XMEN(I)=YMEN(I)
0 FX(I)=X(I)/XMEN(I)
DO 99 I=1,N
MI=0
DO 83 J=1,N
DO 82 K=J,N
DO 981 L=K,N
MI=MI+1
W=0.
IF(FX(I)-FX(J))13,12,13
2 W=W+1
3 IF(FX(I)-FX(K))15,14,15
4 W=W+1
5 IF(FX(I)-FX(L))17,16,17
6 W=W+1
7 Z=W+1
CA=2.*R(I)*((R(I)+R(J)+R(K))/((R(I)+R(J))*R(I)+R(K)))-1.
CB=2.*R(I)*((R(I)+R(J)+R(L))/((R(I)+R(J))*R(L)+R(I)))-1.
CD=2.*R(I)*((R(I)+R(K)+R(L))/((R(I)+R(K))*R(I)+R(L)))-1.
SA=SQRT(1.-CA*CA)
SB=SQRT(1.-CB*CB)
SC=SQRT(1.-CD*CD)
AA=ACOS((CA-CB*CD)/(SB*SC))
BB=ACOS((CB-CA*CD)/(SA*SC))
CC=ACOS((CD-CA*CB)/(SA*SB))
SOL(MI)=((AA+BB+CC-3.14159)/12.56639)
IF(Z-3.)20,18,19
0 P=0.
IF(J-1)927,926,927
26 P=P+1.
27 IF(J-K)929,928,929
28 P=P+1.
29 IF(J-L)931,930,931
30 P=P+1.
31 IF(K-L)933,932,933

```

```

32 P=P+1.
33 IF(K-I)935,934,935
34 P=P+1.
35 IF(I-L)937,936,937
36 P=P+1.
37 IF(P-2.)923,921,18
21 Y=6.
GO TO 981
8 Y=4.
GO TO 981
23 IF(P-1.)925,924,924
24 Y=12.
GO TO 981
25 Y=24.
GO TO 981
9 Y=1.
GO TO 981
81 FREQ(MI)=FX(I)*FX(J)*FX(K)*FX(L)*Y*Z
2 CONTINUE
3 CONTINUE
SUMSOL=0.
SUMFREQ=0.
DO 31 MI=1,M
SUMSOL=SUMSOL+SOL(MI)*FREQ(MI)
SUMFREQ=SUMFREQ+FREQ(MI)
1 CONTINUE
YMEN(I)=SUMSOL/SUMFREQ
3 CONTINUE
IF(ABS(XMEN(I)-YMEN(I))-0.0001)2,2,350
DO 3 I=1,N
WRITE(2,42)R(I),X(I),YMEN(I)
FX(I)=X(I)/YMEN(I)
MI=0
SMOD=0.
SFREQ=0.
SBED=0.
SSPER=0.
SUVOL=0.
DO 899 I=1,N
DO 899 J=I,N
DO 899 K=J,N
DO 899 L=K,N
SPHERES=0.
MI=MI+1
W=0.
IF(1-J)813,812,813
2 W=W+1.
3 IF(1-K)815,814,815

```



```

14 W=W+1.
15 IF(I-L)817,816,817
16 W=W+1.
17 Z=W+1.
    IF(Z-3.)820,818,819
20 IF(Z-2.)822,821,822
21 IF(L-K)827,823,827
22 IF(J-K)828,825,828
25 IF(J-L)827,818,827
28 IF(L-K)829,827,829
29 Y=24.
    GO TO 881
27 Y=12.
    GO TO 881
23 Y=6.
    GO TO 881
18 Y=4.
    GO TO 881
19 Y=1.
81 FREQ(MI)=FX(I)*FX(J)*FX(K)*FX(L)*Y
    SFREQ=SFREQ+FREQ(MI)
    C=1./((R(I)*R(I))+1./((R(J)*R(J))+1./((R(K)*R(K))+1./((R(L)*R(L))))
    D=1./R(I)+1./R(J)+1./R(K)+1./R(L)
    RG=(D/2.+SQRT((.75*D*D)-1.5*C))
    RCELL=1./RG
    VCELL=4.*3.14159*(RCELL**3)/3.
    WRITE(2,43)MI,FREQ(MI),RCELL,VCELL
    FACE,VMOD=0.
1 FACE=FACE+1.
    B1=0.
    RE1=B1
    X1=SQRT((R(I)+R(J)+RE1)/((R(I)+R(J)+R(K))*R(K)))
    X2=SQRT((R(I)+R(K)+RE1)/((R(I)+R(J)+R(K))*R(J)))
    X3=SQRT((R(J)+R(K)+RE1)/((R(I)+R(J)+R(K))*R(I)))
    A1=X1+X2+X3
    R1=1./(A1*A1)
    IF(ABS(R1-RE1)-.0001)4,4,8
    AAA=R(I)*R(J)*R(K)*RCELL
    BBB=R(I)*R(J)+R(I)*R(K)+R(I)*RCELL+R(J)*R(K)+R(J)*RCELL+R(K)*RCELL
    C=1./((R(I)*R(I))+1./((R(J)*R(J))+1./((R(K)*R(K))+1./((RCELL*RCELL))))
    VTEC=SQRT((2.*AAA*BBB-AAA*AAA*C)/9.)
    ARA=SQRT((R(I)+R(J)+R(K))*R(I)*R(J)*R(K))
    CD=2.*R(I)*((R(I)+R(K)+B1)/((R(I)+R(K))*(R(I)+B1)))-1.
    CT=2.*R(I)*((R(I)+R(K)+RCELL)/((R(I)+R(K))*(R(I)+RCELL)))-1.
    XC=CD*(R(I)+B1)-CT*(R(I)+RCELL)
    ZC=3.*VTEC/ARA
    YC=SQRT((1.-CD*CD)*(R(I)+B1)*(R(I)+B1))
    YC=YC-SQRT((1.-CT*CT)*(R(I)+RCELL)*(R(I)+RCELL))-ZC*ZC

```

```

XL1=SQRT(XC*XC+YC*YC+ZC*ZC)-RCELL
VT1=3.14159*R1*B1*XL1
VMOD=VMOD+VT1
WRITE(2,100)I,J,K,B1,VT1
10 FORMAT(3H I=,I2,3H J=,I2,3H K=,I2,4H B1=,F8.6,5H VT1=,F8.6/)
NA=I
I=J
J=K
K=L
L=NA
IF(FACE-4.)21,22,22
VMOD=(VMOD+VCELL)*FREQ(MI)
CA=2.*R(I)*((R(I)+R(J)+R(K))/((R(I)+R(J))*R(I)+R(K)))-1.
CB=2.*R(I)*((R(I)+R(J)+R(L))/((R(I)+R(J))*R(L)+R(I)))-1.
CD=2.*R(I)*((R(I)+R(K)+R(L))/((R(I)+R(K))*R(I)+R(L)))-1.
SA=SQRT(1.-CA*CA)
SB=SQRT(1.-CB*CB)
SC=SQRT(1.-CD*CD)
AA=ACOS((CA-CB*CD)/(SB*SC))
BB=ACOS((CB-CA*CD)/(SA*SC))
CC=ACOS((CD-CA*CB)/(SA*SB))
SOL(MI)=((AA+BB+CC-3.14159)/12.56639)
IF(MI-M)11,11,9
SPHERES=FREQ(MI)*Z*SOL(MI)
AAA=R(I)*R(J)*R(K)*R(L)
BBB=R(I)*R(J)+R(I)*R(K)+R(I)*R(L)+R(J)*R(K)+R(J)*R(L)+R(K)*R(L)
CZ=1./(R(I)*R(I))+1./(R(J)*R(J))+1./(R(K)*R(K))+1./(R(L)*R(L))
VTET=SQRT(((2.*AAA*BBB-AAA*AAA*CZ)/9.))*FREQ(MI)
SMOD=SMOD+VMOD
SBED=SBED+VTET
SSPER=SSPER+SPHERES
9 CONTINUE
UNITS=SSPER
DO 5 I=1,N
UVOL=(4.*3.14159)*X(I)*(R(I)**3)/3.
SUVOL=SUVOL+UVOL
VSPHERES=(UNITS/X(I))*SUVOL
POROSITY=100.*(SBED-VSPHERES)/SBED
REMOIST=100.*(SBED-VSPHERES-SMOD)/(SBED-VSPHERES)
WRITE(2,101)POROSITY,REMOIST
1 FORMAT(10H POROSITY=,F7.5,9H REMOIST=,F7.5/)
DO 7 MI=1,NM
FQ=190.*FREQ(MI)/SFREQ
WRITE(2,102)FQ
2 FORMAT(4H FQ=,F7.3/)
FORMAT(I2)
FORMAT(2F5.2)
FORMAT(6H R(I)=,F9.5,6H X(I)=,F9.5,9H YMEN(I)=,F9.5/)
FORMAT(4H MI=,I2,10H FREQ(MI)=,F15.4,7H RCELL=,F8.6,7H VCELL=,F8.6
1/)
GO TO 50
STOP
END

```



preparation: sieve cut

150/120 specific surface = 514.30 cm<sup>2</sup>/cm<sup>3</sup>

specific gravity = 2.98

microscope count:-

dia. (μ)	73	78	83	88	93	98	102	107	112	117	122
no.	2	3	2	7	9	12	19	26	44	29	26

dia. (μ)	127	132	137	141	146	151
no.	15	12	5	5	3	3

Mixture 1 specific surface = 233.81 cm<sup>2</sup>/cm<sup>3</sup>

specific gravity = 2.96

	mean radius microns	weight grammes	number %
Component 1	90	22.259	52.37
Component 2	124	36.292	32.37
Component 3	170	43.968	15.27

Mixture 2 specific surface = 160.91 cm<sup>2</sup>/cm<sup>3</sup>

specific gravity = 2.98

	mean radius microns	weight grammes	number %
Component 1	128.0	23.322	55.42
Component 2	186.5	43.404	33.32
Component 3	257.7	38.546	11.25

Mixture 3 specific surface = 226.37 cm<sup>2</sup>/cm<sup>3</sup>

specific gravity = 2.98

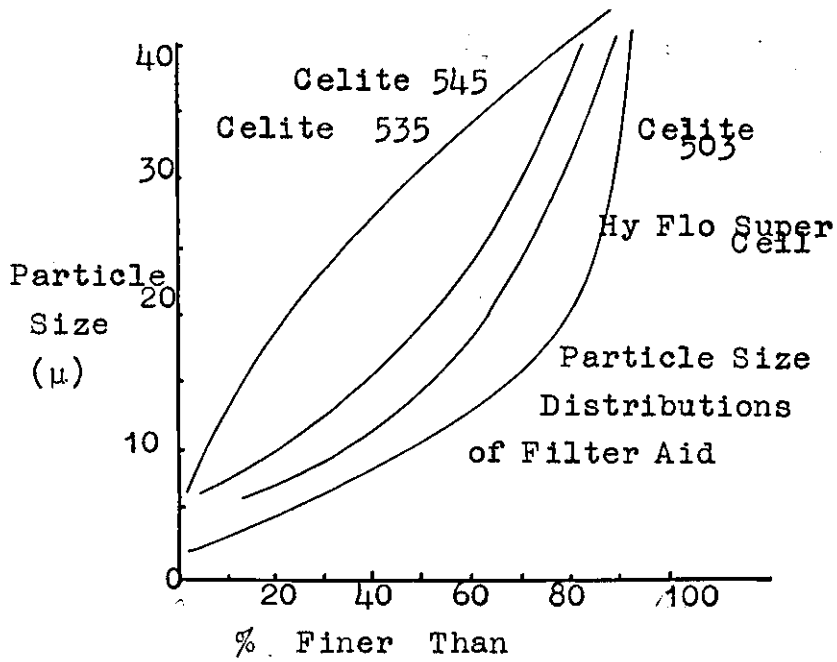
	mean radius microns	weight grammes	number %
Component 1	45.9	5.477	61.64
Component 2	117.0	42.126	28.86
Component 3	186.5	55.478	9.30

Mixture 4      specific surface = 202.16 cm<sup>2</sup>/cm<sup>3</sup>

                  specific gravity = 2.98

	mean radius microns	weight grammes	number %
Component 1	58.3	10.647	66.17
Component 2	102.9	25.750	29.08
Component 3	257.7	65.982	4.75

3.2 Filter Aid Samples



APPENDIX FOUR

EXAMPLE OF OBTAINING CAPILLARY PRESSURE CURVES FROM MODEL

Mixture 2 porosity .2112

				Pressure Drop											
		No	Rad.	Vol.	J	I	H	F	G	E	D	C	B	A	
1111		1	5	.2877	.09972	1			1	1		2			
	111	4	A1	20	.1980									20	
1112		2	20	.3142	.13000	4		1		11	4				
	111	1	A2	20	.1980									20	
	112	3	B2	60	.2221								60		
1113		3	10	.3350	.15744			1	2	6	1				
	111	1	A3	10	.1980									10	
	113	3	C3	30	.2406							30			
1122		4	29	.3449	.17188	1			3	15	10				
	112	2	B4	58	.2221								58		
	112	2	D4	58	.2520							58			
1123		5	30	.3694	.21112					22	8				
	112	1	B5	30	.2221								30		
	113	1	C5	30	.2406									30	
	123	2	E5	60	.2755					48	10	2			
1133		6	8	.3973	.26276				1	6	1				
	113	2	C6	16	.2406								16		
	133	2	F6	16	.3035					8	4	4			
1222		7	18	.3802	.23026	2		2		5	7	2			
	122	1	D7	54	.2520							54			
	222	3	G7	18	.2893				8	8	2				
1223		8	29	.4089	.28643	2			3	13	9	2			
	122	1	D8	28	.2520							28			
	123	2	E8	58	.2755					48	8	2			
	233	1	H8	30	.3194			6	4	12	8				
1233		9	15	.4417	.36092			1	1	6	5	1			
	123	2	E9	30	.2755					20	10				
	133	1	F9	14	.3035				2	2	10				
	233	1	I9	16	.3555				4	8	4				
1333		10	3	.4792	.46089			1	1		1				
	133	3	F10	8	.3035					8					
	333	1	J10	4	.3991					2					
2222		11	4	.4203	.31094				1	2	1				
	222	4	G11	16	.2893				8	4	4				
2223		12	9	.4534	.39036					4	3	2			
	222	1	G12	8	.2893				4	4					
	223	3	H12	28	.3194			4	4	12	4	4			
2233		13	7	.4908	.49519	1	1			1	4				
	223	2	H13	14	.3194			2	2	6	4				
	233	2	I13	14	.3555			2		4	8				
2333		14	3	.5329	.63391					2	1				
	233	3	I14	10	.3555					6	4				
	333	1	J14	2	.3991					2					
3333		15	0												
	333	4	J15	0											

Capillary pressure data given with other results in Appendix Five.  
Network shown in Fig. (61).



APPENDIX FIVE: CAPILLARY PRESSURE RESULTS

$$F = \frac{P_c}{T(1-e)} e \quad F^x = F/S_0 \quad p^x = \text{capillary pressure not corrected for depth of bed}$$

36/52

WT 0.0000 GRMS DIA 10.80 CMS  
 WATER SURFACE TENSION 73.00 DYNES/CM  
 RES MOIST 1.200 WT% 14.582 VOL%  
 POROSITY  $E = .2197$   $E^* = .1917$   
 SPECIFIC SURFACE 157.1291 CM/CM  
 PERMEABILITY KKO 14.1086 KMQ 15.5835

SAT %	PORE RAD	P CM H2O	P*	VOL CCS	F X/100	F* X/100
2.78	3.41	43.6	43.6	0.23	16.814	0.1070
4.57	3.29	45.2	45.2	0.38	17.451	0.1111
5.46	3.20	46.5	46.5	0.45	17.939	0.1142
15.28	3.17	46.9	46.9	1.31	18.092	0.1151
72.23	3.09	48.2	48.2	5.94	18.583	0.1183
79.91	3.06	48.6	48.6	6.58	18.740	0.1193
86.65	3.01	49.5	49.5	7.13	19.077	0.1214
92.69	2.98	49.9	49.9	7.63	19.237	0.1224
98.62	2.91	51.2	51.2	8.12	19.739	0.1256
100.00	2.34	52.5	52.5	8.23	20.243	0.1288

36/52

WT 104.6476 GRMS DIA 10.80 CMS  
 WATER SURFACE TENSION 72.00 DYNES/CM  
 RES MOIST 1.722 WT% 10.182 VOL%  
 POROSITY  $E = .3575$   $E^* = .3245$   
 SPECIFIC SURFACE 160.3254 CM/CM  
 PERMEABILITY KKO 86.1206 KMQ 113.1660

SAT %	PORE RAD	P CM H2O	P*	VOL CCS	F X/100	F* X/100
0.71	25.32	5.8	5.5	0.13	4.481	0.0279
1.45	13.59	10.8	10.5	0.26	8.345	0.0520
2.08	9.92	14.8	14.5	0.37	11.436	0.0713
4.43	7.81	18.8	18.5	0.72	14.527	0.0906
55.69	6.44	22.8	22.5	9.86	17.618	0.1099
78.44	5.92	24.8	24.5	13.89	19.164	0.1195
85.54	5.48	26.8	26.5	15.14	20.710	0.1292
93.23	4.77	30.8	30.5	16.50	23.801	0.1485
99.62	3.43	42.8	42.5	17.64	33.074	0.2063
99.66	2.68	54.8	54.5	17.64	42.348	0.2641
99.85	2.02	72.8	72.5	17.68	56.259	0.3509
100.00	1.38	92.8	92.5	17.70	71.715	0.4473



36/52

WT 510.1600 GRMS DIA 10.80 CMS  
WATER SURFACE TENSION 72.00 DYNES/CM  
RES MOIST 1.458 WT% 8.696 VOL%  
POROSITY E=.3524 E\*=.3242  
SPECIFIC SURFACE 162.2413 CM/CM  
PERMEABILITY KKC 79.2869 KMQ 108.1531

SAT %	PORE RAD	P CM H2O	P*	VOL CCS	F %100	F* %100
0.08	21.15	6.9	5.5	0.07	5.245	0.0323
0.54	9.21	15.9	14.5	0.46	12.047	0.0743
1.92	7.75	18.9	17.5	1.64	14.314	0.0882
22.79	7.01	20.9	19.5	19.49	15.826	0.0975
58.92	6.40	22.9	21.5	50.40	17.338	0.1069
82.06	5.66	25.9	24.5	70.19	19.605	0.1208
95.20	4.60	31.9	30.5	81.43	24.140	0.1488
99.56	3.34	43.9	42.5	85.41	33.209	0.2047
99.92	2.30	63.9	62.5	85.46	48.325	0.2979
100.00	1.56	93.9	92.5	85.53	70.998	0.4376

36/52

WT 1010.3500 GRMS DIA 10.80 CMS  
WATER SURFACE TENSION 72.00 DYNES/CM  
RES MOIST 1.547 WT% 9.241 VOL%  
POROSITY E=.3532 E\*=.3233  
SPECIFIC SURFACE 177.8367 CM/CM  
PERMEABILITY KKC 66.6054 KMQ 91.1623

SAT %	PORE RAD	P CM H2O	P*	VOL CCS	F %100	F* %100
0.22	10.23	14.4	11.5	0.37	10.888	0.0612
14.04	7.21	20.4	17.5	23.75	15.438	0.0868
70.83	5.79	25.4	22.5	119.80	19.230	0.1081
99.63	2.65	55.4	52.5	168.51	41.983	0.2361
99.61	1.95	75.4	72.5	168.48	57.152	0.3214
100.00	1.54	95.4	92.5	169.14	72.321	0.4067

36/52

WT 1010.3500 GRMS DIA 10.80 CMS  
WATER SURFACE TENSION 72.00 DYNES/CM  
RES MOIST 1.213 WT% 7.185 VOL%  
POROSITY E=.3508 E\*=.3273  
SPECIFIC SURFACE 175.5742 CM/CM  
PERMEABILITY KKC 66.4554 KMQ 91.2505

SAT %	PORE RAD	P CM H2O	P*	VOL CCS	F %100	F* %100
0.01	17.59	8.3	5.5	0.02	5.263	0.0357
0.31	9.57	15.3	12.5	0.53	11.516	0.0656
24.38	6.88	21.3	18.5	41.59	16.019	0.0912
62.65	6.03	24.3	21.5	106.87	18.271	0.1041
99.41	3.24	45.3	42.5	169.57	34.031	0.1938
99.93	2.65	55.3	52.5	170.46	41.536	0.2366
99.96	1.95	75.3	72.5	170.51	56.546	0.3221
100.00	1.54	95.3	92.5	170.58	71.556	0.4076

36/52

WT 510.1600 GRMS DIA 10.80 CMS

WATER SURFACE TENSION 72.00 DYNES/CM

RES MOIST 1.545 WT% 9.923 VOL%

POROSITY F= .3528 E\*= .3210

SPECIFIC SURFACE 159.4125 CM/CM

PERMEABILITY KKC 82.5076 KMQ 109.5279

SAT %	PORE RAD	P CM H2O	P*	VOL CCS	F %100	F*
0.09	21.15	6.9	5.5	0.08	5.255	0.0330
0.25	8.18	17.9	16.5	0.21	13.583	0.0852
0.52	9.21	15.9	14.5	0.44	12.069	0.0757
7.20	7.36	19.9	18.5	6.10	15.097	0.0947
34.52	6.69	21.9	20.5	29.25	16.612	0.1042
70.95	6.13	23.9	22.5	60.11	18.126	0.1137
83.63	5.66	25.9	24.5	70.86	19.640	0.1232
93.56	4.90	29.9	28.5	79.27	22.668	0.1422
98.43	4.32	33.9	32.5	83.40	25.697	0.1612
99.86	3.34	43.9	42.5	84.61	33.268	0.2087
99.87	2.30	63.9	62.5	84.62	48.410	0.3037
100.00	1.56	93.9	92.5	84.73	71.123	0.4462

36/52

WT 104.6776 GRMS DIA 10.80 CMS

WATER SURFACE TENSION 72.00 DYNES/CM

RES MOIST 1.578 WT% 9.376 VOL%

POROSITY F= .3547 E\*= .3243

SPECIFIC SURFACE 158.4258 CM/CM

PERMEABILITY KKC 85.3961 KMQ 113.4468

SAT %	PORE RAD	P CM H2O	P*	VOL CCS	F %100	F*
0.91	23.32	5.8	5.5	0.16	4.425	0.0279
2.60	9.92	14.8	14.5	0.46	11.296	0.0713
6.15	7.81	18.8	18.5	1.08	14.350	0.0906
15.18	7.06	20.8	20.5	2.67	15.877	0.1002
33.27	6.73	21.8	21.5	5.86	16.640	0.1050
64.96	6.44	22.8	22.5	11.44	17.403	0.1099
84.16	5.69	25.8	25.5	14.83	19.694	0.1243
91.57	5.10	28.8	28.5	16.13	21.984	0.1388
97.21	4.48	32.8	32.5	17.13	25.038	0.1580
99.69	3.78	38.8	38.5	17.56	29.618	0.1870
99.69	3.01	48.8	48.5	17.56	37.253	0.2351
99.73	2.34	62.8	62.5	17.57	47.941	0.3026
99.89	1.77	82.8	82.5	17.60	63.209	0.3990
100.00	1.58	92.8	92.5	17.62	70.843	0.4472

36/52  
 WT 42.9427 GRMS DIA 10.80 CMS  
 WATER SURFACE TENSION 72.00 DYNES/CM  
 RES MOIST 1.391 WT% 7.523 VOL%  
 POROSITY E=.3725 E\*=.3484  
 SPECIFIC SURFACE 161.1719 CM/CM  
 PERMEABILITY KKC 101.0655 KMQ 138.3099

SAT %	PORE RAD	P CM H2O	P*	VOL CCS	F x100	F* x100
2.36	26.10	5.6	5.5	0.19	4.638	0.0288
4.37	13.82	10.6	10.5	0.35	8.760	0.0544
7.69	10.04	14.6	14.5	0.61	12.058	0.0748
12.14	8.33	17.6	17.5	0.96	14.532	0.0902
25.24	7.48	19.6	19.5	2.00	16.180	0.1004
57.73	6.79	21.6	21.5	4.58	17.829	0.1106
78.07	6.49	22.6	22.5	6.20	18.654	0.1157
92.13	5.13	28.6	28.5	7.31	23.601	0.1464
98.68	4.24	34.6	34.5	7.83	28.548	0.1771
99.21	3.44	42.6	42.5	7.88	35.144	0.2181
100.00	1.58	92.6	92.5	7.94	76.368	0.4738

36/52  
 WT 46.1184 GRMS DIA 10.80 CMS  
 WATER SURFACE TENSION 72.00 DYNES/CM  
 RES MOIST 1.492 WT% 8.671 VOL%  
 POROSITY E=.3583 E\*=.3297  
 SPECIFIC SURFACE 159.2100 CM/CM  
 PERMEABILITY KKC 88.1385 KMQ 117.2890

SAT %	PORE RAD	P CM H2O	P*	VOL CCS	F x100	F* x100
1.92	26.07	5.6	5.5	0.15	4.367	0.0274
4.55	11.62	12.6	12.5	0.36	9.796	0.0615
6.04	8.83	16.6	16.5	0.48	12.898	0.0810
25.31	7.11	20.6	20.5	2.05	16.000	0.1005
62.72	6.49	22.6	22.5	4.98	17.551	0.1102
77.33	5.96	24.6	24.5	6.14	19.102	0.1200
93.34	4.79	30.6	30.5	7.41	23.755	0.1492
93.85	3.44	42.6	42.5	7.84	33.061	0.2077
99.38	2.34	62.6	62.5	7.89	48.571	0.3051
100.00	1.58	92.6	92.5	7.94	71.836	0.4512

36/52  
 WT 45.4990 GRMS DIA 6.60 CMS  
 WATER SURFACE TENSION 72.00 DYNES/CM  
 RES MOIST 1.600 WT% 7.981 VOL%  
 POROSITY E=.3926 E\*=.3636  
 SPECIFIC SURFACE 152.4461 CM/CM  
 PERMEABILITY KKC 141.1558 KMQ 196.9168

SAT %	PORE RAD	P CM H2O	P*	VOL CCS	F x100	F* x100
1.67	11.87	12.4	12.0	0.15	11.102	0.0728
5.25	10.22	14.4	14.0	0.48	12.897	0.0846
24.20	8.97	16.4	16.0	2.21	14.693	0.0964
60.04	7.99	18.4	18.0	5.48	16.488	0.1082
77.39	7.21	20.4	20.0	7.06	18.284	0.1199
91.78	6.02	24.4	24.0	8.37	21.875	0.1435
93.93	4.83	30.4	30.0	9.02	27.261	0.1788
99.77	4.04	36.4	36.0	9.10	32.647	0.2142
99.92	3.17	46.4	46.0	9.11	41.624	0.2730
100.00	2.60	56.4	56.0	9.12	50.602	0.3319

52/60

WT 0.0000 GRMS DIA 10.80 CMS  
 WATER SURFACE TENSION 73.00 DYNES/CM  
 RES MOIST 1.200 WT% 15.143 VOL%  
 POROSITY E=.2135 E\*=.1854  
 SPECIFIC SURFACE 210.3567 CM/CM  
 PERMEABILITY KKC 7.1107 KMQ 7.6820

SAT %	PORE RAD	P CM H2O	P*	VOL CCS	F %/100	F* %/100
1.00	2.59	57.4	57.4	0.08	21.360	0.1015
2.29	2.42	61.6	61.6	0.18	22.895	0.1088
3.51	2.34	63.7	63.7	0.28	23.674	0.1125
21.93	2.27	65.6	65.6	1.74	24.383	0.1159
63.18	2.20	67.6	67.6	5.40	25.139	0.1195
84.48	2.19	68.0	68.0	6.69	25.271	0.1201
86.18	2.16	69.4	69.4	6.83	25.803	0.1227
96.02	2.13	69.8	69.8	7.61	25.941	0.1233
99.66	2.08	71.7	71.7	7.90	26.651	0.1267
100.00	2.02	73.7	73.7	7.92	27.397	0.1302

52/60

WT 96.1847 GRMS DIA 10.80 CMS  
 WATER SURFACE TENSION 73.00 DYNES/CM  
 RES MOIST 1.717 WT% 10.385 VOL%  
 POROSITY E=.3512 E\*=.3188  
 SPECIFIC SURFACE 222.4050 CM/CM  
 PERMEABILITY KKC 41.9483 KMQ 54.2264

SAT %	PORE RAD	P CM H2O	P*	VOL CCS	F %/100	F* %/100
0.48	25.78	5.5	5.5	0.08	4.293	0.0193
0.96	11.65	12.5	12.5	0.15	9.500	0.0427
2.05	6.54	22.5	22.5	0.33	16.938	0.0762
6.27	5.17	28.5	28.5	1.08	21.401	0.0962
35.72	4.68	31.5	31.5	5.68	23.632	0.1063
74.54	4.28	34.5	34.5	11.85	25.864	0.1163
87.63	3.84	38.5	38.5	13.84	28.839	0.1297
95.33	3.32	44.5	44.5	15.16	33.301	0.1497
99.87	2.72	54.5	54.5	15.88	40.739	0.1832
99.92	2.37	62.5	62.5	15.89	46.690	0.2099
99.99	1.80	82.5	82.5	15.90	61.566	0.2768
100.00	1.60	92.5	92.5	15.90	69.004	0.3103

52/60

WT 96.1847 GRMS DIA 10.80 CMS  
 WATER SURFACE TENSION 72.00 DYNES/CM  
 RES MOIST 1.657 WT% 7.974 VOL%  
 POROSITY E=.4003 E\*=.3707  
 SPECIFIC SURFACE 233.6898 CM/CM  
 PERMEABILITY KKC 65.3189 KMQ 92.4852

SAT %	PORE RAD	P CM H2O	P*	VOL CCS	F %/100	F* %/100
0.73	25.33	5.5	5.5	0.15	5.372	0.0230
2.75	7.81	18.5	18.5	0.55	17.424	0.0746
4.97	6.44	22.5	22.5	0.99	21.132	0.0904
15.64	5.92	24.5	24.5	3.13	22.986	0.0984
53.06	5.48	26.5	26.5	10.61	24.841	0.1063
75.20	5.10	28.5	28.5	15.03	26.695	0.1142
88.72	4.48	32.5	32.5	17.73	30.403	0.1301
97.27	3.60	40.5	40.5	19.44	37.820	0.1618
99.94	2.78	52.5	52.5	19.98	48.945	0.2094
99.98	2.02	72.5	72.5	19.98	67.486	0.2888
100.00	1.58	92.5	92.5	19.99	86.028	0.3681

52/60

WT 96.1847 GRMS DIA 10.80 CMS

WATER SURFACE TENSION 73.00 DYNES/CM

RES MOIST 1.558 WT% 9.293 VOL%

POROSITY E=.3528 E\*=.3228

SPECIFIC SURFACE 229.9552 CM/CM

PERMEABILITY KKC 39.6508 KMQ 52.4957

SAT %	PORE RAD	P CM H2O	P*	VOL CCS	F X100	F*
0.60	25.78	5.8	5.5	0.10	4.311	0.0187
1.03	13.82	10.8	10.5	0.17	8.044	0.0350
1.90	7.16	20.8	20.5	0.31	15.512	0.0675
3.06	6.01	24.8	24.5	0.49	18.499	0.0804
4.18	5.36	27.8	27.5	0.67	20.739	0.0902
7.80	5.00	29.8	29.5	1.26	22.232	0.0967
23.34	4.68	31.8	31.5	3.76	23.726	0.1032
61.98	4.41	33.8	33.5	9.99	25.219	0.1097
79.54	4.05	36.8	36.5	12.82	27.459	0.1194
89.07	3.65	40.8	40.5	14.36	30.446	0.1324
99.19	2.93	50.8	50.5	16.00	37.914	0.1649
99.98	2.05	72.8	72.5	16.12	54.342	0.2363
100.00	1.60	92.8	92.5	16.13	69.277	0.3013

52/60

WT 96.1847 GRMS DIA 10.80 CMS

WATER SURFACE TENSION 72.00 DYNES/CM

RES MOIST 1.412 WT% 6.370 VOL%

POROSITY E=.3952 E\*=.3698

SPECIFIC SURFACE 240.7911 CM/CM

PERMEABILITY KKC 58.2072 KMQ 84.2317

SAT %	PORE RAD	P CM H2O	P*	VOL CCS	F X100	F*
0.69	25.34	5.8	5.5	0.10	5.256	0.0218
1.02	16.70	8.8	8.5	0.20	7.979	0.0331
1.72	11.48	12.8	12.5	0.34	11.609	0.0482
2.39	7.81	18.8	18.5	0.47	17.055	0.0708
3.62	6.44	22.8	22.5	0.72	20.685	0.0859
17.27	5.69	25.8	25.5	3.41	23.407	0.0972
70.85	5.10	28.8	28.5	14.01	26.130	0.1085
85.35	4.48	32.8	32.5	16.87	29.760	0.1236
92.90	3.78	38.8	38.5	18.36	35.206	0.1462
93.69	3.01	48.8	48.5	19.51	44.281	0.1839
99.96	2.48	59.3	59.0	19.76	53.811	0.2235
99.85	2.02	72.8	72.5	19.74	66.062	0.2744
100.00	1.58	92.8	92.5	19.77	84.214	0.3497

72/85

WT 0.0000 GRMS DIA 10.80 CMS  
 WATER SURFACE TENSION 73.00 DYNES/CM  
 RES MOIST 1.200 WT% 14.501 VOL%  
 POROSITY E= .2192 E\*= .1921  
 SPECIFIC SURFACE 304.1257 CM/CM  
 PERMEABILITY KKC 3.7735 KMQ 4.1855

SAT %	PORE RAD	P CM H2O	P*	VOL CCS	F %/100	F* %/100
2.36	1.79	83.0	83.0	0.19	32.050	0.1054
3.64	1.71	86.9	86.9	0.30	33.538	0.1103
12.89	1.65	90.4	90.4	1.07	34.923	0.1148
38.78	1.61	92.4	92.4	3.21	35.664	0.1173
90.13	1.58	94.3	94.3	7.46	36.431	0.1198
90.95	1.57	95.0	95.0	7.53	36.698	0.1207
97.15	1.54	96.4	96.4	8.04	37.233	0.1224
99.76	1.51	98.6	98.6	8.26	38.076	0.1252
100.00	1.48	100.9	100.9	8.28	38.953	0.1281

72/85

WT 100.2636 GRMS DIA 10.80 CMS  
 WATER SURFACE TENSION 72.00 DYNES/CM  
 RES MOIST 1.693 WT% 10.634 VOL%  
 POROSITY E= .3445 E\*= .3114  
 SPECIFIC SURFACE 313.3452 CM/CM  
 PERMEABILITY KKC 19.3823 KMQ 24.3981

SAT %	PORE RAD	P CM H2O	P*	VOL CCS	F %/100	F* %/100
1.99	3.75	16.8	16.5	0.32	12.249	0.0391
2.73	5.48	26.8	26.5	0.44	19.548	0.0624
3.98	3.99	36.8	36.5	0.96	26.847	0.0857
9.02	3.43	42.8	42.5	1.44	31.227	0.0997
14.44	3.28	44.8	44.5	2.31	32.687	0.1043
46.61	3.14	46.8	46.5	7.46	34.147	0.1090
63.37	3.01	48.8	48.5	10.18	35.607	0.1136
79.13	2.78	52.8	52.5	12.67	38.526	0.1230
89.71	2.50	58.8	58.5	14.36	42.906	0.1369
96.69	2.20	66.8	66.5	15.48	48.745	0.1556
99.55	1.91	76.8	76.5	15.94	56.045	0.1789
100.00	1.69	86.8	86.5	16.01	63.344	0.2022

72/85

WT 100.2636 GRMS DIA 10.80 CMS  
 WATER SURFACE TENSION 72.00 DYNES/CM  
 RES MOIST 1.672 WT% 8.675 VOL%  
 POROSITY E= .3839 E\*= .3533  
 SPECIFIC SURFACE 311.2222 CM/CM  
 PERMEABILITY KKC 30.7780 KMQ 41.4063

SAT %	PORE RAD	P CM H2O	P*	VOL CCS	F %/100	F* %/100
4.06	7.06	20.8	20.5	0.78	18.000	0.0578
8.80	4.48	32.8	32.5	1.70	28.385	0.0912
12.32	4.22	34.8	34.5	2.38	30.116	0.0968
26.04	3.99	36.8	36.5	3.03	31.847	0.1023
51.19	3.78	38.8	38.5	9.89	33.578	0.1079
68.39	3.60	40.8	40.5	13.22	35.309	0.1135
86.17	3.14	46.8	46.5	16.65	40.501	0.1301
93.10	2.78	52.8	52.5	17.99	45.694	0.1468
98.46	2.34	62.8	62.5	19.03	54.348	0.1746
99.39	2.02	72.8	72.5	19.21	63.002	0.2024
100.00	1.69	86.8	86.5	19.32	75.110	0.2117

72/85

WT 100.2636 GRMS DIA 10.80 CMS  
 WATER SURFACE TENSION 72.00 DYNES/CM  
 RES MOIST 1.570 WT% 8.085 VOL%  
 POROSITY E=3844 E\*=3556  
 SPECIFIC SURFACE 310.0096 CM/CM  
 PERMEABILITY KKC 31.1912 KMQ 42.4504

SAT %	PORE RAD	P CM H2O	P*	VOL CCS	F X100	F*
1.62	8.74	16.8	16.5	0.35	14.569	0.0470
3.55	5.48	26.8	26.5	0.65	23.242	0.0750
11.16	4.48	32.8	32.5	2.17	28.445	0.0918
16.22	4.22	34.8	34.5	3.16	30.180	0.0974
27.94	3.99	36.8	36.5	5.43	31.914	0.1029
54.53	3.78	38.8	38.5	10.58	33.649	0.1085
70.69	3.60	40.8	40.5	13.76	35.383	0.1141
78.72	3.43	42.8	42.5	15.33	37.118	0.1197
86.99	3.14	46.8	46.5	16.94	40.587	0.1309
93.26	2.78	52.8	52.5	18.16	45.791	0.1477
99.00	2.34	62.8	62.5	19.28	54.463	0.1757
100.00	2.02	72.8	72.5	19.47	63.136	0.2037

72/85

WT 100.2636 GRMS DIA 10.80 CMS  
 WATER SURFACE TENSION 72.00 DYNES/CM  
 RES MOIST 1.720 WT% 10.415 VOL%  
 POROSITY E=3517 E\*=3185  
 SPECIFIC SURFACE 315.2132 CM/CM  
 PERMEABILITY KKC 20.8347 KMQ 26.5402

SAT %	PORE RAD	P CM H2O	P*	VOL CCS	F X100	F*
1.09	11.48	12.8	12.5	0.18	9.632	0.0306
2.36	7.81	18.8	18.5	0.39	14.153	0.0449
3.16	5.92	24.8	24.5	0.52	18.674	0.0592
3.87	4.77	30.8	30.5	0.64	23.195	0.0736
5.34	3.99	36.8	36.5	0.88	27.715	0.0879
10.06	3.43	42.8	42.5	1.67	32.236	0.1023
59.67	3.14	46.8	46.5	9.88	35.250	0.1118
71.54	3.01	48.8	48.5	11.85	36.757	0.1166
81.80	2.78	52.8	52.5	13.55	39.771	0.1262
91.52	2.50	58.8	58.5	15.15	44.292	0.1405
97.42	2.20	66.8	66.5	16.13	50.319	0.1596
99.55	1.91	76.8	76.5	16.50	57.854	0.1835
100.00	1.69	86.8	86.5	16.56	65.389	0.2074

150/120  
 WT 0.0000 GRMS DIA 10.80 CMS  
 WATER SURFACE TENSION 73.00 DYNES/CM  
 RES MOIST 1.200 WT% 14.540 VOL%  
 POROSITY  $E = .2195$   $E^* = .1916$   
 SPECIFIC SURFACE 491.1842 CM/CM  
 PERMEABILITY KKO 1.4391 KMQ 1.5824

SAT %	PORE RAD	P CM H2O	P*	VOL CCS	F X100	F* X100
3.14	1.10	134.9	134.9	0.26	51.987	0.1058
6.08	1.05	141.4	141.4	0.50	54.472	0.1109
7.26	1.02	146.4	146.4	0.60	56.396	0.1148
44.20	1.01	148.0	148.0	3.65	56.998	0.1160
62.56	0.97	153.0	153.0	6.81	58.939	0.1200
88.72	0.96	154.6	154.6	7.32	59.552	0.1212
90.39	0.94	158.1	158.1	7.46	60.910	0.1240
97.37	0.93	159.7	159.7	8.04	61.516	0.1252
99.78	0.90	164.8	164.8	8.23	63.497	0.1293
100.00	0.88	170.0	170.0	8.25	65.503	0.1334

150/120  
 WT 47.6986 GRMS DIA 10.80 CMS  
 WATER SURFACE TENSION 72.00 DYNES/CM  
 RES MOIST 2.017 WT% 12.517 VOL%  
 POROSITY  $E = .3504$   $E^* = .3114$   
 SPECIFIC SURFACE 538.6484 CM/CM  
 PERMEABILITY KKO 7.0278 KMQ 8.8267

SAT %	PORE RAD	P CM H2O	P*	VOL CCS	F X100	F* X100
0.09	26.05	5.6	5.5	0.01	4.221	0.0078
0.54	11.62	12.6	12.5	0.04	9.466	0.0176
0.72	6.49	22.6	22.5	0.06	16.957	0.0315
1.08	4.50	32.6	32.5	0.08	24.449	0.0454
1.27	3.44	42.6	42.5	0.10	31.941	0.0593
1.99	2.79	52.6	52.5	0.15	39.433	0.0752
2.98	2.34	62.6	62.5	0.23	46.925	0.0871
8.04	2.02	72.6	72.5	0.62	54.416	0.1010
13.36	1.89	77.6	77.5	1.18	58.162	0.1080
67.39	1.78	82.6	82.5	5.18	61.908	0.1149
82.93	1.68	87.6	87.5	6.37	65.654	0.1219
87.72	1.58	92.6	92.5	6.74	69.400	0.1288
93.13	1.39	105.6	105.5	7.31	79.139	0.1469
99.92	1.08	135.6	135.5	7.68	101.615	0.1886
99.99	0.99	147.6	147.5	7.69	110.605	0.2053
100.00	0.97	150.6	150.5	7.69	112.852	0.2095



150/120  
 WT 190,8000 GRMS DIA 10.80 CMS  
 WATER SURFACE TENSION 72.00 DYNES/CM  
 RES MOIST 1.689 WT% 10.464 VOL%  
 POROSITY E= .3466 E\*= .3138  
 SPECIFIC SURFACE 547,1248 CM/CM  
 PERMEABILITY KKC 6.5161 KMQ 8.5578

SAT %	PORE RAD	P CM H2O	P*	VOL CCS	F X100	F* X100
0.14	24.32	6.0	5.5	0.04	4.447	0.0081
0.18	11.26	13.0	12.5	0.06	9.604	0.0176
0.18	4.44	33.0	32.5	0.06	24.339	0.0445
0.18	2.77	53.0	52.5	0.06	39.074	0.0714
0.65	2.01	73.0	72.5	0.20	53.809	0.0983
40.00	1.88	78.0	77.5	12.32	57.492	0.1051
61.52	1.79	82.0	81.5	18.95	60.439	0.1105
86.23	1.58	93.0	92.5	26.56	68.544	0.1253
93.83	1.38	106.0	105.5	28.90	78.121	0.1428
99.79	1.09	135.0	134.5	30.73	99.487	0.1818
99.96	1.03	142.0	141.5	30.79	104.644	0.1913
100.00	0.97	151.0	150.5	30.80	111.275	0.2034

150/120  
 WT 190,8000 GRMS DIA 10.80 CMS  
 WATER SURFACE TENSION 72.00 DYNES/CM  
 RES MOIST 2.090 WT% 13.258 VOL%  
 POROSITY E= .3469 E\*= .3063  
 SPECIFIC SURFACE 529,8847 CM/CM  
 PERMEABILITY KKC 6.9714 KMQ 8.7808

SAT %	PORE RAD	P CM H2O	P*	VOL CCS	F X100	F* X100
0.05	24.32	6.0	5.5	0.02	4.453	0.0084
0.05	6.37	23.0	22.5	0.02	16.994	0.0321
0.05	3.41	43.0	42.5	0.02	31.749	0.0599
0.19	2.33	63.0	62.5	0.06	46.503	0.0878
2.40	1.96	75.0	74.5	0.72	55.356	0.1045
40.91	1.77	83.0	82.5	21.03	61.257	0.1156
89.37	1.58	93.0	92.5	26.88	68.635	0.1295
99.61	1.27	116.0	115.5	29.96	85.602	0.1615
99.80	1.14	129.0	128.5	30.02	95.193	0.1796
99.90	1.05	140.0	139.5	30.05	103.307	0.1950
100.00	0.97	151.0	150.5	30.08	111.422	0.2103

150/120  
 WT 462,2600 GRMS DIA 10.80 CMS  
 WATER SURFACE TENSION 72.00 DYNES/CM  
 RES MOIST 2.184 WT% 13.757 VOL%  
 POROSITY E= .3495 E\*= .3072  
 SPECIFIC SURFACE 539,2255 CM/CM  
 PERMEABILITY KKC 6.9396 KMQ 8.6310

SAT %	PORE RAD	P CM H2O	P*	VOL CCS	F X100	F* X100
0.08	1.99	73.8	72.5	0.06	55.074	0.1021
69.38	1.75	83.8	82.5	50.92	62.536	0.1160
79.30	1.65	88.8	87.5	58.26	66.267	0.1229
99.34	1.29	113.8	112.5	72.90	84.923	0.1575
99.94	1.02	143.8	142.5	73.34	107.309	0.1990
100.00	0.90	163.8	162.5	73.39	122.234	0.2267

150/120

WT 55.8477 GRMS DIA 10.80 CMS

WATER SURFACE TENSION 72.00 DYNES/CM

RES MOIST 1.979 WT% 12.454 VOL%

POROSITY E= .3471 E\*= .3087

SPECIFIC SURFACE 520.7901 CM/CM

PERMEABILITY KKO 7.2339 KMQ 8.9178

SAT %	PORE RAD	P CM H2O	P*	VOL CCS	F X100	F*
0.31	25.95	5.7	5.5	0.03	4.177	0.0080
0.31	11.60	12.7	12.5	0.03	9.346	0.0179
0.47	7.87	18.7	18.5	0.04	13.776	0.0265
0.63	5.95	24.7	24.5	0.06	18.206	0.0350
1.17	4.79	30.7	30.5	0.10	22.636	0.0435
1.41	4.36	33.7	33.5	0.13	24.851	0.0477
1.64	3.80	38.7	38.5	0.15	28.543	0.0548
2.35	3.15	46.7	46.5	0.21	34.450	0.0661
2.74	2.79	52.7	52.5	0.24	38.880	0.0747
4.07	2.34	62.7	62.5	0.36	46.264	0.0888
8.45	2.02	72.7	72.5	0.75	53.648	0.1030
66.07	1.78	82.7	82.5	5.87	61.032	0.1172
82.49	1.66	88.7	88.5	7.32	65.462	0.1257
96.96	1.39	105.7	105.5	8.61	78.014	0.1498
100.00	1.08	135.7	135.5	8.88	100.165	0.1923

150/120

WT 55.8477 GRMS DIA 10.80 CMS

WATER SURFACE TENSION 72.00 DYNES/CM

RES MOIST 1.979 WT% 12.454 VOL%

POROSITY E= .3471 E\*= .3087

SPECIFIC SURFACE 520.7901 CM/CM

PERMEABILITY KKO 7.2339 KMQ 8.9178

SAT %	PORE RAD	P CM H2O	P*	VOL CCS	F X100	F*
0.31	25.95	5.7	5.5	0.03	4.177	0.0080
0.31	11.60	12.7	12.5	0.03	9.346	0.0179
0.47	7.87	18.7	18.5	0.04	13.776	0.0265
0.63	5.95	24.7	24.5	0.06	18.206	0.0350
1.17	4.79	30.7	30.5	0.10	22.636	0.0435
1.41	4.36	33.7	33.5	0.13	24.851	0.0477
1.64	3.80	38.7	38.5	0.15	28.543	0.0548
2.35	3.15	46.7	46.5	0.21	34.450	0.0661
2.74	2.79	52.7	52.5	0.24	38.880	0.0747
4.07	2.34	62.7	62.5	0.36	46.264	0.0888
8.45	2.02	72.7	72.5	0.75	53.648	0.1030
66.07	1.78	82.7	82.5	5.87	61.032	0.1172
82.49	1.66	88.7	88.5	7.32	65.462	0.1257
96.96	1.39	105.7	105.5	8.61	78.014	0.1498
100.00	1.08	135.7	135.5	8.88	100.165	0.1923

150/120  
 WT 462.2600 GRMS DIA 10.80 CMS  
 WATER SURFACE TENSION 72.00 DYNES/CM  
 RES MOIST 1.936 WT% 12.462 VOL%  
 POROSITY F= .3420 E\* = .3041  
 SPECIFIC SURFACE 532.9602 CM/CM  
 PERMEABILITY KKC 6.5053 KMQ 8.1826

SAT %	PORE RAD	P CM H2O	P*	VOL CCS	F X/100	F* X/100
0.02	21.62	6.8	5.5	0.01	4.901	0.0092
0.02	6.17	23.8	22.5	0.01	17.173	0.0322
0.04	2.73	53.8	52.5	0.03	38.829	0.0729
1.27	1.99	73.8	72.5	0.91	53.267	0.0999
38.14	1.84	79.8	78.5	27.39	57.598	0.1081
60.53	1.75	83.8	82.5	43.47	60.486	0.1135
86.90	1.57	93.8	92.5	62.40	67.703	0.1270
97.25	1.31	111.8	110.5	69.84	80.699	0.1514
99.28	1.07	136.8	135.5	71.29	98.746	0.1853
99.74	1.00	146.8	145.5	71.62	105.965	0.1988
100.00	0.94	156.8	155.5	71.81	113.183	0.2124

150/120  
 WT 51.0038 GRMS DIA 10.80 CMS  
 WATER SURFACE TENSION 72.00 DYNES/CM  
 RES MOIST 1.811 WT% 8.925 VOL%  
 POROSITY F= .3967 E\* = .3642  
 SPECIFIC SURFACE 538.7063 CM/CM  
 PERMEABILITY KKC 11.8208 KMQ 16.3840

SAT %	PORE RAD	P CM H2O	P*	VOL CCS	F X/100	F* X/100
0.20	14.45	10.2	10.0	0.02	9.274	0.0172
0.60	5.61	26.2	26.0	0.06	23.867	0.0443
1.07	3.18	46.2	46.0	0.11	42.152	0.0782
6.31	2.61	56.2	56.0	0.65	51.284	0.0952
35.78	2.40	61.2	61.0	3.70	55.851	0.1037
68.40	2.22	66.2	66.0	7.08	60.417	0.1122
80.28	2.06	71.2	71.0	8.31	64.983	0.1206
86.58	1.93	76.2	76.0	8.96	69.550	0.1291
93.63	1.70	86.2	86.0	9.69	78.682	0.1461
97.86	1.53	96.2	96.0	10.13	87.815	0.1630
99.87	1.38	106.2	106.0	10.34	96.948	0.1800
99.94	1.26	116.2	116.0	10.34	106.080	0.1969
100.00	1.16	126.2	126.0	10.35	115.213	0.2139

MIXTURE 1  
 WT 0.0000 GRMS DIA 10.80 CMS  
 WATER SURFACE TENSION 73.00 DYNES/CM  
 RES MOIST 1.200 WT% 15.214 VOL%  
 POROSITY E= .2122 E\*= .1842  
 SPECIFIC SURFACE 218.2996 CM/CM  
 PERMEABILITY KKC 6.4614 KMQ 6.6864

SAT %	PORE RAD	P CM H2O	P*	VOL CCS	F %100	F* %100
1.26	2.98	49.9	49.9	0.10	18.401	0.0843
4.92	2.66	55.9	55.9	0.39	20.611	0.0944
8.06	2.40	62.0	62.0	0.64	22.894	0.1049
11.05	2.34	63.7	63.7	0.87	23.517	0.1077
13.54	2.18	66.4	66.4	1.07	25.232	0.1156
17.98	2.12	70.2	70.2	6.07	25.894	0.1186
27.52	1.94	76.8	76.8	6.90	28.320	0.1297
32.88	1.89	78.7	78.7	7.33	29.031	0.1330
38.46	1.74	85.4	85.4	7.77	31.509	0.1443
100.00	1.58	94.2	94.2	7.89	34.766	0.1593

MIXTURE 1  
 WT 100.4187 GRMS DIA 10.80 CMS  
 WATER SURFACE TENSION 72.00 DYNES/CM  
 RES MOIST 1.390 WT% 6.814 VOL%  
 POROSITY E= .3924 E\*= .3674  
 SPECIFIC SURFACE 227.2787 CM/CM  
 PERMEABILITY KKC 63.3671 KMQ 87.3010

SAT %	PORE RAD	P CM H2O	P*	VOL CCS	F %100	F* %100
1.55	18.81	7.8	7.5	0.28	7.000	0.0308
2.88	9.92	14.8	14.5	0.59	13.279	0.0584
10.37	7.06	20.8	20.5	2.12	18.661	0.0821
23.27	5.92	24.8	24.5	5.79	22.249	0.0979
37.33	5.10	28.8	28.5	13.79	25.837	0.1137
54.38	4.34	33.8	33.5	17.28	30.322	0.1334
72.68	3.88	37.8	37.5	18.98	33.909	0.1492
92.68	3.43	42.8	42.5	19.80	38.394	0.1689
99.63	2.78	52.8	52.5	20.41	47.364	0.2084
100.00	2.16	67.8	67.5	20.48	60.819	0.2676

MIXTURE 1  
 WT 100.4187 GRMS DIA 10.80 CMS  
 WATER SURFACE TENSION 73.00 DYNES/CM  
 RES MOIST 1.545 WT% 9.282 VOL%  
 POROSITY E= .3503 E\*= .3205  
 SPECIFIC SURFACE 218.3636 CM/CM  
 PERMEABILITY KKC 42.7134 KMQ 53.7352

SAT %	PORE RAD	P CM H2O	P*	VOL CCS	F %100	F* %100
1.08	19.12	7.8	7.5	0.18	5.750	0.0263
1.83	11.64	12.8	12.5	0.31	9.443	0.0432
2.87	7.92	18.8	18.5	0.48	13.874	0.0635
13.04	5.56	26.8	26.5	2.18	19.783	0.0906
36.35	4.83	30.8	30.5	6.08	22.737	0.1041
75.64	4.05	36.8	36.5	12.64	27.169	0.1244
90.72	3.48	42.8	42.5	15.16	31.600	0.1447
99.78	2.82	52.8	52.5	16.68	38.986	0.1785
99.99	2.37	62.8	62.5	16.71	46.372	0.2124
100.00	2.04	72.8	72.5	16.72	53.758	0.2462

MIXTURE 1  
 WT 100.4187 GRMS DIA 10.80 CMS  
 WATER SURFACE TENSION 72.00 DYNES/CM  
 RES MOIST 1.427 WT% 8.376 VOL%  
 POROSITY  $E = .3537$   $E^* = .3264$   
 SPECIFIC SURFACE 228.6961 CM/CM  
 PERMEABILITY KKC 40.5088 KMQ 52.2904

SAT %	PORE RAD	P CM H2O	P* CM H2O	VOL CCS	F /100	F* /100
1.60	18.85	7.8	7.5	0.27	5.918	0.0259
3.70	8.74	16.8	16.5	0.63	12.759	0.0558
6.70	6.44	22.8	22.5	1.15	17.320	0.0757
8.90	5.92	24.8	24.5	1.52	18.840	0.0824
13.70	5.28	27.8	27.5	2.34	21.120	0.0924
29.10	4.77	30.8	30.5	4.98	23.400	0.1023
48.50	4.48	32.8	32.5	8.26	24.921	0.1090
71.70	4.10	35.8	35.5	12.27	27.201	0.1189
82.70	3.78	38.8	38.5	14.15	29.481	0.1289
90.60	3.43	42.8	42.5	15.50	32.522	0.1422
97.40	3.01	48.8	48.5	16.66	37.082	0.1621
99.40	2.58	56.8	56.5	17.01	43.163	0.1887
99.70	2.13	68.8	68.5	17.06	52.284	0.2286
100.00	1.77	82.8	82.5	17.11	62.925	0.2751

MIXTURE 1  
 WT 100.4187 GRMS DIA 10.80 CMS  
 WATER SURFACE TENSION 72.00 DYNES/CM  
 RES MOIST 1.582 WT% 7.731 VOL%  
 POROSITY  $E = .3952$   $E^* = .3668$   
 SPECIFIC SURFACE 231.0226 CM/CM  
 PERMEABILITY KKC 63.2337 KMQ 86.5541

SAT %	PORE RAD	P CM H2O	P* CM H2O	VOL CCS	F /100	F* /100
1.70	18.81	7.8	7.5	0.35	7.084	0.0307
2.70	11.46	12.8	12.5	0.55	11.622	0.0503
5.60	7.81	18.8	18.5	1.15	17.067	0.0739
12.40	6.44	22.8	22.5	2.55	20.697	0.0896
32.30	5.69	25.8	25.5	6.64	23.420	0.1014
66.00	5.10	28.8	28.5	13.56	26.143	0.1132
84.40	4.47	32.8	32.5	17.34	29.773	0.1289
93.60	3.78	38.8	38.5	19.23	35.218	0.1524
99.10	3.07	47.8	47.5	20.36	43.386	0.1878
99.60	2.54	57.8	57.5	20.47	52.462	0.2271
99.90	2.07	70.8	70.5	20.53	64.260	0.2782
100.00	1.77	82.8	82.5	20.55	75.151	0.3253

MIXTURE 2  
 WT 0.0000 GRMS DIA 10.80 CMS  
 WATER SURFACE TENSION 73.00 DYNES/CM  
 RES MOIST 1.200 WT% 15.444 VOL%  
 POROSITY E= .2112 E\*= .1829  
 SPECIFIC SURFACE 149.6656 CM/CM  
 PERMEABILITY KKC 13.5187 KMQ 13.7471

SAT %	PORE RAD	P CM H2O	P*	VOL CCS	F %/100	F* %/100
1.83	4.53	32.9	32.9	0.14	12.054	0.0805
2.61	4.03	36.9	36.9	0.20	13.532	0.0904
3.89	3.62	41.1	41.1	0.46	15.062	0.1006
6.10	3.44	43.2	43.2	0.47	15.851	0.1059
13.00	3.28	45.3	45.3	1.01	16.629	0.1111
54.10	3.13	47.6	47.6	4.20	17.462	0.1167
84.13	2.86	52.0	52.0	6.54	19.090	0.1276
94.21	2.73	54.5	54.5	7.09	19.992	0.1336
98.33	2.52	59.1	59.1	7.64	21.660	0.1447
100.00	2.25	66.2	66.2	7.77	24.296	0.1623

MIXTURE 2  
 WT 100.9798 GRMS DIA 10.80 CMS  
 WATER SURFACE TENSION 72.00 DYNES/CM  
 RES MOIST 1.634 WT% 8.331 VOL%  
 POROSITY E= .3881 E\*= .3583  
 SPECIFIC SURFACE 159.9299 CM/CM  
 PERMEABILITY KKC 122.0789 KMQ 164.8378

SAT %	PORE RAD	P CM H2O	P*	VOL CCS	F %/100	F* %/100
2.42	18.81	7.8	7.5	0.48	6.873	0.0430
3.88	13.59	10.8	10.5	0.77	9.515	0.0595
12.11	9.92	14.8	14.5	2.40	13.039	0.0815
31.14	8.25	17.8	17.5	6.17	15.682	0.0981
53.15	7.41	19.8	19.5	10.53	17.444	0.1091
78.58	6.44	22.8	22.5	15.56	20.086	0.1256
95.18	5.10	28.8	28.5	18.85	25.372	0.1586
99.78	3.60	40.8	40.5	19.76	35.943	0.2247
99.91	2.45	59.8	59.5	19.79	52.680	0.3294
100.00	1.77	82.8	82.5	19.81	72.941	0.4561

MIXTURE 2  
 WT 100.9798 GRMS DIA 10.80 CMS  
 WATER SURFACE TENSION 72.00 DYNES/CM  
 RES MOIST 1.462 WT% 9.104 VOL%  
 POROSITY E= .3434 E\*= .3167  
 SPECIFIC SURFACE 160.4393 CM/CM  
 PERMEABILITY KKC 72.9807 KMQ 92.1056

SAT %	PORE RAD	P CM H2O	P*	VOL CCS	F %/100	F* %/100
1.41	25.39	5.8	5.5	0.23	4.190	0.0262
2.83	13.62	10.8	10.5	0.46	7.831	0.0488
6.46	9.30	15.8	15.5	1.04	11.463	0.0714
14.47	7.61	19.3	19.0	2.35	14.006	0.0873
31.35	6.44	22.8	22.5	5.08	16.548	0.1031
74.01	5.48	26.8	26.5	12.00	19.453	0.1213
96.30	4.22	34.8	34.5	15.62	25.265	0.1575
99.71	3.10	47.3	47.0	16.17	34.344	0.2141
99.88	2.34	62.8	62.5	16.20	45.603	0.2842
100.00	1.77	82.8	82.5	16.22	60.131	0.3748

MIXTURE 2  
 WT 100.9798 GRMS DIA 10.80 CMS  
 WATER SURFACE TENSION 72.00 DYNES/CM  
 RES MOIST 1.101 WT% 6.705 VOL%  
 POROSITY  $E_p = .3434$   $E^* = .3218$   
 SPECIFIC SURFACE 167.3131 CM/CM  
 PERMEABILITY KKC 67.1072 KMQ 88.7275

SAT %	PORE RAD	P CM H2O	P*	VOL CCS	F %	F*
1.26	25.30	5.8	5.5	0.21	4.199	0.0251
1.95	16.72	8.8	8.5	0.32	6.379	0.0381
3.29	11.48	12.8	12.5	0.55	9.284	0.0555
7.89	8.49	17.3	17.0	1.31	12.553	0.0750
14.35	7.42	19.8	19.5	2.38	14.369	0.0859
30.78	6.44	22.8	22.5	5.10	16.548	0.0989
60.14	5.69	25.8	25.5	9.97	18.727	0.1119
80.51	5.10	28.8	28.5	13.35	20.906	0.1250
90.22	4.55	32.3	32.0	14.96	23.449	0.1401
97.46	3.79	38.8	38.5	16.16	28.170	0.1684
99.78	3.01	48.8	48.5	16.54	35.434	0.2118
99.86	2.27	64.8	64.5	16.56	47.056	0.2812
100.00	1.77	82.8	82.5	16.58	60.131	0.3594

MIXTURE 2  
 WT 100.9798 GRMS DIA 10.80 CMS  
 WATER SURFACE TENSION 72.00 DYNES/CM  
 RES MOIST 1.314 WT% 6.621 VOL%  
 POROSITY  $E_p = .3871$   $E^* = .3631$   
 SPECIFIC SURFACE 160.6074 CM/CM  
 PERMEABILITY KKC 119.7262 KMQ 168.3297

SAT %	PORE RAD	P CM H2O	P*	VOL CCS	F %	F*
1.38	25.30	5.8	5.5	0.28	5.089	0.0317
2.72	16.68	8.8	8.5	0.55	7.721	0.0481
6.56	11.47	12.8	12.5	1.31	11.229	0.0699
16.78	9.29	15.8	15.5	3.36	13.861	0.0863
46.61	7.81	18.8	18.5	9.34	16.493	0.1027
75.23	6.73	21.8	21.5	15.08	19.124	0.1191
85.86	5.92	24.8	24.5	17.21	21.756	0.1355
97.36	4.48	32.8	32.5	19.51	28.773	0.1792
99.78	3.07	47.8	47.5	20.00	41.932	0.2611
99.88	2.27	64.8	64.5	20.02	56.844	0.3539
100.00	1.77	82.8	82.5	20.04	72.634	0.4522

MIXTURE 3  
 WT 0.0000 GRMS DIA 10.80 CMS  
 WATER SURFACE TENSION 73.00 DYNES/CM  
 RES MOIST 1.200 WT% 16.967 VOL%  
 POROSITY E=.1975 E\*=.1689  
 SPECIFIC SURFACE 239.1946 CM/CM  
 PERMEABILITY KKG 4.1816 KMQ 3.8719

SAT %	PORF RAD	P CM H2O	P*	VOL CCS	F %	F*
2.30	3.23	45.3	45.3	0.16	15.285	0.0639
3.32	2.76	54.0	54.0	0.23	18.197	0.0761
9.78	2.36	63.1	63.1	0.69	21.269	0.0889
11.96	2.05	72.5	72.5	0.85	24.430	0.1021
41.07	1.75	84.9	84.9	2.90	28.639	0.1197
69.02	1.56	95.7	95.7	6.30	32.253	0.1348
97.37	1.40	106.3	106.3	6.89	35.834	0.1498
98.45	1.11	133.7	133.7	6.96	45.075	0.1884
99.82	1.11	133.8	133.8	7.06	45.121	0.1886
100.00	0.81	184.2	184.2	7.07	62.105	0.2596

MIXTURE 3  
 WT 100.9692 GRMS DIA 10.80 CMS  
 WATER SURFACE TENSION 72.00 DYNES/CM  
 RES MOIST 1.311 WT% 8.532 VOL%  
 POROSITY E=.3316 E\*=.3055  
 SPECIFIC SURFACE 216.9045 CM/CM  
 PERMEABILITY KKG 34.6947 KMQ 44.3151

SAT %	PORF RAD	P CM H2O	P*	VOL CCS	F %	F*
1.48	18.87	7.8	7.5	0.23	5.359	0.0247
2.37	11.49	12.8	12.5	0.37	8.804	0.0406
3.94	7.82	13.8	18.5	0.61	12.938	0.0596
10.30	5.92	24.8	24.5	1.60	17.072	0.0787
12.90	5.48	26.8	26.5	2.00	18.451	0.0851
24.80	4.93	29.8	29.5	3.85	20.518	0.0946
45.00	4.48	32.8	32.5	6.98	22.585	0.1041
64.60	4.11	35.7	35.4	10.02	24.583	0.1133
75.70	3.79	38.8	38.5	11.74	26.719	0.1232
84.50	3.43	42.8	42.5	13.11	29.475	0.1359
92.00	3.01	48.8	48.5	14.27	33.609	0.1550
95.40	2.68	54.8	54.5	14.80	37.744	0.1740
97.50	2.34	62.8	62.5	15.10	43.256	0.1994
98.90	1.99	73.8	73.5	15.34	50.836	0.2344
99.50	1.77	82.8	82.5	15.44	57.037	0.2630
100.00	1.58	92.8	92.5	15.51	63.927	0.2947



MIXTURE 3  
 WT 100.9692 GRMS DIA 10.80 CMS  
 WATER SURFACE TENSION 72.00 DYNES/CM  
 RES-MOIST 1.420 WT% 9.267 VOL%  
 POROSITY E=.3325 E\*=.3045  
 SPECIFIC SURFACE 213.2635 CM/CM  
 PERMEABILITY KKC 36.2802 KMQ 46.9113

SAT %	PORE RAD	P CM H2O	P* CM H2O	VOL CCS	F %/100	F* %/100
1.79	16.72	8.8	8.5	0.28	6.073	0.0285
4.62	7.82	18.8	18.5	0.71	12.991	0.0609
26.02	5.10	28.8	28.5	4.03	19.910	0.0934
54.60	4.48	32.8	32.5	8.45	22.677	0.1063
76.17	3.79	38.8	38.5	11.79	26.828	0.1258
88.15	3.14	46.8	46.5	13.64	32.363	0.1517
93.58	2.59	56.8	56.5	14.48	39.281	0.1842
97.57	1.99	73.8	73.5	15.10	51.043	0.2393
100.00	1.58	92.8	92.5	15.47	64.188	0.3010

MIXTURE 3  
 WT 100.9692 GRMS DIA 10.80 CMS  
 WATER SURFACE TENSION 72.00 DYNES/CM  
 RES-MOIST 1.345 WT% 6.670 VOL%  
 POROSITY E=.3902 E\*=.3658  
 SPECIFIC SURFACE 227.2393 CM/CM  
 PERMEABILITY KKC 61.8800 KMQ 91.1774

SAT %	PORE RAD	P CM H2O	P* CM H2O	VOL CCS	F %/100	F* %/100
1.50	18.81	7.8	7.5	0.31	6.935	0.0305
3.44	9.92	14.8	14.5	0.70	13.156	0.0579
18.24	6.89	21.8	21.0	3.71	18.933	0.0833
51.70	5.92	24.8	24.5	10.53	22.044	0.0970
66.09	5.28	27.8	27.5	13.46	24.710	0.1087
79.28	4.47	32.8	32.5	16.14	29.154	0.1283
89.04	3.60	40.8	40.5	18.13	36.263	0.1596
93.95	3.01	48.8	48.5	19.13	43.373	0.1909
96.30	2.68	54.8	54.5	19.61	48.705	0.2143
97.90	2.34	62.8	62.5	19.93	55.815	0.2456
99.16	2.02	72.8	72.5	20.19	64.703	0.2847
99.84	1.77	82.8	82.5	20.33	73.590	0.3238
100.00	1.58	92.8	92.5	20.36	82.477	0.3630

MIXTURE 3  
 WT 100.9692 GRMS DIA 10.80 CMS  
 WATER SURFACE TENSION 72.00 DYNES/CM  
 RES-MOIST 1.289 WT% 6.476 VOL%  
 POROSITY E=.3867 E\*=.3632  
 SPECIFIC SURFACE 230.9708 CM/CM  
 PERMEABILITY KKC 57.6358 KMQ 85.1732

SAT %	PORE RAD	P CM H2O	P* CM H2O	VOL CCS	F %/100	F* %/100
1.83	14.98	9.8	9.5	0.37	8.584	0.0372
7.70	7.81	18.8	18.5	1.55	16.465	0.0713
30.43	6.44	22.8	22.5	6.12	19.968	0.0865
66.77	5.10	28.8	28.5	13.42	25.223	0.1092
83.76	3.99	36.8	36.5	16.83	32.229	0.1395
92.53	3.14	46.8	46.5	18.60	40.986	0.1775
97.61	2.34	62.8	62.5	19.62	54.997	0.2381
100.00	1.58	92.8	92.5	20.10	81.269	0.3519

## MIXTURE 4

WT 0.0000 GRMS DIA 10.80 CMS  
 WATER SURFACE TENSION 73.00 DYNES/CM  
 RES MOIST 1.200 WT% 19.548 VOL%  
 POROSITY E=1.792 E\*=1.499  
 SPECIFIC SURFACE 199.1460 CM/CM  
 PERMEABILITY KKC 4.3075 KMQ 3.6429

SAT %	PORE RAD	P CM H2O	P*	VOL CCS	F X100	F* X100
8.53	4.52	33.0	33.0	0.52	9.856	0.0495
13.87	3.10	48.0	48.0	0.85	14.343	0.0720
17.76	2.29	64.9	64.9	1.09	19.405	0.0974
18.98	2.29	64.9	64.9	1.17	19.423	0.0975
22.11	1.80	82.5	82.5	1.36	24.685	0.1240
53.65	1.77	83.9	83.9	3.29	25.098	0.1260
69.50	1.45	102.7	102.7	5.49	30.717	0.1542
94.36	1.42	105.1	105.1	5.79	31.420	0.1578
99.23	1.20	124.3	124.3	6.09	37.160	0.1866
100.00	1.02	146.6	146.6	6.14	43.842	0.2201

## MIXTURE 4

WT 60.8327 GRMS DIA 6.60 CMS  
 WATER SURFACE TENSION 72.00 DYNES/CM  
 RES MOIST 1.029 WT% 6.306 VOL%  
 POROSITY E=3.3404 E\*=3.202  
 SPECIFIC SURFACE 196.9240 CM/CM  
 PERMEABILITY KKC 46.7563 KMQ 63.9587

SAT %	PORE RAD	P CM H2O	P*	VOL CCS	F X100	F* X100
2.70	12.82	11.5	11.0	0.27	8.209	0.0417
10.16	8.92	16.5	16.0	1.01	11.793	0.0599
15.64	7.18	20.5	20.0	1.55	14.660	0.0744
32.27	6.00	24.5	24.0	3.20	17.527	0.0890
50.61	5.16	28.5	28.0	5.02	20.394	0.1036
68.02	4.52	32.5	32.0	6.75	23.261	0.1181
78.40	4.03	36.5	36.0	7.78	26.128	0.1327
92.05	3.16	46.5	46.0	9.14	33.296	0.1691
97.66	2.60	56.5	56.0	9.69	40.464	0.2055
99.80	2.05	71.5	71.0	9.91	51.215	0.2601
100.00	1.52	96.5	96.0	9.93	69.134	0.3511

## MIXTURE 4

WT 60.8327 GRMS DIA 6.60 CMS  
 WATER SURFACE TENSION 72.00 DYNES/CM  
 RES MOIST 0.925 WT% 6.748 VOL%  
 POROSITY E=3.3033 E\*=2.841  
 SPECIFIC SURFACE 196.4020 CM/CM  
 PERMEABILITY KKC 29.8033 KMQ 40.3898

SAT %	PORE RAD	P CM H2O	P*	VOL CCS	F X100	F* X100
2.08	12.84	11.4	11.0	0.17	6.910	0.0352
10.83	8.93	16.4	16.0	0.90	9.934	0.0506
19.07	6.85	21.4	21.0	1.59	12.957	0.0660
28.98	5.55	26.4	26.0	2.42	15.980	0.0814
36.97	4.82	30.4	30.0	3.08	18.398	0.0937
47.88	4.26	34.4	34.0	3.99	20.817	0.1060
70.53	3.63	40.4	40.0	5.88	24.445	0.1245
81.77	3.16	46.4	46.0	6.82	28.073	0.1429
99.26	1.92	76.4	76.0	8.28	46.212	0.2353
100.00	1.52	96.4	96.0	8.31	58.301	0.2960

CELITE 560

WT 2.8357 GRMS DIA 3.55 CMS  
 WATER SURFACE TENSION 72.00 DYNES/CM  
 RES MOIST 49.973 WT% 19.710 VOL%  
 POROSITY E=.8747 E\*=.7307  
 SPECIFIC SURFACE \*7414.1252 CM/CM  
 PERMEABILITY KKC 15.5091 KMQ 29.6756

SAT %	PORE RAD	P CM H2O	P*	VOL CCS	F X100	F* X100
0.97	5.87	25.0	24.5	0.07	242.362	0.0327
5.00	2.69	54.5	54.0	0.36	528.383	0.0713
17.28	2.67	55.0	54.5	1.24	533.231	0.0719
52.03	2.26	65.0	64.5	3.74	630.187	0.0850
66.61	1.55	95.0	94.5	4.79	921.055	0.1242
75.39	1.28	115.0	114.5	5.42	*1114.968	0.1504
94.60	0.68	215.0	214.5	6.80	*2084.530	0.2812
100.00	0.47	315.0	314.5	7.19	*3054.092	0.4119

CELITE 560

WT 2.3423 GRMS DIA 3.55 CMS  
 WATER SURFACE TENSION 72.00 DYNES/CM  
 RES MOIST 46.870 WT% 20.228 VOL%  
 POROSITY E=.8650 E\*=.7195  
 SPECIFIC SURFACE \*7163.5347 CM/CM  
 PERMEABILITY KKC 13.8406 KMQ 27.1563

SAT %	PORE RAD	P CM H2O	P*	VOL CCS	F X100	F* X100
1.79	5.90	24.9	24.5	0.10	221.421	0.0309
2.43	4.21	34.9	34.5	0.13	310.413	0.0433
3.45	3.27	44.9	44.5	0.19	399.405	0.0558
4.09	2.67	54.9	54.5	0.22	488.396	0.0662
45.53	2.26	64.9	64.5	2.47	577.388	0.0806
67.78	1.55	94.9	94.5	3.68	844.364	0.1179
85.30	0.95	154.9	154.5	4.63	*1378.314	0.1924
94.89	0.62	234.9	234.5	5.15	*2090.248	0.2918
98.08	0.47	314.9	314.5	5.32	*2802.182	0.3912
99.75	0.35	414.9	414.5	5.41	*3692.100	0.5154
100.00	0.29	514.9	514.5	5.43	*4582.018	0.6396

CELITE 545

WT 1.4055 GRMS DIA 3.55 CMS  
 WATER SURFACE TENSION 72.80 DYNES/CM  
 RES MOIST 45.780 WT% 20.009 VOL%  
 POROSITY E=.8633 E\*=.7194  
 SPECIFIC SURFACE \*9733.0630 CM/CM  
 PERMEABILITY KKC 7.2691 KMQ 11.6417

SAT %	PORE RAD	P CM H2O	P*	VOL CCS	F X100	F* X100
0.65	6.00	24.7	24.5	0.02	214.493	0.0220
2.81	4.27	34.7	34.5	0.09	301.241	0.0310
3.67	2.71	54.7	54.5	0.12	474.738	0.0488
11.45	1.99	74.7	74.5	0.37	648.235	0.0666
31.53	1.49	99.7	99.5	1.01	865.106	0.0889
59.83	1.10	134.7	134.5	1.92	*1168.726	0.1201
76.68	0.85	174.7	174.5	2.47	*1515.720	0.1557
92.01	0.61	244.7	244.5	2.96	*2122.959	0.2181
98.06	0.47	314.7	314.5	3.15	*2730.199	0.2805
100.00	0.34	439.7	439.5	3.22	*3814.554	0.3919

CELITE 535

WT 2.4151 GRMS DIA 3.55 CMS  
 WATER SURFACE TENSION 72.00 DYNES/CM  
 RES MOIST 40.985 WT% 18.738 VOL%  
 POROSITY E= .8566 E\*= .7214  
 SPECIFIC SURFACE \*12389.0993 CM/CM  
 PERMEABILITY KKO 3.9828 KMQ 6.4692

SAT %	PORE RAD	P CM H2O	P* CM H2O	VOL CCS	F %	F* %
1.97	5.90	24.9	24.5	0.10	206.334	0.0167
2.50	3.27	44.9	44.5	0.13	372.264	0.0300
3.02	2.26	64.9	64.5	0.16	538.195	0.0434
3.29	1.96	74.9	74.5	0.17	621.160	0.0501
3.55	1.73	84.9	84.5	0.19	704.126	0.0568
3.68	1.55	94.9	94.5	0.19	787.091	0.0635
3.94	1.40	104.9	104.5	0.21	870.056	0.0702
23.78	1.18	124.9	124.5	1.52	*1035.987	0.0836
61.92	1.01	144.9	144.5	2.21	*1201.917	0.0970
67.54	0.75	194.9	194.5	3.57	*1616.744	0.1305
79.63	0.62	234.9	234.5	4.21	*1948.605	0.1573
92.64	0.47	314.9	314.5	4.89	*2612.327	0.2109
97.90	0.38	384.9	384.5	5.17	*3193.084	0.2577
99.61	0.29	514.9	514.5	5.26	*4271.633	0.3448
99.87	0.23	644.9	644.5	5.28	*5350.182	0.4318
100.00	0.19	774.9	774.5	5.28	*6428.730	0.5189

CELITE 503

WT 2.2615 GRMS DIA 3.55 CMS  
 WATER SURFACE TENSION 72.00 DYNES/CM  
 RES MOIST 47.864 WT% 21.592 VOL%  
 POROSITY E= .8611 E\*= .7082  
 SPECIFIC SURFACE \*14529.0071 CM/CM  
 PERMEABILITY KKO 3.1356 KMQ 6.3456

SAT %	PORE RAD	P CM H2O	P* CM H2O	VOL CCS	F %	F* %
0.55	5.91	24.9	24.5	0.03	214.032	0.0147
3.60	2.68	54.9	54.5	0.18	472.341	0.0325
26.32	1.28	114.9	114.5	1.32	988.960	0.0681
38.36	1.01	144.9	144.5	1.92	*1247.269	0.0858
51.38	0.79	184.9	184.5	2.58	*1591.681	0.1096
64.82	0.63	234.9	234.5	3.25	*2022.197	0.1392
76.04	0.52	284.9	284.5	3.81	*2452.713	0.1688
89.33	0.38	384.9	384.5	4.48	*3313.744	0.2281
96.53	0.29	514.9	514.5	4.84	*4433.084	0.3051
99.44	0.23	644.9	644.5	4.99	*5552.425	0.3822
100.00	0.19	774.9	774.5	5.01	*6671.765	0.4592

HF SP GEL  
 WT 1.7354 GRMS DIA 3.55 CMS  
 WATER SURFACE TENSION 72.00 DYNES/CM  
 RES MOIST 54.169 WT% 26.872 VOL%  
 POROSITY E= .8547 E\* = .6737  
 SPECIFIC SURFACE \*18822.6025 CM/CM  
 PERMEABILITY KKC 1.6693 KMQ 2.5207

SAT %	PORE RAD	P CM H2O	P*	VOL CCS	F X100	E* X100
0.99	4.22	34.8	34.5	0.03	284.004	0.0151
1.98	1.96	74.8	74.5	0.07	610.799	0.0325
3.17	1.18	124.8	124.5	0.11	*1019.293	0.0542
5.75	0.95	154.8	154.5	0.20	*1264.389	0.0672
31.35	0.79	184.8	184.5	1.10	*1509.486	0.0802
40.08	0.68	214.8	214.5	1.40	*1754.582	0.0932
50.20	0.60	244.8	244.5	1.76	*1999.678	0.1062
55.75	0.52	284.8	284.5	1.95	*2326.474	0.1236
70.44	0.41	359.8	359.5	2.46	*2939.214	0.1562
81.74	0.33	439.8	439.5	2.86	*3592.805	0.1909
89.28	0.29	514.8	514.5	3.12	*4205.546	0.2234
96.82	0.23	644.8	644.5	3.39	*5267.630	0.2799
99.40	0.19	774.8	774.5	3.48	*6329.714	0.3363
100.00	0.17	839.8	839.5	3.50	*6860.756	0.3645

APPENDIX SIX : COMPUTER PROGRAM FOR THE PERMEABILITY OF A  
NETWORK

```

FORTRAN G124, J A DODDS
NO TRACE
MASTER MATX
DIMENSION R(171),A(91,91),R(91),NRR(171),REINT(91)
COMMON L,R
666 READ(1,91)L
91 FORMAT(I3)
STVOL=0.0
KT=0
SKER=1.0
IF(L.EQ.999)STOP
READ(1,108)BED,NO
108 FORMAT(A5,A5)
WRITE(2,103)BED,NO
103 FORMAT(//8H BED NO ,A5,A5/)
READ(1,113)DEM
113 FORMAT(F3.1)
NG=2*L*L+L
NF=L*(L+1)+1
DO 104 I=1,NG
104 R(I)=0.0
TOT=0.0
READ(1,198)INDEX
198 FORMAT(I2)
26 IF(INDEX.EQ.10)GO TO 50
READ(1,24)RAD,VOL,NO,NRD
24 FORMAT(F5.4,F6.5,I2,I2,)
GO TO 51
50 READ(1,25)RAD,VOL,NO,NRD
25 FORMAT(F6.5,F6.5,I2,I2,)
51 IF(DEM.EQ.1.0)VOL=VOL*0.1
RSTN=2.00*VOL/(3141.5*RAD**6)
XND=NO
TVOL=VOL*XND
STVOL=STVOL+TVOL
WRITE(2,27)RAD,VOL,NO,RSTN,TVOL,STVOL
27 FORMAT(2X,F5.5,2X,F6.5,2X,I3,2X,F8.5,4X,F8.5,4X,F9.5)
DO 28 I=1,NO
29 RN=ZORNAL(5)
J=RN*171.0+0.5
IF(J=0)0,29,0
IF(R(J)=0.0)29,0,29
R(J)=2.00*VOL/(3141.5*RAD**6)
NRR(J)=NRD
28 TOT=TOT+1.0
IF(TOT=NG)25,111,111
111 CONTINUE
KT=KT+1
DO 30 I=1,NF
30 B(I)=0.0
B(1)=1.0
DO 31 I=1,NF
DO 31 J=1,NF
A(I,J)=Z(I,J)
31 CONTINUE

```

```
N=NF
NA=NF*NF
NB=NF
IN=1
CALL F2SOLVE(A,B,N,NA,NB,IN,D,IO,IT,REINT)
IF(KT.EQ.1)SKER=B(1)
REL P=B(1)/SKER
WRITE(2,37)IT,B(1),REL P,KT
37 FORMAT(I4,2Y,F10.4,2X,F7.4,2X,I4/)
IF(KT.GT.10)GO TO 110
DO 109 J=1,NG
IF(NRR(J).LE.KT)R(J)=999.999
109 CONTINUE
GO TO 111
110 GO TO 566
STOP
END
```

ND OF SEGMENT, LENGTH 374, NAME MATX

```

FUNCTION Z(I,J)
DIMENSION R(171)
COMMON L,R
Z=0.
I1=I
J1=J
II=2*I+1+(I-2)/L
10 IF(I.EQ.1)GO TO 2
IF(J-I)1,5,5
1 K=I
I=J
J=K
II=2*I+1+(I-2)/L
GO TO 10
6 IF(J.EQ.I+L)Z=-R(II-3)
IF(J.GT.L*L+2)GO TO 53
IF(J.EQ.I+1.AND.MOD(J-2,L).NE.0)Z=-R(II-2)
GO TO 53
2 IF(J.EQ.1)GO TO 3
NN=(J-2)/L
IF(MOD(J-2,L).EQ.0.AND.J.LE.(L*L-L+2))Z=-R((2*L+1)*NN+1)
GO TO 53
3 S=0.0
NS=L*L-L+1
DO 4 K=1,NS,L
NN=(K-1)/L
4 S=S+R((2*L+1)*NN+1)
Z=S
GO TO 53
5 IF(I.LE.L+1)GO TO 51
IF(I.GT.L*L+1)GO TO 52
Z=R(II-4)+R(II-3)+R(II-2)+R(II-4-2*L)
GO TO 53
51 IF(II.GT.4)Z=R(II-4)
Z=Z+R(II-3)+R(II-2)
GO TO 53
52 Z=R(II-4-2*L)
53 I=I1
J=J1
RETURN
STOP
END

```

ID OF SEGMENT, LENGTH 409, NAME Z

ORMAL (SEMI-COMPILED)

2SOLVE (SEMI-COMPILED)



Appendix Seven: Computer Program for Relative Permeability and Dewatering Curves from Capillary Pressure Data

```

RTRAN G061, D00DS
MASTER CORP
DIMENSION PC(101),ST(101),R(101),SX(101),RX(101),T(101),NWPER(102)
1,WPER(102),PX(101),SAT(101),V(101),TIM(500),CSAT(500),CSEC(500),YSAT(500)
2AT(500)
REAL L
REAL NWPER
66 READ(1,19)N
19 FORMAT(I3)
IF(N.EQ.999)STOP
NDIV=0
READ(1,28)BED,NO
28 FORMAT(A5,A5)
WRITE(2,29)BED,NO
29 FORMAT(//8H BED NO ,A5,A5/)
READ(1,26)TX,D,DIA,WT,DS,E
26 FORMAT(3F5.2,F9.4,F6.4,F5.4)
READ(1,30)RWM
30 FORMAT(F6.3)
VIS=0.01
IF(E.LE.0.25)WT=100.0
A=3.1415*DIA*DIA/4.0
L=WT/(DS*(1.0-E)*A)
WRITE(2,32)TX,D
32 FORMAT(17H SURFACE TENSION ,F5.2,16H LIQUID DENSITY ,F5.2/)
WRITE(2,33)WT,DIA,L,DS,E,VIS
33 FORMAT(4H WT ,F9.4,5H DIA ,F5.2,8H HEIGHT ,F6.2,4H SG ,F6.4,10H PO
1RSITY ,F5.4,4H VS ,F5.4/)
PC(1)=0.0
ST(1)=0.0
R(1)=1.0
DO 1 I=2,N+1
READ(1,21)PC(I),ST(I)
21 FORMAT(2F7.3)
R(I)=(2.0*TX)/(PC(I)*D*981.0)
1 WRITE(2,23)R(I),PC(I),ST(I)
23 FORMAT(3F10.5)
PC(1)=PC(2)
R(1)=R(2)
I=1
SX(1)=0.
PX(1)=0.
DO 9 J=2,101
X=J-1
SX(J)=X
6 IF(ST(I)-SX(J))3,4,5
4 RX(J)=R(I)
GO TO 2
5 TALP=(R(I-1)-R(I))/(ST(I)-ST(I-1))
RX(J)=R(I-1)-(SX(J)-ST(I-1))*TALP
GO TO 2
3 I=I+1
GO TO 5
2 CONTINUE
PX(J)=(2.0*TX)/(RX(J)*D*981.0)

```

```

9 CONTINUE
PER=0.0
AREA=0.
DO 7 J=2,101
F=(2*J-3)
T(J)=F*RX(J)*RX(J)
SEG=(SX(J)-SX(J-1))*(PX(J)+PX(J-1))*E/2.
AREA=AREA+SEG
7 PER=PER+T(J)
FPER=(E**1.3333)*1250.0*PER
WRITE(2,35)FPER,AREA
35 FORMAT(F10.1,F20.8)
AN=0.
DO 8 J=2,101
AN=AN+T(J)
NWPER(J)=((E*SX(J)/100.)*1.3333)*AN*1250.0/FPER
WPER(J)=((E*(100.-SX(J))/100.)*1.3333)*(PER-AN)*1250./FPER
8 CONTINUE
RX(1)=0.0
NWPER(1)=0.0
NWPER(101)=1.0
NWPER(102)=1.0
WPER(1)=1.0
WPER(101)=0.0
WPER(102)=0.0
NDIV=20
NK=0
VAC=300.0
66 NK=NK+1
DO 10 I=1,NDIV+1
10 SAT(I)=0.0
TIM(I)=0.0
CSAT(I)=0.0
V(I)=0.0
J=1
CSEC(I)=0.0
WRITE(2,36)NDIV
36 FORMAT(6H NDIV=,I3)
BDIV=NDIV
12 NS1=SAT(NDIV+1)
XSAT=0.0
J=J+1
SVER=FPER*WPER(NS1+1)
TSEC=(L*L*VIS*E*1000.)/(SVER*VAC*BDIV)*BDIV
DO 11 I=2,NDIV+1
NS=SAT(I)
SNS=NS*100
SNS2=SAT(I)*100.0-SNS
SPER=FPER*WPER(NS+1)+((FPER*WPER(NS+2)-FPER*WPER(NS+1))*SNS2/100.0
1)
V(I)=((SPER*A*(VAC-PX(NS+1))*TSEC)/(L*VIS.))*D*0.00000981
SAT(I)=SAT(I)+((V(I)-V(I-1))*BDIV*100.0)/(L*A*E)
IF(SAT(I).GE.100.0)SAT(I)=100.0
XSAT=XSAT+SAT(I)
11 CONTINUE
CSAT(J)=CSAT(J-1)+(V(NDIV+1)*100.0)/(L*A*E)
YSAT(J)=XSAT/BDIV
CSEC(J)=TSEC
TIM(J)=TIM(J-1)+TSEC
IF(J.GT.499)GO TO 94
IF(CSAT(J).LE.90.0)GO TO 12
94 DO 13 I=1,J
WRITE(2,31)CSAT(I),TIM(I),CSEC(I),YSAT(I)
13 CONTINUE
31 FORMAT(2X,F8.4,2X,F12.10,2X,F12.10,2X,F10.4)
GO TO 86
STOP

```

## REFERENCES

- ADWICK A.G. and WARMER R.J. (1966) "The Influence of Particle Size Distribution on the Sintering of Ceramic Powders", Soc. Anal. Chem. Part. Size Conf. Loughborough. Paper 27
- ANDREASEN A.H.M. (1940) "The Relation of Fineness to Physical Requirements," J. Soc. Glass Tech. V. 24, 167.
- ANON (1968) "Measurement of Pore Size Distribution," Chem. Proc. V. 14, 34-39.
- ARCHIE G.E. (1942) "The Electrical Resistivity Log as an Aid in Determining Some Reservoir Characteristics," T.A.I.M.E. V. 146, 54.
- ATKINSON D.I.W. (1949) "The Mechanism of the Displacement of Liquids from Porous Solids," Trans. I. Ch. E. V. 27, 259-72.
- AYER J.E. and SOPPETT, E.E. (1965) "Vibratory Compaction I Compaction of Spherical Shapes," J. Am. Ceram. Soc. V. 48, 180-3.
- BARTELL F.E. and OSTERHOF H.J. (1927) "Determination of the Wettability of a solid by a Liquid," Ind. Eng. Chem. V. 19, 1277-80.
- BARTELL F.E. and OSTERHOF H.J. (1928) "The Pore Size of Compressed Carbon and Silica Membranes," J. Phys. Chem. V. 32, 1553-71.
- BATEL W. (1954) "Mechanical Dewatering," Chem. Ing. Tech. V. 26, 497.
- BATEL W. (1955) "The Behaviour of Granular Materials During Sieving," Refract. J. Aug. 468-73.
- BATEL W. (1956) "Properties of Moist Heaps of Bulk Materials," Chem. Ing. Tech. V.28, 195-200.
- BATEL W. (1959) "Characteristics of Pore Volumes in Fixed Beds Related to Unit Operations," Chem. Ing. Tech. V.31, 388-93.
- BATEL W. (1961) "Quantity and Behaviour of the Inter Granular Moisture in Granular Materials," Chem. Ing. Tech. V. 33, 541-7 (C.E.G.B. Trans. No. 2778).
- BEN AIM R. and LE GOFF P. (1968) "Effet de Paroi dans les Empilements Desordonnes de Spheres et Application à la Porosite de Melange Binaires," Pow. Tech. V.1, 281-90.
- BERNAL J.D. (1965) "The Bakerian Lecture 1962: The Structure of Liquids," Proc. Roy. Soc. A. 280, 299-322.

- BERRESFORD R.H. (1967) "Packing of Spheres," Disc. Farad. Soc. No. 43  
76-9.
- BETHEL F.T. and CALHOUN J.C. (1953) "Capillary Desaturation in  
Unconsolidated Beads," T.A.I.M.E. V. 198, 197-202.
- BLUM E.H. and WILHELM R.H. (1968) "A Statistical Geometric Approach  
to Random Packed Beds," A.I. Ch. E./ I. Chem.E. Symp. Ser.  
No. 4, 21-27.
- BO M.K. (1968) "The Flow of Fluids in Porous Media," Ph.D. Thesis,  
Loughborough.
- BO M.K., FRESHWATER D.C. and SCARLETT B. (1965) "The Effect of  
Particle Size Distribution on the Permeability of Filter  
Cakes," Trans. Inst. Chem. Eng. V.43, 228-32.
- BOTSET H.G. (1940) "Flow of Gas Liquid Mixtures Through Consolidated  
Sand," T.A.I.M.E. (Pet. Div.) V. 136, 91-105.
- BROWN J.W. (1951) "Capillary Pressure Investigations," T.A.I.M.E.  
(Pet. Div.) V. 192, 67-74.
- BROWNELL L.E. and CROSIER (1949) "Blower and Heat Requirements of  
Rotary Vacuum Filter Dryer," Chem. Eng. Oct. 124-127.
- BROWNELL L.E. and Gudz G.B. (1949) "Blower Requirements of Rotary  
Drum Vacuum Filters," Chem. Eng. Sept. 112-115.
- BROWNELL L.E. and KATZ D.L. (1947) "Flow of Fluids Through Porous  
Media," Chem. Eng. Prog. V.43, 537-48, 601-12, 703-12.
- BROOKS C.S. and PURCELL W.R. (1952) "Surface Area Measurements on  
Sedimentary Rocks," T.A.I.M.E. V. 195, 289-96.
- BURDINE N.T. (1953) "Relative Permeability Calculations from Pore  
Size Distribution Data," T.A.I.M.E. V. 198, 71-78.
- BURTON G. (1962) "A New Process for Reducing the Moisture Content  
of Filter Cake," 4th Int. Coal. Prep. Cong. Harrogate.
- BURTON G. and THOMAS D.G.A. (1953) "Moisture Retention in Packed  
Beds," N.C.B. REPT No. 1194.
- CARMAN P.C. (1937) "Review of Literature Confirming Validity of  
Kozenys Theory," Trans. Inst. Chem. Eng. V. 150.
- CARMAN P.C. (1941) "Capillary Rise and Capillary Movement of Moisture  
in Fine Sands," Soil Sci. V.52 p. 1. July.
- CARMAN P.C. (1948) "Some Physical Aspects of Water Flow in Porous  
Media," Disc. Farad. Soc. No. 3 72-7.
- CARR J.F. (1964) "Basic Studies of Coal Flow: Surface Tension Forces  
In Wet Powders," Research Mem. 14 C.E.G.B. S.W. Region. Jan.

- CHATENEVER A. and CALHOUN J.C. (1952) "Visual Examinations of Fluid Behaviour in Porous Media, Part I," T.A.I.M.E. Pet. Div. V. 195, 149-56.
- CHILDS E.C. and COLLIS-GEORGE N.C. (1950) "The Permeability of Porous Materials," Proc. Roy. Soc. A.201, 392-405.
- CHRISTENSEN G.N. and BARKAS W.W. (1955) "Stresses Exerted by Water Held in Wet Webs of Paper Making Fibres," Trans. Farad. Soc. V. 51, 130-45.
- COLEMAN J.D. (1963) "Thermodynamics and the Suction of Moisture in Porous Materials," Conf. on Drying Inst. Fuel. Dublin May.
- COULSON J.M. (1949) "The Flow of Fluids Through Granular Beds," T. Inst. Chem. Eng. V. 27, 237-56.
- CRONEY D., COLEMAN J.D. and BRIDGES P.M. (1952) "The Suction of Moisture Held in Soils and other Porous Materials," D.S.I.R. Road Res. Lab. Tech. Ppr 24, H.M.S.O.
- DAHLSTROM D.A. (1966) "New Developments in Continuous Liquid-Solids Separation," Lect. to Filt. Soc. (London) 1 Nov.
- DAHLSTROM D.A. and PURCHAS D.B. (1957) "Scale-up Methods for Continuous Filtration Equipment," A.I.Ch.E./I.Chem.E. Joint Symp. 120-31. (On Scale-up Methods)
- DEBBAS S. and RUMPF H. (1966) "Randomness of Beds of Spheres or Irregular Particles," Chem. Eng. Sci. V. 21, 583-607.
- DODD C.G and KIEL O.G. (1959) "Evaluation of Monte Carlo Methods in Studying Fluid Fluid Displacement and Wettability in Porous Rocks," J. Phys. Chem. V. 63, 1646-52.
- DOMBROWSKI H.S. and BROWNEL L.E. (1954) "Residual Equilibrium Saturation of Porous Media," Ind. Eng. Chem. V. 46, 1207-18.
- DRENNAN J.A. (1964) "Inert Porosity," T. Brit. Cerm. Soc. V.63, 373-88.
- DYKSTRA H. and PARSONS (1951) "Relaxation Methods Applied to Oil Field Research," T.A.I.M.E. Pet. Div. V. 192, 227-232, 367-68.
- EISENKLAM P. (1956) "Porous Masses," Chem. Eng. Prac. V. 2, Ed. Gremer & Davies, 342-463.
- EMMETT R.C. and DAHLSTROM D.A. (1961) "Top Feed Filtration and Drying," Chem. Eng. Prog. V.57, 63-67.
- ENDERBY A.J. (1955) "The Domain Model of Hysteresis I. Independant Domains," Trans. Farad. Soc. V.51, 835-48.

- ENDERBY A.J. (1956) "The Domain Model of Hysteresis 2. Interacting Domains," Trans. Farad. Soc. V. 52, 106-120.
- EPSTEIN N. and YOUNG M.J. (1962) "Random Loose Packing of Binary Mixtures of Spheres," Nature V. 196, 885.
- EVERETT D.H. (1954) "A General Approach to Hysteresis 3 Formal Treatment of the Domain Model," Trans. Farad. Soc. V. 50, 1077-96.
- EVERETT D.H. (1955) "A General Approach to Hysteresis 4 An Alternative Formulation of the Domain Model," Trans. Farad. Soc. V. 51, 1551-7.
- FATT I. (1956) "The Network Model of Porous Media," Trans. A.I.M.E. Pet. Div. V. 207, 144-59, 160-3, 164-81.
- FATT I. (1962) "Deductions from the Network Model Concerning Diffusion and Fluid Flow through Porous Media," I.Chem.E. Symp. Interaction between fluids and particles, London. 304-11.
- FATT I. and DYKSTRA H. (1951) "Relative Permeability Studies," T.A.I.M.E. Pet. Div. V.192, 249-56.
- FISHER R.A. (1926) "On the Capillary Forces in an Ideal Soil Correction of the Formulæ given by W.B. Haines," J.Agric. Sci. V.16, 492-505.
- FISHER R.A. (1928) "Further Note on the Capillary Forces in an Ideal Soil," J. Agric. Sci. V.18, 406-10.
- FLOOD E.A. (1958) "Statistical Descriptions and Physical Properties of Granular and Porous Solids," The Structure & Props. of Porous Materials 10th Symp. of Colston Res. Soc. Bristol, 151-69.
- FRAZER (1935) "Experimental Study of the Porosity and Permeability of Clastic Sediments," J. Geol. V. 43, 910.
- FULLER W.B. and THOMPSON S.E. (1907) "The Laws of Proportioning Concrete," Trans. Am. Soc. Civ. Eng. V. 59, 67.
- FURNAS C.C. (1929) "Flow of Gases through Beds of Broken Solids," V.S. Bur. Mines. Bull. Vo. 307, 60-101.
- FURNAS C.C. (1931) "Grading Aggregates I Mathematical Relations for Beds of Broken Solids of Maximum Density," Ind. Eng. Chem. V.23 1052-58.
- GARDNER W.R. (1956) "Calculation of Capillary Conductivity from Pressure Plate Outflow Data," Soil Sci. Soc. Amer. Proc. V.20, 317-20.

- GATES J.I. and LIETZ W.T. (1950) "Relative Permeability of California Cores by the Capillary-Pressure Method," A.P.I. Drill. Prod. and Prac. 285-302.
- GILLMORE D.W. and WRIGHT C.C. (1952) "Drainage Behaviour and Water Retention Properties of Fine Coal," Min. Eng. Sept. 886-94.
- GRACE H.P. (1953) "Resistance and Compressibility of Filter Cakes," Chem. Eng. Prog. V. 49, 303-18, 367-77, 427-36.
- GRACE H.P. (1959) "The Art and Science of Filtration," Reaction Kinetics and Unit Ops. Chem. Eng. Prog. Sym. Series No. 25, V. 55, 151-162.
- GRATON L.C. and FRASER H.J. (1935) "Systematic Packing of Spheres with Particular Relation to Porosity and Permeability," J. Geol, V. 43, 785-909.
- GRAY V.R. (1958) "The Dewatering of Fine Coal," J. Inst. Fuel. V. 31, 206 Mar. 96-108. Discussion 72-80 V.32 1959.
- GREGG S.J. and HILL K.J. (1953) "The Aggregation of Kaolinite," J. Appl. Chem. V. 3, 169.
- GRICE M.A.K., MAJOR-MAROTHY G., SIMONS C.S., and DAHLSTROM D.A. (1966) "Moisture Control for Pelletization or Shipment of Filter Cakes," Trans. Soc. Min. Eng. Dec. 341-8.
- HACKETT F.E. and STRETTAN J.S. (1928) "The Capillary Pull on an Ideal Soil," J. Agric. Sci. V. 18, 671-81.
- HAINES W.B. (1925) "Studies in the Physical Properties of Soils I Mechanical Properties Concerned in Cultivation," J. Agric. Sci. V. 15, 178-200.
- HAINES W.B. (1925) "Studies in the Physical Properties of Soils II A Note on the Cohesion Developed by Capillary Forces In an Ideal Soil," J. Agric. Sci. V. 15, 529-35.
- HAINES W.B. (1925) "Studies in the Physical Properties of Soils III Observations on the Electrical Conductivity of Soils," J. Agric. Sci. V. 15, 536-43.
- HAINES W.B. (1927) "Studies in the Physical Properties of Soils IV A Further Contribution to the Theory of Capillary Phenomena in Soil," J. Agric. Sci. V. 17, 264-290.
- HAINES W.B. (1930) "Studies in Physical Properties of Soils V The Hysteresis Effect in Capillary Properties and the Modes of Moisture Distribution Associated Therewith," J. Agric. Sci. V. 20, 97-116.

- HARRIS C.C. (1959) "Dewatering of Fine Coal," Ph.D. Thesis, Leeds.
- HARRIS C.C. (1965) "Latin Square as a Network Model of Random Packing," *Nature* V. 205, 353-56.
- HARRIS C.C., JOWETT A. and MORROW N.R. (1964) "Effect of contact Angle on the Capillary Properties of Porous Masses," *Trans. Inst. Min. Met.* V. 73, 355-51, 520-32.
- HARRIS C.C. and MORROW N.R. (1964) "Pendular Moisture in Packings of Equal Spheres," *Nature*, V.203, 706-8.
- HARRIS C.C. and SMITH H.G. (1957) "The Moisture Retention Properties of Fine Coal. A study by Permeability and Suction Potential Methods. I Principles and Summary of Previous Work. II Experimental Results," *Second Sym. on Coal Prep. Leeds*, Oct. 57-98, 211-249.
- HASSAN M.E. and NIELSEN R.F. (1953) "How to Calculate Relative Permeability of Bradford Sand from Capillary Pressure Data," *The Petl. Engr.* March, 61-62.
- HENDERSON A.F., CORNELL C.F., DUNYON H.F. and DAHLSTROM D.A. (1957) "Filtration and Control of Moisture Content on Taconite Concentrates," *Min. Eng.* V. 9, 349-55.
- HIGUTI I. (1961) "A Statistical Study of Random Packing of Unequal Spheres," *Annals Inst. Stat. Maths.* V. 12, No. 3, 257-71.
- HIMUS G.W. (1958) "The Elements of Fuel Technology 2nd Ed.," Leonard Hill, London.
- HOGENDIJK M.J. (1963) "Random Dense Packing of Spheres with a Discrete Distribution of the Radii," *Phillips Res. Repts.* V.18, 109-126.
- HORSFIELD H.T. (1934) "The Strength of Asphalt Mixtures," *J. Soc. Chem. Ind.* V. 53, 107-115.
- ICZKOWSKI R.P. (1966) "Mercury Penetration into Aggregates of Spheres," *Ind. Eng. Chem (Fund.)* V. 5, 516.
- ICZKOWSKI R.P. (1967) "Breakthrough Pressures for Random Sphere Packings," *Ind. Eng. Chem.* V.6, 263-5.
- KEEN B.A. (1924) "On the Moisture Relations in an Ideal Soil," *J. Agric. Sci.* V. 14, 170-7.
- KING F.H. (1899) "Principles and Conditions of the Movements of Ground Water," 19th Ann. Rep. U.S. Geol. Survey, 59-294.
- KRON G. (1939) "Tensor Analysis of Networks," Chapman & Hall, London.
- KRUYER S. (1958) "The Penetration of Mercury and Capillary Condensation in Packed Spheres," *Trans. Farad. Soc.* V. 54, 1758-64.



- LALIBERTE G.E., BROOKS R.H. and COREY A.T. (1968) "Permeability Calculation from Desaturation Data," Am. Civ. Eng. Soc. (Irig. & Drain Div.) Mar. 57-72.
- LE GOFF P. (1967) "Geometric Problems in the Study of Porous and Dispersed Media," 3rd Davis-Swindin Mem. Lect. Loughborough.
- LEWIS H.D. and GOLDMAN A. (1966) "Theorems for Calculation of Weight Ratios to Produce Maximum Packing Density of Powder Mixtures," J. Am. Ceram. Soc. 323-327.
- LEVA.M. and GRUMMER M. (1947) "Pressure Drop through Packed Tubes III Prediction of Voids in Packed Tubes," Chem. Eng. Prog. V. 43, 713-718.
- LEVERETT M.C. (1939) "Flow of Oil-Water Mixtures through Unconsolidated Sands," T.A.I.M.E. Pet. Div. V. 132, 149-71.
- LEVERETT M.C. (1941) "Capillary Behaviour in Porous Solids," T.A.I.M.E. Pet. Div. & Tech. V. 142, 152-169.
- LEVERETT M.C. and LEWIS W.B. (1941) "Steady Flow of Gas-Oil-Water Mixtures through Unconsolidated Sands," T.A.I.M.E. Pet. Div. & Tech. V. 142, 107-116.
- LYONS O.R. (1950) "Dewatering and Thermal Drying," Coal Prep. Am. Inst. Min. Met. Eng. New York. Ed. D.R. Mitchell.
- LYONS O.R. (1951) "Filter Cake Size Consist and Moisture Relationships," Min. Eng. Oct. 868-70.
- LYONS O.R. (1951) "An Approximate Method of Predicting and Comparing Expected Results when Dewatering Coal by Centrifuges," Min. Eng. May, 417-25.
- MACRAE J.C., FINLAYSON P.C. and GRAY W.A. (1957) "Vibration Packing of Dry Granular Solids," Nature, V. 179, 1365-66.
- MACRAE J.C. and GRAY W.A. (1961) "Significance of the Properties of Materials in the Packing of Real Spherical Particles," Brit. J. Appl. Phys. V. 12, 164-71.
- MARSHALL T.J. (1958) "A Relation Between Permeability and the Size Distribution of Pores," J. Soil Sci. V. 9, 1-8.
- MARSHALL T.J. (1962) "Permeability Equations and their Models," Sym. on Int. between Fluids & Partics. London.
- MASON G. (1967) "Computer Model for Sphere Packing," Disc. Farad. Soc. 75-6.
- MAYER R.P. and STOWE R.A. (1965) "Mercury Porosimetry-breakthrough Pressure for Penetration between Packed Spheres," J. Coll. Sci. V. 20, 893-911.
- MAYER R.P. and STOWE R.A. (1966) "Mercury Porosimetry: Filling of Toroidal Void Volume Following Breakthrough between Packed Spheres, J.Phys. Chem. V.70, 3867-73.

- MCGEARY R.K. (1961) "Mechanical Packing of Spherical Particles,"  
J. Am. Ceram. Soc. V. 44, 513-22.
- MCGEARY R.K. (1967) "Mechanical Packing of Spherical Particles,"  
Perspectives in Pow. Met. V. 2, Vibratory Compacting.  
209-36, Plenum. Press, New York.
- MELROSE J.C. (1966) "Model Calculations for Capillary Condensation,"  
J.A.I. Chem. E. V. 12 986-94, Sept.
- MELROSE J.C. and WALLICK G.C. (1967) "Exact Geometrical Parameters  
for Pendular Ring Fluid," J. Phys. Chem. V.71, 3676-8.
- MEYER H.I. (1953) "Pore Distribution in Porous Media," J. Appl.  
Phys. V. 24, 510-2, May.
- MILLINGTON R.J. and QUIRK J.P. (1961) "Permeability of Porous  
Solids," Trans. Farad. Soc. V. 57, 1200-7.
- MORROW N.R. (1962) "Measurement and Interpretation of Capillary  
Pressures in Porous Materials," Ph.D. Thesis, Leeds.
- MORROW N.R. and HARRIS C.C. (1965) "Capillary Equilibrium in Porous  
Materials," J. Soc. Pet. Eng. V. 5, 15-24.
- NAAR J. and WYGAL R.J. (1962) "Structure and Properties of  
Unconsolidated Aggregates," Canad. J. Physics, V. 40,  
818-31.
- NAAR J., WYGAL R.J. and HENDERSON J.H. (1962) "Imbibition Relative  
Permeability in Unconsolidated Porous Media," Soc. Pet.  
Eng. J. V. 13, 61-70.
- NELSON P.A. and DAHLSTROM D.A. (1957) "Moisture Content Correlation  
of Rotary Vacuum Filter Cakes," Chem. Eng. Prog. V.53, 320-327.
- NENNIGER E. (1956) "Drainage of Packed Beds in Gravitational and  
Centrifugal Force Fields," Ph. D. Thesis, Manchester.
- NENNIGER E. and STORROW J.A. (1958) "Drainage of Packed Beds in  
Gravitational and Centrifugal Force Fields," J.A.I.Ch.E.  
V. 4, 305-316.
- NEWITT D.M. and CONWAY-JONES J.M. (1958) "A Contribution to Theory  
and Practice of Granulation," T. Inst. Chem. Eng. V. 36, 422.
- OSOBA J.S., RICHARDSON J.G., KERVER J.K., HAFFORD J.A. and  
BLAIR P.M. (1951) "Laboratory Measurements of Relative  
Permeability," T.A.I.M.E. V. 192, 47-56.
- PARRISH J.R. (1961) "Packing of Spheres," Nature, V. 190, 800.
- PAYNE D. (1953) "A Method for the Determination of the Approximate  
Surface Areas of Particulate Solids," Nature, V.172, 261.

- PAYNE D. (1954) "The Determination of the Approximate Surface Area of Soil Crumbs," Trans. 5th Int. Cong. Soil Sci. Leopoldville (Kinshasa) V. 2, 46-52.
- PEARCE K.W. and DONALD M.B. (1959) "The Shrinkage Forces Developed in Porous Substances by Capillary Effects," Chem. Eng. Sci, V. 10, 212-224.
- PHILIP J.R. (1964) "Similarity Hypothesis for Capillary Hysteresis in Porous Materials," J. Geophys. Res. V. 69, 1553-63.
- PHILLIPS J.W. and THOMAS D.G.A. (1955) "Removal of Water from Fine Coal," Colliery Eng. Jan, 15-21.
- PIETSCH and RUMPF H. (1967) "Adhesive Force, Capillary Pressure Liquid Volume and Wetting Angle of a Liquid Bridge between Two Spheres," Chem. Ing. Tech. V. 39, 885-893.
- PIROS R.J., BRUSENBACK R.A. and DAHLSTROM D.A. (1952) "Theory, Scale-up, and Operating Variables of the Peterson Top Feed Reservoir," Min. Eng. 1236-44.
- POOLE J.B. and DOYLE D. (1965) "Research in Solid/Liquid Separation," The. Chem. Engr. 169-72.
- POOLE J.B. and DOYLE D. (1965) "Solid Liquid Separation: A Review and a Bibliography," H.M.S.O.
- POULOVASSILIS A. (1962) "Hysteresis of Pore Water an Application of the Concept of Independant Domains," Soil Sci. V. 93, 405-12.
- PRESTON J.M. and NIMKAR M.V. (1952) "Capillary Phenomena in Assemblies of Fibres," J. Textile Inst. V. 43, 402.
- PRILL R.C., JOHNSON A.I. and MORRIS D.A. (1965) "Specific-Yield-Laboratory Experiments Showing the Effect of Time on Column Drainage," Geol. Survey Water Supply Washington, 1662.
- PROBINE M.C. (1958) "Electrical Analogue Method of Predicting Permeability of Unsaturated Porous Materials," Brit. J. Appl. Phys. V. 9, 144-8.
- PURCELL W.R. (1949) "Capillary Pressures their Measurement Using Mercury and the Calculation of Permeability Therefrom," T.A.I.M.E. Pet. Div. V. 186, 39-48.
- RAPPOPORT L.A. and LEAS W.J. (1951) "Relative Permeability to Liquid In Liquid-Gas Systems," T.A.I.M.E. Pet. Div. V. 192, 83-98.
- RICHARDS B.G. (1965) "Determination of the Unsaturated Permeability from Pressure Plate outflow Data with Non-Negligible Membrane Impedance," Moisture Equilibria in Soils Beneath Covered Areas, Aust. 47-54.
- RICHARDS L.A. and FIRMAN M. (1943) "Pressure Plate Apparatus for Measuring Moisture Sorption and Transmission by Soils," Soil Sci. V. 56, 395-404.

- RICHARDSON J.G., KERVER J.K., HAEFORD J.A. and OSOBA J.S. (1952) "Laboratory Determination of Relative Permeability," T.A.I.M.E. Pet. Div. V. 195, 187-96.
- RIDGEWAY K. and TARBUCK K.J. (1967) "Random Packing of Spheres," B.C.E. V. 12, 384-7.
- RIDGEWAY K. and TARBUCK K.J. (1968) "Particulate Mixture Bulk Densities," C.P.E V. 49, 103-5.
- RINGQVIST G. (1955) "A Method for Determination of Specific Surfaces Applied to Coarse Grained Powders," Proc. Swedish Cement & Concrete Res. Inst. Stockholm, V. 28.
- RITTER H.L. and DRAKE L.C. (1945) "Pore Size Distributions in Porous Materials I Pressure Porosimeter and Determination of Complete Macro-Pore Size Distributions," Ind. Eng. Chem. (Anal. Ed.) V. 17, 782-6.
- RITTER H.L. and DRAKE L.C. (1945) "Pore Size Distributions in Porous Materials II Macro-Pore Size Distributions in Some Typical Substances," Ind. Eng. Chem. (Anal. Ed.) V. 17, 787.
- ROSE W. (1957) "Studies of Water Flood Performance III Use of Network Models," Illinois Ste. Geol. Srvy. Urbana Ill.
- ROSE W. (1958) "Volumes and Surface Areas of Pendular Rings," J. Appl. Phys. V. 29, 687-91.
- ROSE W. and BRUCE W.A. (1949) "Evaluation of Capillary Character in Petroleum Reservoir Rock," T.A.I.M.E. Pet. Div. V. 186, 127-42.
- ROSE H.E. and ROBINSON D.J. (1965) "The Density of Packing of Two Component Powder Mixtures," Pow. Met. V. 8, 20-38.
- ROZKYDALEK J. (1967) "Measurement with X-Rays of Cake Moisture as A Function of Dewatering Time," Mech. Sep. of Liquids, Magdesburg, Oct. (Filt. & Sep. V. 5, 40 1968)
- RUTGERS B. (1962) "Packing of Spheres," Nature, V. 193, 465-6.
- SCARLETT B. (1968) "Private Communication,"
- SCHEIDEGGER A.E. (1953) "Theoretical Models of Porous Matter," Prod. Monthly Aug. 17-23.
- SCHEIDEGGER A.E. (1954) "Statistical Hydrodynamics in Porous Media," J. Appl. Phys. V. 25 994.
- SCHEIDEGGER A.E. (1956) "The Physics of Flow Through Porous Media," Univ. of Toronto Press 2nd Ed. (1960).
- SCHEPMAN B.A., MARTIN B. and DAHLSTROM D.A. (1956) Continuous Rotary Filtration of Corn Gluten," Chem. Eng. Prog. V. 52, 423-427.Oct.

- SCOTT G.D. (1960) "Packing of Spheres," Nature, V. 188, 908-9.
- SHOENBERGER R.W. and BURCH E.F. (1964) "Improved Dewatering of Coal by Steam Filtration: Continuous Pilot Scale Filter Tests," T.A.I.M.E. (S. Min.E.) V. 229, 379-83.
- SILVERBLATT C.E. and DAHLSTROM D.A. (1954) "Moisture Content of a Fine Coal Filter Cake," Ind. Eng. Chem. June, 1201-07.
- SILVERBLATT C.E. and DAHLSTROM D.A. (1964) "Improved Dewatering of Coal by Steam Filtration: Experimental Bench Scale Tests," T.A.I.M.E. (S. Min. E.) V. 229, 341-47.
- SIMONS C.S. and DAHLSTROM D.A. (1965) "Application of Steam to the Dewatering of Metallurgical Concentrates," Ann. C.I.M.M. Toronto, Mar. (Also Bull. Can. I.M.M. V. 59, 961-7, 1966).
- SIMONS C.S. and DAHLSTROM D.A. (1966) "Steam Dewatering of Filter Cakes," Chem. Eng. Prog. V. 62, 75-81.
- SLICHTER C.S. (1899) "Theoretical Investigation of the Motion of Ground Water," 19th Ann. Rep. V.S. Geol. Survey.
- SMALLEY I.J. (1962) "Packing of Equal O-Spheres," Nature, V. 194, 1271.
- SMITH E.B. and LEA (1960) "A Monte Carlo Equation of State for Mixtures of Hard Sphere Models," Nature, V. 186, 714.
- SMITH W.O., FOOTE P.D. and BUSANG P.F. (1929) "Packing of Homogeneous Spheres," Phys. Rev. V. 34, 1271-4.
- SMITH W.O., FOOTE P.D. and BUSANG P.F. (1931) "Capillary Rise in Sands of Uniform Spherical Grains," Phys. V. 34, 18-26.
- STIGANT S.A. (1964) "Matrix and Tensor Analysis in Electrical Network Theory," MacDonal, London.
- SULLIVAN R.R. and HERTEL K.L. (1942) "Advances in Colloid Science," Int. Sci. V. 1. New York.
- TEMPLETON C.C. (1954) "A Study of Displacements in Microscopic Capillaries," T.A.I.M.E. V. 201, 162-8.
- THOMEER J.H.M. (1960) "Introduction of a Pore Geometrical Factor Defined by the Capillary Pressure Curve," J. Pet. Tech. Mar. 73-7.
- THORNTON O.F. (1949) "A Note on the Valuation of Relative Permeability," T.A.I.M.E. Pet. Div. V. 186, 328-28.
- TROPPER A.M. (1962) "Matrix Theory for Electrical Engineering Students," Harrap, London.

- VERSLUYS J. (1917) "Die Kapillarität der Boden," Int. Mitt. Fur. Bodenkunde, V. 7, 117-40.
- VON ENGELHARDT W. (1955) "Interstitial Water of Oil Bearing Sands and Sandstones," Proc. 4th World Pet. Cong. sect.1 C 399.
- WALL C.G. (1965) "Permeability: Pore Size Distribution Correlations," J. Inst. Pet. V. 51, 195-200.
- WALKLEY I. and HILLIER I.H. (1967) "Computer Model for Sphere Packing," Disc. Farad. Soc. 79-81.
- WEICKOWSKI, A. and STREK F. (1966) "Voidage in Mixtures of Granular Materials Multi-Component Systems," Chem. Stos 1B 95 4 B 431-47.
- WESTMAN A.E.R. and HUGILL H.R. (1930) "The Packing of Particles," J. Am. Ceram. Soc. V. 13, 767-79.
- WHITE H.E. and WALTON S.F. (1937) "Particle Packing and Particle Shape," J. Am. Ceram. Soc. V. 20, 155-66.
- WICKSELL S.D. (1925) "The Corpuscle Problem - A Mathematical Study of a Biometric Problem," Biometrika, V. 17, 84-99.
- WILSDON G. (1924) "A Physical Theory of Soil Moisture Relations," J. Agric. Sci. V. 14, 473-89.
- WINSAVER W.O., SHEARIN H.M., MASSON P.H. and WILLIAMS M. (1952) "Resistivity of Brine-Saturated Sands in Relation to Pore Geometry," Bull. Am. Assoc. Pet. Geol. V. 36, 253-77.
- WISE M.E. (1952) "Dense Random Packing of Unequal Spheres," Philips Res. Rep. V. 7, 321-343.
- WISE M.E. (1960) "On the Radii of Five Packed Spheres in Mutual Contact," Philips Res. Rep. V. 15, 101-6.
- WYCOFF R.D. and BOTSET H.G. (1936) "The Flow of Gas-Liquid Mixtures Through Unconsolidated Sands," Phys. V. 7, 325-45. Sept.
- WYLLIE M.R.J. and GARDNER G.H.F. (1958) "Permeability and the Size Distribution of Pores," Nature, V. 181, 477.
- WYLLIE M.R.J. and GARDNER G.H.F. (1958) "The Generalized Kozeny-Carman Equation 2 A Novel Approach to Problems of Fluid Flow," World Oil, V. 146, 121-8, 210-28.
- WYLLIE M.R.J. and GREGORY A.R. (1955) "Fluid Flow in Unconsolidated Porous Aggregates Effect of Porosity & Particle Shape," Ind. Eng. Chem. V. 47, 1379-88.
- WYLLIE M.R.J. and ROSE (1950) "The Application of Kozeny-Carman Equation to Consolidated Porous Materials," Nature, V. 165, 972.
- WYLLIE M.R.J. and SPANGLER M.B. (1952) "Application of Electrical Resistivity Measurements to the Problem of Fluid Flow in Porous Media," Bull. Am. Ass. Pet. Geol. V. 36, 359-403.

